Investigation of an N5-glutamine methyltransferase, a novel partner of α2-chimaerin

A thesis by

Adamantios Mamais

Submitted to

University College London

for the degree of

Doctor of Philosophy, PhD.

April 2010

Department of Molecular Neuroscience

UCL Institute of Neurology

University College London

Queen Square

London WC1N 3BG

I, Adamantios Mamais, confirm that the work presented in this thesis is my own. Where information has been derived from other sources, I confirm that this has been indicated in the thesis.

Acknowledgments

I would like to thank Professor Louis Lim and Dr Christine Hall for giving me the opportunity to study and perform research in their laboratory. To my supervisor Dr Christine Hall, thank you for your guidance, advice and encouragement over the course of this project. To Professor Louis Lim, thank you for the numerous inspiring discussions on the secrets of molecular pathways in an effort to unravel the beautiful blue-prints of nature. I would like to thank my Mother and Father for their immense support and encouragement, and for inspiring persistence, dedication and positive thinking. To Dr Sheila Govind, thank you for your advice and guidance, and for bringing warmth and light in the lab. To Bhav for always being there to sort things out, and under-taking the super-human task of organising a research team! To Cassie, thank you for sharing this long trip down the bumpy road of a PhD research project. To Anthony, thank you for taking care of everyone, and for providing a great inspiration of patience and self-contentment. Also, I want to thank Jana and Connie, for their tremendous help and bugging to get this finished, and for being such great friends.

I want to thank my brothers Costas and Vaggelis, for making life so fun and for their immense guidance on data analysis and statistics. A huge thank you to Yasmin for her support, patience, advice and lovely cooking through what may be my last student years. Lastly I want to thank my extended brothers George, Van, Aris and Dimitris for all the laughs and philosophies over cups of coffee.

Abstract

Differentiating neurones respond to extracellular signalling cues that affect the actin cytoskeleton and influence the outgrowth and retraction of cellular processes. Rac1 belongs to the family of Rho GTPases that play a key role in actin organisation during neuronal development. Rac1 promotes lamellipodia formation and neurite outgrowth, and is also involved in axonal retraction pathways. α2-Chimaerin down-regulates Rac1 and is involved in neuronal plasticity and axonal guidance through a wide spectrum of interacting partners. The N5-glutamine methyltransferase HemK1 was previously identified in our lab as a novel interacting partner of α2-chimaerin, in a yeast two-hybrid screen. The aim of this study was to characterise HemK1 and investigate its role in neurite outgrowth.

N5-glutamine methyltransferases are universally conserved in nature and little studied in vertebrates. HemK1 and related protein HemK2 are implicated in the control of translation termination by methylating the polypeptide chain release factors, a modification that mediates efficient translation termination in their bacterial and yeast homologues. Analyses of their transcript levels in rat embryonic brains by quantitative real-time PCR indicated that both HemK1 and HemK2 are expressed at comparable levels to α2-chimaerin in the brain and also in hippocampal neurones. HemK1 monoclonal antibodies detected an endogenous protein in brain mitochondrial fractions, but not in cytosol. When over-expressed, HemK1 co-localised with its proposed mitochondrial substrate mtRF1a in cells and also exhibited partial co-localisation with Dcp1b, a component of the mRNA decay machinery. Both HemK1 and HemK2 associated with α2-chimaerin, as well as with their proposed substrates, mtRF1a and eRF1. α2-Chimaerin influences neuronal morphology and dendritic pruning. ShRNA knock-down of HemK1 or HemK2 in primary rat hippocampal neurones in culture promoted increased branching and complexity of neurites as assessed by confocal microscopy and Sholl analysis. These results suggest a novel link between translational control mechanisms and Rac signalling pathways in developing neurones.

Contents

List of Figures

Chapter 1 [Introduction]

Chapter 2 [Materials and Methods]

Chapter 3 [Results I]

Chapter 4 [Results II]

Chapter 5 [Results III]

Chapter 6 [Results IV]

Chapter 7 [Discussion]

List of Tables

Abbreviations

Amp	Ampicillin
APS	Ammonium Persulphate
ATP	Adenosine Triphosphate
BDNF	Brain-Derived Neurotrophic Factor
BCR	Breakpoint Cluster Region
BSA	Bovine Serum Albumin
Cdc	Cell Division Cycle
Cdk	Cyclin Dependent Kinase
cDNA	Complementary DNA
CIAP	Calf Intestinal Alkaline Phosphatase
CMV	Cytomegalovirus
CRMP	Collapsin Response Mediator Protein
Cy5	Cyanine 5
DAG	Diacylglycerol
ddH_2O	Deionised purified water
Dcp	mRNA Decapping Protein
DEPC	Diethylpyrocarbonate
DLC	Deleted in Liver Cancer
DMEM	Dulbecco's Modified Eagles Medium
DNA	Deoxyribonucleic Acid
dNTP	Deoxyribonucleotide Triphosphate
DOCK	Dedicator of Cytokinesis Proteins
DTT	Dithiothreitol
E.coli	*Escherichia coli*
ECL	Enhanced Chemiluminescence
EDTA	Ethylenediamine Tetraacetic Acid
eEF	Eukaryotic Elongation Factor
EGF	Epidermal Growth Factor
eIF	Eukaryotic Translation Initiation Factor
EJC	Exon Junction Complex

ER	Endoplasmic Reticulum
eRF	Eukaryotic Release Factor
ESCRT	Endosomal Sorting Complex Required for Transport
F-actin	Filamentous Actin
FCS	Foetal Calf Serum
FGF	Fibroblast Growth Factor
FITC	Fluorescence Isothiocyanate
FMRP	Fragile X Mental Retardation Protein
G3BP	Ras-GAP SH3 domain binding protein
G-actin	Monomeric Actin
GAP	GTPase Activating Protein
GDI	Guanine Nucleotide Dissociation Inhibitor
GDP	Guanosine Diphosphate
GEF	Guanine Nucleotide Exchange Factor
GFP	Green Fluorescent Protein
GIT	G-protein Coupled Receptor Kinase Interacting Targets
GSK	Glycogen Synthase Kinase
GST	Glutathione-S-Transferase
GTP	Guanosine Triphosphate
HA	Haemagglutinin
HPRT	Hypoxanthine Phosphoribosyltransferase
HRP	Horseradish Peroxidase
IPTG	Isopropyl-Thio-D-Galactoside
IRS	Insulin Receptor tyrosine kinase Substrate
LB	Luria-Bertani
MAP	Microtubule Associated Protein
MAPK	Mitogen Activated Protein Kinase
mRNA	Messenger Ribonucleic Acid
MTOC	Microtubule Organising Centre
mtRF	Mitochondrial Release factor
NF	Neurofilament
NGF	Nerve Growth Factor
NMD	Nonsense-Mediated mRNA Decay
N-WASP	Neural-Wiskott Aldrich Syndrome Protein

OCRL	Oculocerebrorenal Syndrome of Lowe
PABP	Poly-(A) Binding Protein
PAGE	Polyacrylamide Gel Electrophoresis
PAK	p21 Activated Kinase
PBS	Phosphate Buffered Saline
PCR	Polymerase Chain Reaction
PDGF	Platelet Derived Growth Factor
PI3K	Phosphoinositide 3 Phosphate Lipid Kinase
PIP	Phosphatidylinositol Phosphate
PKC	Protein Kinase C
PKD	Protein Kinase D
PLC	Phospholipase C
PMA	Phorbol Myristate Acetate
PMSF	Phenylmethyl-Sulfonyl Fluoride
PRMT	Protein Arginine Methyltransferase
PTB	Phosphotyrosine Binding Domain
PVDF	Polyvinylidene Fluoride
Rac	Ras-related C3 Botulinum Toxin Substrate
Rho	Ras Homologous Member A
RF	Release Factor
RFU	Relative Fluorescence Units
ROK	RhoA Kinase
ROS	Reactive Oxygen Species
SBS	Staufen Binding Site
SDS	Sodium Dodecyl Sulphate
SH2	Src Homology 2 Domain
SH3	Src Homology 3 Domain
shRNA	Short Hairpin RNA
TEMED	N, N, N', N'-Tetramethylethylenediamine
TRITC	Tetramethylrhodamine Isothiocyanate
tRNA	Transfer RNA
WAVE	WASP family verprolin homologous protein
USP	Ubiquitin Specific Protease
Vps	Vacuolar Protein Sorting Protein

“If the brain were so simple we could understand it,
we would be so simple we couldn't.”

Lyall Watson
April 12, 1939 - June 25, 2008

Chapter 1
[Introduction]

The Brain

The brain is the most complex part of the central nervous system in all vertebrate and most invertebrate animals, while it is the less-understood of the human organs. Electrochemical processes originating in the brain order the conscious and unconscious behaviour of an individual, be it thought, memory or involuntary actions and sensory perception among others. The complex functions of the brain are undertaken largely by neuronal cells whose well-being is maintained by glial cells that provide support and protection maintaining a stable environment for their growth and survival. It is estimated that the adult human brain contains an average of 86.1 billion neurones (Azevedo et al, 2009) while the total number of synapses in the neocortex, the outer layer of the cerebral hemispheres, can reach as much as 164 trillion (Tang et al, 2001a). The human brain develops in a series of orchestrated stages that give rise to the complex topology, compartmentalisation and organisation of this organ. In early embryonic development neurulation gives rise to the neural tube that eventually forms a closed cylinder that separates from the surface ectoderm. Differentiation of the neuronal tube gives rise to the brain and the spinal cord. On an anatomical level the neural tube and its lumen constrict to give rise to the chambers of the brain and the spinal cord. At the tissue level the cells of the neural tube wall rearrange to form the different functional regions of the central nervous system. At the cellular level the neuroepithelial cells differentiate to give rise to neurone cells and glial cells, the main components of the brain. The newly formed neurone cells migrate to different parts of the brain to self-organise to the different functional brain regions (Gilbert, 2003). At the final step of embryonic brain development the neurones extend dendrites and axons to form synapses with neighbouring cells, and thus give rise to the complex neural circuitry of the brain.

The Neurones

The neurones provide the lines of communication of the nervous system sending signals to each other and other cells in the body including muscle and endocrine cells. Neuronal cells are highly differentiated with complex morphology allowing specialisation of function. A generic representation of a neurone gives a picture of a polarised cell consisting of cell body, the long process of the axon that features a

growth cone ending, and smaller processes that protrude from the cell body that constitute the dendrites (Figure 1.1). Neuronal cells communicate through the release of chemical signals propagating action potentials from cell to cell through synapses. Synaptic connections between neurones can occur between axons, dendrites and the cell body, forming dendrodendritic, axoaxonic, axodendritic and axosomatic synapses (Figure 1.1).

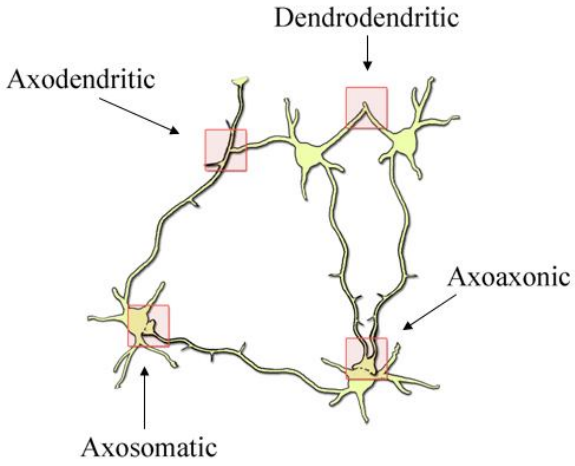

Figure 1.1 Synapses between neurones. Neurones can form synapses between axons (axoaxonic), axons and dendrites (axodendritic), axons and the cell soma (axosomatic) and also between dendrites (dendrodendritic).

The early stages of neuronal differentiation see the development of an axon and multiple dendrites that will eventually form connections with neighbouring cells through synapses and mediate the formation of a neuronal network. Primary cultures of dissociated hippocampal neurones are a widely used model system in the study of neurone polarisation and axonal development (Arimura and Kaibuchi, 2007). An early study by Dotti et al described the development of hippocampal neurones in culture in five distinct stages (Figure 1.2) (Dotti et al, 1988). The freshly plated neurones initially extend lamellipodia around the soma (stage 1) that give rise to multiple processes of approximately equal length described as immature neurites (stage 2). Approximately 1.5 days in culture the cells begin to acquire polarisation with one of the immature neurites rapidly elongating and exhibiting axonal characteristics (stage 3). After 2-3 days in culture the remaining neurites develop to give rise to multiple dendrites (stage 4). The final stage of neuronal development in culture comes with the further maturation of axons and dendrites and the formation of synaptic contacts after 7 days in vitro (stage 5) (Dotti et al, 1988; Yoshimura et al, 2006). Studies have suggested that while neurites have equal chances of becoming an axon, the neurite

that is finally specified to become an axon negatively regulates the remaining neurites preventing them from becoming axons (Dotti and Banker, 1987; Goslin and Banker, 1989). This suggests a model where neurites regulate their growth against each other, each one sending a growth promoting signal to it self and an inhibitory signal to neighbouring neurites maintaining a balance of opposite signals that gives rise to the symmetrical morphology of stage 2 neuronal development (Andersen and Bi, 2000). This balance is broken when one neurite elongates and over-takes the negative feed-back from other neurites while sending growth inhibitory signals preventing simultaneous elongation of other neurites. This gives rise to initial polarisation observed in stage 3 neurones in culture, resulting in the formation of a single axon and multiple dendrites (Figure 1.2) (Bradke and Dotti, 2000).

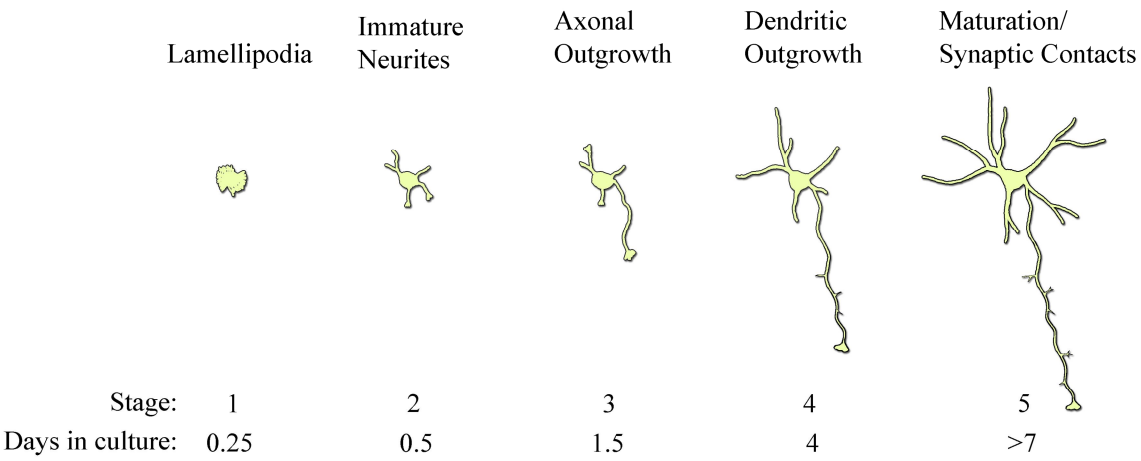

Figure 1.2 Stages of development of hippocampal neurones in culture.
The development of hippocampal neurones in culture can be described in five stages that see the development of neurites subsequently giving rise to an axon and dendrites. (adapted from Dotti et al, 1988).

Studies on the intracellular signalling pathways that govern the axonal and dendritic development have revealed a series of factors that play a role in neuronal polarisation. The family of Rho GTPases regulates the actin cytoskeleton in developing processes in response to extracellular stimuli. The three best studies Rho GTPases, Rho that regulates the formation of stress fibers and focal adhesions (Ridley and Hall, 1992), Rac that is responsible for the formation of lamellipodia (Ridley et al, 1992) and Cdc42 that mediates filopodia formation (Kozma et al, 1997), all play an important role in regulating cell polarity. Furthermore the signalling pathway of

phosphatidylinositol 3-kinase (PI3-kinase), Akt and GSK-3β has been shown to play a role in neuronal polarity. PI3-kinase is important in determining axonal specification and elongation (Shi et al, 2003). PI3-kinase activates Akt that in turn mediates the phosphorylation of GSK-3β, resulting in downregulation of GSK-3β activity, a step required for neuronal polarisation (Scheid and Woodgett, 2001; Yoshimura et al, 2005; Jiang et al, 2005). GSK-3β regulates neuronal polarity by phosphorylating the collapsin response mediator protein-2 (CRMP-2) (Yoshimura et al, 2005), a protein that promotes microtubule assembly in vitro (Fukata et al, 2002), is highly expressed in axons and plays an important role in axonal formation (Yoshimura et al, 2005)

Defects in neuronal development can give rise to cognitive disorders as well as motor disability and autism. The family of Rho GTPases is implicated in neuronal morphogenesis by regulating the actin cytoskeleton and directing morphological events of cell development, differentiation and establishment of polarity. A number of effector and regulator proteins have been identified mediating the effects of Rho GTPases to the cytoskeleton and mutations in these genes have been associated with neurological disorders, including mental retardation and amyotrophic lateral sclerosis (Kasri and Aelst, 2008). A number of Rho GTPase effectors and regulators involved in neuropathology are summarised in table 1.1.

Gene (locus)	Protein	Function	Clinical Manifestation
OPHN1 (X-q12)	Oligophrenin-1	Rho family GAP for RhoA/Rac1/Cdc42	non-syndromic X-linked Mental Retardation
PAK3 (Xq22)	PAK3	Ser/Thr kinase effector of Rac1/Cdc42	non-syndromic X-linked Mental Retardation, Alzheimer's Disease
ARHGEF6 (Xq26)	Cool2	GEF for Rac/Cdc42 interacts with PAK	non-syndromic X-linked Mental Retardation
FDG1 (Xp11)	FDG1	GEF for Cdc42	non-syndromic X-linked Mental Retardation, faciogenital dysplasia
OCRL1 (Xq24)	OCRL1	Rac GAP	Lowe syndrome
FMR1 (Xq27)	FMRP	RNA binding protein that interacts with CYFIP, a Rac effector	Fragile X syndrome
LIMK1 (7qQ11)	LIMK1	Ser/Thr kinase effector of Rac and RhoA that inactivates cofilin	Williams syndrome, Alzheimer's Disease
MEGAP (3p25)	MEGAP	GAP for Cdc42 and Rac1	3p-syndrome

Table 1.1 Mutations in Rho GTPase regulators and effectors are linked to neurodegenerative diseases. (Adapted from Kasri and Aelst, 2008).

The Cytoskeleton

The cytoskeleton is a system of microscopic filaments that exist all through the cytoplasm of prokaryotic and eukaryotic cells and delivers shape, stability and movement to the cell while organising the position of the cellular organelles. The cytoskeleton consists of three main types of protein filaments: Actin filaments (also called microfilaments), microtubules, and intermediate filaments. The highly dynamic nature of the cytoskeleton allows for cell migration and morphological alterations in response to extracellular stimuli. The cytoskeleton is also responsible for cell division resulting into two daughter cells and also chromosome separation during mitosis and meiosis.

Actin Filaments (microfilaments)

Actin is one of the most highly conserved proteins in nature and participates in many important cellular processes including cell shape and motility, cell division, vesicle and organelle movement and cell signalling. Actin exists in two forms in the cell, as globular actin monomers (G-actin) and as actin filaments (F-actin). F-actin filaments are polarised fibres consisting of G-actin monomers, with a fast growing (+) end, and a relatively inert (-) end. The equilibrium observed between actin polymerisation at the plus end and depolymerisation at the minus end has been described as treadmilling process (Wegner, 1976). Actin forms structures at the edge of cells forming different network arrays. Filopodia and microspikes are formed when F-actin arranges in parallel bundles, in a way that the filaments have the same polarity. Stress fibres are formed across the cell when actin filaments are organised in opposite polarities, in structures called contractile bundles. Lamellipodia formation is the result of actin being organised in a network of open arrangement, where F-actin forms a meshwork of interconnecting filaments at the cell edge. (Pollard et al, 2000)

Microtubules

Microtubules are polar helical structures formed by the non-covalent polymerisation of tubulin, consisting of α- and β-tubulin heterodimers arranged in a head to tail fashion (Amos and Klug, 1974; Burns, 1991). Important to the function of microtubules is their polarity raised with the opposite arrangement of the two

monomers. Microtubules have a fast growing (+) end and a slower growing (-) end and β-tubulin is orientated towards the plus end while α-tubulin points the minus end (Desai and Mitchison, 1997). Microtubules form the mitotic spindle during cell division, physically segregating the chromosomes and orientating the point of cleavage. In some non-dividing cells the microtubules are the structural elements of flagella and cilia while they also organise the cytoplasm and position the nucleus and organelles. Tubulin is a GTPase and its activity is stimulated by polymerisation. Stable microtubules form when tubulin polymerises in the presence of GTP (Hymen et al, 1992). Microtubules can solely exert forces on the cell membrane and also act as tracks for the transport of organelles through the motor proteins kinesin and dynein (Vale and Fletterick, 1997; Reviewed in Howard & Hyman, 2003; Hirokawa, 1998). Dynamic microtubules also play a role in neurite morphogenesis, assisting in axonal guidance and dendritic spine maturation coupling with actin filaments (Geraldo and Gordon-Weeks, 2009; Arnold, 2009). While growing tips of both dendrites and axons exhibit increased microtubule polymerisation, dendrites exhibit more immature dynamic microtubules throughout their entire arbour compared to more stable microtubule structures observed in axons (Kollins et al, 2009). Local stabilisation of microtubules in a neurite gives a physiological signal for this process to develop to an axon (Witte et al, 2008). Microtubule associated proteins (MAPs) act as regulatory elements binding to microtubules and stabilising them while regulating the polymerisation of tubulin. The family of MAPs present in the brain includes the large proteins MAP-1 and MAP-2 and the smaller protein Tau. Neuronal MAPs strongly suppress the transition from microtubule polymerisation to depolymerisation (Desai and Mitchison, 1997). MAP-2 shows a dendrite specific localisation where microtubules show mixed orientation, with the plus end facing either the cell body or the process end. Tau is active primarily in axons where it provides stabilisation and flexibility on the microtubule assembly that shows a uniform orientation with the plus end facing the axon tip (Bernhardt and Matus, 1984; Cone and Cáceres, 2009). The microtubule associated protein Tau is the centre of a great scientific interest since it has been linked to neurodegeneration in Alzheimer and Parkinson's disease and other tauopathies. While normal Tau is involved in microtubule assembly and stabilisation, abnormally hyperphosphorylated Tau can promote microtubule disruption (Iqbal et al, 2009).

Intermediate Filaments

Intermediate filaments have an average diameter in between that of actin filaments and microtubules, ranging from 8-10 nm. Intermediate filaments are the most insoluble part of the cell and while being cell specific they are prominent in cells that withstand mechanical stress, offering shock-resistance characteristics. Intermediate filaments exhibit conserved domain structure featuring an α-helical rod domain surrounded by a globular non-α-helical domain at the N and C termini. Intermediate filaments consist of different proteins in different cells. In astrocytes the main component of intermediate filaments is the glial fibrillary acidic protein (Eng, 1985), while in neuronal cells the neurofilaments NF-L, NF-M and NF-H compose intermediate filaments (Fuchs and Cleveland, 1998). NF-M and NF-H integrate on a backbone formed by NF-L, forming peripheral dimer arrays with protruding tails, allowing them to associate with microtubules in the cytoplasm. Two other examples of abundant intermediate filaments are keratins and lamins. Lamins are nuclear intermediate filaments offering functional structure to the nucleus. Keratins are the most diverse among intermediate filaments forming junctions between cells (desmosomes) and also attaching cells to the extracellular matrix (hemidesmosomes) (Herrmann et al, 2009). Mutations in intermediate filament genes have been linked to the Hutchinson-Gilford progeria syndrome and the fatal Alexander disease that affects the nervous system causing abnormal development of the brain and skull (Mounkes and Stewart, 2004; Li et al, 2002). Furthermore mutations in Lamin A have been associated with cardyopathy and muscular dystrophies (Gotzmann and Foisner, 2006).

The Arp2/3 complex

Actin-related proteins (Arp) feature sequence similarity to actin while the diverse Arp protein groups perform distinct and very different function in cells. The actin related protein 2/3 complex (Arp2/3) in an important regulator of the actin cytoskeleton. Its two subunits Arp2 and Arp3 closely resemble the structure of actin monomers promoting synthesis of new actin filaments by serving as nucleation sites for polymerisation (Machesky and Gould, 1999). Arp2/3 is responsible for the creation of branched actin networks by forming nucleation cores on the sides of already existing

actin filaments (mother) and initiating the synthesis of new filaments (daughter) at a distinctive 70° angle. The activity of Arp2/3 is regulated by proteins of the Wiskott-Aldrich syndrome family including N-WASP and WAVE (Blanchoin et al, 2000). Arp2/3 requires ATP and activating proteins to initiate actin polymerisation. The activating factors in the presence of ATP cause a conformational change that allows Arp2 and Arp3 to come in close proximity activating the complex (Robinson et al, 2001). The Arp2/3 complex rearranges the actin cytoskeleton in response to signals mediated by the activator proteins that in turn are part of signalling pathways governed by the Rho GTPases.

The Rho GTPases

The Rho GTPases comprise a family of small monomeric G proteins that belong to the Ras superfamily and are found in all eukaryotic cells. The Rho GTPases coordinate diverse cellular functions including the cell cycle, gene expression, vesicular trafficking and cell polarity (reviewed in Bustelo et al, 2007). While more than twenty Rho GTPases have been discovered, RhoA, Rac1 and Cdc42 are the best characterised members. In neurones Rac1 promotes the formation of lamellipodia and ruffles playing an important role in growth cone and neurite formation, while Cdc42 is generally accepted to be involved in the formation of filopodia, and RhoA in cell contraction and formation of stress fibres and focal adhesions. Axon guidance cues mediated by the semaphorins, ephrins, netrins, and slit proteins are received by membrane receptors at the growth cone and initiate intracellular signal transduction pathways that converge onto the Rho GTPases. The Rho GTPases orchestrate the morphological changes of the developing neurone signalling pathways that affect the actin cytoskeleton organisation (Govek et al, 2005).

Rho GTPases are guanine nucleotide binding proteins and function as molecular switches cycling between an active GTP-bound state and an inactive GDP-bound state (Figure 1.3) (Nobes and Hall, 1994). While their inactive state is usually cytosolic, when active the Rho GTPases associate with the cell membrane mediating signals

from membrane receptors to effector proteins that in turn rearrange the actin cytoskeleton of the cell (Figure 1.4).

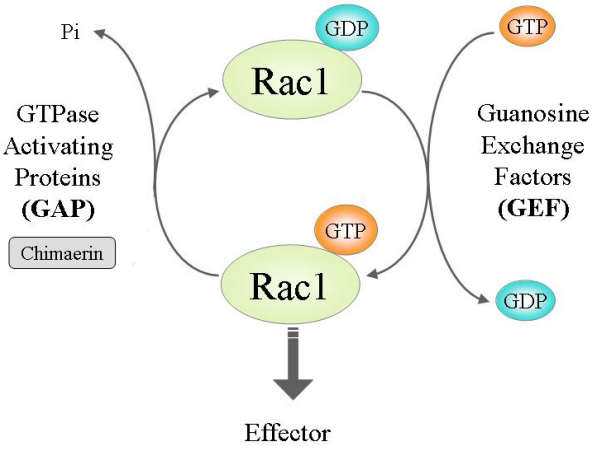

Figure 1.3 The cycling of Rho GTPases. Rho GTPases are activated by GEFs that exchange bound GDP for GTP. GTP-bound Rho GTPases rearrange the actin cytoskeleton through effectors. Their intrinsic GTPase activity is enhanced by GAPs and hydrolysis of GTP to GDP deactivates them. A GAP specific for Rac1 is chimaerin.

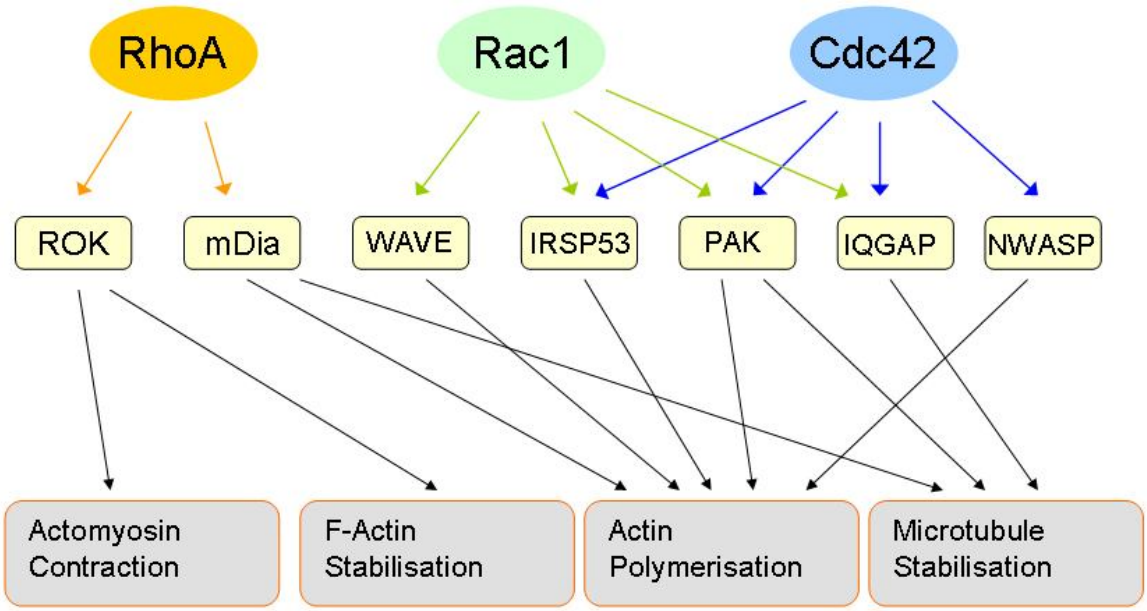

Figure 1.4 Rho GTPases act through effectors to rearrange the actin cytoskeleton. Rho GTPases interact with effector proteins when active and mediate changes in the actin cytoskeleton of the cell. Some effector proteins interact with more than one Rho GTPase establishing a cross-talk between different signalling pathways that can involve a co-ordinated regulation led by several Rho GTPases (Adapted from Iden and Collard, 2008)

Rho GTPase Regulatory Proteins

An immediate control of the activity of Rho GTPases is achieved by the GTPase Activating Proteins (GAPs), the Guanine nucleotide Exchange Factors (GEFs) and the Guanine nucleotide Dissociation Inhibitors (GDIs). All three families of proteins regulate the GTPase cycle and hence specific functions in signalling pathways that rely on the intrinsic activity of the Rho GTPases as molecular switches.

Guanine nucleotide Exchange Factors (GEFs)

Guanine nucleotide Exchange Factors (GEFs) activate Rho GTPases by promoting the exchange of the bound GDP for a GTP molecule (Schmidt and Hall, 2002). GEF's mediate their activity through two functional domains, a dbl homology domain (DH) and a pleckstrin homology domain (PH), in tandem placement. The dbl homology domain comprises the catalytic core while the pleckstrin homology domain mediates the intracellular localisation of the protein by recruiting the protein on the cell membrane or by assisting in interactions with other proteins. GEF's can have a single specific substrate or can also activate different Rho GTPases. An example is the GEF Trio that features two DH/PH cassettes, one is specific for RhoA while the second can activate both Rac1 and RhoG (Bellanger et al, 1998; Blangy et al, 2000; Chhatriwala et al, 2007). Trio has been involved in neurite outgrowth in netrin-1 signalling through Rac1 (Briançon-Marjollet et al, 2008) and also in nerve growth factor differentiation signalling through RhoG (Estrach et al, 2002). A GEF protein family that features a novel domain structure, different to the Dbl/DH arrangement, is comprised of the dedicator of cytokinesis proteins (DOCK) that can catalyse both Rac1 and Cdc42 (Yang et al, 2009a).

Guanine nucleotide Dissociation Inhibitors (GDIs)

The Guanine nucleotide Dissociation Inhibitors (GDIs) keep the GTPases in an inactive state by inhibiting the dissociation of GDP while also preventing the activation by GEFs (Fukumoto et al, 1990). GDIs can also prevent the Rho GTPases

from localising on the membrane, where they can be activated and mediate signalling cascades, by forming a complex with the GTPases in the cytoplasm. Furthermore Rho GDIs can interact with GTP bound Rho GTPases and block the interaction of these proteins with downstream effectors while inhibiting the hydrolysis of GTP by the intrinsic GTPase activity (reviewed in DerMardirossian and Bokoch, 2005).

GTPase Activating Proteins (GAPs)

The GTPase Activating Proteins bind to activated Rho GTPases and stimulate their intrinsic GTPase activity thereby promoting the hydrolysis of GTP and rendering the GTPase inactive, terminating the signalling event. The activity of GAPs is regulated by a variety of mechanisms including protein-protein interactions, phosphorylation, subcellular translocation, phospholipid interactions and proteolytic degradation (reviewed in Bernards and Settleman, 2004). GAPs outnumber the Rho GTPases they regulate by 2- to 3- fold, and recent findings have suggested three main reasons for this: a) GAPs can show preferential tissue expression and exhibit tissue-specific functions, b) the GAP domain may act as recognition module so the GAPs mediate cross-talk between Rho GTPases and their effectors, and c) some GAPs may regulate specific Rho GTPase signalling pathways, a notion supported by the fact that Rho GTPases are involved in a large number of biological processes (Tcherkezian and Lamarche-Vane, 2007). GAPs, like GEFs, can have a specific target or can down-regulate a series of Rho GTPases. Plexin-B1 is a semaphorin 4D receptor and is an example of a GAP that has two substrates. By regulating the activity of both R-Ras and M-Ras GTPases it affects axonal and dendritic morphology respectively (Saito et al, 2009).

A series of domains have been discovered in Rho GAPs that mediate their activation and specificity. As well as the GAP domain of Rho GAPs that mediates their binding to Rho GTPases and the down-regulation of Rho GTPase activity other domains may regulate their function. The cysteine-rich C1 domain found in a series of GAPs mediates binding to diacylglycerol and in the case of the Rac1 specific GAP chimaerin it mediates phorbol ester induced membrane translocation (Caloca et al, 1999; Brown et al, 2004). While pleckstrin homology domains (PH) are mainly

associated with dbl homology domains in Rho GEFs, they are also found in some GAPs, as in the case of PSGAP, a PH containing GTPase that can regulate the activity of Cdc42 (Ren et al, 2001). Src homology 3 domains are well represented in Rho GAPs mediating interactions with other proteins and expanding their role in complex signalling pathways. The SH3 domain of p120Ras-GAP is responsible for its interaction with the Rho GAP DLC1, and this association can inhibit DLC1 GAP activity (Yang et al, 2009b). Moreover the two SH2 domains of p120Ras-GAP can individually bind p190Rho-GAP, suggesting a means of coordination between Rho- and Ras- mediated signalling pathways (Bryant et al, 1995). Chimaerin contains an SH2 domain that mediates its interaction with EphA4 and links this Rac1 GAP to EphA4 growth cone collapse signalling (Shi et al, 2007).

Downstream signalling effectors of the Rho GTPases

p21-activated kinases (PAK)

One of the families of Rac1 and Cdc42 effector proteins are the p21-activated kinases (PAK). PAK was the first serine/threonine kinase identified to associate and be activated by Rho GTPases (Manser et al, 1994). PAK proteins have been involved in the regulation of actin dynamics and gene transcription. PAK proteins are found in an autoinhibitory state in the cytoplasm, where the conformation of an N-terminal region renders the C-terminal kinase domain unable to be activated (Lei et al, 2000). The autoinhibitory conformation of PAK is disrupted upon binding to Rac1-GTP and Cdc42-GTP resulting in its activation and autophosphorylation (Manser et al, 1994). Active PAK phosphorylates and activates LIM-domain kinase 1 (LIMK1) which in turn phosphorylates cofilin, an actin binding protein that causes depolymerisation at the minus end of actin filaments (Yang et al, 1998; Edwards et al, 1999). Rac1, Cdc42 and PAK have also been implicated in microtubule dynamics, through the ability of PAK to phosphorylate the microtubule-destabilising protein stathmin and in turn promote microtubule stabilisation (Daub et al, 2001). As well as their role in actin dynamics, PAK proteins function in centrosome dynamics by regulating Aurora-A, an important factor in spindle assembly and stability during mitosis (Zhao et al, 2005).

Wiskott-Aldrich syndrome protein family

Another family of downstream effectors for the Rho GTPases are the Wiskott-Aldrich syndrome family of scaffolding proteins that mediate signals to the actin cytoskeleton (reviewed in Smith and Li, 2004). Five members comprise this proteins family: WASP, the neuronal N-WASP, and WAVE1-3 also known as Scar proteins. Cdc42 regulates the activity of the Wiskott-Aldrich syndrome proteins WASP and N-WASP (Rohatgi et al, 2000). The interaction of WASP and N-WASP with the activated Cdc42 causes a conformational change in these effectors that releases the WASP VCA region from autoinhibition and allows it to activate the Arp2/3 complex that in turn forms nucleation cores for actin polymerisation (Kim et al, 2000). WAVE1-3 have been found to be part of Rac1 signalling mediating actin remodelling in the production of ruffles on the cell edges (Miki et al, 1998; Machesky et al, 1999; Yan et al, 2003).

IRSp53 and IQGAP-1

GTP bound Rac1 associates with the scaffolding proteins IRSp53 and IQGAP-1. IQGAP-1 appears to be involved in polarised actin organisation linking actin dynamics with microtubule stability (Fukata et al., 2002). IRSp53 binds both Rac1 and Cdc42 (Govind et al. 2001; Miki and Takenawa, 2002) and links Rac1 to WAVE promoting actin polymerisation through the Arp2/3 complex.

Rho kinase protein family and Diaphanous

The Rho GTPase RhoA regulates the actin cytoskeleton through two prominent effectors, the Rho kinase family (ROK/ROCK) and Diaphanous (mDia). ROK associates with RhoA and translocates to the membrane playing a role in stress fibre and focal adhesion formation (Leung et al, 1995). ROK has been reported to phosphorylate the collapsin response mediator protein-2 (CRMP-2) (Arimura et al, 2000) a protein that promotes microtubule assembly (Fukata et al, 2002) and has been involved in pathways of growth cone collapse (Goshima et al, 1995) and neuronal polarity (Inagaki et al, 2001). The Diaphanous gene mDia has been suggested to have

a role in forming and stabilising microtubules as well as actin dynamics (Palazzo et al, 2001; Eng et al, 2006).

Chimaerins

Rac1 is down-regulated by the GTPase activating protein α2-chimaerin, which is involved in neurite formation and axonal guidance (Hall et al. 2001; Brown et al. 2004). The family of chimaerins is involved in a variety of signalling cascades mediating control over pathways of cell morphology, proliferation and migration.

The first member of the family of Chimaerin splice-variants was identified by Hall et al (Hall et al, 1990). The N-terminal of n-Chimaerin was found to share 50% identity with the C1 regulatory domain of protein Kinase C (PKC). The C-terminal was shown to have 42% identity with the C-terminal region of Breakpoint Cluster Region protein (BCR) involved in the Philadelphia chromosome translocation. The name Chimaerin was invented to represent the novel nature of this protein, consisting of two apparently unrelated domains and indicating an important function in neural outgrowth.

There are two chimaerin genes each with two splice variants. The variants have related structures, with α1-chimaerin and β1-chimaerin consisting of an N-terminal C1 domain and a C-terminal GAP domain, and α2- and β2- having an N-terminal Src homology domain (SH2). α2-Chimaerin is highly expressed in the brain and also in testis and the highest expression pattern is observed in the hippocampus and the cerebral cortex (Hall et al, 1993). The biological functions of the members of the chimaerin family are been examined, and to the present, chimaerins have been reported to play a role in important biological processes including neural growth cone collapse (Brown et al, 2004; Iwasato et al, 2007; Beg et al, 2007, Shi et al, 2007; Takeuchi et al, 2009), inhibition of cancer proliferation (Yang et al, 2005) and the regulation of dendritic morphology and spine density in cultured hippocampal neurones (de Ven et al 2005, Buttery et al 2006). Chimaerins have also been implicated in the proliferation and migration of vascular smooth muscle cells (Maeda

et al, 2006) and in the regulation of cell number, cell-cell contacts, and the stability of adherens junctions in the Drosophila eye (Bruinsma et al, 2007).

Structure and Function of α2-Chimaerin

α2-Chimaerin has three functional domains: C1, SH2 and GAP domain (Figure 1.5).

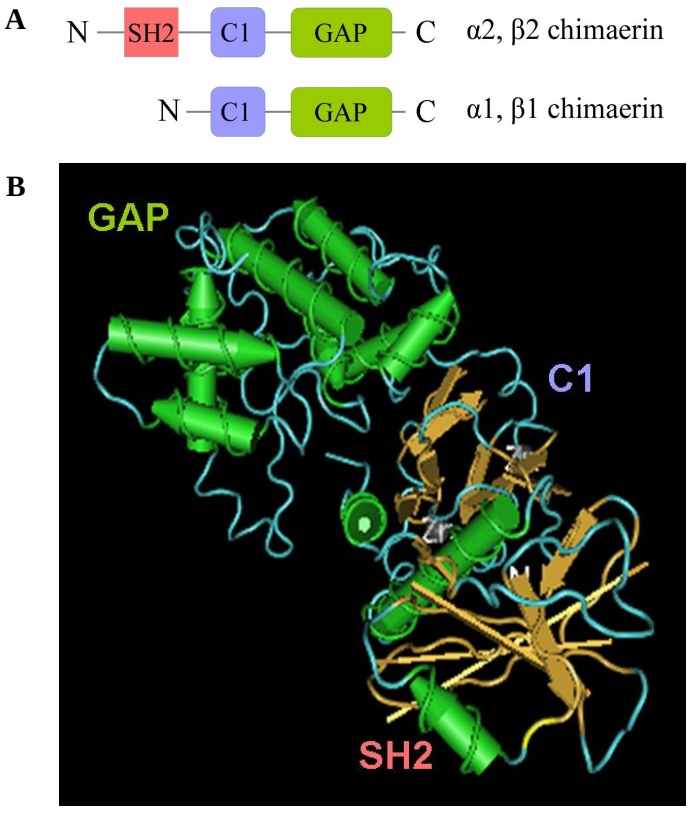

Figure 1.5 Chimaerin domains and structure. (A) The family of chimaerins is comprised of two genes: α- and β-chimaerin. Each is expressed as two splice variants with one encoding for an SH2 domain. (B) α2-Chimaerin consists of an SH2, a C1 and a GAP domain. The auto-inhibitory conformation brought about by intermolecular interactions is released upon diacylglycerol binding to the C1 domain.

The SH2 domain of α2-chimaerin

The SH2 domain mediates protein interactions that depend on tyrosine phosphorylation. It was first identified in the oncogenic v-Fps cytoplasmic tyrosine kinase as a sequence of 100 amino acids that although appeared to modulate the kinase activity and substrate recognition of the protein, was not necessary for the catalytic activity of the kinase. This domain was named Src homology since it was found conserved in the Src and Abl kinases (Sadowski et al, 1986). The SH2 domain is important in both intermolecular and intramolecular interaction involved in protein

tyrosine kinases signalling pathways, primarily recognising phosphotyrosine as a prime target and in some cases phosphorylated serine and threonine. Also non-phosphorylated ligands have been reported amongst the negatively charged binding targets of the Src homology domain.

It was recently shown that α2-chimaerin is part of the EphA4 signalling pathway of axonal guidance (Figure 1.6) (Wegmeyer et al, 2007; Beg et al, 2007; Iwasato et al, 2007; Shi et al, 2007). EphA4 (ephrin type-A receptor 4) belongs to the family of ephrin receptors of the protein-tyrosine kinase family that are key players in cell migration and synapse formation and plasticity in the developing nervous system (Lai and Ip, 2009; Wilkinson, 2001). α2-Chimaerin binds to the activated EphA4 receptor via its SH2 domain and this association is required for ephrin-induced growth cone collapse in cortical neurones (Beg et al, 2007). The ligand ephrin-B3 is an important molecule in neurite outgrowth, axonal guidance and synapse formation (Kadison et al, 2006; Aoto et al, 2007, Benson et al, 2005). Active EphA4 stimulates an increase of tyrosine phosphorylation of α2-chimaerin and enhances chimaerins Rac1 specific GAP activity via the ephrin-B3/EphA4 signalling pathway (Iwasato et al, 2007, Shi et al, 2007). It was therefore suggested that ephrin-B3/EphA4 signalling prevents growth cone extension in motor circuit formation through inactivation of Rac1, mediated by α2-chimaerin.

α2-Chimaerin also interacts with CRMP-2 via its SH2 domain and is involved in the Sema3A pathway (Figure 1.6) (Brown et al, 2004). Collapsin Response Mediator Protein-2 (CRMP-2) is involved in axonal outgrowth and microtubule dynamics. CRMP-2 is part of the growth cone collapse signalling pathway induced by Semaphorin 3A (Sema3A). Sema3A induces growth cone collapse through a Rac-GTP dependent signalling pathway (Jin and Strittmatter, 1997). α2-Chimaerin can associate with Plexin A, that together with neuropilin-1 make up the Sema3A membrane receptor (Brown et al, 2004). Sema3A can act through Fyn that in turn will phosphorylate and activate Cyclin dependant kinase 5 (Cdk5) (Sasaki et al, 2002). Cdk5 can phosphorylate CRMP-2, priming it for phosphorylation by GSK3β, and this action is required for the collapse induced by Sema3A (Brown et al, 2004). CRMP-2 is regulated via phosphorylation by Rho kinase (Arimura et al, 2000), to reversibly switch between RhoA (retraction) and Rac (outgrowth) phenotypes (Hall et al, 2001).

The association between α2-chimaerin and CRMP-2 appears to be promoted by phorbol ester binding to chimaerin's C1 domain, possibly because of the release of the auto-inhibitory conformation that makes the SH2 domain accessible (Canagarajah et al, 2004; Colón-González et al, 2008).

The C1 domain of α2-chimaerin mediates interactions with Phorbol Esters.

The C1 domain was first identified in Protein Kinase C (PKC), where it was found to bind phorbol esters analogues of diacylglycerol causing PKC activation and initiation of intracellular signalling pathways (Figure 1.6). The C1 region of PKC has been shown to consist of one or two copies of a cysteine-rich domain that bind phorbol esters and diacylglycerol in a phospholipid and zinc-dependant manner. Chimaerin was the first non-PKC protein to be shown to bear a C1 domain and bind phorbol ester (Ahmed et al, 1990). Subsequently the C1 domain has been identified in other proteins including RasGRP, a GEF for Ras that links diacylglycerol binding with activation of Ras GTPases (Lorenzo et al, 2001), and protein kinase D (PKD), a protein involved in signal transduction and important biological functions including cell survival, proliferation and differentiation (Chen et al, 2008; Rozengurt et al, 2005).

The GAP domain of α2-chimaerin mediates its Rac1 GAP activity.

The conserved Rho-GAP domain of α2-chimaerin is composed of seven alpha helices and mediates its Rac1-specific GAP activity. The GAP domain of GTPase Activating Proteins is responsible for the enhanced hydrolysis of the GTP molecule to GDP and inorganic Pi by Rho GTPases. This offers a level of control over the activation state of the Rho family of small GTPases that transduce signals from plasma membrane receptors and regulate cytoskeletal dynamics. Chimaerin stimulates the intrinsic GTPase activity of Rac and promotes the inactive (GDP bound) Rac conformation. Rendering the GAP domain inactive by mutation inhibits the growth cone collapse induced via the Sema3A pathway indicating the importance of the Rac GAP activity on the signalling role of α2-chimaerin in neural retraction (Brown et al, 2004). The

GAP domain of α2-chimaerin is also responsible for its association with cyclin-dependent kinase 5 (Cdk5) and its activator p35, that mediate CRMP-2 phosphorylation as part of the Sema3A pathway (Brown et al, 2004).

A structural study on β2-chimaerin revealed that the C1 residues involved in DAG phorbol ester binding are buried in the tertiary structure and form intermolecular interactions (Canagarajah et al, 2004). This suggests that intermolecular contacts compete with phospholipids for binding on the C1 domain while activation of β2-chimaerin would cause a large conformational change in the protein. The current model of chimaerin activation proposes a conformational opening of the structure upon interaction of basic residues with acidic membrane phospholipids (Colón-González and Kazanietz, 2006). This releases the auto-inhibitory constraints of the N-terminal and unmasks the C1 domain enabling DAG and phospholipid binding and also GAP activity.

Figure 1.6 outlines the two main signalling pathways that α2-chimaerin has been implicated in, and signifies parallels to PKC activation by DAG upon receptor activation on the membrane. Diacylglycerol is an activator of both PKC and chimaerins, through interaction with related C1 domains in both proteins. Protein kinase C phosphorylation of multiple substrates including MARCKS, GAP-43 and kinases can influence neuronal development (Ramakers et al, 1999; Girard and Kuo, 1990). Furthermore PKC phosphorylation as a regulator of β2-chimaerin has recently been reported (Griner et al 2010).

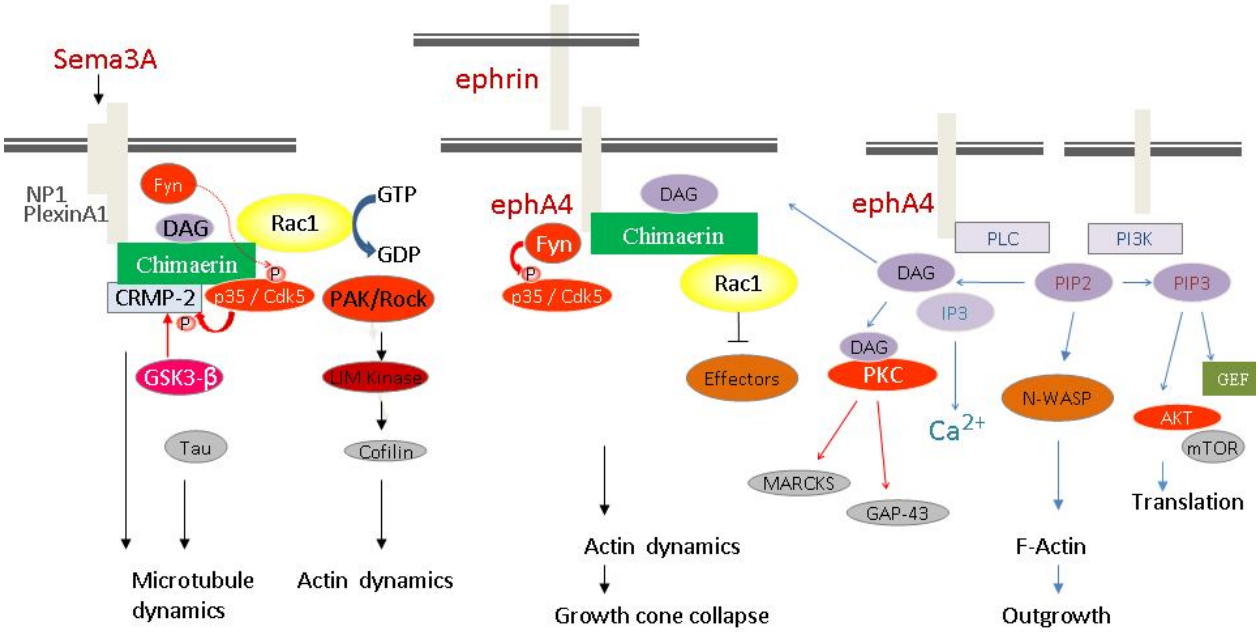

Figure 1.6 Signalling pathways of α2-Chimaerin, lipid activation and PKC.
α2-Chimaerin is implicated in Sema 3A signalling through its interaction with CRMP-2 and p35/Cdk5, via the SH2 and GAP domains respectively and may be part of the Plexin A receptor complex (Brown et al, 2004). Cdk5 phosphorylates CRMP-2, priming for phosphorylation by GSK3β, a further component of Sema 3A signalling (Brown et al, 2004; Eickholt et al 2003). Inactivating mutations of α2-chimaerin GAP domain and SH2 domain inhibit growth cone collapse while Rac1 is an essential component of this pathway (Jin and Strittmater 1997; Brown et al 2004). Cdk5 is itself activated by Fyn phosphorylation of Cdk5Y15 (Sasaki et al 2002). Kinases such as ROCK and PAK modulate actin regulatory proteins downstream of Rac1 activation. α2-Chimaerin was also identified as a key component of EphA4 forward signalling involving Cdk5 and Fyn activation, and mediating growth cone collapse (Fu et al 2007; Shi et al 2007). In tyrosine receptor kinase signalling, phospholipase C is also activated, generating DAG and IP3 (which mobilizes Ca^{2+}) from PIP2. PKC is activated by DAG and can phosphorylate many substrates affecting axonal growth cone development. PIP2 is also an activator of actin regulatory proteins including N-WASP and IRSp53 that rearrange the actin cytoskeleton and modulate outgrowth of neuronal processes.

Novel interacting partners for α2-chimaerin

Research has granted α2-chimaerin with an array of interacting factors mediating morphogenetic effects in diverge signalling pathways. It associates with Rac1 via its GAP domain and mediates down-regulation of Rac1 activity. α2-Chimaerin associates with CRMP-2 through its SH2 domain and with Cdk5/p35 through its GAP domain mediating growth cone collapse in the Sema3A pathway (Brown et al, 2004). It also associates with Plexin A, a protein part of the Sema 3A receptor (Brown et al, 2004). Recently, α2-chimaerin was reported to associate with the EphA4 receptor mediating motor neurone growth cone extension control via the ephrin-B3/EphA4 signalling pathway (Wegmeyer et al, 2007; Beg et al, 2007; Iwasato et al, 2007; Shi et al, 2007). Research is increasingly supporting that chimaerins play important roles in diverge biological processes and a search for novel interacting partners for these multi-functional proteins is of high scientific interest. A yeast two-hybrid screen in our lab has recently identified the N5-glutamine methyltransferase HemK1 as a possible interacting partner for α2-chimaerin. The interaction of the little studied N5-glutamine methyltransferase HemK1 with α2-chimaerin is the subject of this study.

N5-glutamine methyltransferases

HemK/PrmC family of proteins and their role in translation termination

The function of HemK or PrmC has been misidentified twice in literature. The *hemK* gene encoding for the bacterial HemK homologue was first identified in *E.coli* as a member of the *hem* family of genes that encode enzymes involved in the biosynthesis of heme (Nakayashiki et al, 1995). *HemK* was initially thought to be involved in the oxidation of protoporphyrinogen, a function that was questioned when in 1999 Guen and colleagues published data of yeast phenotypic analyses and enzyme activity measurements that failed to suggest a direct involvement of HemK in the heme biosynthetic pathway (Guen et al, 1999). Sequence analysis of HemK identified the catalytic motif NPPY initially thought to be restricted to cytosine N4 and adenine N6 DNA methylases. This suggested a possible S-adenosyl-L-methionine (SAM/AdoMet) dependent DNA methyltransferase activity for the HemK1 homolog in yeast (Bujnicki and Radlinska, 1999). However no evidence has ever been published that HemK can methylate DNA.

Homologues of the bacterial HemK are found in eukaryotes including yeast, fly, mouse and humans, suggesting an important biological role for the ubiquitously expressed protein (Heurgué-Hamard et al, 2002). The HemK family of proteins has been characterised as a methyltransferase involved in translation termination by modifying the glutamine residue of the conserved GGQ motif of polypeptide chain release factors. HemK has been shown to be important for the correct translation termination mediated via the release factors.

HemK in Prokaryotes

In *E.coli* the HemK gene lies in the *hemA-prfA-hemK* operon where *prfA* encodes for polypeptide chain release factor 1 (RF1). In two studies published in the same year the bacterial HemK (PrmC) was found to methylate the two polypeptide chain Release Factor proteins RF1 and RF2, on the glutamine residue of a highly conserved GGQ motif *in vitro* (Nakahigashi et al, 2002; Heurgué-Hamard et al, 2002). HemK was also

shown to be required for the methylation of RF1 in the tryptic fragment containing the GGQ in RF1 *in vivo*. Furthermore Nakahigashi and colleagues showed an increased read-through rate of UAG and UGA stop codons recognised by RF1 and RF2 respectively during protein translation in *hemK* knock-out *E. coli* K12 derivative strains, as well as an impaired growth of the cells and a global shift of gene expression to anaerobic respiration (Nakahigashi et al, 2002). HemK inactivation reduces the specific termination activity of RF1 and RF2 by approximately 3 to 4 fold in *E.coli* K12 strain (Mora et al, 2007). The growth defects of *hemK* knock-out in K12 strain *E.coli* are suppressed by recombinant HemK of *Chlamydia Trachomatis* origin whose ability to methylate release factors within the tryptic fragment containing the GGQ motif has also been shown in vivo (Pannekoek et al, 2005). Similarly the growth defects of a HemK deletion mutant in *E.coli* were complemented by a predicted HemK homologue in *Porphyromonas gingivalis* (Kusaba et al, 2003).

The name PrmC was proposed for the N5-glutamine methyltransferase HemK in the light of the two previously identified methyltransferases PrmA and PrmB that are close orthologues of HemK and are involved in translation (Heurgué-Hamard et al, 2002). PrmA methylates the large ribosomal subunit L11 in bacteria and this modification affects translation accuracy by modulating nonsense suppression at specific stop codons (Colson et al, 1979; Vanet et al, 1994; Bouakaz et al, 2006). PrmB has been shown to methylate the L3 ribosomal subunit that is believed to play a role in coordinating the binding of elongation factors during translation (Colson et al, 1979; Heurgué-Hamard et al, 2002; Meskauskas and Dinman, 2007). A protein family involved in gene transcription are the protein arginine methyltransferases (PRMTs). PRMTs have been shown to methylate proteins involved in signal transduction, transcriptional regulation and RNA processing and recently have been implicated in the expression of translation elongation factor eIF4E and the synthesis of tumour suppressor protein p53 (Mowen et al, 2001; Yoshimoto et al, 2006; Scoumanne et al, 2009; Lee and Stallcup, 2009). The terms HemK and PrmC have both been used in literature.

HemK in yeast

In 2005, Heurgué-Hamard et al published their results on the *YDR140w* gene in *Saccharomyces cerevisiae*, encoding a HemK/PrmC homolog. Their findings suggest that the product of *YDR140w* gene is required for the methylation of the GGQ motif of eRF1 *in vivo* in yeast, and is necessary for optimal cell growth. This protein was able to methylate both yeast and human eRF1. The authors also propose that the substrate for the YDR140w methyltransferase is the ternary complex eRF1-eRF3-GTP (Heurgué-Hamard et al, 2005). The product of the *YDR140w* gene was later described as Mtq2p (HemK2) in yeast by Polevoda and colleagues (Polevoda et al, 2006). This study was the first to report the existence of two HemK homologues in eukaryotes that recognise different substrates. The authors show evidence that the HemK homologues Mtq1p (also termed HemK1) and Mtq2p (also termed HemK2 and Ydr140w) methylate the mitochondrial Mrf1p and the cytoplasmic Sup45p (yeast orthologue of mammalian eRF1) release factors respectively (Polevoda et al, 2006). Deletion of Mtq1 causes moderate growth defects in yeast, while deletion of Mtq2 was responsible for multiple phenotypes including sensitivity to translation fidelity antibiotics. Furthermore the deletion of Mtq1 suppressed a mitochondrial mit(-) mutation cox2-V25 containing a premature stop codon. In a further study by Heurgué-Hamard et al, methylation of eRF1 by the yeast HemK2 required the 15-kDa zinc-binding protein Ynr046w as a co-factor (Heurgué-Hamard et al, 2006).

HemK in mice

In mice a HemK2 homologue was identified as PRED28 initially (also termed N6amt1 as a putative DNA methyltransferase) which has two splice variants termed PRED28α and PRED28β that differ in a missing exon but both contain the NPPY motif (Ratel et al, 2006). The two splice variants were ubiquitously detected in the tissues examined including mouse brain and testis, with PRED28α showing higher levels to PRED28β. The two splice variants of HemK2 were reported to exist in humans too, with one of them missing the NPPY motif (Ratel et al, 2006). A later study confusingly designated the two mouse HemK2 splice variants PRED28α and PRED28β as mHemK1 and mHemK2 (Nie et al, 2009). This study confirmed the previous findings of Ratel and colleagues (Ratel et al, 2006) that the two splice

variants are found in testis and brain and that over-expressed HemK2 can localise in the cell nucleus (Nie et al, 2009). The same team also reported that a HemK2 knock-down by RNAi in mice led to a decrease in cell proliferation (Liu et al, 2009). The authors also report an association between HemK2 and polypeptide chain release factor eRF1.

HemK in human

The functions of the human HemK homologues were very recently described. A study by Ishizawa and colleagues indicated that the human mitochondrial HemK/PrmC homologue HMPrmC (HemK1) methylates the mitochondrial release factor HMRF1L (also termed mtRF1a in Soleimanpour-Lichaei et al, 2007). They show that HemK1 is targeted to mitochondria and depletion of this protein in HeLa cells leads to decreased mitochondrial translation activity in the presence of translation fidelity antibiotics (Ishizawa et al, 2008). Figaro and colleagues reported that the human HemK2 homologue can methylate both human and yeast eRF1-eRF3-GTP complexes in vitro and the catalytic subunit of human HemK2 can complement growth defects caused by deletion of Mtq2p in yeast (Figaro et al, 2008).

HemK1 and HemK2 are highly conserved in nature

Homologues of the bacterial PrmC exist in all organisms and the function of these N5-methyltransferases are conserved in yeast, mice and human (Heurgué-Hamard et al, 2002; Polevoda et al, 2006; Ratel et al, 2006; Ishizawa et al, 2008; Figaro et al, 2008). The mouse and rat gene orthologues of HemK1 show higher than 80% similarity to the human HemK1 gene that is located in chromosome 3 (http://www.genecards.org/). HemK1 is a 338 amino-acids long protein of 38.2kDa size. HemK2 is encoded in chromosome 21 in human and is predicted to be a 22.9kDa protein. Close HemK2 gene orthologues are found in chimpanzee, mouse and rat. HemK proteins share two highly conserved motifs: the catalytic motif comprised of the GxGxG sequence, and the substrate binding site of the NPPY motif (Figure 1.7). The human HemK1 and HemK2 protein sequences share only 25.7% identity, while HemK2 has two splice-variants with one of them missing the exon containing the substrate binding NPPY motif. The yeast HemK1 homologue mtq1p shares 20.6%

sequence identity with the human HemK1, while the yeast HemK2 homologue, mtq2p, share a 34.6% identity with human HemK2.

In a phylogenetic analysis the HemK homologues show their common origin through their related conserved sequences. Both HemK1 and HemK2 are highly related to their homologues in Rhesus monkey, following a similar pattern of sequence divergence through domestic cow, mouse, chicken, zebrafish and bacteria (Figure 1.8). The HemK1 yeast homologue mtq1p seems to have diverged more than HemK2 homologue mtq2p to an extent that is widely different to the HemK1 primary sequences in all tested organisms including bacteria. (Figure 1.8).

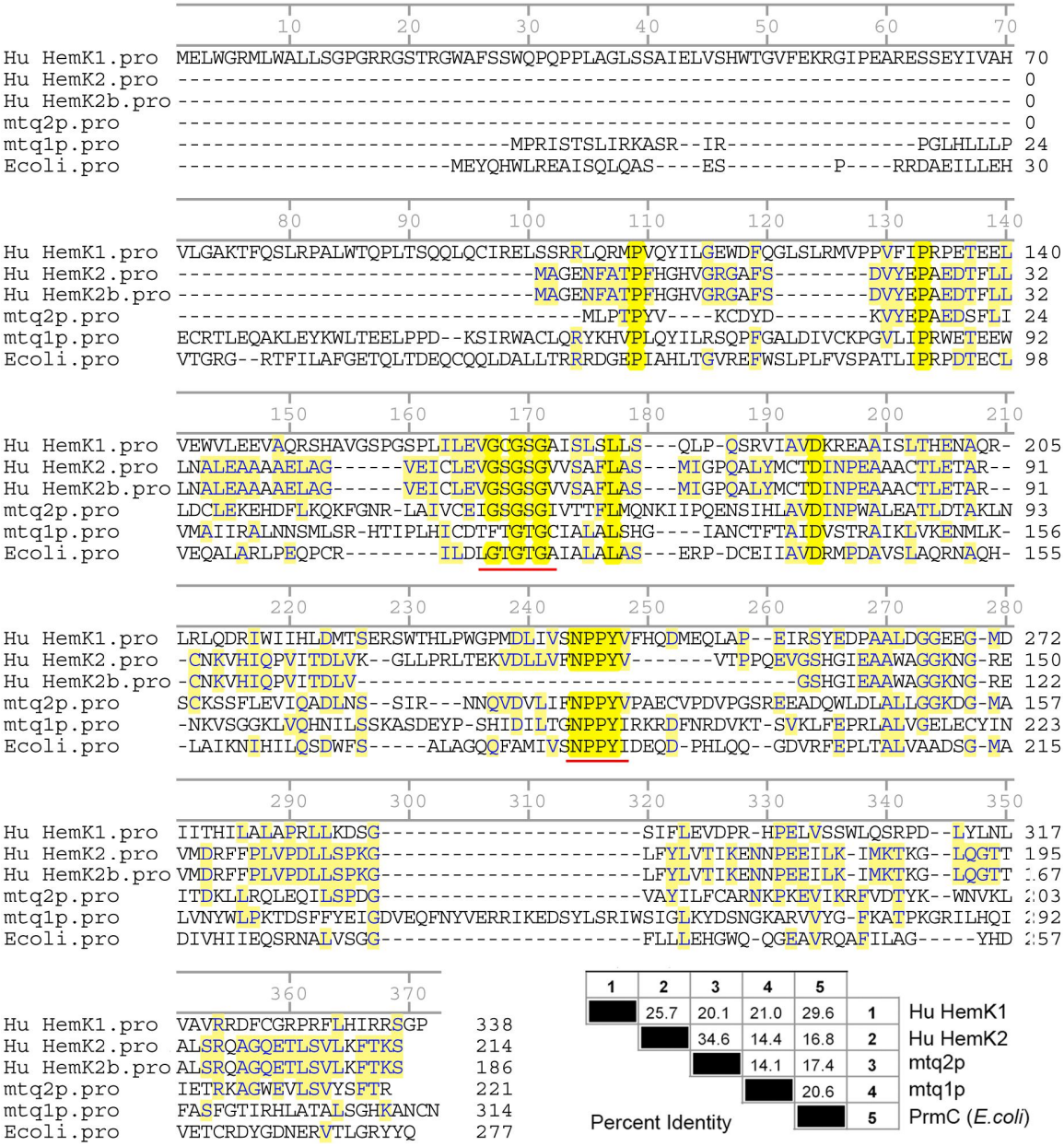

Figure 1.7 Sequence alignment of HemK homologues reveals highly conserved motifs. Primary sequences of HemK1 and HemK2 proteins in human (Hu), *Saccharomyces cerevisiae* (mtq1p and mtq2p) and *E.coli* were aligned by the Clustal W method in Lasergene MegAlign. The conserved AdoMet binding site GxGxG and the release factor binding site NPPY are underlined in red. The panel on the bottom right shows the percent identity in the protein sequences of HemK homologues.

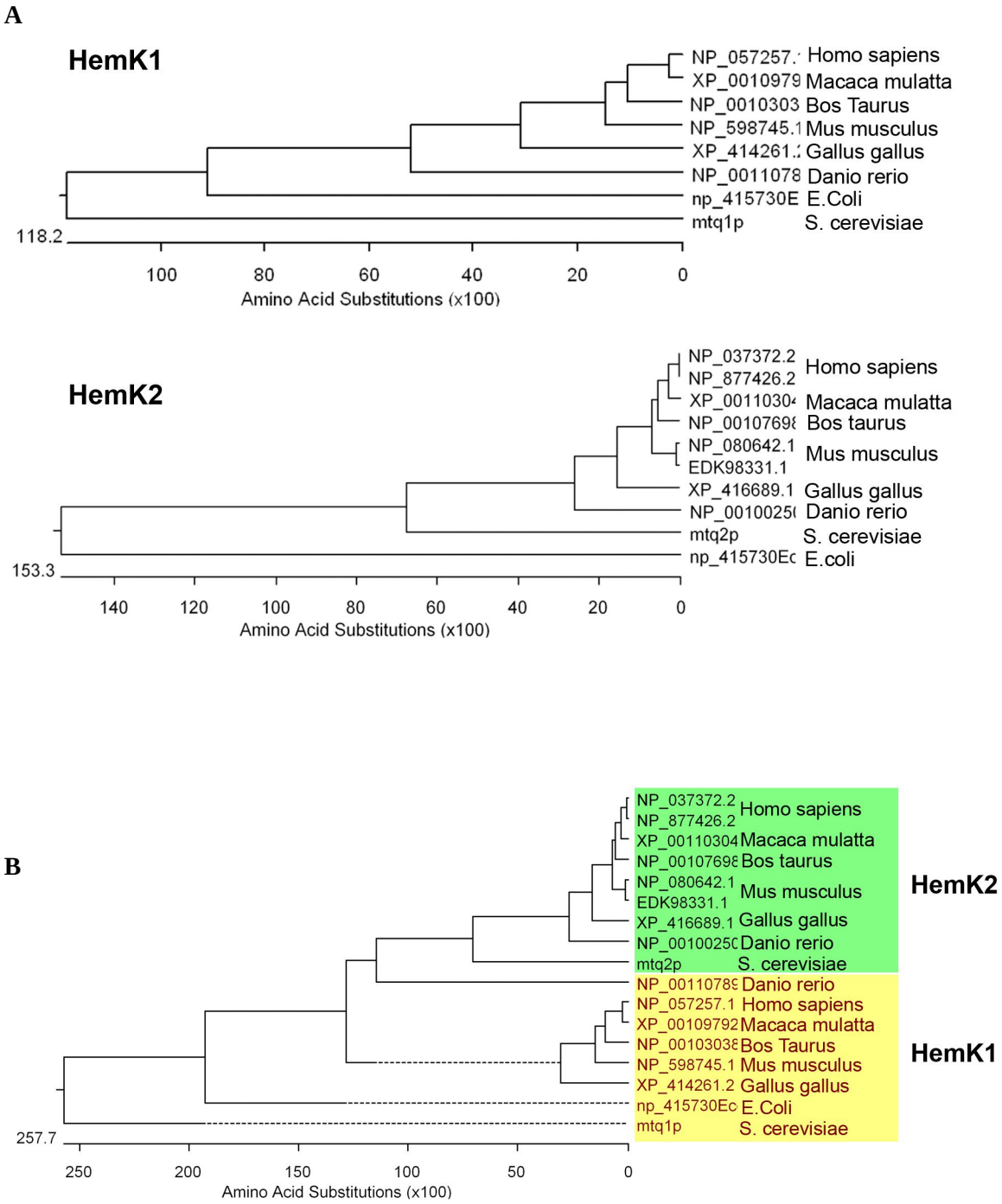

Figure 1.8 Phylogenetic analysis of HemK homologues. Phylogenetic analysis of HemK1 and HemK2 homologues in human, Rhesus monkey, cow, mouse, chicken, zebrafish, *E.*coli and *Saccharomyces cerevisiae* was performed in Lasergene Megalign. (A) Macaca mulata holds the closest relative to the human HemK1 and HemK2, while the most distant is the yeast mtq1p for HemK1 and the bacterial PrmC for HemK2. (B) The yeast HemK1 homologue mtq1p is more diverged than the bacterial PrmC when the two phylogenies are combined.

HemK/PrmC structure

Structural analyses by Schubert and colleagues described similarities in structure of the active site of HemK in *Thermotoga maritima* to that of DNA methyltransferases, namely the (D/N)PPY motif, and also suggest a common mechanism for all methyltransferases of orienting and modifying their substrates, signifying a high flexibility of these enzymes to select and modify a wide variety of substrates involving the highly conserved AdoMet-binding motif (Schubert et al, 2003). In a further study by Yang and colleagues, the structure of the E.coli HemK was found similar to that of the Thermotoga maritima consisting of two domains: a putative RF1 substrate binding domain comprised of a five helix bundle containing the NPPY motif, and a catalytic domain with a seven-stranded β-sheet that harbours the AdoMet binding sequence GxGxG (Figure 1.9) (Yang et al, 2004a). The authors describe the binding of S-adenosyl-L-homocysteine, which is the chemical that AdoMet is converted to upon donation of a methyl group, to the GxGxG motif. (Yang et al, 2004a). Furthermore an apparent hinge mobility of approximately 10°of the two domains has been described, suggesting a functional importance during substrate binding and modification (Yang et al, 2004a). Figure 1.10 shows the structure of RF1 in complex with HemK1, where the close proximity of the catalytic NPPY motif and the GGQ motif on the release factor glutamine mediates methylation that ensures efficient dissociation of the nascent peptide from the ribosome mediated by RF1. The HemK proteins mediate addition of a methyl group on the nitrogen at position 5 of glutamine, in the GGQ motif of release factors (Figure 1.11).

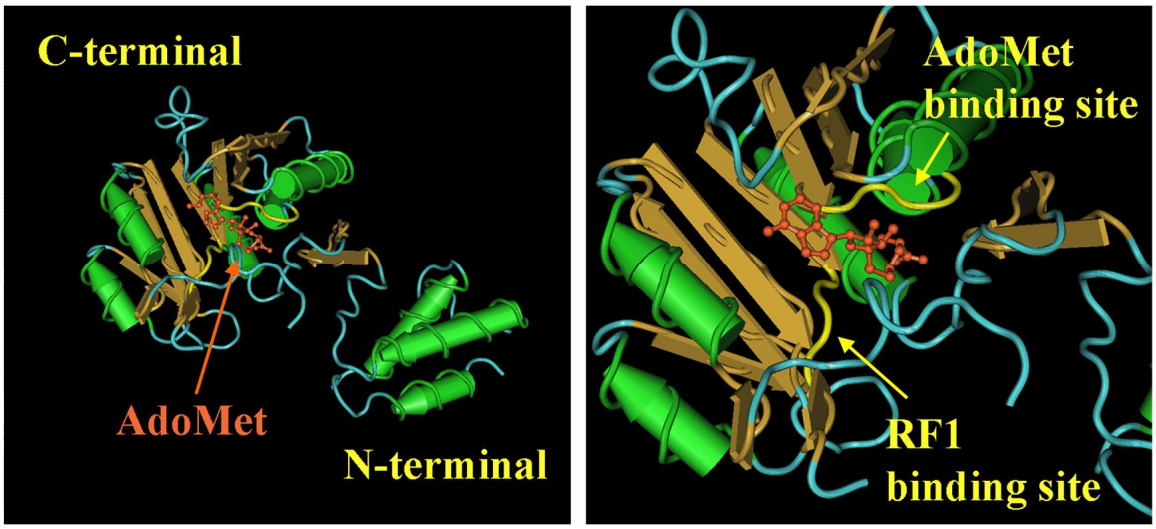

Figure 1.9 HemK1 structure. The structure of HemK1 was described in *Thermotoga maritime*. (A) The seven-stranded catalytic domain harbors the GxGxG sequence motif where AdoMet binds. (B) The substrate binding NPPY motif is in close proximity to the AdoMet binding site allowing for the addition of a methyl group on to RF1 (Schubert et al, 2003; Yang et al, 2004a) (PDB ID: 1NV9)

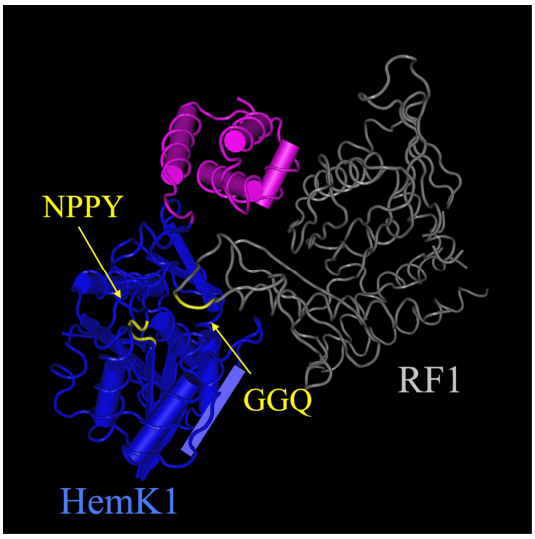

Figure 1.10 The RF1 GGQ motif comes in proximity to HemK1 NPPY motif. The glutamine side residue in RF1 GGQ motif is methylated by HemK1, and the HemK1 NPPY motif is important for this modification. The structure of RF1 in complex with HemK1 reveals a compact RF1 structure where the GGQ motif is in contact with HemK1 NPPY motif (Heurgue-Hamard et al, 2005) (PDB ID: 2B3T).

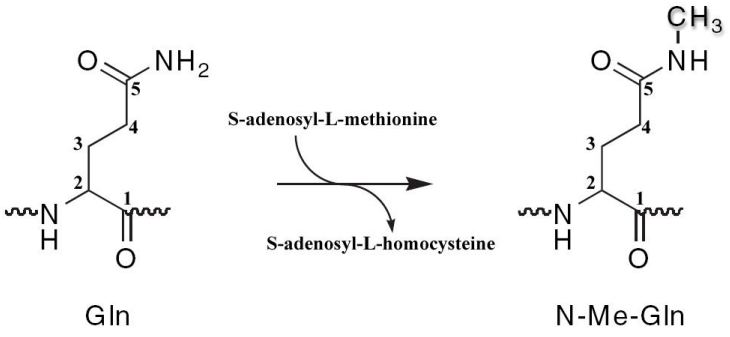

Figure 1.11 Methylation of Glutamine in the GGQ motif of release factors. The addition of a methyl group on the nitrogen at carbon 5 (N5) of the GGQ motif of release factors is mediated by the HemK proteins, mediating efficient translation termination. S-adenosyl-L-methionine is the methyl donor that is converted to S-adenosyl-L-homocycteine upon efficient methylation.

Mechanisms of Translational Control

Translation of mature mRNA into protein is the final stage of protein synthesis, and the process is scrutinised by a wide range of control mechanisms. Translation is tightly controlled from embryonic development to cell differentiation in a spatial and temporal manner, and specifically in polarised cells like neurons, the processes of localised translation provides a means of stimulus-induced local protein synthesis that takes place in the growing tips of cell processes and synapses (Twiss and Minnen, 2006; Campbell and Holt, 2001). The mechanisms of translational control can provide global control, where by modulating initiation factor acivity the translation of most mRNAs is affected, or mRNA-specific control, where factors that recognise specific elements on target mRNAs regulate their translation (reviewed in Gebauer and Hentze, 2004). Elements on mRNA that provide recognition sites for translational control complexes include the m7G cap on 5′ end and the poly(A) tail on the 3′ end that strongly promote translation initiation. Furthermore, Internal Ribosome-Entry Sequences (IRES) which mediate translation intitiation in a cap-independent manner, Upstream Open Reading Frames (uORF) which can mediate translation of the normal ORF, secondary or tertiaty RNA structures such as hairpins, and recognition sites of translation control complexes, all provide control on the translation fate of the specific mRNA (Figure 1.12) (reviewed in Gebauer and Hentze, 2004). A mature mRNA, once exported from the nucleus, can be targeted for local translation mediated by Staufen, a protein involved in microtubule-dependent transport of mRNAs (Lasko, 1999; Kloc et al, 2002). Another level of control is ordered by microRNA-mediated gene silencing, where RNA-induced silencing complexes (RISC) mediate degradation of target mRNA sequences (Liu et al, 2005). Repression of translation of specific mRNAs can be mediated by FMRP, a protein also involved in mRNA local translation (Zalfa et al, 2003). The best studied and most accredited mechanisms of translational control involve modulation of the activity of intitiation factors, eventhough control of translation elongation and termination mechanisms also constitute important processes of translational control. At the translation initiation stage, eIF2 bound to GTP delivers the Methionine-tRNA to the 40S ribosomal subunit to initiate start codon recognition, and once a start codon has been recognised eIF2-GTP is hydrolysed to eIF2-GDP and translation can commence (Figure 1.12). The

GTP/GDP binding state of eIF2 is modulated by the guanine nucleotide exchange factor eIF2B, and the phosphorylation of eIF2 by RNA-regulated protein kinase (PKR) and eIF2α kinase (PERK) (de Haro et al, 1996; Gebauer and Hentze, 2004). The formation of the closed-loop mRNA model, that is believed to occur in the initial stages of translation, is mediated by recruitment of initiation factors eIF3 and eIF4G, to form a complex with eIF4E that binds to the 5′ mRNA cap and poly(A)-binding protein PABP that binds to the poly-A 3′ end of mRNA (Gingras et al, 1999). Signaling events initiated by membrane-receptor substrate-binding can also modulate translation initiation. The stability of the 40S small ribosomal subunit is regulated by phosphorylation of ribosomal subunit S6 by S6K1, in downstream signalling events of ERK activation, upon recognition of NMDA by its specific receptor (Chiaberge et al, 1998; Banko et al, 2004). Furthermore, mTOR (Mammalian Target of Rapamycin) is activated by downstream signalling of PI3K initiated by growth factors or insulin, and phosphorylates the eIF4E-binding protein 4E-BP that allows eIF4E to join the pre-initiation complex (Figure 1.12) (Gingras et al, 2004; Foster and Fingar, 2010). The elongation stage sees the delivery of an aminoacyl-tRNA to the A site of the ribosomal complex by eEF1A-GTP, whose GTP binding is controlled by eEF1B (Andersen et al, 2001). eEF2 mediates the shift of the translation machinery to the next codon upon formation of a peptidyl-tRNA bond, and its activity is regulated by PP2A (Chung et al, 1999). Translation termination is initiated by stop codon recognition by release factors, and methylation of eRF1 by HemK mediates efficient termination and release of the newly formed peptide (Schubert et al, 2003). Upon recognition of a premature stop codon the release factors form a complex with SMG-1 and Upf1, factors involved in mRNA decay (Kashima et al, 2006).

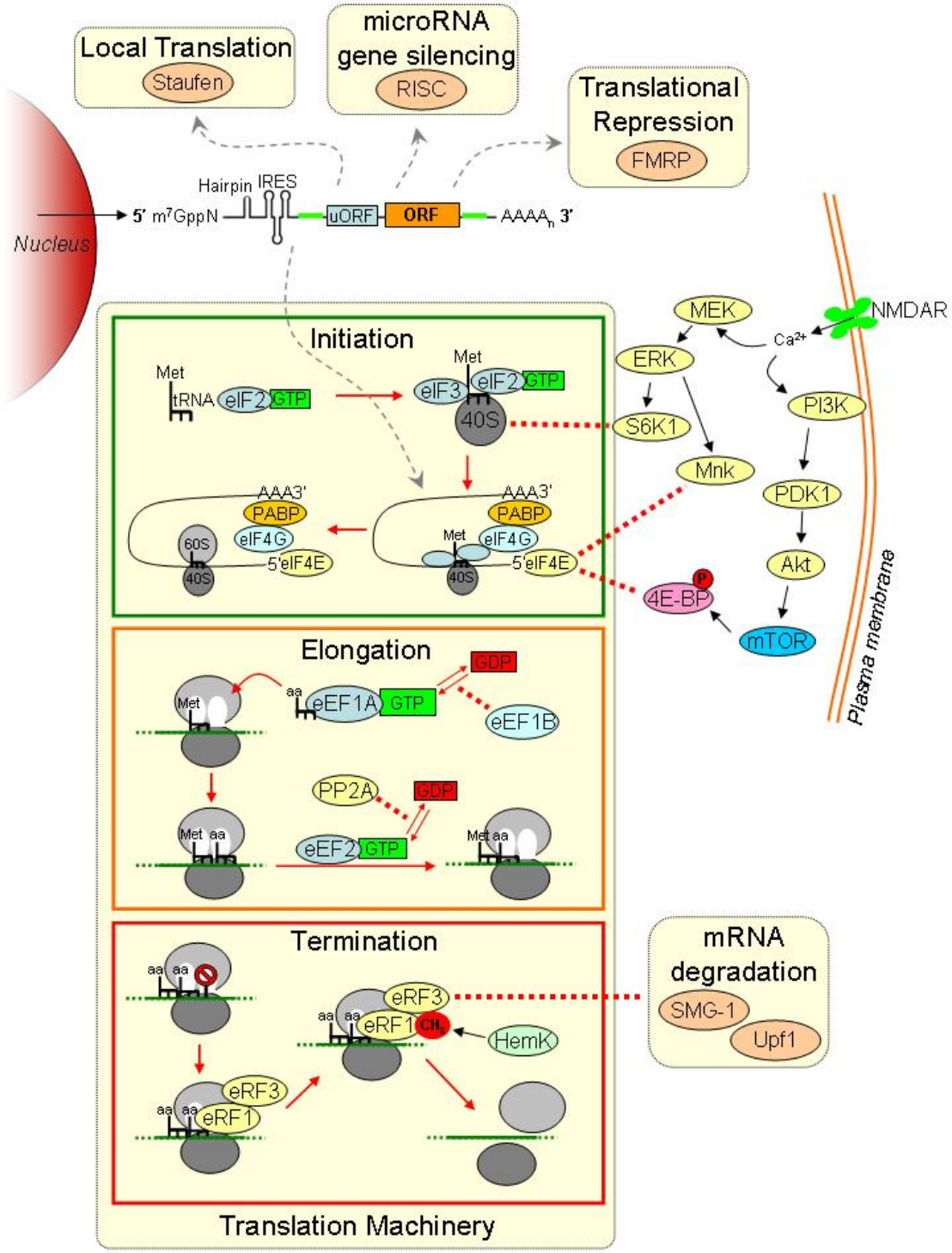

Figure 1.12 General diagram of translational control mechanisms. A wide variety of mechanisms exist that regulate the translation of mRNA into protein. Signaling cascades in response to extracellular cues mediate translation initiation, while control mechanisms also regulate elongation and termination of translation. Elements on the mRNA that can mediate translation control include secondary structures, Internal Ribosome-Entry Sequences, the m7G cap and the poly(A) tail situated on either end of the transcript. The areas in green on the depicted mRNA denote further recognition sites of factors that can modulate translation. The mRNA depicted is adapted from a review by Gebauer and Hentze (Gebauer and Hentze, 2004).

Polypeptide Chain Release Factors in Translation Termination

"DNA makes RNA makes Protein" (Crick, 1970). This has been the central dogma of molecular biology since the second half of the 20th century, and many mechanisms of this complex machinery still remain elusive. Translation, the process by which RNA is used as a template to synthesise proteins in cells is driven and also tightly controlled by a myriad of components that raise check-points for correctly synthesised proteins. Translation termination occurs when a stop codon occupies the ribosomal A site and the newly synthesised polypeptide chain is released from the P site tRNA. The decoding of stop codons and initiation of translation termination occur through release factor proteins that recognise the three almost universal trinucleotide sequences on mRNA and signal for the ultimate hydrolysis of the completed peptide chain from the ribosome. The first report on proteins regulating translation termination was published more than forty years ago (Capecchi, 1967) and even though our understanding of these processes has since greatly advanced, elucidation of the complex interactions between protein and RNA in the last stages of protein synthesis is still ongoing.

Class I Polypeptide Chain Release Factors

Two types of polypeptide chain release factor proteins have been identified as part of translation termination machinery. The class I release factors recognise the stop codons and occupy the A site of the prokaryotic 50S ribosomal subunit initiating the peptide release reaction. In bacteria there are two class I release factors: RF1 and RF2. RF1 recognises the UAA and UAG stop codons and similarly RF2 recognises UAA and UGA in mRNA (Scolnick et al, 1968). This stop codon specificity of RF1 and RF2 arises through their tripeptide motifs Proline-Alanine-Threonine and Serine-Proline-Phenylalanine respectively (Ito et al, 2000). Class I RFs cause polypeptide chain release by preventing peptidyl transferase from adding amino acids to the chain and triggering hydrolysis of the bond between peptide chain and tRNA.

In eukaryotic organisms there is only one class I release factor, eRF1 that recognises all three stop codons (Konecki et al, 1977; Frovola et al, 1994). Class I release factors

in both eukaryotic and prokaryotic kingdoms share a universally conserved GGQ motif surrounded by positively charged amino acids which is located near the site of the peptidyl-tRNA ester bond that is cleaved during translation termination. This tripeptide motif is thought to be involved in translation termination but not stop codon recognition (Frovola et al, 1999). Mutation or deletion of the conserved GGQ motif abolishes peptidyl-tRNA hydrolysis induced by RF1 and therefore translation termination (Moffat and Tate, 1994; Frovola et al, 1999). This GGQ motif is methylated by HemK1 and this modification is important for efficient translation termination mediated by the release factors (Figure 1.10) (Schubert et al, 2003).

Class II Polypeptide Chain Release Factors

The class II release factors are GTPases in both prokaryotic and eukaryotic kingdoms and share distinct functions. The bacterial Class II release factor RF3 is required for the release of RF1 and RF2 after polypeptide chain release and the dissociation of the ribosomal complex (Freistroffer et al, 1997). Ribosomes in complex with RF1 or RF2 act as guanine nucleotide exchange factors (GEF) promoting the exchange of GDP for GTP on RF3 (Zavialov et al, 2001). Binding of RF3 to the ribosomal complex induces great conformational changes in both the GTPase-associated centre and the decoding centre of the ribosome that break the interactions with class I release factors and lead to their release from the translation machinery (Gao et al, 2007). The eukaryotic class II release factor eRF3 shares homology with RF3 in the GTP-binding domain. eRF1 and eRF3 form a stable complex in cells through their C-terminal domains (Stansfield et al, 1995; Ebihara and Nakamura 1999) and eRF1 acts as a GTP dissociation inhibitor on eRF3 stabilising the ternary complex GTP-eRF1-eRF3 (Pisareva et al, 2006). The interaction between the two release factors is required for eRF3 to stimulate peptide chain release mediated by eRF1 (Figure 1.13) (Alkalaeva et al, 2006).

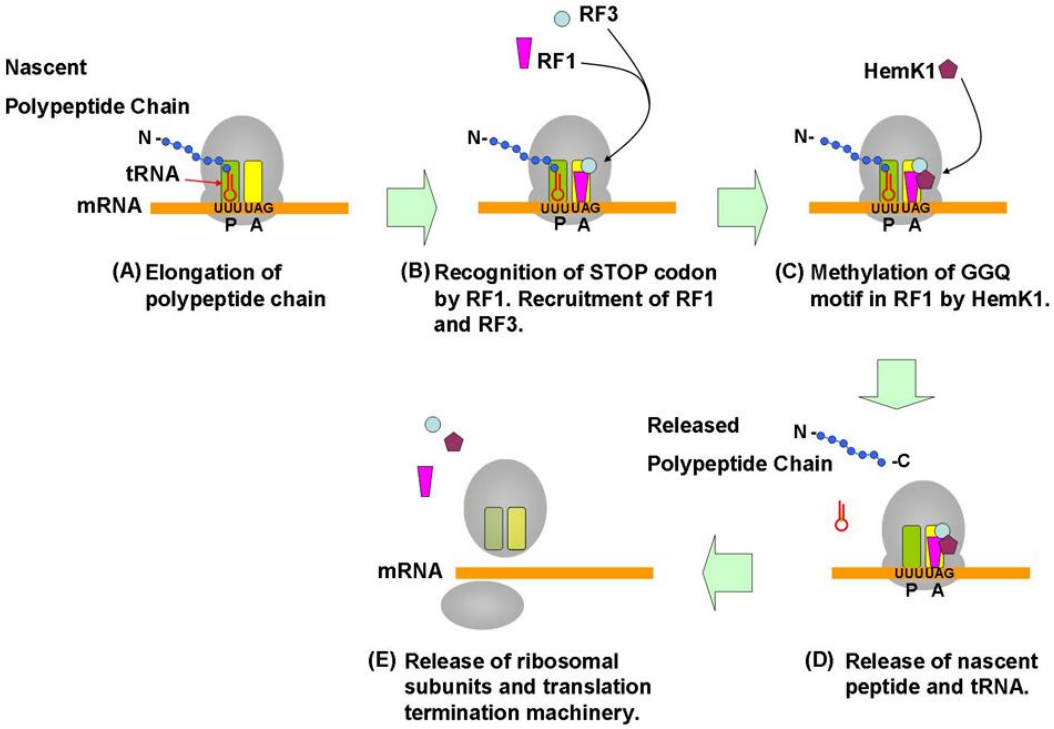

Figure 1.13 A basic model of translation termination. Normal translation termination involves the recognition of a stop codon on mRNA and recruitment of release factors RF1 and RF3 (B). HemK1 methylates RF1 in the conserved GGQ motif (C) and mediates the release of the synthesized peptide and tRNA (D). The final stage sees the dissociation of the ribosomal subunits and the translation termination machinery (E).

Mitochondrial Polypeptide Chain Release Factors

In mitochondria the metabolic process of oxidative phosphorylation produces the required ATP for the cell to maintain life. Thirteen of the proteins that are important for this process are encoded by the mitochondrial genome (Anderson et al, 1981). The process of mitochondrial protein translation is not fully understood and data so far suggest that it employs a distinct translation machinery. Factors involved in mitochondrial protein synthesis are encoded by nuclear genes that have been related to human diseases through pathological mutations that could affect the mitochondrial peptide translation system (Jacobs and Turnbull, 2005; Valente el at, 2007). Translation in mitochondria employs a different codon recognition system to the universally standard code of prokaryotes and eukaryotes that seems to differ between organisms (Elzanowski and Ostell, 2008). The decoding of AUA as methionine and the universal stop codon UGA as tryptophan is found in but not restricted to human mitochondria (Barrell et al, 1979; Elzanowski and Ostell, 2008). Soleimanpour-Lichaei and colleagues identified the release factor mtRF1a in human mitochondria that shows sequence similarity to many other release factors and also retains the universally conserved GGQ motif (Soleimanpour-Lichaei et al, 2007). The authors show that mtRF1a is targeted to mitochondria and is capable of terminating translation termination at stop codons UAA and UAG but not UGA, both *in vivo* and *in vitro*. Finally depletion of mtRF1a in HeLa cells caused growth defects and led to elevation of reactive oxygen species production. In a similar study mtRF1a was renamed HMRF1L and the authors presented results that are in accordance with the previous study (Nozaki et al, 2008).

Polypeptide Chain Release Factors in RNA degradation

In eukaryotic organisms protein expression is tightly regulated by mRNA quality check-points that ensure translation of functioning peptides. Before mRNA is exported from the nucleus it undergoes post-transcriptional modifications that include the removal of introns and the addition of a poly(A) tail on the 3′ end. The fate of mature mRNA is decided upon exiting the nucleus where it can be a) immediately

translated, b) maintained in a translationally repressed state, c) transferred to a specific cellular location to be translated, or d) degraded. Translational repression and mRNA degradation can be directed by specific RNA binding proteins and also by small complementary RNAs (miRNAs) that eventually target mRNA for degradation. A number of the factors involved in mRNA surveillance, degradation and translation repression are found in the cytoplasm localising in cytoplasmic foci described as mRNA processing bodies (P-bodies) and stress granules.

Besides their role in mediating translation termination, the eukaryotic polypeptide chain release factors eRF1 and eRF3 are also involved in normal and nonsense-mediated mRNA decay (NMD) through its association with certain mRNA processing factors. eRF3 associates with the poly(A)-binding protein (PABP) that mediates mRNA stability and also with DCP1 (mRNA decapping protein 1) that removes the 5′ mRNA cap prior to degradation. eRF1 and eRF3 can also exist in a complex with the nonsense mediated mRNA decay proteins Upf1 and SMG1.

General mRNA decay mechanism

The stability of mRNA in the cytoplasm is sustained by its 5′ N7-methyl guanosine (m7G) cap. The m7G cap protects mRNA from 5′→3′ degradation and offers control over translation in the cytoplasm (Cougot et al, 2004a). Stability of the transcript and translation is mediated through the interaction of the eukaryotic initiation factor complex eIF4F with the mRNA cap and with the poly(A)-binding protein (PABP) that resides on the poly(A) tail of the message. The components of the eIF4F complex, the eukaryotic initiation factors eIF4E and eIF4G associate with the 5′ cap and PABP respectively (Cougot et al, 2004a; Amrani et al, 2008). RNA degradation is initiated by deadenylation, where the poly(A) tail of mRNA is removed by specific deadenylase complexes. eRF3 interacts with PABP via its N-terminal domain and it regulates the initiation of deadenylation and normal mRNA decay through this association that is conserved from yeast to humans (Hoshino et al, 1999; Hosoda et al, 2003). Furthermore eRF3 has been shown to exist in a complex with the initiation factor eIF4G through PABP suggesting a role in ribosome recycling taking place upon translation termination (Uchida et al, 2002). Following deadenylation the mRNA can be degraded by either 3′→5′ exonucleolytic digestion catalysed by the exosome

whose activity is regulated by the SK1 complex, or by 5′→3′ digestion that requires the removal of the 5′ cap. Removal of the 5′ cap halts translation and targets the mRNA for degradation (Eulalio et al, 2007a). The mRNA decapping proteins DCP1 and DCP2 have been shown to be responsible for decapping the messenger RNA prior to degradation. Removal of the 5′ mRNA cap structure allows XRN1 to proceed with exonucleolytic degradation of the mRNA. In yeast DCP2 interacts with DCP1 and this interaction is required for decapping *in vivo* and *in vitro* (Dunckley and Parker, 1999; Sakuno et al, 2004; She et al, 2008). DCP1 also binds the release factor eRF3 in yeast (Kofuji et al, 2006). In human there is one DCP2 homologue and two DCP1 homologue proteins, hDcp1a and hDcp1b. While hDcp1a, hDcp1b and hDcp2 have been shown to localise in mRNA processing bodies (Cougot et al, 2004b; van Dijk et al, 2002), hDcp1a and hDcp2 have also been shown to associate with the nonsense mediated mRNA decay protein Upf1 (Cho et al, 2009; Lykke-Andersen, 2002). This suggests that mRNA decapping factors may be recruited by the mRNA surveillance complex at premature translation-termination sites as part of nonsense mediated mRNA decay. The majority of the proteins involved in 5′→3′ mRNA decay localise in P-bodies.

Nonsense-mediated mRNA decay

In eukaryotes the nonsense-mediated mRNA decay (NMD) is a mechanism that is highly conserved through evolution. NMD ensures that mRNAs that feature a premature termination codon are degraded (Figure 1.14) (Conti and Izaurralde, 2005; Isken and Maquat, 2007). Premature termination codons in mRNA translation result in the production of non-functioning and potentially toxic proteins. Approximately 30% of disease-linked mutations generate premature termination codons, and mutations in the factors involved in NMD resulting in abnormal function of the mRNA degradation pathway have been implicated in human disease highlighting the medical significance of this process (Tarpey et al, 2007; Holbrook et al, 2004). Furthermore recent studies have suggested that NMD may constitute a translation-dependent post-transcriptional control mechanism for gene expression, as non-aberrant mRNAs have been reported substrates for this mRNA decay pathway (reviewed in Stalder and Mühlemann, 2008). This is also supported by the observation that approximately one third of alternatively spliced transcripts contain a premature

termination codon, while as much as 95% of multi-exon genes undergo alternative splicing in human (Lewis et al, 2003; Pan et al, 2008). These observations suggest a wider role of NMD in gene expression control beyond aberrant transcript degradation.

The factors involved in NMD comprise the so called mRNA surveillance complex that is recruited upon recognition of a nonsense termination codon, and include the proteins UPF1, UPF2 and UPF3 that are conserved from yeast to humans and the effectors SMG-1, SMG-5, SMG-6 and SMG-7 (Conti and Izaurralde, 2005; He et al, 1997). The process of mRNA intron splicing sees the deposition of a protein complex 20-24 nucleotides upstream of the splice junction called the exon junction complex (EJC) (Kataoke et al, 2000; Hir et al, 2000). In mammals UPF3 is a component of the EJC interacting with the EJC core factor Y14 (Kim et al, 2001). UPF2 binds directly to UPF3 in yeast (Weng et al, 1996) and mammals (Lykke-Andersen et al, 2000) and recruits the RNA helicase UPF1 to the EJC. UPF1 binds to eRF1 and eRF3 and is phosphorylated by the phosphatidylinositol 3-kinase-related protein kinase SMG1 kinase upon premature translation termination, in a complex described as SMG-1–Upf1–eRF1–eRF3 (SURF) (Kashima et al, 2006). SMG-1 is thought to be recruited to the NMD machinery by the recently discovered SMG-8, while its kinase activity is modulated by SMG-8 and SMG-9, two protein components of the SMG-1 complex (Yamashita et al, 2009). A kinase-deficient point mutant of SMG-1 suppressed premature termination codon dependent mRNA degradation, while wild type SMG-1 enhanced it in experiments by Yamashita and colleagues (Yamashita et al, 2001) indicating the importance of UPF1 phosphorylation by SMG-1 in NMD. In fact a later study described that phosphorylation of UPF1 by SMG-1 induces an association with SMG-5 and SMG-7 that eventually lead to its dephosphorylation, suggesting a important role of the UPF1 phosphorylation/dephosphorylation cycle in remodeling of the mRNA surveillance complex and NMD (Ohnishi et al, 2003).

The association of the yeast eRF3 orthologue with poly(A)-binding protein (PABP) is important for the dissociation of the terminating ribosome from mRNA (Amrani et al, 2004). In recent experiments mammalian cells not expressing PABP exhibited increased read-through of termination codons (Ivanov et al, 2008). The association between eRF3 and PABP is antagonised by UPF1 in the case of premature termination codons resulting in NMD (Singh et al, 2008). In fact when PABP is

tethered downstream of a premature termination codon it abolishes NMD (Silva et al, 2008). A recent study suggested that binding of the GTP to the eRF1-eRF3 complex accompanies major structural rearrangements upon the formation of the eRF1-eRF3-GTP complex, and this is essential for the association of eRF3 with PABP (Kononenko et al, 2009).

Figure 1.14 Premature translation termination and nonsense-mediated mRNA decay. Translation of an mRNA transcript (step 1) leads to recognition of a premature stop codon by eRF1 and eRF3 that recruit Upf1 (step 2). UPF1 recruits SMG-1 which together with eRF1 and eRF3 form the SURF complex (step3). The SURF complex interacts with the exon junction complex downstream (step 3) and this association leads to phosphorylation of UPF1 by SMG-1 (step 4). Translation termination sees the dissociation of release factors and the 40S and 60S ribosomal subunits (step 5). Recruitment of SMG-5 and SMG-7 by UPF1 leads to dephosphorylation of UPF1 and this may lead to dissociation of SMG-5 and SMG-7, and loss of the m7G mRNA cap mediated by decapping enzyme Dcp1 (step 7). mRNA not protected by the m7G cap is rapidly degraded by the 5′→3′ exonuclease Xrn (step 8).

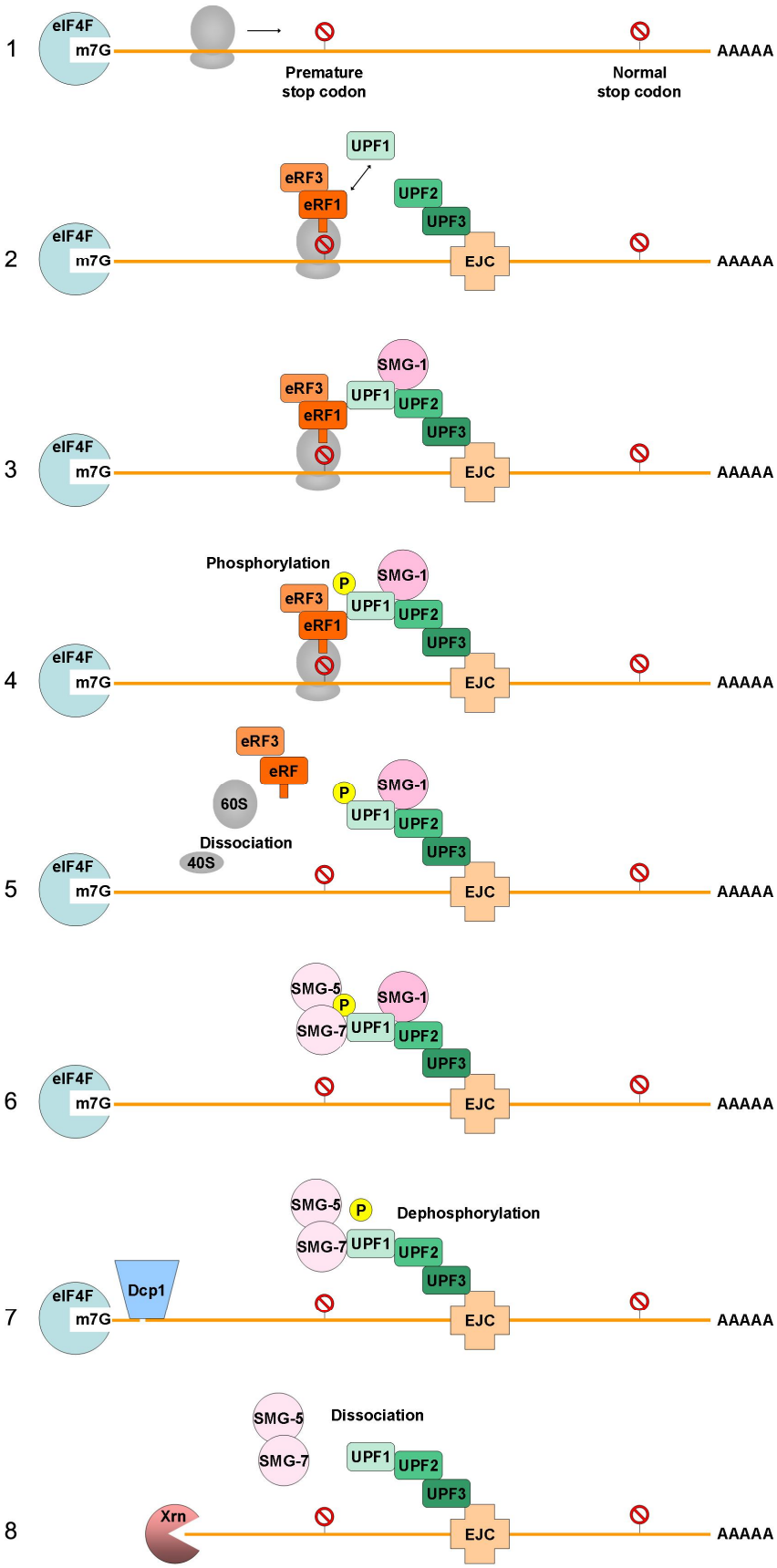
1
eIF4F
m7G
AAAAA
Premature
stop codon
Normal
stop codon
2
UPF1
eRF3
eRF1
UPF2
UPF3
EJC
3
SMG-1
4
Phosphorylation
P
5
eRF
60S
Dissociation
40S
6
SMG-5
SMG-7
7
Dcp1
Dephosphorylation
8
Xrn

Staufen and its role in mRNA processing

Staufen is an mRNA binding protein that is principally known to be involved in the transport of mRNAs to achieve their localised translation (Johnston et al, 1991; Ferrandon et al, 1994; Wickham et al, 1999; Kim-Ha et al, 1995). Staufen was initially described in *Drosophila* oocytes, where it was found to localise in granules involved in microtubule-dependent localisation of maternal mRNAs (Lasko, 1999; Kloc et al, 2002).

In mammals the two homologues Staufen1 and Staufen2 are components of ribonucleoprotein complexes that travel along microtubules from the cell soma to the dendrites (Vessey et al, 2008). Staufen1 is ubiquitously expressed in human tissues and is involved in translation control and mRNA decay (Kim et al, 2005, Kim et al, 2007). In human Staufen2 is primarily found in neuronal cells where it is involved in mRNA transport and dendritic spine morphogenesis (Goetze et al, 2006; Tang et al, 2001b). Human Staufen1 has been shown to localise in RNA granules together with ribosomes, the proteins PABP1 and FMRP that are involved in protein synthesis, cytoskeletal proteins tubulin and actin as well as Rac1, Cdc42 and IQGAP1 (Villacé et al, 2004). These Staufen1 RNA granules were found to localise in the dendrites of differentiated neuroblasts supporting a role of Staufen1 in mRNA transport and localised translation control (Villacé et al, 2004). Mammalian Staufen1 has also been shown to enhance translation in experiments of translationally repressed mRNAs (Dugré-Brisson et al, 2005). It was suggested that Staufen1 can facilitate translation of mRNAs by associating with their 5′ end. Staufen has also been found to localise in stress granules in rodent oligodendrocytes upon oxidative stress (Thomas et al, 2005). It has become evident that Staufen can exist in a number of different ribonucleoprotein complexes localising in different mRNA granules, and this is considered an important attribute for mediating its multiple functions (Dahm et al, 2008).

A mammalian mRNA decay mechanism responsible for degrading mRNAs that feature a stop codon upstream of a Staufen1 (STAU1) binding site (SBS) is the Staufen1-mediated mRNA decay pathway (SMD) (Kim et al, 2005; Kim et al, 2007). When translation terminates sufficiently upstream of a SBS, the dsRNA binding protein Staufen1 recruits Upf1 to the SBS triggering the SMD pathway (Kim et al,

2005; Kim et al, 2007). In NMD Upf1 is recruited to an exon-junction complex by Upf2 triggering the RNA decay mechanism (Lykke-Andersen et al, 2000). In a recent study it was shown that the NMD and SMD mechanisms are in fact competitive pathways (Gong et al, 2009). The sites on Upf1 where Staufen1 and Upf2 bind overlap, suggesting that the association of the two proteins with Upf1 is mutually exclusive. Furthermore, inhibition of SMD by down-regulating Staufen1 cellular abundance increases the efficiency of NMD, and similarly SMD efficiency is increased when NMD is inhibited by down-regulating Upf1 abundance. Therefore it appears that there is a balance between the NMD and SMD pathways in translation termination-dependent mRNA degradation (Gong et al, 2009).

In recent studies Staufen1 has been implicated in dendrite development and synapse formation in neurones. In experiments in mice a Staufen1 loss of function allele caused significant decrease in Staufen1-containing ribonucleoprotein particles delivered down the dendrites of cultured hippocampal neurones (Vessey et al, 2008). Furthermore it was demonstrated that cultured hippocampal neurones from mice lacking Staufen1 showed deficits in dendritic length and branching during development, and exhibited fewer synapses (Vessey et al, 2008). Staufen1 was also shown to be important for long-term potentiation in hippocampal synapses suggesting a role in maintaining synaptic efficacy (Lebeau et al, 2008). The emerging involvement of Staufen1 in dendritic spine morphogenesis is in parallel with its homologue Staufen2 that is expressed mainly in the brain and plays a role in the dendritic development (Goetze et al, 2006).

RNA processing bodies (P-bodies)

The RNA processing bodies (P-bodies / Dcp bodies / GW bodies) are discrete cytoplasmic domains that contain proteins involved in mRNA degradation, mRNA surveillance, translational repression and RNA-mediated gene silencing along with their substrate mRNAs (Eulalio et al, 2007a). P-bodies were first discovered with the observation that the mRNA decapping enzymes Dcp1 and Dcp2 involved in NMD localise in specific cytoplasmic foci (van Dijk et al, 2002). Exogenously expressed

human Dcp1a and Dcp1b localise in the cytoplasm, nearly exclusively concentrated in bright foci (Cougot et al, 2004b). Subsequently the proteins Lsm1-7 and Xrn1 that are also involved in mRNA degradation were found to localise in cytoplasmic foci containing Dcp1 and Dcp2. (Ingelfinger et al, 2002). Another component of P-bodies is the conserved family of GW182 proteins that associate with the miRNA-induced silencing complex and have been shown to be crucial factors in microRNA-mediated gene silencing (Ding et al, 2007). GW182 co-localises in ribonucleoprotein P-body cores with Dcp1 and Lsm4 (Eystathioy et al, 2003) and is important for maintaining P-bodies stability during the cell cycle (Yang et al, 2004b). Moreover, shRNA targeting of GW182 and Lsm1 and 4 inhibits the assembly of P-bodies (Ohn et al, 2008) while cells induced to proliferate show an incremental expression of GW182 and larger as well as more numerous P-bodies (Yang et al, 2004b).

Translational inhibitors are known to stabilise mRNA and therefore down-regulate mRNA degradation pathways (Jacobson and Peltz, 1996). When mRNA decay is inhibited by treatment with the translation inhibitor cycloheximide the P-bodies disappear indicating that they are sites of active mRNA decay (Cougot et al, 2004b). Furthermore blocking P-body assembly does not inhibit mRNA degradation, indicating that proteins of the mRNA degradation machinery are fully competent even when not recruited in P-bodies (Eulalio et al, 2007b). Therefore P-bodies may also function as sites of mRNA storage, harbouring untranslated mRNAs awaiting for the decay machinery, and thus regulating translational silencing (Parker and Sheth, 2007; Franks and Lykke-Andersen, 2007). While arsenite treatment can induce P-body assembly in a signalling pathway distinct to that of stress granule induction, the stress-induced P-body assembly mechanism still remains elusive (Ohn et al, 2008).

P-bodies have also been visualised in neuronal cells. Dcp1a containing P-bodies have been shown to assemble in the soma and dendrites of mammalian neurones, while they can also relocate to distant sites in response to synaptic activation (Cougot et al, 2008). While these foci are heterogeneous compared to the non-neuronal P-bodies, they were positive for GW182 and other P-body markers. These P-bodies observed in hippocampal neurones may mediate local translation in dendrites by storing translationally repressed ribonucleoprotein complexes and releasing them upon synaptic activation (Cougot et al, 2008). In *Drosophila* neurones, P-body-like

ribonucleoprotein particles have been visualised containing Dcp1, Xrn1, Upf1 as well as FMRP (Barbee et al, 2006). Another conserved P-body protein, Me31B, is present in staufen-containing neuronal ribonucleoprotein complexes and has been shown to be required for dendrite morphogenesis and microRNA-mediated gene silencing *in vivo* while also regulating P-body assembly in the Drosophila wing disk (Hillebrand et al, 2007). These emerging studies indicate an important role of neuronal P-body proteins in the regulation of dendrite localised mRNAs and synaptic plasticity.

Stress Granules

Stress granules are ribonucleoprotein granules compositionally related to P-bodies (Anderson and Kedersha, 2006). Stress granules are non-membranous cytoplasmic foci whose assembly is triggered by a variety of environmental stresses, including oxidative stress, heat shock, hyperosmolarity and viral infection (Anderson and Kedersha, 2009). Stress-induced translation arrest sees mRNAs encoding constitutively expressed "housekeeping" genes being redirected from polysomes to stress granules (Kedersha et al, 2005). Pharmacological studies have indicated that polysome stability and stress granule assembly are in a dynamic equilibrium (Kedersha et al, 2000). Treating cells with polysome stabilising drugs like cycloheximide inhibits the assembly of stress granules and results in stress granule disassembly under conditions of prolonged stress. In contrast, drugs like puromycin that release ribosomes from mRNAs and therefore destabilise polysomes promote stress granule assembly. (Kedersha et al, 2000). It was therefore proposed that stress granules may be the sites of mRNA triage where untranslated mRNAs accumulate during stress, and are either degraded or repackaged in ribonucleoprotein complexes to reinitiate translation (Kedersha et al, 2000).

In mammalian cells the assembly of stress granules is initiated by the phosphorylation of the translation initiation factor eIF2α, an event that inhibits translation initiation and promotes the accumulation of untranslated mRNAs (Anderson and Kedersha, 2009). Unlike P-bodies, stress granules are primarily composed of the translationally

silent 48S preinitiation complexes that contain mRNAs bound to small ribosomal subunits and translation initiation factors (Kedersha et al, 2002; Kimball et al, 2003). Stress granules also contain PABP (Kedersha et al, 1999), Xrn1 (Kedersha et al, 2005) and the mRNA binding proteins TIA-1 and TIAR that act downstream of eIF2α phosphorylation to promote stress granule assembly (Anderson and Kedersha, 2002). A protein that is required for stress granule assembly and localises in stress granules but not P-bodies is the RasGAP-associated G3BP that has a phosphorylation-dependent sequence-specific endoribonuclease activity *in vitro* (Tourrière et al, 2001; Tourrière et al, 2003).

P-bodies and stress granules have a lot of similarities. They are simultaneously assembled in cells under environmental stress, both are in dynamic equilibrium with polysomes assembling on untranslated mRNAs and both have been linked to microRNA-mediated gene silencing while they also share a subset of identical component proteins. However they do have distinctive differences. P-bodies contain factors of the mRNA decay machinery while stress granules are defined by translation initiation factors. Stress granules are only found in cells under environmental stress and their assembly requires the phosphorylation of eIF2a (reviewed in Anderson and Kedersha, 2008). Finally stress granules are relatively fixed in the cytoplasm where they change shape and appear to fuse and divide, while P-bodies change their position without changing their shape, as observed by time-lapse video microscopy (Kedersha et al, 2005).

Local translation in Neurones

Asymmetric localisation of mRNAs is an evolutionary conserved mechanism of restricting protein translation to specific subcellular locations and is widely exploited in nature (Lécuyer et al, 2007). The concept of mRNAs being translated locally in neurones, in contrast to translation occurring only in the cell soma, was introduced in the early 1980's with a study that revealed a preferential localisation of polyribosomes to dendritic spines (Steward and Levy, 1982). It is now well established that stimulus-induced local translation allows neurones to alter the protein composition of synapses with great spatial and temporal resolution and provides a fast and efficient mechanism

of adjusting to novel environmental conditions (reviewed in Schuman et al, 2006). Local translation in axons allows the growth cone to autonomously respond to guidance cues by rapidly changing its direction of outgrowth (Twiss and Minnen, 2006). Guidance cues that require local axonal translation to induce chemotropic responses include netrin-1, Sema3A (Campbell and Holt, 2001), Slit2 (Piper et al, 2006) and brain-derived neurotrophic factor (BDNF) (Yao et al, 2006). A large number of mRNAs encoding for a wide variety of proteins have been shown to be transported to distal dendritic sites. mRNAs encoding for receptors, ion channels, translation factors, RNA-binding proteins, ribosomal proteins, cytoskeletal proteins and growth factors are among the identified dendritic messages (Zhong et al, 2006). Most notably dendritic mRNAs encoding for RhoA have been discovered, whose local translation is enhanced by BDNF stimulation (Troca-Marín et al, 2010). RhoA transcripts have also been described to localise in developing axons and growth cones where their local translation is induced by Sema3A (Wu et al, 2005). Intra-axonal translation of RhoA is in fact necessary and sufficient for Sema3A-mediated growth cone collapse (Wu et al, 2005). Other transcripts found to localise in dendrites include mRNAs encoding for the eukaryotic translation elongation factor 1A (eEF1A) and also for ribosomal proteins (Zhong et al, 2006). The presence of ribosomal protein mRNAs in dendrites raises the intriguing possibility of local ribosome assembly in distal sites (Zhong et al, 2006).

Regulatory proteins that couple synaptic activity to local translation include staufen (Vessey et al, 2008) and Fragile-X Mental Retardation Protein (FMRP) (Zalfa et al, 2006). The role of staufen in mRNA transport in neurones has been discussed previously.

Fragile-X Mental Retardation Protein (FMRP)

Fragile-X Mental Retardation Protein is encoded in humans by the Fmr1 gene. Mutations in the Fmr1 gene that resides on the X chromosome are causative of the Fragile X Syndrome, a major cause of inherited mental retardation (D'Hulst and Kooy, 2009). In the majority of cases the Fragile X Syndrome is caused by the expansion of a polymorphic CGG repeat located in the 5′ untranslated region of Fmr1

gene. This expansion up to more than 200 CGG repeats triggers hypermethylation of the upstream CpG island of the gene promoter causing transcriptional silencing (Verkerk et al, 1991; Zalfa et al, 2006). FMRP is highly conserved in vertebrates and is expressed in various organs, showing a particularly high expression in the brain. In the brain FMRP is restricted to differentiated neurones particularly in the hippocampus and granular layer of the cerebellum, while its expression has been localised to proximal dendrites and synapses but not axons (Hinds et al, 1993; Feng et al, 1997). FMRP regulates the expression of specific mRNAs at synapses (Zalfa et al, 2003). It has been suggested that FMRP forms ribonucleoprotein complexes with target mRNAs in the nucleus which are transported to dendrites and spines where FMRP is involved in the regulation of local translation in response to stimuli (Bassell and Warren, 2008). Targets of FMRP translation regulation include mRNAs encoding Rac1 (Lee et al, 2003), profilin (Reeve et al, 2005) and microtubule-associated protein 1B (Lu et al, 2004). FMRP has been shown to modulate actin organisation in the brain by directly controlling profilin, an actin-binding protein that regulates the actin cytoskeleton (Reeve et al, 2005). FMRP binds to mRNA encoding for the profilin homolog in Drosophila and negatively regulates profilin protein synthesis. Up-regulation of profilin expression mimics the phenotype of FMRP mutants, while down-regulation suppresses the phenotype (Reeve et al, 2005). The function of FMRP has been linked to actin cytoskeleton remodelling and specifically Rac1 signalling. In Drosophila the CYFIP protein, orthologue of the vertebrate Cytoplasmic-FMR1-interacting proteins 1 and 2, interacts with FMRP and Rac1, acting as a Rac1 effector that antagonises FMRP function (Schenck et al, 2003). FMRP has been shown to associate physically and functionally with known components of the microRNA pathway (Li et al, 2009) and recent advances indicate that phosphorylation of FMRP modulates its function in microRNA-mediated gene silencing (Cheever and Ceman, 2009). FMRP may regulate the expression of the RasGAP-associated endoribonuclease G3BP that has been linked to stress granule assembly and the ubiquitin proteosome pathway (Zhong et al, 1999; Tourrière et al, 2001; Tourrière et al, 2003; Soncini et al, 2001).

G3BP in RAS signalling and RNA processing

RasGAP SH3-Domain Binding Protein, G3BP, is an evolutionarily conserved endoribonuclease that was initially characterised through its interaction with a Ras GTPase-activating protein (p120 RasGAP) (Parker et al, 1996). The endoribonuclease activity of G3BP can initiate mRNA degradation and this RNase activity is phosphorylation dependent (Gallouzi et al, 1998). It has been suggested that G3BP regulates the transport and translation of mRNAs encoding for proteins involved in cellular proliferation and migration (Solomon et al, 2007). High expression of G3BP has been described in several human cancer derived cell lines and various cancer tissues, while G3BP can stimulate S phase entry in cultured cells in a function dependent on its RNA binding ability (Guitard et al, 2001). Furthermore, the expression of G3BP has been found to be closely related to the lymph node metastasis and survival in oesophageal squamous carcinoma patients (Zhang et al, 2007).

G3BP is recruited to stress granules in cells exposed to arsenite while over-expressing G3BP can dominantly induce stress granule assembly, suggesting a role in determining the fate of mRNAs during cellular stress (Tourrière et al, 2003). In fact G3BP has been implicated in the transport and translation of mRNAs encoding for proteins involved in synaptic plasticity in neurones (Solomon et al, 2007). G3BP has been shown to directly down-regulate the translation of Tau mRNA through an interaction mediated by the 3′ untranslated region of the Tau transcript (Atlas et al, 2007).

G3BP has been implicated in ubiquitin-dependent protein degradation via its association with the ubiquitin-specific protease USP10, where data suggests that it inhibits the ability of USP10 to disassemble ubiquitin chains (Soncini et al, 2001). A study on fragile X lymphoblast cell lines revealed lowered levels of G3BP mRNA compared to controls, suggesting a regulation of G3BP mRNA by microRNA-mediated gene silencing involving FMRP (Zhong et al, 1999).

Aim of this study:

A yeast two-hybrid screen previously identified HemK1 as a potential binding partner for the neuronal α2-chimaerin. HemK1 is a ubiquitously expressed but little studied protein and the function of mammalian HemK1 has been described to a little extent very recently. α2-Chimaerin is a brain specific protein and an established player in signalling pathways of neuronal development and differentiation. The aim of this study was to characterise HemK1 and elucidate its function in neuronal morphology.

Objectives:

The objectives of this study were to:

a) Investigate and map the interaction between HemK proteins and α2-chimaerin.

b) Investigate the expression of HemK1 and HemK2 mRNA in the developing brain and characterise three monoclonal and two polyclonal anti-HemK1 antibodies in order to investigate native protein expression in rat brain.

c) Characterise the interaction of HemK1 and HemK2 with release factors eRF1 and mtRF1a and investigate their intracellular localisation in respect to subcellular organelle markers, release factors, and proteins involved in RNA processing.

d) Investigate the effects of HemK proteins in neuronal morphology by shRNA knock-down in rat hippocampal neurones.

Chapter 2
[Materials and Methods]

Reagents/Materials

General reagents

Water was distilled and deionised through an ELGA purification system and was autoclaved prior to use. The general laboratory chemicals used were from BDH.

Reagents for bacterial work

Bacto Tryptone, Bacto Yeast Extract and Agar were from DIFCO. An initial stock of competent XL1-BLUE E.coli was obtained from Stratagene and subsequent stocks of competent cells were prepared by the $CaCl_2$ method as described in the Bacterial Procedures section.

Reagents for DNA procedures

Agarose was from Sigma and the DNA ladder markers were φx174 (HaeIII) and λ (HindIII) from Invitrogen. Tris-Acetone-EDTA buffer was from Millipore and ethidium bromide was from Sigma. The kit for DNA agarose gel extraction and kits for plasmid DNA purification from bacterial cultures were from Qiagen. Restriction enzymes used in cloning were from New England Biolabs. Calf intestinal alkaline phosphatase was from Promega and DNA ligase from Invitrogen. The site-directed mutagenesis kit was from Stratagene.

The vectors used were the mammalian expression pXJ40 vectors (with FLAG, HA, GST, GFP and RFP tags) and the bacterial expression pGEX vector (GST tag). The HIS-Biotin dual-tag vectors used were the mammalian pXJ40-8xHIS-precission-SBP and the bacterial pGEX-T4.

Reagents for RNA procedures

The DNase/RNase-free water (DEPC-treated) and TRIzol were obtained from Invitrogen. DNase/RNase-free disposable consumables were from Greiner Bio-One. The RNeasy kit from Qiagen was used for RNA purification from cultured mammalian cells. The SuperScript III First-Strand Synthesis System by Invitrogen

was used for first-strand cDNA synthesis and the SYBRGreen PCR Master Mix by the same company was used for RT-PCR.

Reagents for protein procedures

In mammalian cell lysis and protein pull-down assays, the protease inhibitors used were the reducing agent dithiothreitol (DTT) and the phosphatase inhibitors Sodium ortho-Vanadate, Sodium Fluoride and Phenylmethanesulfonyl Fluoride (PMSF) obtained from Sigma and a protease inhibitor cocktail obtained from Roche. Anti-FLAG and anti-HA antibody conjugated affinity beads were from Sigma. The BCA protein assay kit was from Thermo Scientific.

In Sodium Dodecyl Sulfate Polyacrylamide Gel Electrophoresis (SDS-PAGE), Acrylamide/Bis-acrylamide (37.5:1) was from Severn Biotech, TEMED from Bio-Rad, β-mercaptoethanol from BDH and prestained protein size-standards were from Invitrogen (SeeBlue Plus2). In western blotting Triton X-100 was from BDH and the PVDF membrane from Perkin-Elmer. Dried skimmed milk powder was from Marvel. Autoradiography film, ECL Hyperfilm and the ECL solutions were from Amersham and the film developing and fixing solutions were from Kodak. Glutathione Sepharose was from Amersham Biosciences, Centriprep Concentrators from Amicon and S-Adenosyl[methyl-3H]methionine from GE Healthcare. The autoradiography enhancer spray was En3hance from Perkin-Elmer.

Reagents for tissue culture procedures

Dulbecco's Modified Eagle's medium (DMEM), Minimal Essential Eagle's media (MEM), Opti-MEM, Neurobasal Medium, B-27, Lipofectamine, Lipofectamine 2000, DMSO, Hanks Buffered Saline Solution, Antibiotics/Antimytotics, Trypsin and FBS were from Gibco-Invitrogen. Disposable supplies were from Greiner and Bovine Serum Albumin (BSA) from Jackson Laboratories. Poly-D-lysine was from ICN. The slides and coverslips were from BDH and the mountant was from DAKO. G-418 Sulfate was from Calbiochem. The electroporator device (Nucleofector) and the solutions used in primary neurone electroporation were from Amaxa.

cDNA constructs

The cDNA constructs used in this project and their source is summarised in table 2.1,

Construct	Gene ID	Chromosome	Clone ID	DNA accession
N6AMT1/ HemK2	21904	21q21.3	NIH MGC 119	BI520047, BI520047, BI520950
TRMT112	51504	11q13.1	IMAGE 30524659	CF780526.1
DCP1b	196513	12p13.33	IMAGE 5296928	BC043437
STAU1 Staufen1	6780	20q13.1	IMAGE 30528051	CF594111, BC095397
eRF1	2107	5q31.1	IMAGE 3677482	BE561367, BC014269
eRF3b	23708	Xp11.23	IMAGE 5313878	BC036077, BI669954

Table 2.1 List of constructs cloned during this project.

The constructs that were obtained from others are summarised in table 2.2.

Construct	Gene ID	Chromosome	Source	DNA accession
HemK1	51409	3p21.3	In house(C.Monfies)	NM_01617.3
G3BP1	10146	5q33.1	E. Manser (sGSK,IMCB)	NM_005754
FMR1	54516	6q25-q26	E. Manser (sGSK,IMCB)	NM_002024
mtRF1	9617	13q14.1	Z. Chrzanowska-Lightowlers	
mtRF1a	54516	6q25-q26	Z. Chrzanowska-Lightowlers	

Table 2.2 List of constructs that were kindly provided by others.

Bacterial procedures

Luria-Bertani (LB) media

The LB medium used in the bacterial procedures was 10% (w/v) Bacto Tryptone, 5% Bacto Yeast Extract and 10% NaCl diluted in distilled/deionised water and subsequently autoclaved. Amount of 15% (w/v) agar was added before sterilisation to make the agar plates. A final concentration of 100mg/ml Ampicillin was added when selection was needed.

Preparation of competent cells

XL-1 BLUE E.coli were spread on a $10cm^2$ agar plate using a sterile plastic loop and incubated inverted at 37°C overnight. A colony was picked with a sterile plastic loop and used to inoculate 100ml of LB medium (in a ventilated flask) that was subsequently incubated in a shaking incubator (approximately 225-250 rpm) at 37°C. When the absorbance of the culture at 600nm wavelength reached A=0.35 the flask was placed on ice for 5 minutes. The cells were pelleted by centrifugation at 3,000 g for 10 minutes at 4°C in pre-chilled 50ml polypropylene tubes and the supernatant was decanted. Remaining medium was removed by inverting the tubes and blotting on absorbent paper. The cell pellet was resuspended in a total of 30ml of ice-cold 50mM $CaCl_2$ and incubated on ice for 10 minutes. The cells were re-pelleted as above and the supernatant removed. The final cell pellet was resuspended in 50mM $CaCl_2$/15% glycerol and stored at -80°C.

Transformation of competent E.coli

Transformation of XL1-Blue competent cells (Stratagene)

Competent E.coli obtained from Stratagene were thawed on ice and β-mercaptoethanol was added to a final concentration of 24.12mM (1.7µl of 1.42M in 100µl) to 100µl of bacteria, and incubated on ice for 10 minutes. A total of 5µg for miniprep or 1µg for maxiprep plasmid DNA was added and the tubes were incubated on ice for 30 minutes after gentle mixing. The difference in the DNA amount used depending on the method of DNA purification takes in consideration the higher concentration and purity of maxiprep DNA (250ml starting culture) compared to miniprep DNA (5ml starting culture). The tubes were heat-pulsed in a 42°C water bath for 45 seconds and subsequently incubated on ice for two minutes. When maxiprep DNA was used the cells were plated on ampicillin-containing agar plates and incubated at 37°C overnight. When miniprep DNA was used, 1ml of pre-warmed LB medium was added and the tubes were incubated at 37°C for 1 hour with shaking at 225–250 rpm. The cells were then pelleted by pulse-centrifugation and 800µl of the

supernatant were decanted. The cells were resuspended in the remaining 200µl LB and streaked on ampicillin-containing agar plates and incubated at 37°C overnight.

Transformation of XL1-Blue $CaCl_2$ prepared competent cells

Competent E.coli prepared by the $CaCl_2$ method were thawed on ice and 100µl of bacteria were mixed with a total of 5µg for miniprep or 1µg for maxiprep plasmid and incubated on ice for 30 minutes. The tubes were heat-pulsed in a 42°C water bath for 90 seconds and subsequently incubated on ice for two minutes. The last steps of this procedure were as described above for the commercial competent cells obtained from Stratagene, depending on the purification scale of the DNA used.

Bacterial cultures for DNA purification

For a maxi-prep scale of DNA purification, a single bacterial colony was picked with the aid of a sterile plastic loop and used to inoculate 5ml of ampicillin-containing LB medium that was subsequently incubated at 37°C with shaking at 225-250 rpm, for 4-6 hours. This starter culture was then used to inoculate a total of 250ml of ampicillin-containing LB that was incubated at 37°C in a shaking incubator.

For mini-prep scale of DNA purification a single colony was used to inoculate 5mls of ampicillin-containing LB that was incubated at 37°C with shaking at 225-250 rpm overnight.

Bacterial stocks

Glycerol stocks of transformed bacteria were made by transferring 700µl of an overnight culture to a 1.5ml tube and adding 300µl of 50% sterile glycerol solution to obtain a final 15% (v/v) glycerol content. After mixing the tubes were stored at -80°C.

Plasmid DNA purification

Plasmid DNA was purified using the relevant kits from Qiagen and following the commercial protocol. Briefly, the overnight bacterial cultures were pelleted by centrifugation and resuspended in a Tris-based buffer. Subsequent alkaline lysis of the cells followed neutralisation of the lysate by the addition of a low-salt and low-pH

buffer. An anion-exchange resin was used to bind the DNA while RNA, proteins and low molecular weight impurities were removed by washing with a medium-salt buffer. The plasmid DNA was purified in a high-salt buffer and subsequently concentrated and desalted by isopropanol precipitation. The purified DNA was finally resuspended in 1ml of 10mM Tris-HCl pH8.0.

Determination of purified DNA concentration and purity

Amount of 10μl of the purified DNA was added to a cuvette containing 1ml of 10mM Tris pH 8.0. The absorbance was measured with the aid of a spectrophotometer at wavelengths 260 and 280 nm, against a blank sample of Tris pH 8.0. DNA absorbs ultraviolet light with an absorption peak at 260 nm, and protein shows an absorption peak at 280 nm. A ratio of the absorptions at the two wavelengths (A_{260}/A_{280}) gives an indication of the purity of the DNA with respect to protein contamination, with a product of 1.8 to be considered a “pure” DNA sample. The concentration of DNA is assessed by the formula:

Concentration (mg/ml) = [(total volume/DNA volume) x A_{260} reading x 50] / 1000

DNA procedures

In cloning the various cDNAs in mammalian and bacterial expression vectors, a sequence of techniques was used. Initially the cDNAs were amplified by PCR that generated restriction enzyme recognition sites on either end of the amplified product. These restriction sites generated by the primers were chosen to allow ligation of the amplified cDNA in the multiple cloning site of the target plasmid. It was therefore important that these generated sites are unique in the cDNA and the relevant restriction enzymes will only cut at the designed sites. The PCR product was subjected to agarose gel electrophoresis and the corresponding band was excised off the gel and the DNA was purified. The DNA was digested with the corresponding restriction enzymes and purified, before it was ligated to the target plasmid, also digested with the same enzymes. The ligation products were used to transform E.coli, and select for the positive colonies. All these techniques are outlined here.

Polymerase Chain Reaction (PCR)

The method of PCR was used to (a) amplify cDNA to clone in vectors, (b) test if bacterial colonies were positive in carrying a plasmid containing the cDNA insert, (c) raise a mutation in a cDNA by site-directed mutagenesis and (d) investigate on the expression of different transcripts in cells/tissues by quantitative Real-Time PCR (explained in RNA methods).

PCR in cloning

The method of PCR was used to clone cDNAs of HemK1, HemK2, eRF1, eRF3, Dcp1b, Staufen1 and TRMT112 in (a) mammalian expression vectors pXJ40 carrying an HA, FLAG, GST, GFP or RFP tag, and (b) bacterial expression vector pGEX carrying a GST tag. HemK1 and HemK2 cDNAs were also cloned in the HIS-Biotin dual tag vectors pXJ40-8xHIS-precission-SBP (for mammalian expression) and pGEX-T4 pBIOTIN-HIS (for bacterial expression).

For PCR in cloning, the Taq Polymerase (bacterial recombinant) from SIGMA was used, as well as the 10x PCR buffer and 25mM $MgCl_2$ solutions provided. The amounts of PCR buffers, cDNA, dNTPs, primers and Taq Polymerase used in a 50µl reaction volume are outlined:

Component	Final concentration	Volume in reaction
PCR buffer	10mM Tris-HCl Ph8.3, 50mM KCl	5µl of 10x reaction buffer
$MgCl_2$	1.5mM	3µl of 25mM $MgCl_2$ solution
Primer 1	0.8µM	0.4µl of 100µM stock
Primer 2	0.8µM	0.4µl of 100µM stock
dNTPs	200µM of each dNTP	1µl of 10mM [dATP, dTTP, dCTP, dGTP] mix (1:1:1:1)
DNA template	0.5µg	
Taq Polymerase	0.05units/µl	0.5µl of 5units/µl
ddH_2O		Up to 50µl total reaction volume

Table 2.3 Reaction condition in PCR in cloning.

The conditions used in the PCR varied depending on the predicted T_m of the primers and the length of the cDNA amplified in each case. A general outline is as follows:

	94°C	1′	Initial Denaturation step
30 Cycles	94°C	45″	Denaturation
	50-60 °C	30″	Annealing
	72°C	1′/1000 bp of cDNA	Elongation
	72°C	5′	Final Elongation step

The primers used to clone each cDNA into each vector are listed in table 2.4.

cDNA	Target vector	Primers (5′ to 3′). Complementary to cDNA sequence in BLACK, Restriction Enzyme site in GREEN and extra sequence allowing restriction enzyme positioning in BLUE		Restriction Enzyme site generated
Human HemK1	C-terminal FLAG pXJ40	F	GACGTCAAGCTTATGGAGCTTTGGGGCCGAATGC	HindIII
		R	GACGTCCTGCAGCCTGGCCCAGACCTCCGGATATG	PstI
Human HemK1	pGEX T4 Biotin-His	F	GACGTCGAATTCATGGAGCTTTGGGGCCGAATGC	EcoRI
		R	GACGTCGTCGACTGGCCCAGACCTCCGGATATG	SalI
Human HemK2	pGEX T4 Biotin-His	F	GACGTCGAATTCATGGCAGGGGAGAACTTCG	EcoRI
		R	GACGTCGTCGACAGACTTGGTGAACTTGAGG	SalI
Human HemK2	pXJ40-8xHIS-precision-SBP vector	F	GACGTCAAGCTTATGGCAGGGGAGAACTTCGCTACG	HindIII
		R	GACGTCGCGGCCGCCTAAGACTTGGTGAACTTGAG	NotI
Human HemK2	pXJ40 (N term. GST, FLAG, HA)	F	(a) CTTATGGCAGGGGAGAACTTCGCTACG (b) GACGTCAAGCTTATGGCAGGGGAG	HindIII
		R	GACGTCCTGCAGCTAAGACTTGGTGAAC	PstI
eRF1	pXJ40 (N term. GST, FLAG, HA)	F	GACGTCAAGCTTATGATATCATTGATCATTCC	HindIII
		R	GACGTCCTGCAGCTAGTAGTCATCAAGGTC	PstI
eRF3	pXJ40 (N term. GST, FLAG, HA)	F	GACGTCAAGCTTATGGATTCGGGTAGCAGC	HindIII
		R	GACGTCCTGCAGTTAGTCCTTCTCTTGGAC	PstI
Human TRMT112	pGEX-GST	F	GACGTCCCATGGATGAAACTGCTTACCC	NcoI
		R	GACGTCGTCGACCTCAACTCTCAGTTTCC	SalI
Human TRMT112	pXJ40 (N term. GST, FLAG, HA)	F	GACGTCAAGCTTATGAAACTGCTTACCC	HindIII
		R	GACGTCAGATCTTCAACTCTCAGTTTCC	BglII
Staufen1	GFP(n)-Pxj40	F	GACGTCGCGGCCGCCATGAAACTTGGAAAAAAACGA	NotI
		R	GACGTCAGATCTTCAGCACCTCCCACACAC	BglII
Dcp1b	GFP(n)-Pxj40	F	GACGTCCTCGAGATGGCAGCCGTGGCG	XhoI
		R	GACGTCCCCGGGTCACATAGTCTTTTTCAT	SmaI

Table 2.4 Primers used in cloning of cDNA constructs.

The antibodies and probes used in this project are summarised in table 2.5.

Antibody/Probe	Dilution for immunoblotting	Dilution for cell immunostaining	Donor Animal	Company
Primary Antibodies				
α2-Chimaerin	1:2,000	1:100	Rabbit	In House
FLAG	1:2,000	1:100	Rabbit/ Mouse	Sigma
HA	1:2,000		Rabbit	Bethyl Laboratories
GST	1:1,000		Rabbit/Mouse	Sigma
Lamp-1		1:100	Mouse	BD Biosciences
EEA1:FITC		1:100	Mouse	BD Biosciences
GM130:FITC		1:100	Mouse	BD Biosciences
Clathrin Heavy Chain:FITC		1:100	Mouse	BD Biosciences
HSP60:FITC		1:100	Mouse	BD Biosciences
6D2 anti-HemK1	1:500	1:100	Mouse	In House
8F3 anti-HemK1	1:500	1:100	Mouse	In House
7D7 anti-HemK1	1:500	1:100	Mouse	In House
Rabbit-5 anti-HemK1	1:500	1:100	Rabbit	In House
Rabbit-6 anti-HemK1	1:500	1:100	Rabbit	In House
Mouse anti-HemK1 H00051409-B01	1:500		Mouse	Abnova
Mouse anti-HemK2 H00029104-A01	1:500		Mouse	Abnova
Rabbit anti-HemK2 H00029104-M01	1:500		Rabbit	Abnova
MitoTracker Green FM (M-7514)		1:100		Molecular probes
Dcp1a (ab47998)		1:100	Goat	Abcam
Secondary Antibodies				
Mouse HRP	1:1,000		Rabbit	DAKO
Rabbit HRP	1:1,000		Swine	DAKO
Trueblot HRP	1:1,000		Mouse	eBioscience
Trueblot HRP	1:1,000		Rabbit	eBioscience
Rabbit:Cy5		1:100	Donkey	Jackson Laboratories
Mouse:FITC		1:100	Donkey	Jackson Laboratories

Table 2.5 Antibodies used in immunoblotting and immunostaining.

PCR testing for positive colonies

The PCR method was used to test for positive colonies in cloning. Colonies of bacteria transformed with cDNA-vector ligation products were picked from LB-agar plates with a yellow tip and used to inoculate 20µl of 10mM Tris-HCl Ph8.0 in a 1.5ml tube. Amount of 10µl of the bacterial suspension was used to inoculate 5ml of LB containing ampicillin, and incubated at 37° C with shaking at 225-250 rpm overnight. The rest 10µl of the bacterial suspension were used as template in a PCR designed to amplify the specific insert cDNA (same primers used for amplifying the cDNA before ligating with the vector). The products of this PCR were analysed by

agarose gel electrophoresis to identify the colonies that contained a vector+cDNA construct, as opposed to an empty re-ligated vector (only the positive colonies would give a product of the expected size in the PCR). The positive colonies were analysed further by purifying the plasmid DNA of the 5ml cultures and performing restriction digests that would give products of predicted sizes.

The final volume of this PCR was 25µl and the amounts of reaction components used are outlined in table 2.6.

Component	Final concentration	Volume in reaction
PCR buffer	10mM Tris-HCl Ph8.3, 50mM KCl	2.5µl of 10x reaction buffer
$MgCl_2$	1.5mM	1.5µl of 25mM $MgCl_2$ solution
Primer 1	0.8µM	0.2µl of 100µM stock
Primer 2	0.8µM	0.2µl of 100µM stock
dNTPs	200µM of each dNTP	0.5µl of 10mM [dATP, dTTP, dCTP, dGTP] mix (1:1:1:1)
DNA template		10µl
Taq Polymerase	0.05units/µl	0.25µl of 5units/µl
ddH_2O		9.85µl total reaction volume

Table 2.6 Reaction conditions used in PCR in positive clone identification.

All the cloned constructs were sequenced to check for sequence integrity and possible errors incorporated during PCR. The primers used in sequencing are listed bellow:

cDNA	Target Vector	Primers used in sequencing
eRF1	pXJ40	F: GATCATTCCTCCCAAAGACC F: CAAAGTGAATGTGGCTGGTC R: CTTTTGATTGTAACCTCTGATC
eRF3	pXJ40	F: CCATGGATTCGGGTAGCAG F: GTGCACCTAAGAAAGAACACG F: CATTCACTTTATGCCCTGCTCAGG R: CTGAGCAGGGCATAAAGTG R: CTTCTGGGGGCCCTGAATC
HemK1	pXJ40	F: ATGGAGCTTTGGGGCCGAATGCTG R: CCACCTCTTCCAGCACCCACTC
primers upstream and downstream of pXJ40 multiple cloning site		T7: TAATACGACTCACTATAGGG R: CGACCAGACATGATAAGATAC

Table 2.7 Primers used in PCR of positive clones.

PCR in site-directed mutagenesis

The conserved substrate binding NPPY motif of the human HemK1 was mutated in order to investigate the methyltransferase activity and possible effect in neuronal growth. The NPPY motif in the bacterial HemK1, PrmC, has been shown to be important for the interaction with, and methylation of, release factor RF1. As published by Graille et al (Graille et al, 2005), the Asparagine to Alanine mutation in the NPPY motif inhibits the interaction with RF1 and abolishes methylation by PrmC. The QuikChange XL Site-Directed Mutagenesis Kit from Stratagene was used to raise the Asn239Ala mutation in the human HemK1 homologue. This kit is based on PCR, where the pXJ40-HemK1 plasmid constructs carrying a FLAG, HA or GST tag were amplified. The primers incorporated a nucleotide mismatch that generated the desired mutation. The primers used are outlined below and the mismatch nucleotides are highlighted in red:

Forward:
5′ GACCTGATTGTCAGCGCCCCTCCCTACGTCTTC 3′
Reverse:
3′ GAAGACGTAGGGAGGGGCGCTGACAATCAGGTC 3′

Figure 2.1 illustrates the principle of this technique, where the primers bind on either side of the target sequence. The mismatch nucleotides that give rise to the Asn239Ala mutation are in lower case, and the red nucleotides at the forward primer indicate the affected codon:

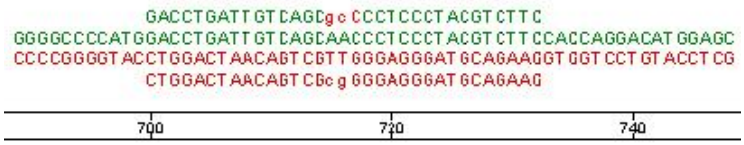

Figure 2.1 Principle of N239A site-directed mutagenesis of HemK1 by PCR.

In the PCR, the Pfu polymerase was used to take advantage of its high fidelity so as no random mutations are incorporated in the long elongation steps. The amounts and conditions used are outlined bellow:

PCR:
5µl 10x reaction buffer (provided in kit)
10ng of double-stranded plasmid DNA (cDNA: HemK1)
125ng primer 1
125ng primer 2
1µl dNTP mix (provided in kit)
3µl QuickSolution (provided in kit)
ddH_2O to final volume 50µl

	94°C	1′	Initial Denaturation step
18 Cycles	94°C	50″	Denaturation
	60 °C	50″	Annealing
	68°C	5′	Elongation
	68°C	7′	Final Elongation step

After the completion of the PCR, the samples were incubated with the restriction enzyme Dpn1, to digest the methylated parental DNA template. The PCR products were used to transform E.coli, that were subsequently plated on ampicillin containing LB agar plates. The colonies picked were used to prepare DNA that was sequenced to reveal the colonies containing the successfully mutated HemK1 construct.

DNA agarose gel electrophoresis

DNA was analysed by agarose gel electrophoresis when a) purification of a digestion product was needed (in preparing the insert for ligation in cloning), b) to test for positive colonies by restriction digest of bacterial colony plasmid DNA and c) to check PCR products in optimising reaction conditions. The agarose gels used ranged from 1 to 2% agarose, depending on the size of the expected DNA. The recipe was as follows:

1-2g of Agarose
100ml TAE buffer (40mM Tris, 20mM Acetate, 1mM EDTA)

After dissolving the agarose by heating the solution, the mix was cooled to about 50°C and ethidium bromide was added at a final concentration of 5µg/ml. The gel was poured in a gel-tray than incorporated 20 wells, and left to set before use.
The DNA samples were prepared by adding 1/5 volume of 6x DNA loading buffer and mixing. The DNA loading buffer consist of 30% glycerol, 0.25% Bromophenol blue, made up in Tris-Acetate-EDTA buffer.

The gel then immersed in a TAE buffer containing running tank, and the samples containing 6x DNA loading buffer were loaded in the wells. The gel was run for 1 hour at 125V before visualising on a UV light source. A digital camera and the Kodak Molecular Imaging software were used to obtain pictures of the DNA gel electrophoresis.
To excise bands off the agarose gel, a scalpel was used to cut off the band in the gel visualised under UV. DNA was extracted from the agarose piece by using the QIAquick Gel Extraction kit by Qiagen.

DNA Phenol-Chloroform extraction and Ethanol precipitation

To purify DNA from protein contaminants the method of Phenol-Chloroform extraction was used. An equal volume of Phenol/Chloroform/Isoamyl alcohol (25:24:1) was added to the DNA sample and was mixed by brief vortexing. It was centrifuged in a microcentrifuge at 14,000rpm for 5 minutes. The upper aqueous phase was carefully transferred to a fresh tube, avoiding the white interphase containing the protein impurities. The process was repeated and the final aqueous phase was transferred to a fresh tube.

Amount of two volumes of pure Ethanol was added to the sample and Sodium Acetate pH 5.2 was added to a final concentration of 0.3M. The solution was mixed and incubated on dry-ice for 10 minutes. The tube was centrifuged in a microcentriguge at 14,000rpm for 10 minutes. The supernatant solution was carefully

removed and the DNA pellet was washed with 200 µl of 70% ethanol. The tube was centrifuged for 2 minutes at 14,000rpm and the solution was carefully removed. The pellet was dried in a vacuum centrifuge for 5 minutes and the DNA was finally resuspended in 10mM Tris pH8.

DNA restriction enzyme digestion

Digestion of DNA was used when preparing insert and plasmid DNA for ligation and also when testing for positive bacterial colonies, in cloning. In digesting the insert (often a PCR product that was extracted/purified by agarose gel electrophoresis) and the plasmid in cloning, amount of 10µg of DNA were used in the reaction. The reaction was set up as follows:

DNA (10µg)
Restriction enzyme(s) [7% of reaction volume]
ddH_2O up to the desired volume

When needed amount of 0.1mg/ml BSA was also included in the reaction (provided by New England Biolabs as a 100x stock containing 20mM KPO_4 pH 7.0, 50 mM NaCl, 0.1 mM EDTA and 5% glycerol).
The reaction was mixed and incubated at 37° C overnight. The digested DNA in the reaction was then purified by Phenol/Chloroform extraction and Ethanol precipitation.

Dephosphorylation of linearised vector DNA prior to insert ligation

Linearised vector DNA was dephosphorylated prior to insert ligation to avoid re-ligation of the vector and false positives, when the vector ligates back to itself without containing an insert. The Calf Intestinal Alkaline Phosphatase (CIAP) from Invitrogen was used. The dephosphorylation reaction was set up at the end of a restriction digest of the vector, without purifying the DNA. The provided buffer and Phosphatase were added directly to the completed restriction reaction as follows:

100 µl of vector digestion reaction
13 µl of 10x CIAP buffer
11 µl of 1:100 diluted CIAP enzyme

The samples were mixed and incubated for 30 minutes at 37 °C.

A further amount of 11 µl 1:100 CIAP enzyme was added and the samples were incubated for 30 minutes at 37 °C. The samples were run on agarose gel electrophoresis and the desired linearised vector was excised off the gel and purified with the QIAquick Gel Extraction Kit before setting up an insert ligation reaction.

DNA ligation

Linearised vector DNA was ligated with insert DNA, that is the purified cDNA to be cloned in a mammalian or bacterial expression vector. The T4 DNA ligase from Invitrogen was used. The two purified DNA fragments were briefly checked for purity and concentration by running a small amount in an agarose gel and visualising on a UV light source. The vector and insert DNA were mixed in a tube and initially heated up to 65° C for 5 minutes, to break any secondary structures. Then they were allowed to cool at room temperature and transferred on ice so as the ligation buffer and ligase enzyme can be added. The amounts of vector and insert DNA varied on each cloning experiment, depending on the concentration of the purified DNA samples, but a general initial set up would use 3:1 insert to vector amounts. Also when a ligation reaction would yield no colonies the reaction would be repeated increasing the amount of insert. As an example, the reaction set up for cloning HemK1 and HemK2 in the His-Biotin pXJ40 vectors were as follows:

0.5 µl of linearised/dephosphorylated Vector DNA
7 µl of Insert DNA
2 µl of 10x T4 DNA Ligase Buffer
1 µl of T4 Ligase Enzyme

A negative control reaction was set up in parallel, were no insert DNA was included, so as to control for the re-ligation of the vector and false positives.

The reaction was incubated at 16° C overnight and was then used to transform bacteria, as explained in the Bacterial Procedures section. The transformed bacteria were plated on ampicillin containing plates to select for successfully transformed E.coli. Six colonies were picked and a used to inoculate 5mls of LB with ampicillin selection. This starter culture was used to make a mini-prep of DNA as described in the Bacterial Procedures section.

A small amount of the DNA purified from the colonies was digested with restriction enzymes to check if they successfully contain the insert. The enzymes used were most often the same used to clone the insert at the first place. Running the digestion products on an agarose gel, the positive colonies would produce two DNA bands, the linearised vector and the insert, and colonies that do not contain the insert would produce only the linearised vector band. DNA from the positive colonies was used to transform E.coli and make a maxi-prep of DNA.

RNA procedures

Knock-down of gene expression by shRNA

To investigate the effect of HemK1 and HemK2 in neurite morphogenesis, the expression of the two genes was knocked-down by double-stranded RNA interference. The siSTRIKE U6 hairpin cloning system by Promega was used, that utilises a psiSTRIKE vector containing the U6 promoter. We designed oligonucleotides that contain the hairpin shRNA target and U6 terminator sequence, that were ligated in the psiSTRIKE vector. In cells, RNA polymerase III recognises the U6 promoter driving the transcription of the hairpin RNAs. The antisense RNA molecules generated bind to complementary RNA molecules in the cell that target the complex to cleavage by the RNA-induced silencing complexes (RISCs). The oligonucleotides were cloned in two psiSTRIKE vectors, one containing a GFP marker (for detection of transfected cells in rat embryonic hippocampal primary neurones experiments) and one containing a neomycin gene giving resistance to G-418 for selecting transfected cells in experiments with N1E-115 cells. Also the two

vectors contain an Amp^r gene that offers selection of E.coli, in cloning the oligonucleotides in the psiSTRIKE vectors.

All the oligonucleotides were HPLC purification grade and ordered from Sigma. The oligonucleotides were designed using the on-line shRNA oligonucleotide designer tool provided by Invitrogen. The target sequence of HemK1 and HemK2 returned 20 possible oligonucleotide pairs, three of which were chosen that were not complementary to the human sequence (so HemK1/2 expression can be restored by transient transfection of human cDNA) and were complementary to both rat and mouse cDNAs. The oligonucleotides used are outlined in the following table:

Target RNA	Complementary to species	name	Oligonucleotide sequence (5′ to 3′)
HemK1	Rat, mouse	1A	ACCGGATGCCGGTGCAGTATATTTCAAGAGAATATACTGCACCGGCATCCTTTTTC
			TGCAGAAAAAGGATGCCGGTGCAGTATATTCTCTTGAAATATACTGCACCGGCATC
	Rat, mouse	2A	ACCGGAACCCATGACTGATTCTTTCAAGAGAAGAATCAGTCATGGGTTCCTTTTTC
			TGCAGAAAAAGGAACCCATGACTGATTCTTCTCTTGAAAGAATCAGTCATGGGTTC
	Rat, mouse	3A	ACCGGGAATCCAGTGAGTACATTTCAAGAGAATGTACTCACTGGATTCCCTTTTTC
			TGCAGAAAAAGGGAATCCAGTGAGTACATTCTCTTGAAATGTACTCACTGGATTCC
HemK2	Rat, mouse	1B	ACCGGGCTGTTCTACTTAGTTATTCAAGAGATAACTAAGTAGAACAGCCCTTTTTC
			TGCAGAAAAAGGGCTGTTCTACTTAGTTATCTCTTGAATAACTAAGTAGAACAGCC
	Rat, mouse	2B	ACCGAAACGGCCGGGAAGTCATTTCAAGAGAATGACTTCCCGGCCGTTTCTTTTTC
			TGCAGAAAAAGAAACGGCCGGGAAGTCATTCTCTTGAAATGACTTCCCGGCCGTTT
	Rat, mouse	3B	ACCGGAGGACACGTTCCTGTTATTCAAGAGATAACAGGAACGTGTCCTCCTTTTTC
			TGCAGAAAAAGGAGGACACGTTCCTGTTATCTCTTGAATAACAGGAACGTGTCCTC

Table 2.8 Primers used in shRNA knock-down of HemK1 and HemK2.

Also, two pairs of scrambled sequence oligonucleotides were used, as a control for non-specific RNA interference. These scrambled oligonucleotides were based on pairs 1A and 2A described above, and their sequences are as follows:

Scrambled 1:
ACCGGATGCCGGTGCAGTATATTTCAAGAGAATATACTGCACCGGCATCC
TTTTTC

TGCAGAAAAAGGATGCCGGTGCAGTATATTCTCTTGAAATATACTGCACC
GGCATC

Scrambled 2:

ACCGTTTGGCTCGATGATTATCTTCAAGAGAGATAATCATCGAGCCAAAC
TTTTTC

TGCAGAAAAAGTTTGGCTCGATGATTATCTCTCTTGAAGATAATCATCGAG
CCAAA

Initially the oligonucleotides were diluted in nuclease-free water to a final concentration of 1 µg/µl. The annealing reaction was set up as follows:

Oligonucleotide A (1 µg/µl)	2 µl
Oligonucleotide B (1 µg/µl)	2 µl
Oligo annealing buffer	46 µl

The reaction was incubated at 90° C for 3 minutes, and then transferred to a 37° C water-bath and incubated for 15 minutes. The annealed hairpin nucleotides were diluted further to a final concentration of 4ng/ µl to set up a ligation reaction with the already linearised psiSTRIKE vectors:

2x rapid ligation buffer	5 µl
psiSTRIKE vector (50ng/µl)	1 µl
Annealed oligonucleotides A and B (4ng/ µl each)	1 µl
Nuclease-free water	2 µl
T4 DNA ligase (3 units/µl)	1 µl

The reactions were mixed by pipetting and incubated at room temperature for 3 hours. The ligation products were used to transform E.coli bacteria as described in the Bacterial Procedures section. Five colonies were picked from each oligonucleotide-pair and were used to purify DNA to screen for positives. The psiSTRIKE vectors contain a single PstI restriction site. Successful ligation of the annealed oligonucleotides in these vectors results in the creation of a second PstI site. Therefore the colonies were screened for positives by digesting the DNA with PstI, since empty religated vectors would produce in linearised plasmids (one ~4.5kb band in agarose

gel electrophoresis) and the insert-containing vectors would produce two bands (~3.6kb and 1kb). The PstI digestion was set up as follows:

DNA	10 µl
NEB Buffer 2	2 µl
Pst 1	1 µl
ddH_2O	7 µl

The digestion reactions were incubated at 37° C for three hours before they were analysed by agarose gel electrophoresis. The positive colonies were used to re-transform E.coli and finally prepare DNA to be used for mammalian cell transfections.

Quantification of gene expression by Real-Time RT-PCR

RNA purification from cells

To investigate the expression of HemK1 and HemK2 genes in specific cells and the effectiveness of knocking-down their expression by shRNA, RNA was purified and used in a real-time PCR. The purification of RNA from cells was performed using the RNeasy mini kit from Qiagen. RNA was purified from e18 rat brain hippocampal neurones plated on PDL/Laminin coated $5cm^2$ plates, 3 days in vitro. RNA was purified from N1E-115 cells plated on $10cm^2$ plates. The whole purification was performed on ice, using RNase-free solutions and consumables. Briefly, the medium was removed from the plates and the cells were washed once in PBS that was subsequently completely aspirated. The cells were lysed on the plates by addition of a denaturing guanidine-thiocyanate containing buffer (buffer "RLT" in the kit). The cells were harvested using a rubber policeman and the lysate was homogenised by centrifugating through a QIAshredder spin column (Qiagen). Ethanol was added to the lysate and total RNA was bound to a silica-based column (RNeasy Mini spin column) and was subsequently washed with provided buffers and eluted in 35µl RNase/DNase-free water. Amount of 1µl of purified RNA was used to measure the

RNA concentration with the aid of a NanoDrop spectrophotometer. The purified RNA was stored at -80° C.

RNA purification from tissues

RNA was purified from brain sections to quantify the gene expression of HemK1 and HemK2. The TRIzol reagent used (Invitrogen) is a phenol and guanidine isothiocyanate solution that disrupts the cells in the lysis/homogenisation step while suppressing the activity of RNases by being a strong protein denaturant and therefore maintaining RNA integrity.

Initially, sections from embryonic rat brains were dissected and weighted out. Amount of 1ml of TRIzol was added to 0.1g of tissue. The tissue was pulverised with the aid of a glass homogeniser, on ice. The homogenate was transferred to RNase-free tubes and incubated at room temperature to allow for the complete dissociation of nucleoprotein complexes. Amount of 0.2ml of chloroform was added and the tubes were vigorously mixed by hand for 15 seconds and incubated at room temperature for 3 minutes. The samples were subsequently centrifuged at 12,000g for 15 minutes at 4° C. The resulting aqueous phase was transferred to new tubes and 0.5mls of isopropyl alcohol were added. After incubating the tubes for 10 minutes at room temperature they were centrifuged at 12,000g for 10 minutes at 4° C. The supernatant was subsequently removed and the RNA precipitate was washed by the addition of 1ml of 75% ethanol and brief vortexing. The tubes were further centrifuged at 7,500g for 5 minutes at 4°C. The ethanol was removed and the pellet was briefly air-dried for 10 minutes. The purified RNA was resuspended in 35µl of RNase-free water, and stored at -80° C.

Determination of purified RNA concentration and purity

The concentration and purity of purified RNA was assessed with the aid of the cuvette-free spectrophotometer Nanodrop that allows for the analysis of 1µl sample volume. That allowed for the normalisation of RNA amounts used in reverse-transcription reactions where comparable amounts of cDNA product were desired, assuming that the total mRNA content in the reaction will be transcribed to cDNA.

Reverse Transcription of cDNA

RNA purified from tissues/cells was used to reversely transcribe cDNA from mRNA, to be subsequently used in quantitative Real-Time PCR. The amounts used in the "SuperScript III First-Strand Synthesis for qRT-PCR" kit from Invitrogen, and the conditions used are outlined in table 2.9.

Component	Amount used
2X RT Reaction Mix	10 µl
RT Enzyme Mix	2 µl
RNA	(up to 1 µg)
DEPC-treated water	to 20 µl total reaction volume

Table 2.9 Reaction conditions used in Reverse Transcription of mRNA.

The reaction was set up in an RNase/DNase free 0.2ml PCR tube on ice and incubated at 25°C for 10 minutes. Subsequently, the tube was incubated at 50°C for 30 minutes, before terminating the reaction at 85°C for 5 minutes. The tube was chilled on ice and 1 µl (2 U) of E.coli RNase H was added, and incubated at 37°C for 20 minutes. The tube was finally stored at -20°C.

Quantitative Real-Time PCR

The method of real-time PCR allowed us to estimate the relative abundance of specific transcripts in cells and tissues. In this PCR, we amplify the transcript of a gene of interest, so the template used is the cDNA made from RNA purified from cells/tissues, while the primers used are specific for the cDNAs in question (i.e. HemK1, HemK2, α2-chimaerin, β-actin and HPRT1). Real-time PCR employs a DNA-binding fluorescent reporter molecule to monitor the reaction in real-time. We used the dye SYBR Green that binds to the minor groove of the DNA double helix, and when excited it exhibits fluorescence that is detected by the real-time thermal-cycler. The fluorescence of the reporter increases as the product accumulates in each cycle. This allows us to create an amplification curve, where the reading of the fluorescence emission on each cycle is plotted against the cycle. The software will automatically set a threshold of fluorescence, at the point where fluorescence of amplified product is first detected above the "noise" level. The cycle at which the fluorescence from a sample crosses the threshold is called C_t, and that parameter is

used to compare amounts of specific mRNA transcripts. In this method, we used the dye ROX in the reactions as a passive signal to normalise experimental results for non-PCR-related fluctuations in fluorescence signal. To quantitate the alteration of the HemK1 and HemK2 transcript by shRNA knock-down, a standard curve was constructed using cDNA from untransfected cells, in a series of known dilutions. The standard curve was then used as a reference standard for extrapolating quantitative information for mRNA targets of unknown concentrations.

The real-time thermal cycler determines the melting point of the product at the end of the amplification reactions. It constructs a dissociation curve, where the temperature is raised while the fluorescence is being measured. At the melting point, the DNA strands will denature and the fluorescence reading will drop rapidly. Since SYBR Green will bind any double-stranded DNA, it will also give fluorescence in the case of DNA contamination in the reaction, formation of primer-dimer and also mispriming, where DNA products are made due to primers annealing to non-target DNA. Thus, this reading is an important quality control, since the melting temperature of a DNA double helix depends on its length and base composition and so the PCR products of a particular primer pair should have the same melting temperature. The plot constructed by the software shows the rate of change of fluorescence with time (-d(RFU)/dT where RFU is Relative Fluorescence Units and T is time) versus the temperature. The peak in the graph represents the melting temperature (Tm) (see Chapter 4). All reactions of each primer-pair were checked for similar melting temperatures as a non-similar peak would indicate contamination or non-specific priming and primer-dimers would manifest in lower melting temperatures. Negative controls were also included in the reaction set up, to check for possible DNA contamination and also primer-dimers.

The Power SYBR Green PCR Master Mix (Invitrogen) was used for the real-time PCR analysis. The real-time PCR thermal cycler used was the Stratagene Mx3000P along with the MxPro QPCR software for reaction set up and data analysis. The primers were designed so the amplicons (cDNA target sequence to be amplified) span two introns to avoid amplification of genomic DNA. The amplicon size was kept to the range of 180-250 base-pairs. The GC content of the primers was kept in the 20 to

80% range and runs of an identical nucleotide were avoided. The primers were designed to have a melting temperature between 58.5 and 61 °C.

The primers used in the real-time PCR are listed in table 2.10.

Transcript	Species	Product size (bb)	Primers	T_m (°C)
α2-Chimaerin	Rat	211	F: TTGCGAGGTAGAAAACAGACC	59.4
			R: CCCAACAAAGTGCTTTCCAT	59.9
HemK1	Rat	201	F: CCAGGAGCTGTGTAACCATAGA	59.3
			R: AGAATGAGGGGACCATCTTG	58.9
HemK1	Mouse	211	F: ATGGTACCCCCAGTGTTCAT	59.0
			R: CAGCAGCTTCCTCCTTATCC	58.9
β-Actin	Rat	247	F: TCCTTCCTGGGTATGGAATC	58.8
			R: CCAGGATAGAGCCACCAATC	59.5
β-Actin	Mouse	177	F: CTAGGCACCAGGGTGTGAT	58.5
			R: CCACACGCAGCTCATTGTA	59.4
HPRT-1	Rat	229	F: GGAAAGAACGTCTTGATTGTTG	58.7
			R: TCAAATCCCTGAAGTGCTCA	59.4
HPRT-1	Mouse	216	F: TCAGTCAACGGGGGACATA	59.9
			R: CCAACAAAGTCTGGCCTGTA	58.8
HemK2	Mouse	181	F: CGAGCTAGCAGGAGTGGAAA	60.7
			R: GATCACTGGCTGAACATGGA	59.6
HemK2	Rat	186	F: GGGTGGTGTCTGCATTCCTA	60.9
			R: GCAGGTCTACTTTCCCCTTCA	60.6

Table 2.10 Primers used in real-time PCR.

The reactions were set up in an RNase-DNase free 96-well PCR plate on ice. Filter tips were used to avoid cross-contamination. The reactions were set up as follows:

Component	Final concentration	Volume in reaction
SYBR Green PCR MasterMix (2x)	1x	12.5µl
Primer 1	1.5mM	3µl of 25mM $MgCl_2$ solution
Primer 2	0.8µM	0.4µl of 100µM stock
cDNA template	0.8µM	0.4µl of 100µM stock
ddH_2O		Up to 25µl total reaction volume.

Table 2.11 Reaction conditions used in real-time PCR.

The 96-well plate was sealed with PCR cap strips and pulse-centrifuged at 500g before placing in the ABI 7300 PCR thermal cycler and initiating the reaction cycles.

The conditions used in the PCR are as follows:

	94°C	1′	Initial Denaturation step
30 Cycles	94°C	45″	Denaturation
	50-60 °C	30″	Annealing
	72°C	1′/1000 bp of cDNA	Elongation
	72°C	5′	Final Elongation step

The reaction data collected by the ABI 7300 were exported from the MX Pro software and processed in Microsoft Excel.

Protein Procedures

Analysis of proteins by Western Blotting

Sodium Dodecyl Sulfate Polyacrylamide Gel Electrophoresis (PAGE)

Proteins were separated according to their size by polyacrylamide gel electrophoresis, using a Tris based 12% polyacrylamide gel. The recipe for making a 12% polyacrylamide gel was as follows:

ddH_2O	3.4ml
3M Tris pH 8.8	1.25ml
10% SDS	100µl
Acrylamide/Bis-acrylamide (37.5:1)	4ml
10% ammonium persulfate (APS)	50µl
Temed	10µl

The stacker gel used was as follows:

ddH_2O	3ml
Stacking mix (0.4% SDS, 1.5M Tris pH6.8)	1.25ml
Acrylamide/Bis-acrylamide (37.5:1)	650µl
10% ammonium persulfate (APS)	25µl
Temed	10µl

An amount of 4x SDS loading buffer was added to the protein samples that were incubated for 10 minutes in a heat-block set at 100° C (volume of 4x loading buffer added equals 1/3rd of the initial sample volume). The samples were then pulsed-centrifuged and 20-35µl were loaded in the gel. The gels were ran at 170 Volts for one hour, or until the ion front (marked by the migration of the bromophenol blue dye) reached the bottom end of the gel.

The 4x SDS loading buffer was made as follows: 200mM Tris pH6.8, 8% (w/v) SDS, 0.4% (w/v) bromophenol blue, 40% (v/v) glycerol and 400mM β-mercaptoethanol.

Electroblotting of proteins to PVDF membrane

The proteins resolved in the polyacrylamide gel were transferred to PVDF membrane to facilitate the detection of specific proteins by immunodetection. The PVDF membrane was first soaked in methanol and then in transfer buffer together with a total of eight 3mm chromatography paper pieces (of equal size to the membrane). The gel was removed from the electrophoresis apparatus and the stacker was removed. The gel was immersed in transfer buffer and left to equilibrate for 5 minutes with gentle shaking. A semi-dry blotter was used, where a sandwich of the membrane and the gel was placed with four chromatography papers on either side. The gel was placed on the side of the negative pole while the membrane on the side of the positive pole and air-bubbles between the gel and membrane were removed with the aid of a roller. The transfer was at 22V for 40 minutes.

The transfer buffer was made as a 10x stock as follows:
48mM Tris, 39mM glycine, 1.3mM SDS. To make the 1x working solution 100ml of 10x were mixed with 200ml of methanol and 700ml of ddH_2O.

Coomassie Blue staining of the PVDF membranes

The PVDF membrane were removed from the transfer apparatus and left to dry. A pen was used to mark on the standard protein sizes on the membrane and the membrane was immersed in Coomassie Blue stain solution for 15 minutes with gentle shaking. Excess Coomassie stain was washed off with water and the membrane was destained

in destain solution for a total of 20 minutes. This allowed us to visualise the proteins as well as check for equal loading and quality of samples (in the case of brain extracts where excess lipids will cause a smear on the gel that will not resolve to a clean immunodetection).

The Coomassie stain was as follows:
0.1% (w/v) Coomassie Brilliant Blue, 45% (v/v) methanol, 45% ddH_2O and 10% (v/v) acetic acid. After dissolving the solution was filtered through 3mm chromatography paper to remove and Coomassie Brilliant Blue lumps.

The destain solution was as follows:
45% (v/v) methanol, 45% ddH_2O and 10% (v/v) acetic acid.

Immunodetection of proteins

After destaining the PVDF membrane was washed in PBS and blocked in 5% milk/0.1% Tween/PBS at room temperature for 30 minutes. It was then washed five times for five minutes in PBS/0.1% Tween and incubated with the appropriate antibodies in PBS/0.1% Tween for one hour at room temperature. After washing as above the membrane was incubated with the HRP-conjugated secondary antibody in PBS/0.1% Tween for an hour. After washing as above the membrane was immersed in ECL reagent for one minute. The excess ECL reagent was then carefully blotted off the bottom end of the membrane with a tissue, and the membrane was wrapped in plastic wrap before it was placed in a cassette with an ECL-hyperfilm to detect the immunofluorescence.

Cell Biology procedures

Solutions

Growth Media for COS-7 and N1E-115 cells: DMEM, 10% FCS, 1% Antibiotic/antimycotic.
Growth Media for HeLa cells: Eagle Minimum Media, 10% FCS, 1% Antibiotic/antimycotic, 4 mM L-Glutamine.
Freezing stock Solution: 10% DMSO, 90% FCS.

Primary Neurones Plating Media: OptiMEM, 10 % FCS, 20 mM Glucose, 1 % Antibiotic/ antimycotic.

NB plus Media: Neurobasal media, 1:50 dilution of B-27 supplement, 0.5 mM L-glutamine, 1 mM Sodium Pyruvate, 0.06 mg/ml Cysteine, 1% Antibiotic/ antimycotic.

COS-7 Lysis Buffer: 20 mM TrisHCl pH 7.4, 5 mM EDTA, 150 mM NaCl, 10% glycerol, 1% triton-X100.

N1E-115 Lysis Buffer: 25 mM HEPES pH 7.5, 0.3 M NaCl, 1 mM MgCl, 1 mM EGTA, 20 mM p-glycerophosphate, 5% glycerol, 1% triton-X100.

Inhibitors: 0.1 mM Sodium Vanadate, 10 mM Sodium Flouride, 5 mM DTT, 1x Protein inhibitor cocktail, 1 mM PMSF.

Recovery of Cells from Frozen Stocks

Vials of cells stored in liquid nitrogen were thawed in a 37° C water bath. Cells were re-suspended in pre-warmed media and centrifuged at 150 g for 5 minutes. The medium was decanted the cell pellet re-suspended in fresh media and plated onto cell culture dishes.

Freezing Down Cell Stocks

Cells were removed from the plate by pipetting or trypsinisation and centrifuged at 150 g for 5 minutes. Supernatant was decanted and the cell pellet was re-suspended in 1.5 ml of freezing stock solution and placed into a Cryovial. Cells were frozen gradually to -80 °C over night in an isopropanol-insulated container, before being stored in liquid nitrogen.

Cell Maintenance

All mammalian cells used in this study were maintained in 37° C, 5 % CO_2 incubators.

COS-7 cells (monkey) were maintained at the required density by splitting the culture. Cells were washed in PBS, trypsinised, and centrifuged at 150 g for 5 minutes. The supernatant was aspirated and the cells were re-suspended in media and plated at the desired densities.

Neuroblastoma N1E-115 cells (mouse) were plated on laminin-coated tissue culture dishes. They were maintained by detaching the cells from the tissue culture plate by pipetting, and re-plated at the required densities. The shRNA transfected neuroblastoma N1E-115 cells were selected in 400 μg/ml neomycin G418-containing media.

HeLa cells (human) were maintained at the desired density by trypsinisation and re-plating like COS-7 cells.

The primary hippocampal neurones isolated from e18 rat brains were maintained by replacing half of their NB plus media every 2-3 days.

Preparation of Coverslips

Glass coverslips (24 x 24mm^2, thickness 1) were treated with 40 % HCl/60 % ethanol for 10 minutes with shaking, and washed thoroughly with water. Coverslips were dried on blotting paper and baked overnight at 80° C wrapped in foil.
Coverslips were coated with laminin (1 hour in 10 μg/ml laminin) when used in N1E-115 neuroblastoma experiments. In plating primary neurones the coverslips were treated with 30μg/ml Poly-D-Lysine and 2 μg/ml laminin for an hour. The coverslips were washed in water and dried before being used in cell culture experiments.

Transient Transfection

For Pull-Down assays: COS-7 and N1E-115 neuroblastoma were plated at around 70% confluency in 10cm^2 dishes. A mix of 1 ml of DMEM, 2-5 μg DNA and 15 μl lipofectamine reagent (COS-7) or lipofectamine 2000 (N1E-115) was prepared and incubated at room temperature for 45 minutes. Cells were serum starved in DMEM for 45 mins and the transfection mix was added for 4 hours. The DMEM was replaced with normal media for 16 hours before harvesting.
For Immunocytochemistry: COS-7 and N1E-115 neuroblastoma were plated at around 70% confluency on coverslips in 3cm^2 dishes. A mix of 200 μl of DMEM, 1 μg DNA and 7 μl lipofectamine reagent (COS-7) or lipofectamine 2000 (N1E-115) was prepared and incubated at room temperature for 45 minutes. Cells were serum starved

in DMEM for 45 mins and the transfection mix was added for 4 hours. The DMEM was replaced with normal media for 16 hours before staining the cells.

HeLa cells were only used in immunocytochemistry experiments and were treated as above, while the cells were starved in 1 ml of Optimem medium and the transfection mix consisted of 100 µl Optimem medium, 6 µl Lipofectamin reagent and 1.5 µg DNA.

Cell Treatment with Phorbol 12-myristate 13-acetate (PMA)

PMA stock solution was made at 1 mM in DMSO and added to cells at a final concentration of 1 µM for 1 hour at 37° C, 5% CO_2.

Cell Treatment with Pervanadate

A 20 mM Na_3VO_4 stock was made in 600 µl of PBS, and activated by the addition of 1 µl of 30% v/v H_2O_2, followed by a 5 minute incubation at room temperature. A 20 mg/ml catalase stock was made in 50 mM Potassium Phosphate buffer pH 7.0, and 0.6 µl were added to the activated pervanadate solution, and incubated at room temperature for 5 minutes. The pervanadate stock was used at 1:200 dilution in the culture media and the cells were treated for 30′ at 37° C, 5% CO_2.

Affinity Purification of Proteins (pull-down assay)

Culture dishes (10cm^2) of COS-7 or N1E-115 transfected cells were placed on ice while the media was aspirated and the cells gently washed in cold PBS. Amount of 500 µl COS-7 or N1E-115 lysis buffer containing protease/phosphatase inhibitors was added to the dish and incubated for 30 minutes on ice. The cells were harvested using a rubber-policeman and the lysates centrifuged at 14,000 g for 15 minutes at 4° C. Amount of 100 µl of the soluble lysate was kept to be analysed by SDS-PAGE and western blotting for protein expression. The rest of the supernatant was incubated with 30 µl of the appropriate affinity beads (FLAG / HA antibody conjugated or glutathione sepharose beads) for 3 hours at 4° C on a rotary shaker. The beads were washed three times in 1 ml lysis buffer and re-suspended in 4x SDS sample buffer. Samples were stored at -20° C for further analysis by SDS-PAGE and western blot.

Preparation of dissociated e18 rat hippocampal neurones

Hippocampi were dissected from e18 rat brains while the procedure was performed in ice cold Hanks buffered saline solution (HBSS). The dissected tissue was incubated in 2 ml HBSS, 0.2 µg/ml of DNase 1, 0.05% trypsin for 15 minutes at 37° C. The solution was aspirated and the tissue was washed three times with 1 ml of plating media. The tissue was dissociated by pipetting with a glass Pasteur pipette. The end of the pipette had been narrowed by briefly holding in a Bunsen burner flame. Amount of 9 ml of plating media were added to the homogeneous cell suspension and the cells were counted by flow cytometry and centrifuged for a 5 minutes at 20 g. If the cells were to be plated they were re-suspended in plating media and plated at 200,000 cells per coverslip. The media was then replaced with NB plus media after allowing the cells to adhere to the coverslip for 3 hours. If cells were to be transfected by electroporation, they were treated as described below.

Electroporation of Neuronal Cells

After centrifugation the cells were resuspended in 100 µl of rat neurone nucleofector solution (Amaxa) per 2 million cells. Amount of 2 µg of DNA was transferred into the electroporation cuvettes and 100 µl of the resuspended cells added. The cuvettes were placed in the Nucleofector II electroporator and the standard programme 0-003 was used, recommended for electroporation of rat primary hippocampal neurones. Subsequently amount of 100 µl of plating media was added and the whole mix was plated onto coverslips in plating media. After 3 hours the plating media was changed to NB plus media.

Cell Immunostaining

Cells on coverslips were fixed in 4 % paraformaldehyde/PBS for 10 minutes at room temperature and subsequently washed two times in PBS for 10 minutes. Cells were permeabilised in 0.2 % triton/PBS for 7 minutes and blocked in PBS/3 % BSA for 30 minutes incubated at 37° C tissue culture incubator with controlled humidity. Primary antibodies were added at the appropriate dilution (see antibody table) in PBS/1 % BSA and the cells incubated in a 37° C incubator for 2 hours. The cells were washed three times for 10 minutes each in PBS. Secondary antibodies or probes were added at

the appropriate dilution and the cells were incubated for one hour at 37° C. Cells were washed three times for 10 minutes each in PBS. The coverslips were dried and mounted onto slides to be analysed by microscopy.

Microscopy

The cells were visualised using a Zeiss Axioplan fluorescent microscope or a Zeiss LSM 510 confocal microscope. The excitation channels FITC (488 nm), TRITC (568 nm) and Cy5 (633 nm) were used.

Subcellular fractionation of rat brain

Subcellular fractions were prepared from e14, e18 and adult rat brain homogenate in isotonic sucrose. The procedure was adapted from pioneering fractionation studies and is outlined in figure 2.2 (Whittaker and Barker, 1972; Booth and Clark, 1978). The tissue was homogenised in 10% (w/v) 50mM Tris/HCl pH 7.4, 75mM KCl, 5mM $MgCl_2$, 1mM DTT, 0.32M sucrose plus Protease Inhibitors and an initial centrifugation at 1000 g for 11 minutes obtained the crude nuclear fraction. The supernatant was spun at 17,000 g for 13 minutes to obtain a pellet fraction containing mitochondria, myelin, and synaptosomes. This pellet was resuspended in 50mM Tris/HCl pH 7.4, 75mM KCl, 5mM $MgCl_2$, 1mM DTT, 0.32M sucrose plus Protease Inhibitors and was fractionated through a discontinuous sucrose gradient (0.8M and 1.2M sucrose), separating the myelin, synaptosomal and pure mitochondria fractions under centrifugation at 63,000 g for 2 hours. The 17,000 g supernatant fraction was centrifuged at 100,000 × g for 1 hour to obtain the microsomal and cytosolic fractions. Pellet fractions were washed in isotonic solution before solubilising in SDS electrophoresis buffer, and soluble fractions were concentrated using Centriprep concentrators (Amicon, Beverly, MA).

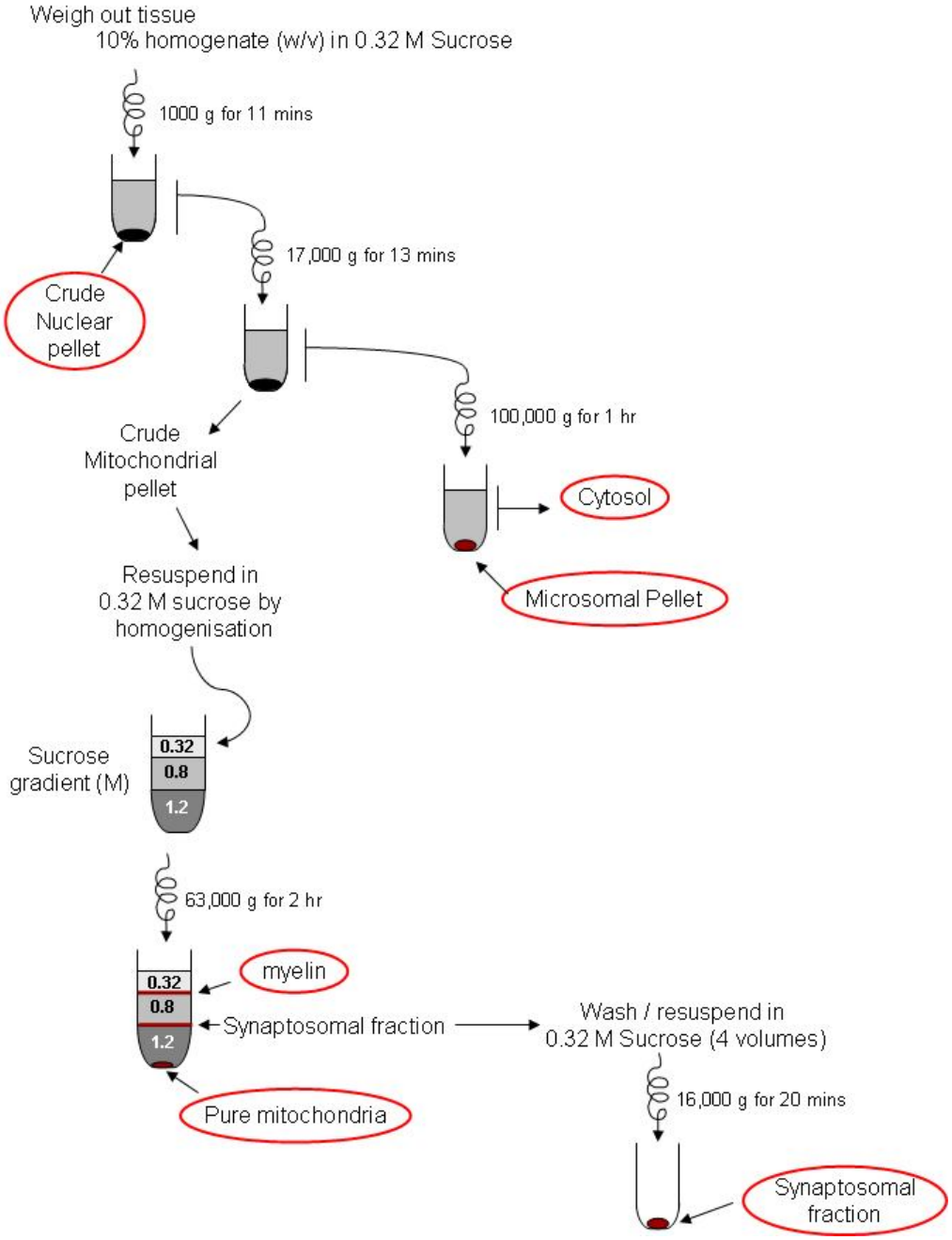

Figure 2.2 Subcellular fractionation of rat brain. Brains from e14, e18, 5d and 20d old rats were fractionated by a series of centrifucagtions in isotonic sucrose solution and through sucrose gradient cushions. The fractions obtained were crude nuclear, microsomal, myelin, pure mitochondria, synaptosomal and cytosolic.

Methyltransferase Assay

For the two *in vitro* methyltransferase assays presented here, two different reaction set-ups were followed. The reaction conditions were adapted from the work of Heurgué-Hamard and colleagues (Heurgué-Hamard et al, 2002). The reactions were carried in methylation assay buffer, that was prepared as 10x stock.

Methylation Assay Buffer:
10mM Tris/HCl, pH 7.6
50mM KCl
10mM MgAcetate
1mM DTT

Methylation Assay 1:
For the preparation of the enzyme proteins, three confluent COS-7 plates were transfected with HA-HemK1, two with HA-HemK1 and three with HA-HemK1 + HA-TRMT112. After 16 hrs expression the cells were lysed in 0.5 ml/plate hypotonic buffer: 20mM Tris/HCl pH 7.0, 10mM KCl, 2mM PMSF, 1mM NaF, 1mM $NaVO_4$, 0.5mM DTT, Roche Protease Inhibitor Cocktail. The cells were harvested with a rubber policeman and centrifuged for 10 mins at 14,000 rpm, 4° C in a microcentrifuge. The supernatant was kept on ice and used in the methylation assay.

For the preparation of the substrate proteins, six confluent plates of COS-7 cells were transfected with GST-eRF1 + HA-eRF3. After 16 hrs expression the cells were lysed in 1ml/plate COS-7 lysis buffer, the cells were harvested and the lysates centrifuged for 10 min at 14,000 rpm, 4° C in a microcentrifuge. The supernatant was incubated with 350µl of GST beads for 3hrs, rotating at 4° C. The beads were washed three times in methylation assay buffer and resuspended in 500µl methylation assay buffer.

The methylation reactions were prepared in 1.5ml microcentrifuge tubes on ice, and the enzyme protein lysate and S-adenosyl-L-[methyl-^{3}H]methionine were added last. Table 2.12 summarises the reaction set-up.

	1	2	3	4	5	6
eRFs	-	120	120	120	-	-
HA-HemK1 COS-7 lysate	-	700	-	-	300	-
HA-HemK1+TRMT112 COS-7 lysate	-	-	700	-	-	300
HA-HemK1 N239A+TRMT112 Cos 7 lysate	-	-	-	500	-	-
10x Methylation Assay Buffer	96	96	96	96	36	36
S-adenosyl-L-[methyl-^{3}H]methionine	25	25	25	25	18	18
GTP (50mM stock)	19	19	19	19	7	7
ddH_2O	820	-	-	200	-	-
Total Volume	960	960	960	960	361	361

Table 2.12 Reaction conditions of Methylation Assay 1. The amounts of each reagent used in each reaction are stated in µl.

The reactions were incubated for 2 hrs at 37° C with rotation. After the completion of the reaction, amount of 10µl of samples 1, 2, 3 and 4 was washed with methylation buffer to wash off the COS-7 lysate from the GST beads, and blotted on a PVDF membrane. Amount of 10µl of samples 5 and 6 was blotted on PVDF membranes. The membranes were washed with methylation buffer and a scintillation counter was used to measure the radioactivity of the washed membranes. Furthermore, 30µl of the same samples was analysed by SDS-PAGE, where the polyacrylamide gel was transferred on a PVDF. The membrane was dried, sprayed with enhancer spray (En3hance) and left to expose an autoradiography film for 3 weeks at -80° C.

Methylation Assay 2:

For the preparation of the enzyme proteins, three confluent COS-7 plates were transfected with each of the constructs GST-HemK1 and FLAG-HemK1. The cells were lysed in COS-7 lysis buffer after 16 hrs expression. GST and FLAG beads were used to immunopurify the expressed proteins.

For the preparation of the substrates, *E.coli* cells were transformed with mtRG1 and mtRF1a GST constructs, plated on agar plates and incubated at 37° C overnight. Colonies were inoculated in 400ml of LB media supplemented with ampicillin and grown at 37° C until an absorbance of OD_{600} = 1 was achieved. Protein expression was induced by addition of 0.25 mg/ml IPTG and the cells were incubated for 3 hrs at

room temperature with agitation. The cells were centrifuged for 10 minutes at 6,000 rpm at 4° C and the cell pellet was frozen at -80° C. The pellet was thawed on ice and resuspended in 40ml of cold bacteria cell lysis buffer (PBS, 1 % Triton X-100, 0.5 mM $MgCl_2$, Protease Inhibitors). The cells were sonicated for five minutes (with 5 seconds pause every 20 seconds sonication) on ice and centrifuged at 14,000 g, 4° C for 30 minutes. Amount of 500µl of Glutathione sepharose (GST) beads were incubated in the supernatant for 3 hrs at 4° C and subsequently washed three times in cold bacterial lysis buffer. The proteins were eluted off the beads by incubation in 10ml of elution buffer (10mM glutathione, 50mM Tris-HCL pH 8.0, 5% glycerol) for 15 minutes at room temperature. The protein eluate was concentrated in Centricon columns, down to 150µl final volume.

The methylation reactions were set-up as described in table 2.13.

	1	2	3	4	5	6	7	8	9	10	11
GST-HemK1	45	-	-	-	-	45	80	80	-	-	-
FLAG-HemK1	-	45	-	-	-	-	-	-	45	80	80
GST-mtRF1	-	-	50	-	-	-	50	-	-	50	-
GST-mtRF1a	-	-	-	50	-	-	-	50	-	-	50
COS-7 lysate	-	-	-	-	50	50	-	-	50	-	-
GTP (50mM stock)	3.2	3.2	3.2	3.2	3.2	3.2	3.2	3.2	3.2	3.2	3.2
S-adenosyl-L-[methyl-^{3}H]methionine	10	10	10	10	10	10	10	10	10	10	10
BSA	5	5	-	-	-	-	-	-	-	-	-
ddH_2O	80	80	80	80	80	35	-	-	35	-	-
10x Methylation Assay Buffer	16	16	16	16	16	16	16	16	16	16	16

Table 2.13 Reaction conditions of Methylation Assay 2. The amounts of each reagent used in each reaction are stated in µl.

The reactions were incubated rotating for 2 hrs at 37 °C. Amount of 10µl of the reactions were blotted on PVDF membranes that were washed in methylation buffer

and radioactivity was measured in a scintillation counter. Amount of 40µl of the reactions was analysed by SDS-PAGE and transferred on PVDF membrane that was dried, sprayed with enhance spray and placed in a cassette with an autoradiography film for two weeks at -80° C, before developing the film.

Chapter 3

[Results I]

HemK proteins associate with α2-chimaerin

α2-Chimaerin interacts with HemK1

The neuronal protein α2-Chimaerin is involved in EphA4 signalling pathways via its GAP and SH2 domains, and also interacts with CRMP-2 and Cdk5 as part of the Sema3A collapse pathway. There has been an increasing amount of findings supporting an important role of α2-chimaerin in Rac1-dependent signalling pathways and neurite morphology, and therefore an investigation of novel interacting partners is of great interest. In previous experiments in our laboratory a yeast two-hybrid screen on a human brain cDNA library identified HemK1 as a possible novel partner. The screen involved the deletion mutant Δ1-39 α2-chimaerin, which renders chimaerin active by abolishing intra-molecular interactions mediated by the N-terminal that would otherwise support an auto-inhibitory conformation. In order to verify the interaction between α2-chimaerin and HemK1 in mammalian cells, the two proteins were used in pull-down experiments in COS-7 cells. Both proteins had been cloned in pXJ40 mammalian expression vectors carrying N-terminal GST, HA or FLAG tags. A brief over-expression experiment in COS-7 cells indicated that FLAG-fusion HemK1 protein was highly insoluble in COS-7 cells in 1% Triton-containing buffer (Figure 3.1). The GST-HemK1 construct was therefore used in these pull-down experiments (Figure 3.2).

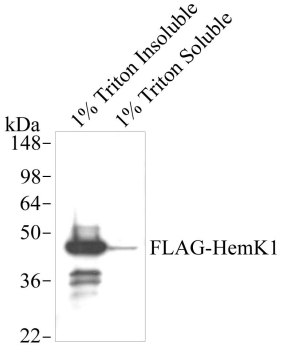

Figure 3.1 FLAG-HemK1 is predominantly insoluble in 1% Triton-containing lysis buffer. Lysates of COS-7 cells transfected with FLAG-HemK1 were analysed by western blotting (mouse anti-FLAG antibody). In 1% Triton X-100 lysis buffer FLAG-HemK1 was mostly detected in the insoluble fraction.

α2-Chimaerin associates with HemK1 in over-expression studies

In order to verify the interaction between HemK1 and α2-chimaerin in mammalian cells, the two cDNA constructs were used in a pull-down assay performed in COS-7 cells. The human α2-chimaerin and HemK1 cDNA clones were co-expressed as FLAG and GST tag fusion proteins constructs respectively. The cells were lysed and SDS-PAGE and western blot analysis using anti-FLAG and anti-GST antibodies revealed the expression of FLAG-α2-chimaerin and GST-HemK1. FLAG-α2-chimaerin was affinity purified from cell lysates using anti-FLAG conjugated beads and western blot analysis with anti-GST-antibodies revealed association with GST-HemK1 (Figure 3.2A). The association was further enhanced when the cells were treated with the phorbol ester analogue PMA that can activate chimaerin by binding to its C1 domain. The negative control for this experiment is presented in figure 3.2B where it is shown that GST-HemK1 or GST-HemK2 do not associate with anti-FLAG beads, when over-expressed in COS-7 cells.

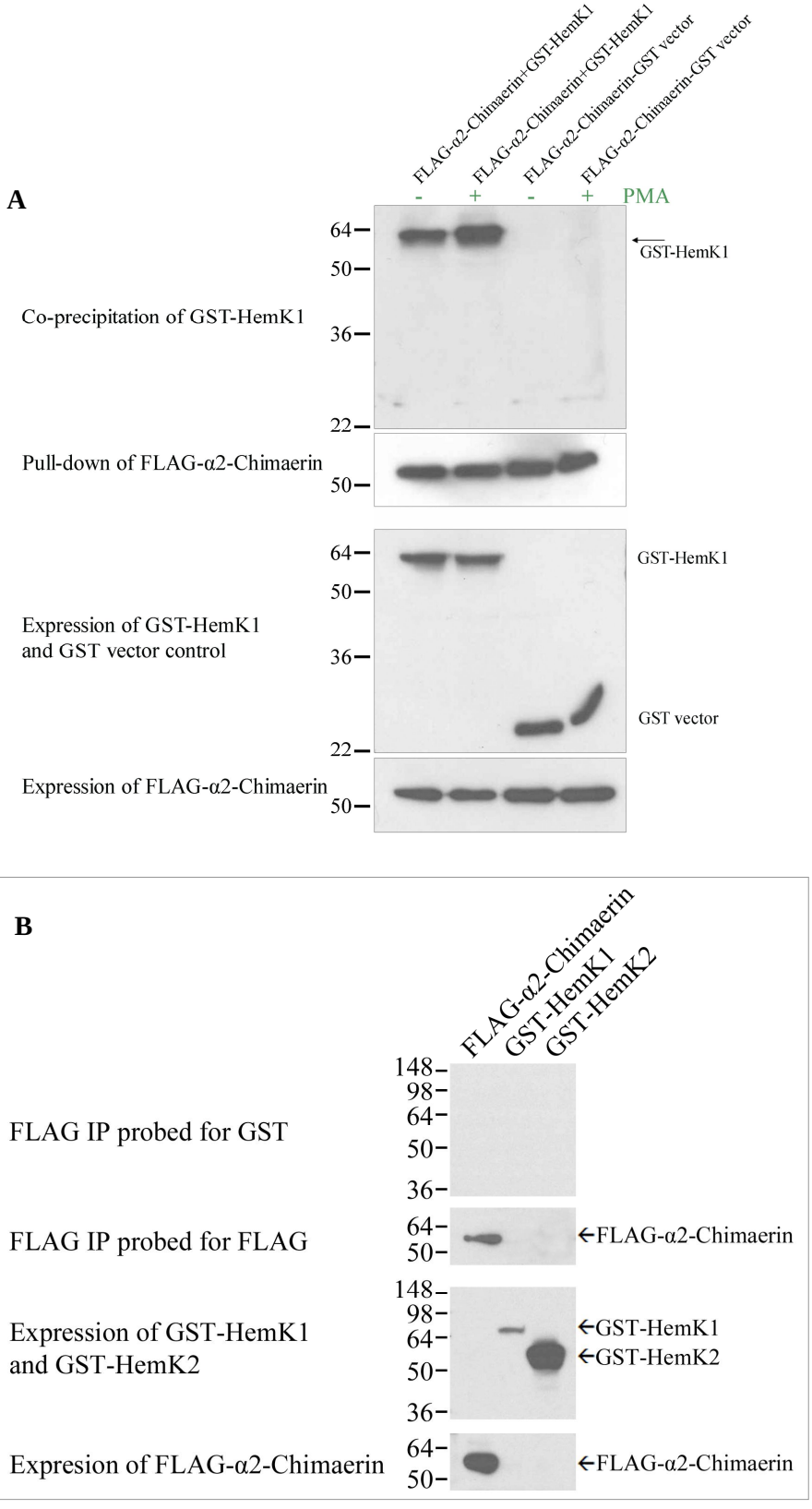

Figure 3.2 α2-Chimaerin and HemK1 can associate in cells. (A) COS-7 cells were transfected with FLAG-α2-chimaerin, GST-HemK1 and GST-vector control construct and were lysed after over-night expression. FLAG beads were used to affinity purify α2-chimaerin and analysed by SDS-PAGE. Western blot with rabbit anti-FLAG and mouse anti-GST antibodies revealed co-precipitated HemK1, while no co-precipitation of the GST-vector control protein was detected (top panel). (B) Control experiment showing that GST-HemK1 and GST-HemK2 do not associate with anti-FLAG beads when over-expressed in COS-7 cells.

To identify the α2-chimaerin domains responsible for the association with HemK1, a series of α2-chimaerin deletion constructs encoding for different parts of the protein were used in a similar pull-down assay (Figure 3.3). The constructs used were: a) full-length α2-chimaerin, b) amino acids 39-459 where the short N terminal region important for the inactive auto-inhibiting conformation is deleted, c) amino acids 196-459 that include the C1 and GAP domains, d) amino acids 268-459 that comprise the GAP domain and e) amino acids 1-137 that contain the SH2 domain. All constructs were able to associate with HemK1 as shown in the pull-down with a clear increase in association when chimaerin is missing the first 38 amino acids. The association was observed with all the chimaerin constructs indicating a number of interacting residues between the two proteins. The best binding was observed with the SH2 domain of chimaerin (aa 1-137), and this finding was reproducible, raising the possibility of a phosphotyrosine-dependent association.

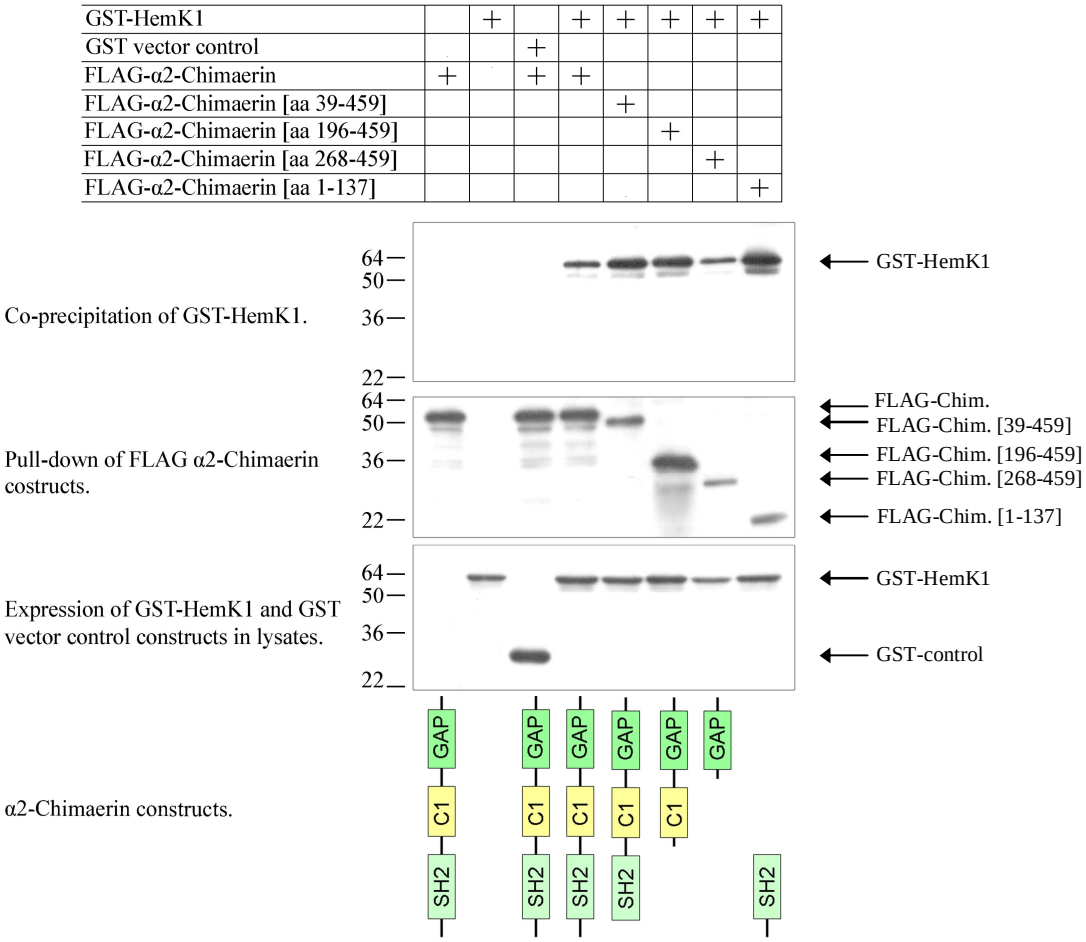

Figure 3.3 HemK1 can associate with deletion constructs of α2-Chimaerin in cells. COS-7 cells were transfected with FLAG-conjugated α2-chimaerin deletion constructs, GST-HemK1 and GST-vector control constructs and were lysed after over-night expression. FLAG beads were used to affinity purify the α2-chimaerin proteins and SDS-PAGE analysis with relevant antibodies revealed co-precipitated HemK1 with all α2-chimaerin deletion constructs, while no co-precipitation of the GST-vector control protein was detected.

It was observed that HemK1 showed the highest association with the SH2 domain of α2-chimaerin [aa 1-137]. This raised the possibility of a phospho-tyrosine dependent interaction. To investigate if the association between HemK1 and chimaerin is phospho-tyrosine dependent, a pull-down experiment was carried out in which GST-HemK1 and FLAG-α2-chimaerin [aa 1-137] were co-expressed in COS-7 cells and immuno-precipitated with anti-FLAG beads. The COS-7 cells were treated with pervanadate before lysis, a protein-tyrosine phosphatase inhibitor, to upregulate tyrosine phosphorylation. The immunoprecipitated samples were analysed by SDS-PAGE and western blot, and probed for anti-GST antibody to check for increased amount of co-immunoprecipitated HemK1 in pervanadate-treated cells, and with 4G10 anti-phospho-tyrosine antibody to detect if co-immunoprecipitated HemK1 is tyrosine phosphorylated (Figure 3.4). An increase in tyrosine-phosphorylated species present in the lysates of pervanadate-treated COS-7 cells was observed as probed with 4G10 (data not shown). No increase in the amount of HemK1 that co-immunoprecipitated with FLAG-α2-chimaerin [aa 1-137] was observed in pervanadate-treated cells. Probing the immunoprecipitation blot with 4G10 did however detect GST-HemK1, indicating that co-immunoprecipitated HemK1 is tyrosine phosphorylated (Figure 3.4). This suggests that the association between FLAG-α2-chimaerin and HemK1 is unlikely to be phospho-tyrosine dependent, while the SH2 domain of α2-chimaerin is adequate to mediate association between the two proteins, and co-immunoprecipitated HemK1 is tyrosine-phosphorylated. The SH2 domain of α2-chimaerin is slightly atypical and so far no phospho-tyrosine peptide target sequences have been identified, nevertheless mutation of the essential arginine amino acid of the SH2 domain inactivates chimaerin in the growth cone collapse EphA4 pathway (Songyang et al, 1993; Shi et al, 2007).

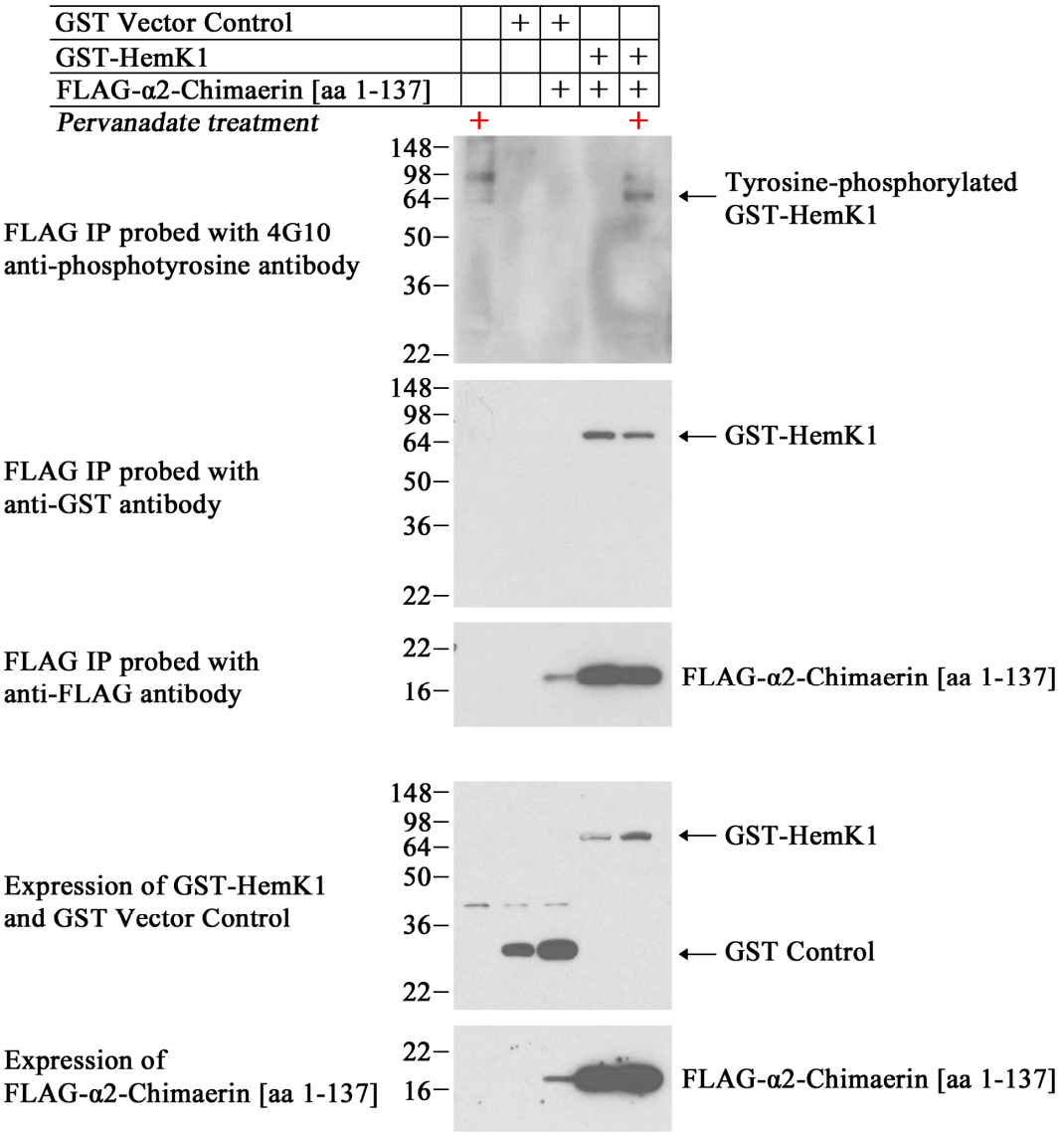

Figure 3.4 HemK1 is tyrosine phosphorylated but this does not increase association with the SH2 domain of α2-Chimaerin in cells. COS-7 cells were transfected with FLAG-conjugated α2-chimaerin [aa 1-137], GST-HemK1 and GST-vector control constructs and were treated/untreated with pervanadate after over-night expression, before being lysed. FLAG beads were used to affinity purify α2-chimaerin [aa 1-137] and SDS-PAGE analysis with relevant antibodies revealed co-precipitated HemK1, while no co-precipitation of the GST-vector control protein was detected. Pervanadate treatment did not increase the association between HemK1 and α2-chimaerin [aa 1-137]. The immunoprecipitation blot was probed with 4G10 anti-phospho-tyrosine antibody revealing phosphorylated GST-HemK1, co-immunoprecipitated with FLAG- α2-chimaerin [aa 1-137]. A contaminating band of around 40kD can be seen in the expression of GST-HemK1 and GST Vector Control blot.

α2-Chimaerin interacts with HemK2

The unique function of HemK1, to methylate glutamine residues at the conserved GGQ motif of polypeptide chain release factors, is shared with close homologue HemK2. HemK1 is predicted to be mitochondrial, something not supported for HemK2. α2-Chimaerin has not been linked to mitochondria and HemK1 and HemK2 are closely related and highly conserved in species. The possibility that α2-chimaerin can associate with HemK2 was therefore investigated, that if true it could constitute HemK2 as α2-chimaerin's real biological partner.

Cloning of human HemK2 cDNA

The cDNA encoding for the human HemK2 was obtained from Source Bioscience Gene Service (clone ID: 5163231). The cDNA obtained was missing the first eight nucleotides of the coding region, so the primers used in cloning were designed to incorporate the missing nucleic acids as well as the restriction sites HindIII and PstI for insertion in the vector (see Materials and Methods chapter). HemK2 cDNA was cloned in pXJ40 vectors carrying the tags FLAG, HA and GST. These vectors carry the mammalian CMV promoter and the AmpR gene used in *E.coli* selection in cloning. The HemK2 cDNA was amplified by a two step PCR, since the missing base pairs from the 5′ end had to be incorporated along with the restriction sites for cloning, and thus the extra sequence that had to be generated was too long to be accomplished by using one set of primers. The initial amplification incorporated the first eight base pairs of the coding sequence on the 5′ end and a PstI site on the 3′ end of the cDNA. This PCR product was subjected to a second amplification using the same 3′ end primer and a 5′ end primer that incorporated the HindIII site (Figure 3.5).

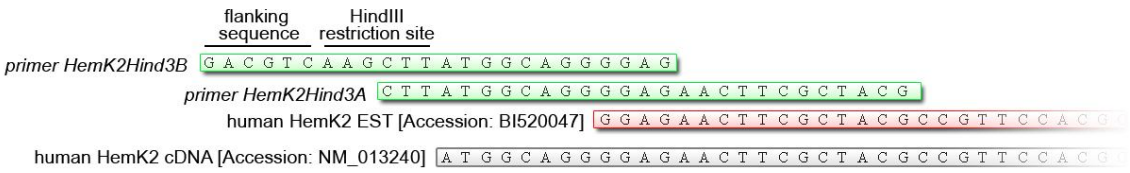

Figure 3.5 PCR strategy followed in cloning HemK2. The HemK2 cDNA obtained was missing the first 8 base pairs of the 5′ end. A two step PCR strategy incorporated the missing base pairs along with the restriction sites used to clone HemK2 in pXJ40 mammalian expression vectors.

The conditions of the PCR were optimised by increasing the annealing temperature of the reaction, to give one clean band on the gel and to ensure that the correct and complete sequence would be cloned in the expression vectors (Figure 3.6A). After successful cloning all the positive clones were sequenced using a universal primer complementary to the pXJ40 T7 promoter region and a designed oligo that primes downstream of the multiple cloning site of the pXJ40 vectors (see Materials and Methods). The clones were tested for protein expression in COS-7 mammalian cells (Figure 3.6B).

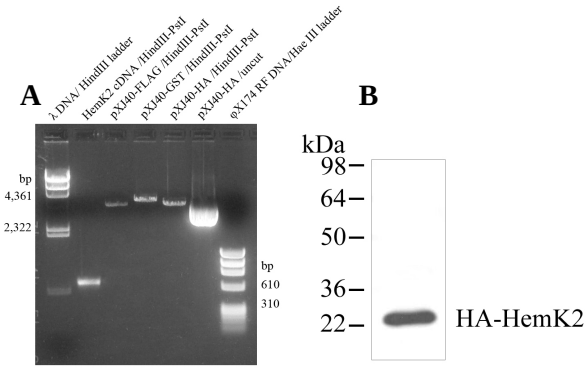

Figure 3.6 Cloning of HemK2 in mammalian expression vectors. (A) The amplified HemK2 DNA and vector constructs digested with the restriction enzymes were analysed by agarose gel electrophoresis before ligation. (B) HemK2 expression of HA-fused protein as analysed by western blot of lysates of transfected COS-7 cells.

α2-Chimaerin interacts with HemK2 in over-expression studies

The hypothesis that HemK2 can associate with α2-chimaerin was tested in over-expression pull-down experiments in COS-7 cells (Figure 3.7). In this experiment HemK1 and HemK2 were co-expressed as GST fusion constructs and over-expressed FLAG-α2-chimaerin was immunoprecipitated using anti-FLAG antibody associated beads. Both HemK1 and HemK2 associated with chimaerin in the pull-down.

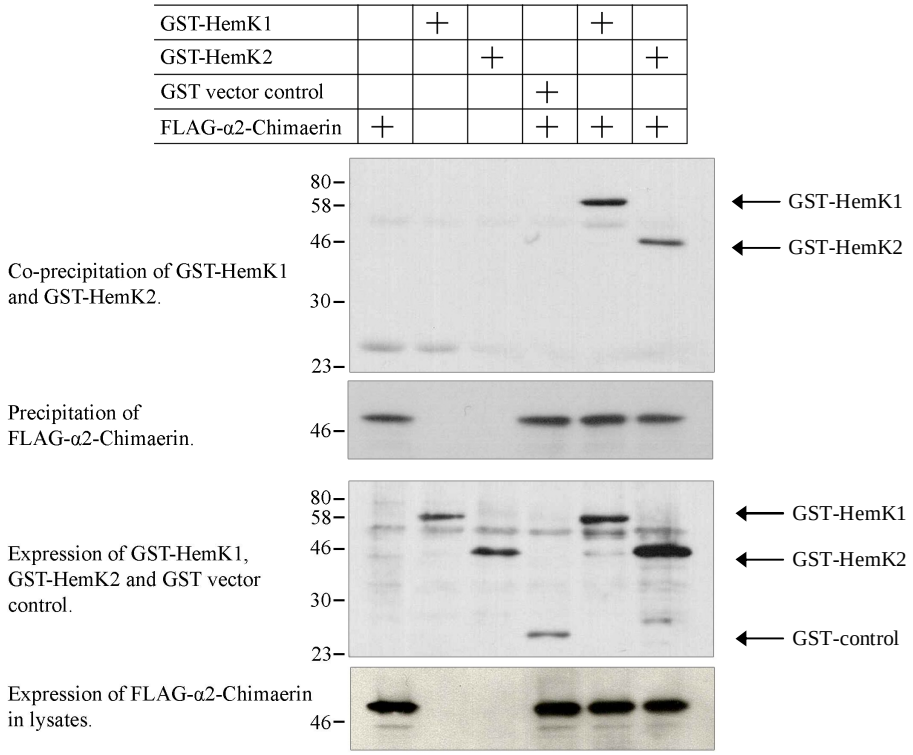

Figure 3.7 HemK1 and HemK2 can associate with α2-chimaerin in cells. COS-7 cells were transfected with FLAG-α2-chimaerin, GST-HemK1, GST-HemK2 and GST-vector control constructs and were lysed after over-night expression. FLAG beads were used to affinity purify the α2-chimaerin and SDS-PAGE analysis with relevant antibodies revealed co-precipitated HemK1 and HemK2, while no co-precipitation of the GST-vector control protein was detected.

To determine which part of chimaerin is responsible for the observed association with HemK2. A series of FLAG-tag chimaerin constructs were used in a similar pull-down assay where GST-HemK2 was co-precipitated with chimaerin deletion constructs. HemK2 associated with α2-chimaerin [39-459] where the deletion of the first 38 amino acids allows for an "open" conformation and would allow access of HemK1 to interacting sites. Weaker association was observed with full length and the C1-GAP, GAP and SH2 domains separately, suggesting a number of sites on α2-chimaerin that are involved in HemK2 association (Figure 3.8)

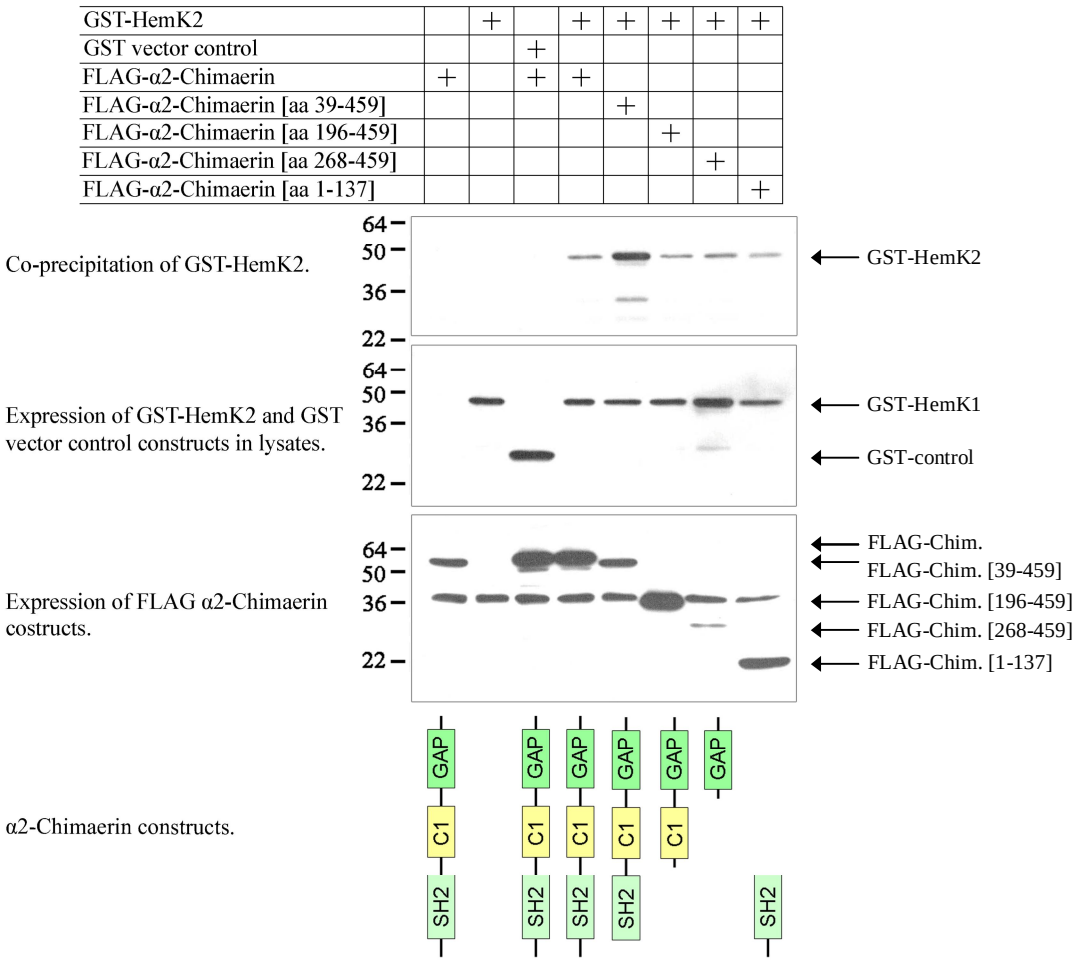

Figure 3.8 HemK2 can associate with deletion constructs of α2-Chimaerin in cells. COS-7 cells were transfected with FLAG-conjugated α2-chimaerin deletion constructs, GST-HemK2 and GST-vector control constructs and were lysed after over-night expression. FLAG beads were used to affinity purify the α2-chimaerin proteins and SDS-PAGE analysis with relevant antibodies revealed co-precipitated HemK2 with all α2-chimaerin deletion constructs, while no co-precipitation of the GST-vector control protein was detected. The highest association was observed with FLAG-α2-chimaerin [39-459] that is believed to exist in an open conformation making possible interacting sites more accessible. A contaminating band is observed in the lower panel where expression of α2-chimaerin constructs is detected using a rabbit anti-FLAG primary antibody. The non-specific band recognised by the rabbit-anti-FLAG antibody is between 36 and 50 kDa and partially overlaps with FLAG-α2-chimaerin [196-459], that can be observed directly below it.

HemK1 but not HemK2 can associate with CRMP-2

α2-Chimaerin associates with CRMP-2, a protein involved in growth cone collapse through the Rac dependent Sema3A pathway (Brown et al, 2004). The association of both HemK1 and HemK2 with α2-chimaerin raises the possibility the two N5-methyltransferases are involved in signalling pathways affecting neuronal morphology through α2-chimaerin and its interacting partners. The hypothesis that HemK1 and HemK2 are involved in an α2-chimaerin signalling pathway involving CRMP-2 was tested by pull-down experiments in mammalian cells. In a pull-down experiment in N1E-115 neuroblastoma cells over-expressed FLAG-CRMP-2 co-precipitated HA-HemK1 but not HA-HemK2 (Figure 3.9). This preliminary finding was not investigated further due to time restrictions. It does however suggest that HemK1 is the *bona fide* partner of α2-chimaerin implicating HemK1 in pathways of neuronal morphology.

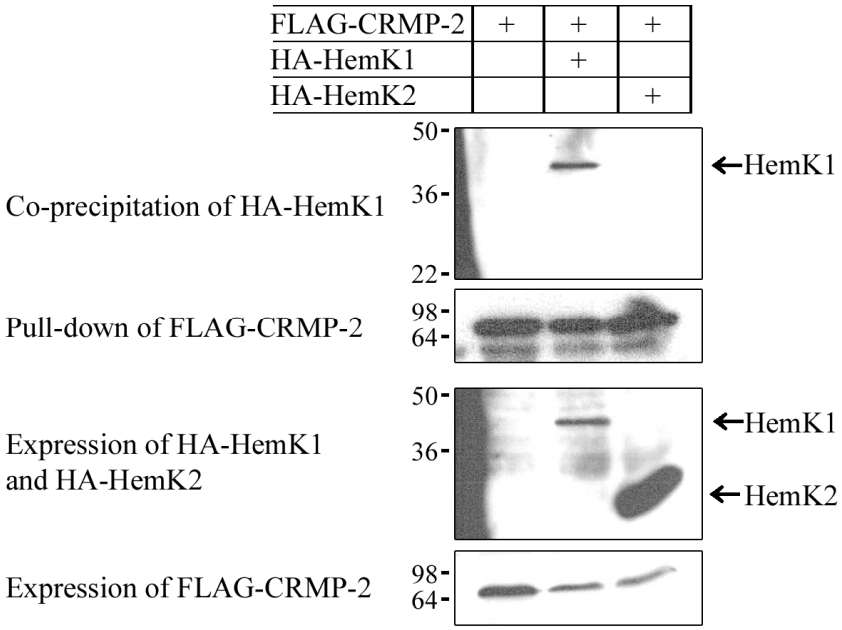

Figure 3.9 HemK1 can associate with CRMP-2 in cells. COS-7 cells were transfected with FLAG-conjugated CRMP-2, HA-HemK1 and HA-HemK2 and were lysed after over-night expression. FLAG beads were used to affinity purify CRMP-2 and SDS-PAGE analysis with relevant antibodies revealed co-precipitated HemK1, while no co-precipitated HemK2 was observed.

Summary

Following an initial observation of HemK1 associating with α2-chimaerin in a yeast two-hybrid screen, the interaction was verified in a mammalian system. The two proteins were over-expressed and affinity purified revealing an association between the two full length proteins. This association was enhanced under treatment with PMA, a phorbol ester analogue that causes a conformational change on chimaerin rendering it more accessible to interacting proteins. A GST tag conjugated HemK1 construct was used in this assay since it was found to be more soluble in 1% Triton X-100, than the FLAG and HA tag conjugated constructs. HemK1 associated with partial clones of α2-chimaerin indicating a number of sites on chimaerin that are responsible for the association.

The HemK1-related protein HemK2 was tested for association with α2-chimaerin since the two related proteins share a conserved function across species, methylating release factors as part of translation termination machinery. HemK2 was found to associate with full length and also partial constructs of α2-chimaerin in pull-down assays. In both HemK1 and HemK2 pull-down studies, the two proteins showed increased association with the α2-chimaerin constructs that were missing the first 38 amino acids that contribute to the auto-inhibiting closed conformation of chimaerin. HemK1 but not HemK2 was able to associate with CRMP-2, suggesting possible involvement of HemK1 in signalling pathways led by α2-chimaerin and involving its established interacting partner CRMP-2.

Chapter 4

[Results II]

HemK1 and HemK2 expression in the brain

HemK1 and HemK2 transcript levels in brain

The mRNA transcript levels of N5-methyltransferases HemK1 and HemK2 were investigated and compared to α2-chimaerin in rat brains using quantitative real-time PCR methodology. RNA was purified from rat brains and reverse transcribed to cDNA to be used in the real-time PCR analysis.

Assessment of RNA purity and integrity

The quality of the purified brain RNA was determined by formaldehyde agarose gel electrophoresis and spectrophotometric analysis. Formaldehyde agarose gel electrophoresis was used to check the integrity of the purified RNA. Figure 4.1 shows RNA purified from embryonic day 12 and 18, and from cortex and cerebellum of day 5 and day 20 rat brains. The 28S and 18S ribosomal RNA complexes are clearly visible on the gel. The 28S rRNA band is approximately twice as intense as the 18S and this is a good indicator that the purified RNA is not degraded.

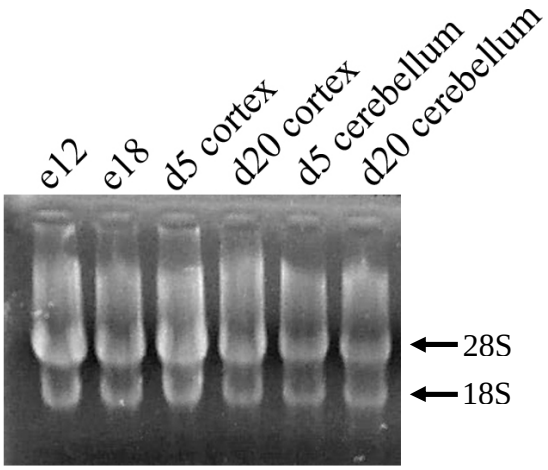

Figure 4.1 Integrity check for purified rat cortex and cerebellum RNA. RNA purified from e12 and e18 rat brains, and from cortex and cerebellum of d5 and d20 rat brains was analysis by formaldehyde agarose gel electrophoresis and visualised by UV after staining with ethidium bromide. The 28S rRNA band is approximately twice as intense as the 18S and smaller degradation products were also absent.

Purity and concentration of the purified RNA were analysed by using a Nanodrop spectrophotometer. The absorbance ratios A_{260}/A_{280} and A_{260}/A_{230} give an indication of possible protein and guanidium thiocyanate contamination respectively. All RNA preparations had A_{260}/A_{280} and A_{260}/A_{230} ratios of ≥ 2.0, which indicates high RNA purity.

Real-Time PCR setup/analysis

The primers used in the real-time PCR analysis to amplify sections of the mature mRNA sequences were designed to intercept mRNA intron-exon boundaries, to avoid possible genomic DNA amplification. This was initially tested by using the on-line In-Silico PCR on the UCSC Genome Browser website (http://genome.ucsc.edu/cgi-bin/hgPcr) that retrieved no genomic amplification products using the designed primers. The size of the amplified regions varied between 180-250 base-pairs, and the PCR conditions were optimised by varying the annealing temperature of the reaction. The specificity of the real-time primers and the reaction conditions were tested by agarose gel electrophoresis of the reaction products that revealed a single band of the expected size for each amplification reaction (Figure 4.2).

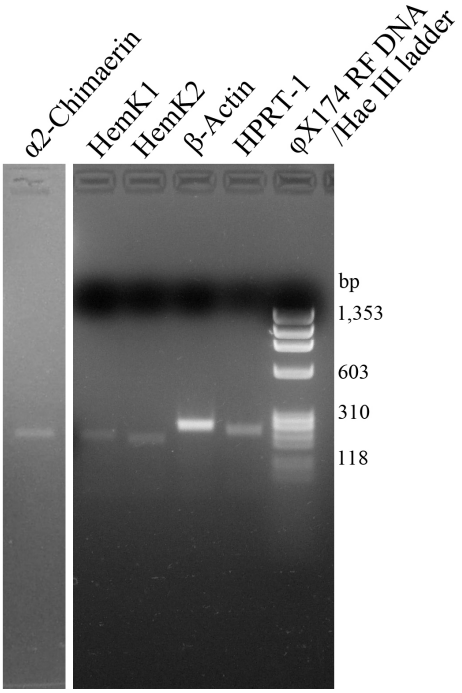

Figure 4.2 Agarose gel electrophoresis of Real-Time PCR products. The specificity of the real-time primers PCR primers and the reaction conditions were checked by agarose gel electrophoresis of the reaction products. The template was cDNA reverse transcribed from e18 rat brain mRNA. The gel shows a single band for all real-time amplification reactions: α2-chimaerin, HemK1, HemK2 and the house-keeping genes β-actin and HPRT-1.

The efficiency of each reaction was calculated by the real-time PCR software MxPro, based on the values obtained from the constructed standard curve (Figure 4.3). A standard curve of amplification was constructed for each primer pair by the amplification of a series of dilutions of a known concentration cDNA template. The standard curve shows the C_t values for each reaction plotted against the initial template quantity of each of the dilutions. This is used by the software to calculate the efficiency of the reaction, a value that reflects on the specificity of the primers as well as the reaction conditions. All primer pairs featured a calculated PCR efficiency of higher than 90% indicating optimal conditions. The standard curve is used by the software to calculate the relative levels of transcripts in "unknown" samples by extrapolating initial template quantity data from the standard curve dilution samples. The standard curve also gives an indication of pipetting error, since each reaction was set in triplicate, and the plot shows all three values of each reaction.

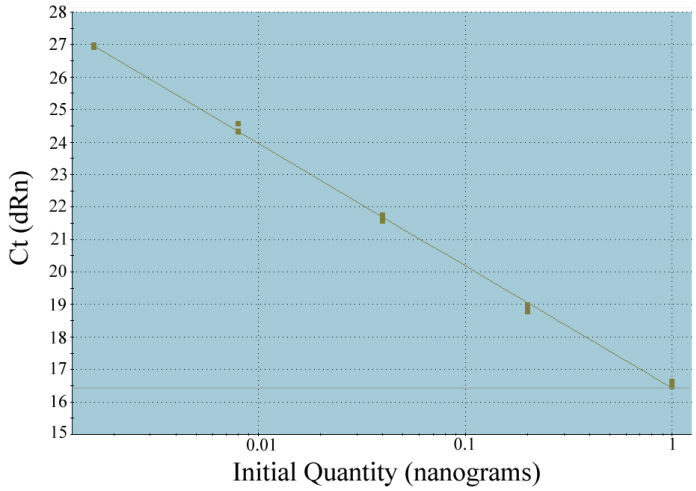

Figure 4.3 Standard Curve for β-actin real-time PCR. The construction of a standard curve on known cDNA dilutions allows the researcher to estimate by extrapolation the initial quantity amounts of unknown samples. The efficiency of the real-time reaction is also calculated by the Standard Curve and triplicate values can give an indication of possible pipetting error.

A second checkpoint for the conditions used in the PCR was provided by the real-time PCR program MxPro that generates a dissociation curve for each PCR run. At the end of the reaction the temperature is raised in step-wise fashion and the fluorescence of SYBR Green is measured, revealing a big drop in emission when the PCR products denature to single stranded DNA. Since SYBR Green intercalates with all double stranded DNA the dissociation curve will show an additional peak of fluorescence change in the case of DNA contamination, non-specific priming and also formation of primer-dimer complexes. The software plots the rate of fluorescence change with time (-d(RFU)/dT) versus the temperature of each step. Dissociation curves were constructed for all reactions and the real-time PCR of HemK1, HemK2, β-actin and

HPRT-1 all showed a single peak of fluorescence drop, indicating the presence of a single product (Figure 4.4).

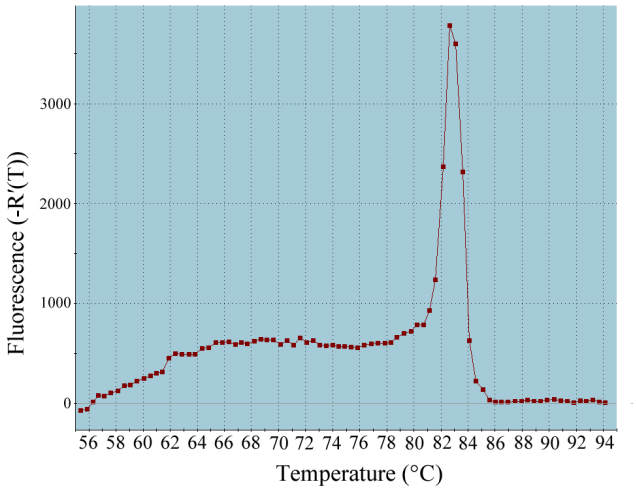

Figure 4.4 Dissociation Curve of β-actin real-time PCR. The construction of a dissociation curve allows for the detection of non-specific PCR products, DNA contamination or primer-dimers. A single peak of fluorescence-change was detected indicating the presence of a single PCR product.

Figure 4.5A shows the dissociation curves of three α2-chimaerin real-time amplification reactions on rat brain RNA. The dissociation curve of α2-chimaerin PCR showed two peaks, indicating the presence of two products (Figure 4.5A). The two peaks featured very close melting temperatures (approximately 2 °C difference) and also comparable -d(RFU)/dT values. These data indicate that if there are indeed two products of the PCR, they are very similar in length and GC content and their final quantities at the completion of the amplification reaction are comparable. On the dissociation curves plot (Figure 4.5A) the red graph represents a PCR with 9.52 ng of corresponding initial RNA template and the orange a reaction with 0.38 ng initial RNA template, so the two reactions differed by a factor of 1:25 in initial cDNA template. The green graph represents the negative control where no cDNA template was included in the reaction. The fact that both peaks drop when less template is used and that the negative control does not show any peaks indicate that there are no primer-dimer products formed under the conditions used. When the PCR products were analysed by agarose gel electrophoresis only a single band was observed (Figure 4.5B). Sequencing of the α2-chimaerin real-time PCR products retrieved a sequence that matched the human α2-chimaerin cDNA. It was therefore concluded that the two peaks in the dissociation curve represent an anomaly in respect to the PCR product's denaturation that could be a consequence of its GC content or the formation of a secondary structure.

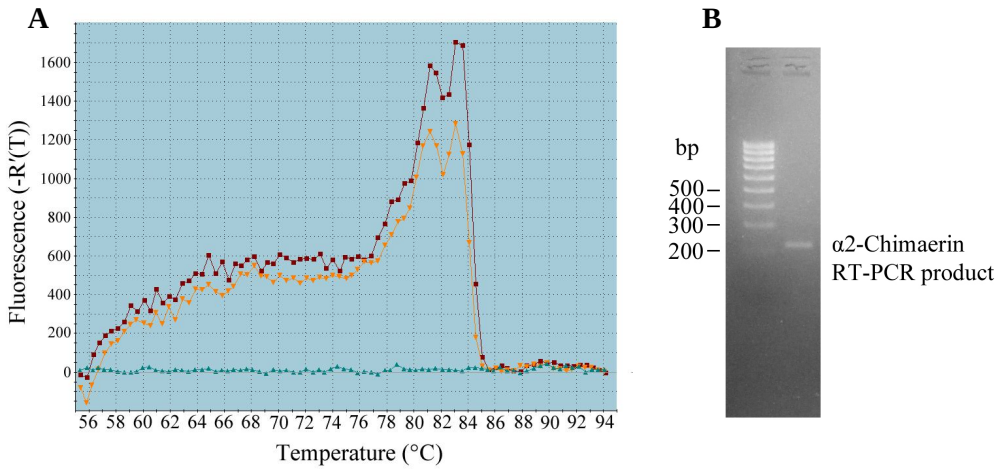

Figure 4.5 Dissociation Curve of α2-chimaerin real-time PCR. (A) The Dissociation Curve of α2-chimaerin revealed two peaks of similar melting temperature and fluorescent change amplitude indicating that the two possible products have similar length, GC content and also final quantity after the reaction completion. (B) Agarose gel electrophoresis of the real-time reaction product revealed a single band indicating that the two peaks in the Dissociation Curve represent an anomaly in the detection of a single PCR product.

Relative transcript levels of HemK1 and HemK2

The transcript levels of HemK1, HemK2, β-Actin and HPRT1 were investigated by real-time PCR in RNA purified from rat e18 primary hippocampal neurones. Figure 4.6 shows the relative mRNA levels of the two N5-methyltransferases and the house-keeping gene HPRT1, normalised to β-actin as calculated by the linear equation generated by the standard curve method.

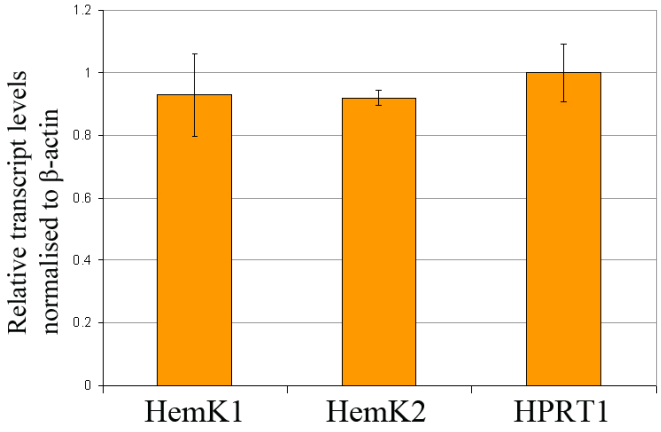

Figure 4.6 Relative transcript levels of HemK1, HemK2 and HPRT1 in e18 rat hippocampal neurones. Real-time PCR analysis revealed comparable levels of HemK1, HemK2 and HPRT1 trancripts in e18 rat hippocampus. The relative transcript quantities were normalised to β-actin levels.

The mRNA transcript levels of HemK1, HemK2 and α2-chimaerin were investigated in e12, e18, 5d and 20d rat brains (Figure 4.7). RNA was purified from e12 and e18 whole brain and 5d and 20d cortex and cerebellum sections. The levels of the two N5-methyltransferases were found comparable to those of α2-chimaerin, following a similar pattern of increase in the developing brain. The green bars represent relative HemK1 transcript levels, showing an increase from pre-natal to post-natal brain. HemK2 transcript levels, represented by the blue bars, show higher levels in e12 brain compared to HemK1 but follow a similar increase with development. α2-Chimaerin levels are relatively low in e12 brain and show an increase in the e18, 5d and 20d cortex as previously shown by Hall and colleagues (Hall et al, 1993). Furthermore the levels of α2-chimaerin transcript drop from 5d to 20d cerebellum, as suggested in the aforementioned study.

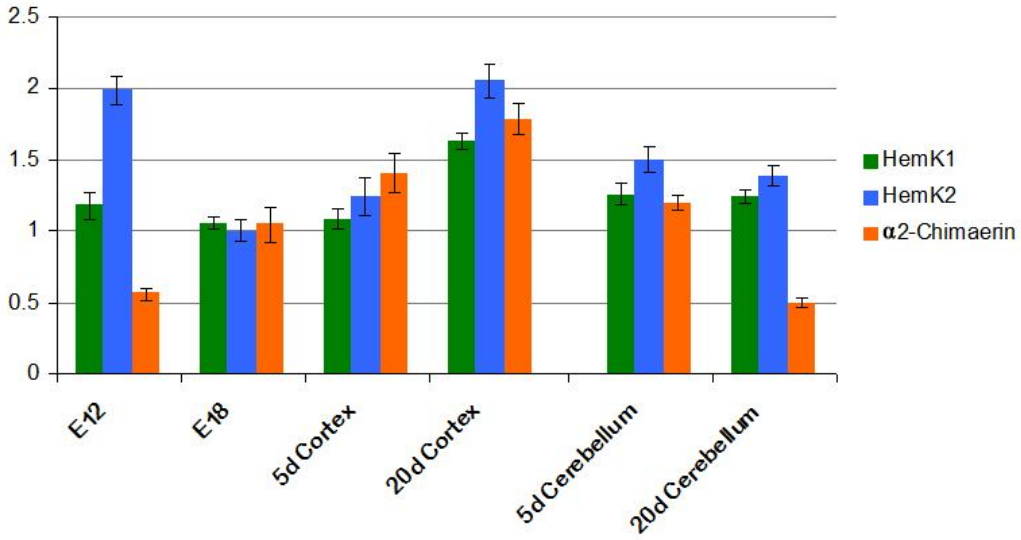

Figure 4.7 Relative transcript levels of HemK1, HemK2 and α2-chimaerin in e12, e18, 5d and 20d rat brains. Real-time PCR analysis was used to examine the transcript levels of HemK1, HemK2 and α2-chimaerin in different ages rat brain sections. HemK1 and HemK2 showed different levels in e12 brain, but followed a similar increase with age thereafter. α2-Chimaerin showed low levels in e12, an increase with development and a drop comparing 5d and 20d cerebellum sections. The relative transcript quantities were normalised to β-actin levels. The samples were generated once while the real-time PCRs were performed in triplicate. The error bars represent standard deviations of triplicate real-time PCRs.

Characterisation of HemK1 and HemK2 antibodies

A series of antibodies have been raised against the human HemK1. Three monoclonal antibodies were raised against a C-terminal partial clone of human HemK1 protein (C. Monfries). Two polyclonal antibodies were also raised against a synthesised peptide of the last 16 amino acids on the C-terminal of the human HemK1 protein. The three monoclonal (7D7, 8F4 and 6D2) and the two polyclonal antibodies (R5 and R6) were initially tested for specificity on detecting the cloned HemK1 protein, and the antibodies that gave promising results were tested further in the investigation of endogenous HemK1 expression in brain and localisation in cells.

Antibodies against HemK1

The three monoclonal and two polyclonal antibodies were tested on western blots of lysates of COS-7 cells transfected with HA-fused or GST-fused HemK1 constructs (Figure 4.8). 6D2 and 7D7 detected a single band compared to a number of smaller proteins detected by the 8F3 antibody. This could suggest that the 8F3 antibody recognises an epitope present in HemK1 degradation products. The polyclonal antibodies detected a number of proteins in COS-7 lysates indicating low specificity to HemK1 protein. The monoclonal antibodies were further used on western blots of rat brain homogenates and fractions.

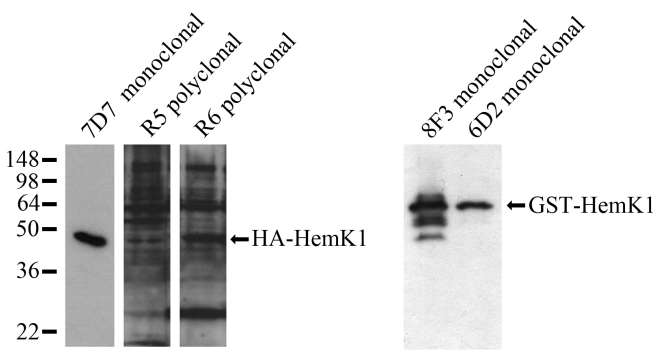

Figure 4.8 Antibody specificity to cloned HemK1 protein. Lysates of COS-7 cells transfected with HA-HemK1 and GST-HemK1 were used in a western blot analysis where the specificity of the anti-HemK1 antibodies was tested. The monoclonal antibodies 7D7 and 6D2 detected a single band of the expected size, while 8F3 also detected a number of smaller proteins. The two polyclonal antibodies were not specific to the cloned HemK1 protein.

Antibodies against HemK1 on fractionated rat brains

HemK1 has an N-terminal mitochondrial localisation sequence and cloned HemK1 was highly insoluble when conjugated to a small tag like HA or FLAG. A preliminary western blot experiment with monoclonal 6D2 antibody used on total rat brain homogenates revealed no apparent bands (Figure 4.9). This suggests that the endogenous HemK1 protein is expressed at low levels in the brain, and/or that the antibody cannot detect the native protein (in the case of a structurally-buried epitope). To test whether the native protein can be detected in enriched brain fractions, e14, e18 and adult rats brains were fractionated to the following enriched fractions: (a) Crude Nuclear, (b) Mitochondrial, (c) Myelin, (d) Synaptosomal, (e) Microsomal and (f) Cytosolic fractions.

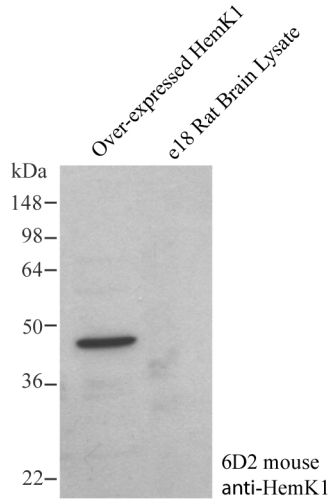

Figure 4.9 Native HemK1 cannot be detected in e18 rat brain homogenate. Homogenate from e18 rat brain was analysed by western blot where the monoclonal 6D2 anti-HemK1 antibody did not detect an endogenous protein.

The three monoclonal antibodies 7D7, 6D2 and 8F3 were used on western blots of brain fractions from e14, e18 and adult rat brains.

The 8F3 antibody detected bands of higher molecular weight compared to the cloned HA-HemK1 in all fractions including the cytosolic fraction. This raises doubts on the specificity of 8F3 since HemK1 bears a mitochondrial localisation sequence and the cloned protein was predominantly insoluble in earlier experiments. It was therefore concluded that the 8F3 antibody was not specific to the HemK1 protein and was not investigated further (Figure 4.10).

The 7D7 antibody detected a strong band of similar size to the cloned HA-HemK1 in the crude nuclear, mitochondrial, microsomal and synaptosomal fractions of e14 rat brains, between 36 and 50 kDa. In e18 brains a similar pattern was observed but the protein band was detected in the myelin fraction too. In adult brains a band of similar size to the cloned HA-HemK1 was detected only in the microsomal fraction. A band of smaller size was detected in the microsomal fractions of e18 and adult brains, just under the 36kDa size marker and in most fractions of e14 brains. The 7D7 antibody did not detect any proteins in the enriched cytosolic fraction as opposed to the 8F3 antibody.

The 6D2 antibody detected a distinct band in the e14 brain mitochondrial fraction of smaller size compared to the cloned HA-HemK1 protein. This could represent the endogenous HemK1 protein localised in mitochondria where the mitochondrial localisation sequence has been cleaved off.

Moreover, both 6D2 and 8F3 antibodies detected a number of bands in the crude nuclear fraction of e18 and adult rat brains (Figure 4.10).

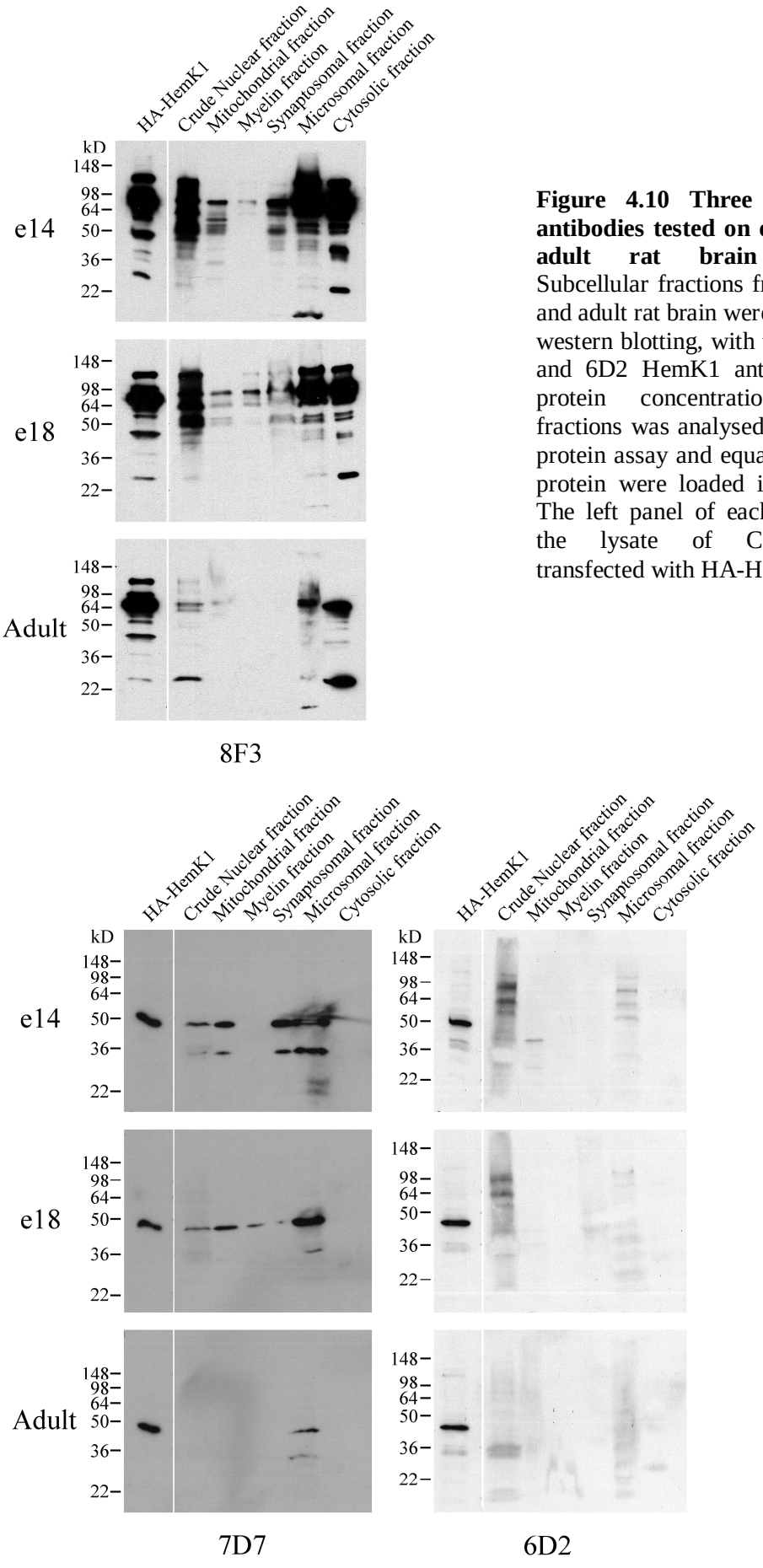

Figure 4.10 Three monoclonal antibodies tested on e14, e18 and adult rat brain fractions. Subcellular fractions from e14, e18 and adult rat brain were analysed by western blotting, with the 8F3, 7D7 and 6D2 HemK1 antibodies. The protein concentration of the fractions was analysed by the BCA protein assay and equal amounts of protein were loaded in each well. The left panel of each blot shows the lysate of COS-7 cells transfected with HA-HemK1.

The specificity of the 7D7 antibody was further investigated by western blot analysis of Triton X-100 insoluble and soluble fractions of COS-7, N1E-115 neuroblastoma and HeLa cells. The untransfected cells were lysed in 1% Triton X-100 containing buffer and were centrifuged to separate the two fractions that were subsequently analysed by western blotting (Figure 4.11). A strong band of similar size to the cloned HemK1 was detected in the soluble fractions of both mouse and monkey origin cells but not in HeLa cells. Considering that each well represents cells from only one confluent $10cm^2$ dish and the blot shown below is a 1′ exposure when the primary antibody 7D7 mouse anti-HemK1 was used in the same dilution as in the rat brain fractions experiment (1:100), the band detected is surprisingly strong.

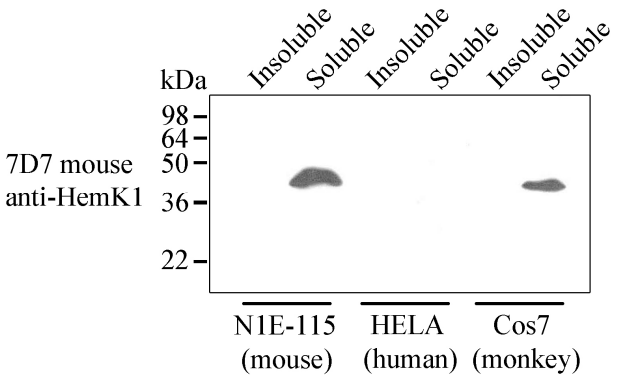

Figure 4.11 The monoclonal 7D7 antibody detects a strong band of similar size to cloned HemK1 in mammalian cells. N1E-115, HeLa and COS-7 cells were lysed in 1% Triton X-100 containing buffer and the soluble and insoluble fractions were separated by centrifugation and analysed by western blotting. The monoclonal 7D7 antibody detected a strong band of similar size to the cloned HemK1 in the Triton X-100 soluble fraction of mouse and monkey cells, but not human.

We therefore aimed to characterise the mouse monoclonal 7D7 anti-HemK1 antibody further by using it on a western blot of cell lysates where HemK1 expression has been knocked down by shRNA (see Chapter 5). HemK1 expression was knocked-down using two HemK1-specific shRNA sequences cloned in the psiSTRIKE shRNA vector that carries the neomycin resistance gene and offers growth selection in neomycin G418. In the first experiment (Figure 4.12A) the cells were transfected with the psiSTRIKE constructs shRNA1, shRNA2 and a scrambled sequence and then selected in Neomycin G418 for five days. Figure 4.12A shows the successful knock-down of HemK1 transcript levels as analysed by real-time PCR (upper panel). The middle panel in figure 4.12A shows western blot analysis of cell lysates with the 7D7

mouse anti-HemK1 antibody, and the lower panel shows the expression of β-actin as detected by a rabbit anti-β-actin antibody. The different levels of the protein band detected by the 7D7 antibody do not correspond to the HemK1 RNA transcript levels. The untransfected cells show the highest HemK1 mRNA levels while the protein band detected is the weakest of all samples. Transfecting N1E-115 cells with the psiSTRIKE vectors affects their growth. ShRNA1 transfected cells showed the greatest growth abnormalities, with more than 50% of transfected cells loosing their adherence and detaching from the dish, and the remaining cells exhibiting a much contracted morphology. These growth effects are amplified when the cells are treated with G418. It is known that G418 affects polypeptide synthesis and reduces the efficiency of translation termination (Manuvakhova et al, 2000) so it is possible that HemK1 protein levels in the cells are affected by this treatment. The experiment was therefore repeated by transfecting with the same psiSTRIKE shRNA vectors and without G418. Figure 4.12B shows the HemK1 RNA transcript levels and western blot analysis of cell lysates using the 7D7 mouse anti-HemK1 antibody. Not treating with G418 resulted in more consistent data between RNA and protein levels, even though the scrambled and shRNA2 samples show protein bands of equal intensities and very different RNA levels.

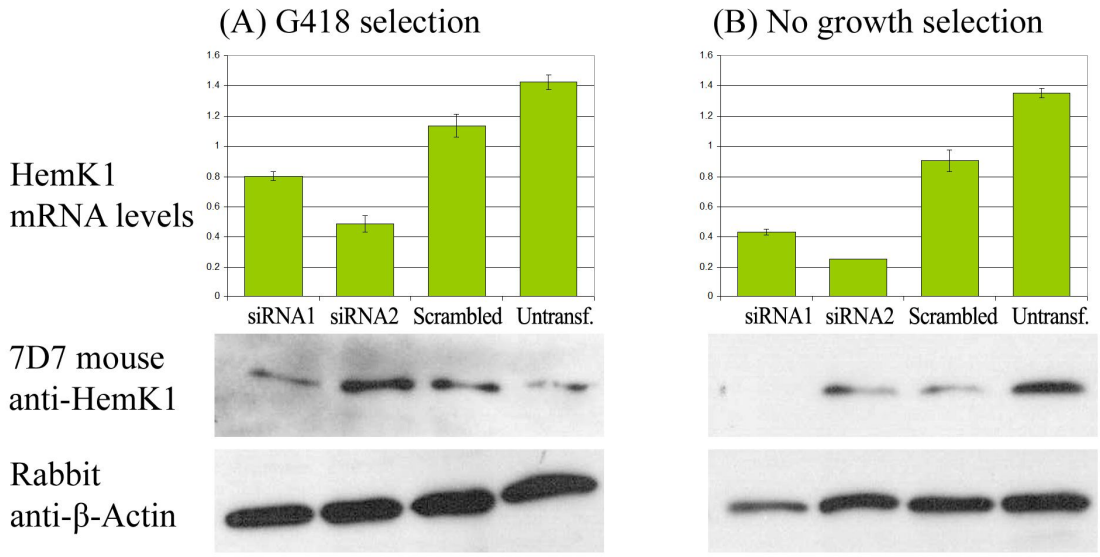

Figure 4.12 Protein levels detected by 7D7 antibody do not correspond to HemK1 mRNA levels. N1E-115 were transfected with the psiSTRIKE vector carrying shRNA1, shRNA2 or a scrambled sequence. Cells were treated with neomycin G418 (A) or untreated (B) and HemK1 mRNA levels were analysed by real-time PCR showing efficient HemK1 mRNA knock-down. The difference in levels of the band detected by the monoclonal 7D7 antibody in western blots of knock-down cells lysates did correspond to the mRNA levels. The cell lysate and purified RNA samples were generated once and the error bars represent standard deviation of transcript levels from real-time PCR performed in triplicate.

The monoclonal and polyclonal antibodies used in these experiments were raised against human HemK1 sequences and the rat and human HemK1 protein sequences show 79% sequence conservation. We investigated the possibility that the antibodies were species specific only detecting the human sequence. Human frontal cortex brain homogenates in PBS were analysed by western blot using the mouse and rabbit anti-HemK1 antibodies (Figure 4.13). Interestingly the monoclonal 7D7 antibody did not detect any strong bands, and this is consistent to the HeLa lysate western blot shown in figure 4.11. The monoclonal 6D2 antibody detected a band between 36 and 50 kDa in size, consistent with the data from the mitochondrial fraction of adult rat brain in figure 4.10. The 8F3 antibody detected a higher molecular weight band as it did in rat brains. The two rabbit polyclonal antibodies gave much cleaner results although different. The rabbit 5 antibody detected a strong band between the 36 and 50 kDa markers of comparable size to the cloned HemK1. The rabbit 6 antibody detected a band closer to the 36 kDa marker that matched the results of a commercially available mouse monoclonal anti-HemK1 antibody raised against full-length human HemK1 (Cat#: H00051409-B01 from Abnova).

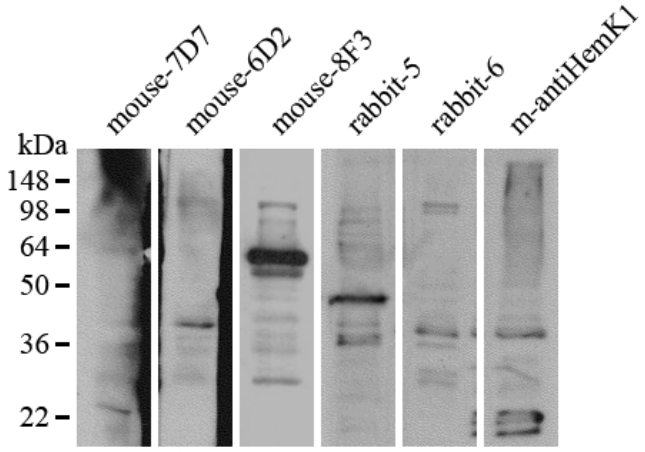

Figure 4.13 Antibodies against HemK1 tested on human frontal cortex brain homogenate. Human frontal cortex homogenate in PBS was analysed by SDS-PAGE and the available anti-HemK1 antibodies were used to detect endogenous protein in a western blot. 7D7 does not recognise a band of the expected size, while 6D2, rabbit-6 and a commercially available monoclonal antibody detect a band between 36 and 50 kDa that could represent native HemK1 after cleavage of the mitochondrial localisation sequence.

Antibodies against HemK1 on cells

To investigate the efficiency of the monoclonal and polyclonal anti-HemK1 on detecting endogenous and exogenously expressed HemK1 in cells, untransfected or HemK1 expressing N1E-115 neuroblastoma cells were fixed and stained with the relevant antibodies (Figure 4.14). The monoclonal 6D2 and 8F3 successfully detected the exogenous HA-HemK1 in loci in the cytoplasm (Figure 4.14B and D) while they showed non-specific cytoplasmic and nuclear staining on untransfected cells (Figure 4.14A and C). The 7D7 antibody stained all through the cytoplasm and nucleus and did not show high specificity for HemK1 protein when compared to HA-HemK1 staining by an anti-HA antibody (Figure 4.14 E).

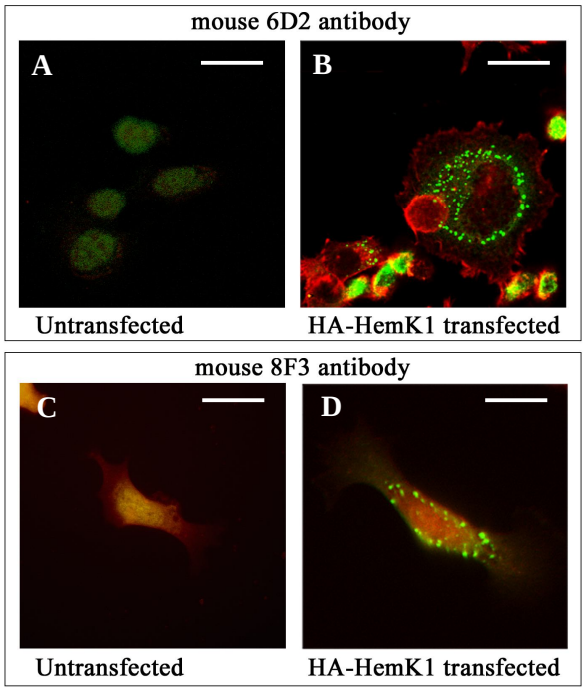

Channels:
(A) FITC(green):m6D2 antibody (endogenous staining) and TRITC(red):Phalloidin,
(B) FITC(green):m6D2 antibody (HA-HemK1) and TRITC(red):Phalloidin,
(C) FITC(green):m8F3 antibody (endogenous staining) and TRITC(red):Phalloidin,
(D) FITC(green):m8F3 antibody (HA-HemK1) and TRITC(red):Phalloidin,
(E) FITC(green):m7D7 antibody, TRITC(red):HA-HemK1 (anti-HA antibody) and Cy5(blue):Phalloidin.

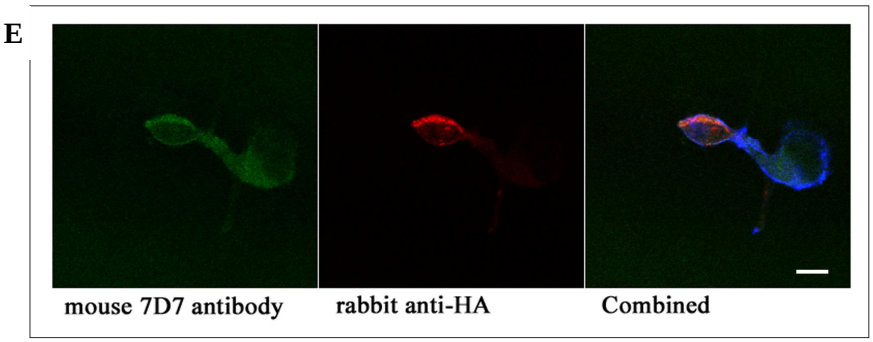

Figure 4.14 Immunocytochemistry with monoclonal antibodies against HemK1. N1E-115 neuroblastoma cells were untransfected or transfected with HA-HemK1 and were fixed and stained with mouse 6D2, 8F3 and 7D7 anti-HemK1 antibodies. The 6D2 antibody revealed a weak non-specific cytoplasmic and nuclear staining when used on untransfected cells (A) while it detected the over-expressed HA-HemK1 when used on transfected cells (B). The 8F3 antibody showed weak staining through the cytoplasm in untransfected cells (C) while it successfully detected over-expressed HA-HemK1 (D). The 7D7 antibody did not show high specificity for HA-HemK1 as revealed by comparing with HA-HemK1 staining by anti-HA antibody (E). The scale bar represents 10μm.

The specificities of the two rabbit polyclonal antibodies rabbit-5 and rabbit-6 were tested on untransfected and HA-HemK1 transfected HeLa and N1E-115 cells respectively (Figure 4.15). They both revealed a cytoplasmic punctate staining in untransfected cells that could represent endogenous HemK1. When the antibodies were used on HA-HemK1 transfected cells they did not show high specificity towards the exogenously expressed protein when compared to anti-HA antibody staining.

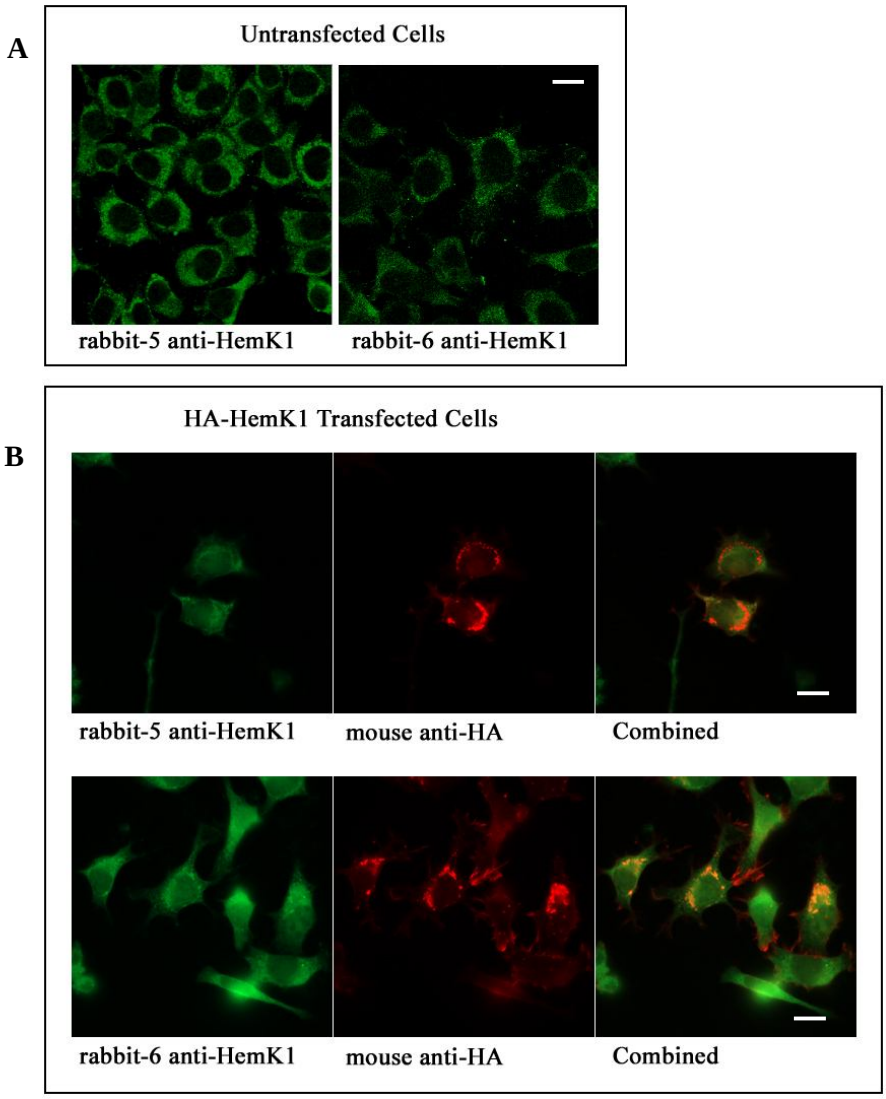

Figure 4.15 Immunocytochemistry with polyclonal antibodies against HemK1. (A) HeLa cells were fixed and stained with the polyclonal rabbit-5 and rabbit-6 antibodies. No nuclear staining was observed while a punctate staining was observed in the cytoplasm. (B) N1E-115 neuroblastoma cells were transfected with HA-HemK1 and were fixed and stained with rabbit-5 and rabbit-6 antibodies. Both antibodies showed background staining in the cytoplasm and the nucleus. Comparison of the polyclonal antibodies staining with that of anti-HA antibody revealed that both rabbit antibodies could detect some exogenously expressed HA-HemK1. The scale bars represent 10μm.

Channels: (A) FITC(green):endogenous HemK1 (rabbit anti-HemK1 antibodies), (B) FITC(green):HA-HemK1 (rabbit anti-HemK1 antibodies) and TRITC(red):HA-HemK1 (mouse anti-HA antibody).

Antibodies against HemK2

For the detection of endogenous HemK2 two commercially available antibodies were obtained from Abnova. (Cat#: polyclonal H00029104-A01, monoclonal H00029104-M01). The two antibodies were initially tested on lysates of COS-7 cells over-expressing FLAG-HemK2 (Figure 4.16). The polyclonal anti-HemK2 antibody was able to detect the cloned HemK2 protein that was partially insoluble in Triton X-100 containing lysis buffer. The monoclonal antibody did not successfully detect the protein.

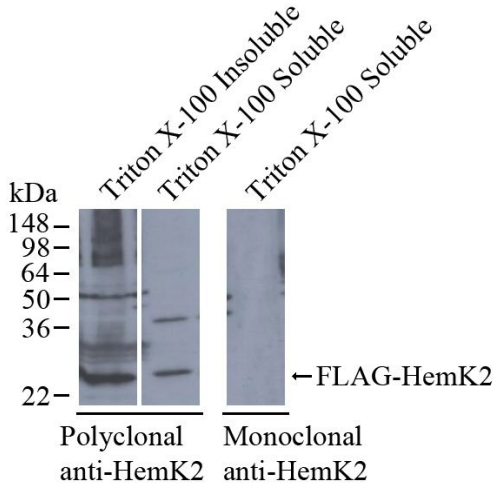

Figure 4.16 Antibody specificity to cloned HemK2 protein. COS-7 cells were transfected with FLAG-HemK2 and lysed in 1% Triton X-100 containing buffer. Two anti-hemK2 antibodies were tested on western blots where the polyclonal antibody detected FLAG-HemK1 in the soluble and insoluble fractions. The monoclonal antibody failed to detect the cloned protein in the soluble fraction.

The two antibodies were used to detect endogenous HemK2 on western blots of E13, E17 and 5d rat brain homogenates (Figure 4.17A). The two antibodies gave similar results detecting a number of protein bands in the two embryonic stages that could correspond to the HemK2 protein size. On a western blot of human frontal cortex brain homogenate in PBS the monoclonal anti-HemK2 antibody detected a strong band between 50 and 64 kDa in size and a faint band that could correspond to the expected size, between 22 and 36 kDa (Figure 4.17B).

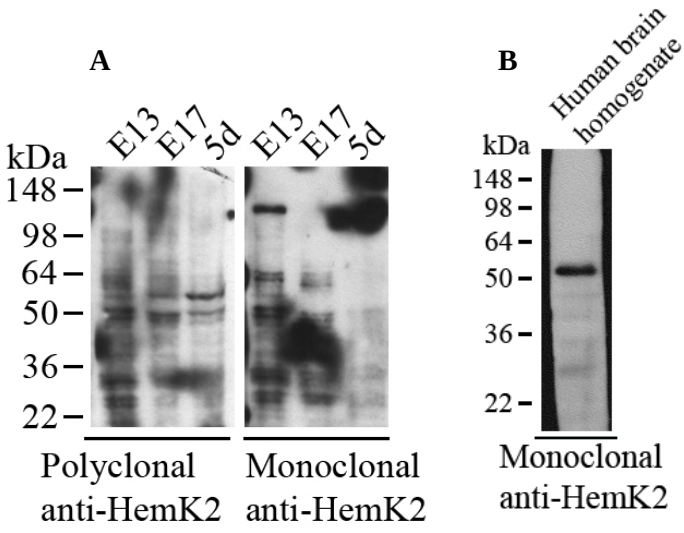

Figure 4.17 Antibodies against HemK2 tested on rat brain and human frontal cortex brain homogenates. (A) Brain homogenates from e13, e17 and 5d rats were analysed by western blotting. The polyclonal antibody detected two bands mostly in the e13 rat brain that could correspond to the cloned HemK2 protein size. The monoclonal antibody gave similar results with the same two bands being detected in e17 brains as well. (B) Human frontal cortex homogenate in PBS was analysed by western blot and the commercially available monoclonal anti-HemK2 antibody detected a strong band ~55kDa in size, and a faint band between 22kDa and 36kDa that could match the predicted size of HemK2.

HemK1 expression in cells

Human HemK1 cDNA was transiently transfected in COS-7 cells that were subsequently fixed and stained to reveal the subcellular localisation of the expressed protein by confocal microscopy analysis.

HemK1 subcellular localisation

When FLAG-HemK1 was expressed in COS-7 cells it localised in distinct dots in the cytoplasm (Figure 4.18). The HemK1 construct used in these experiments carried the FLAG tag on the N-terminal of the full length protein. A series of organelle markers were used to investigate the localisation of HemK1 in co-staining experiments. Figure 4.18 shows COS-7 cells expressing FLAG-HemK1 (red) and co-stained with antibodies targeting: a) Clathrin, a marker for Clathrin-coated vesicles involved in receptor-mediated endocytosis, b) GM130, a marker for the Golgi apparatus, c) EEA1, a protein localising in early endosomes, d) HSP60, a heat shock protein that localises in the mitochondria and e) Lamp-1, a lysosomal membrane protein. HemK1 showed partial co-localisation with the mitochondrial marker HSP60, while its localisation was largely distinct from the lysosomal, clathrin, early endosomes and Golgi markers. It was noted however than in some cells HemK1 staining partially over-lapped with the markers for clathrin and early endosomes, mainly in cell expressing high levels of FLAG-HemK1. The partial co-localisation between HemK1 and HSP60 was consistent and reproducible, observed in low and high expressing cells too.

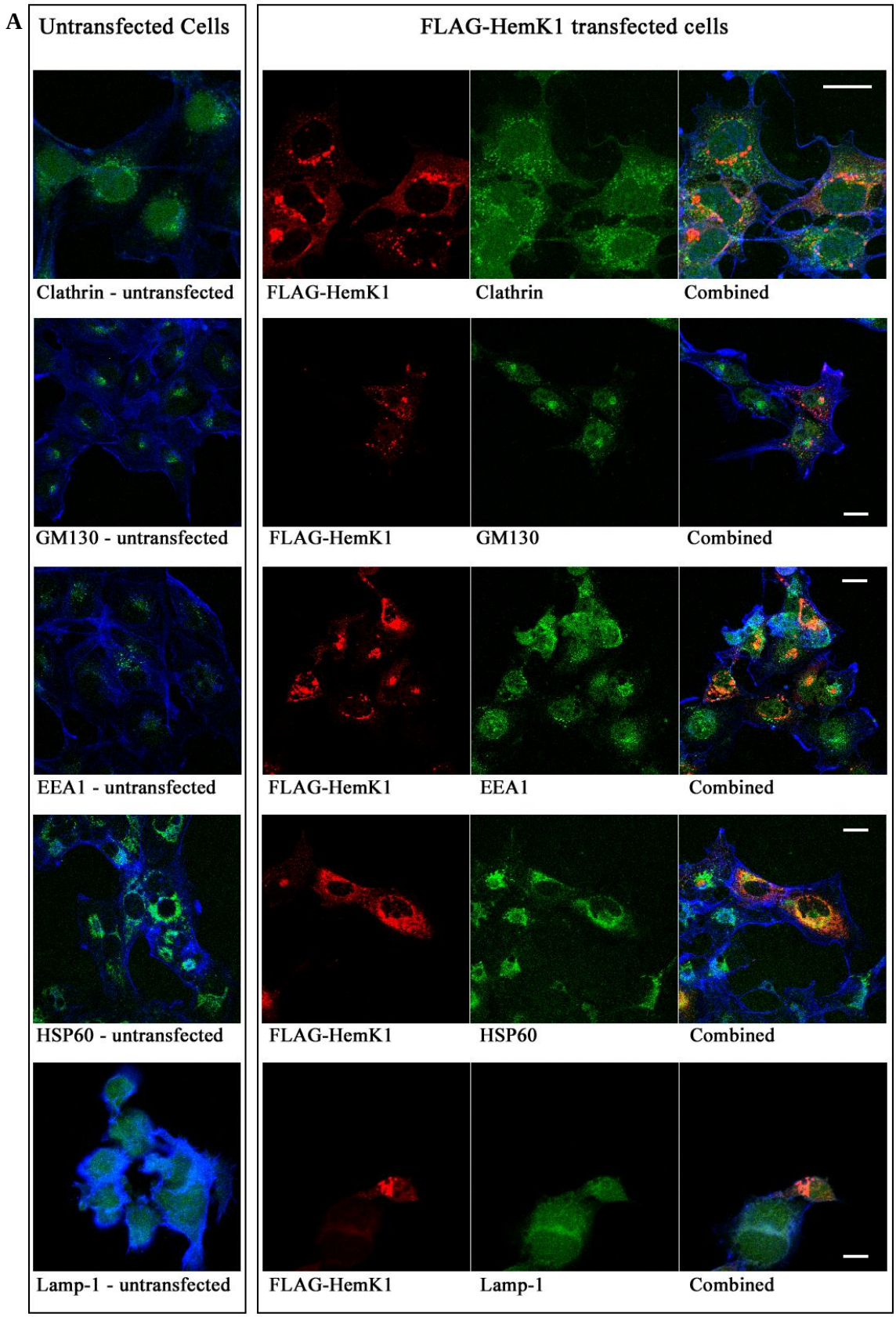

Figure 4.18 HemK1 cellular localisation as compared to organelle markers. (A) The localisation of exogenously expressed FLAG-HemK1 was compared to antibody staining of markers for Clathrin, golgi (GM130), early endosomes EEA1, mitochondria (HSP60) and lysosomes (Lamp-1). Partial co-localisation was observed between FLAG-HemK1 and HSP60. (B) A close up of the combined staining images. Scale bars: 10µm.

Channels: FITC(green):relevant cell organelle antibodies, TRITC(red):FLAG-HemK1 (rabbit anti-FLAG antibody), Cy5(blue):Phalloidin.

B

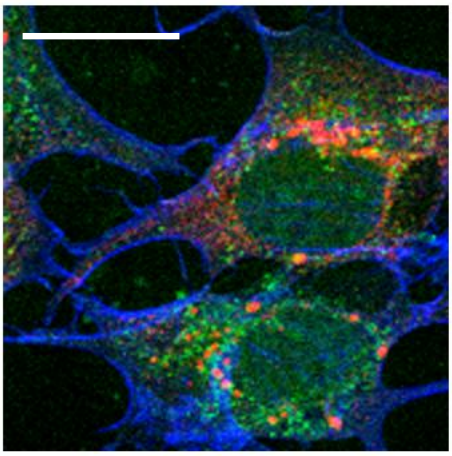

Clathrin (FITC)
FLAG-HemK1 (TRITC)
Phalloidin (Cy5)

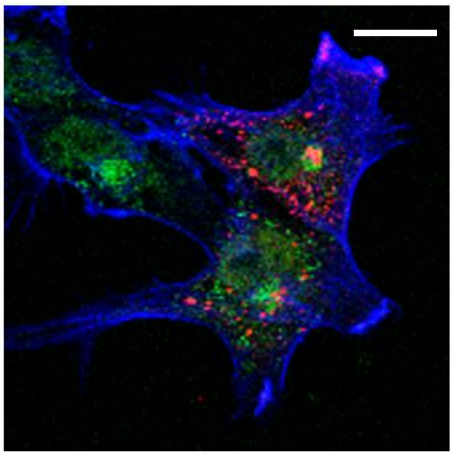

GM130 (FITC)
FLAG-HemK1 (TRITC)
Phalloidin (Cy5)

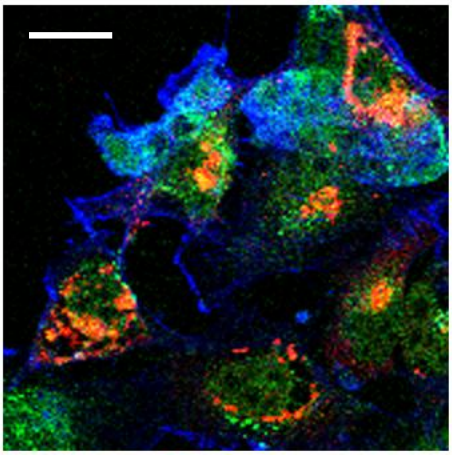

EEA1 (FITC)
FLAG-HemK1 (TRITC)
Phalloidin (Cy5)

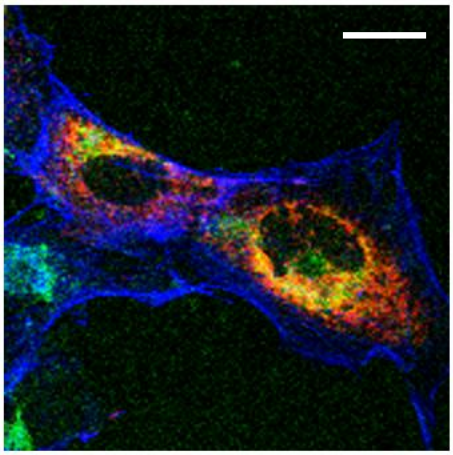

HSP60 (FITC)
FLAG-HemK1 (TRITC)
Phalloidin (Cy5)

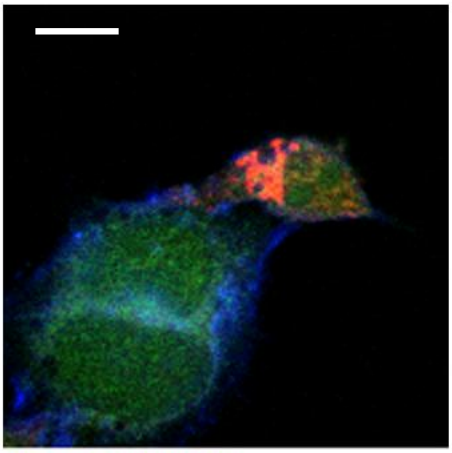

Lamp-1 (FITC)
FLAG-HemK1 (TRITC)
Phalloidin (Cy5)

HemK1 is predicted to localise in the mitochondria through a mitochondrial leader sequence on the N terminal of the protein (see Chapter 1 - Introduction). To minimise the possibility that the FLAG tag on the N terminal of the cloned human HemK1 interferes with the function of the mitochondrial sequence, HemK1 was cloned in a mammalian expression vector incorporating a FLAG tag on the C-terminal of the protein (Figure 4.19D). To investigate the localisation of HemK1 in mitochondria the human N- and C- terminal FLAG-tag HemK1 proteins were expressed in HeLa cells and compared to the green-fluorescent mitochondrial stain MitoTracker Green FM. Both N- and C-terminal FLAG-HemK1 constructs showed strong co-localisation with the mitochondrial stain (Figure 4.19A, B). Some nuclear staining is evident for HemK1 in these experiments, which is a characteristic of the mouse anti-HemK1 6D2 antibody used. In an experiment where the N- terminal HA and C-terminal FLAG conjugated HemK1 constructs were co-expressed in N1E-115 cells the two proteins exhibited very high co-localisation as analysed by confocal microscopy, suggesting that the FLAG tag on the N-terminal of the protein does not interfere with the mitochondrial localisation sequence (Figure 4.19C).

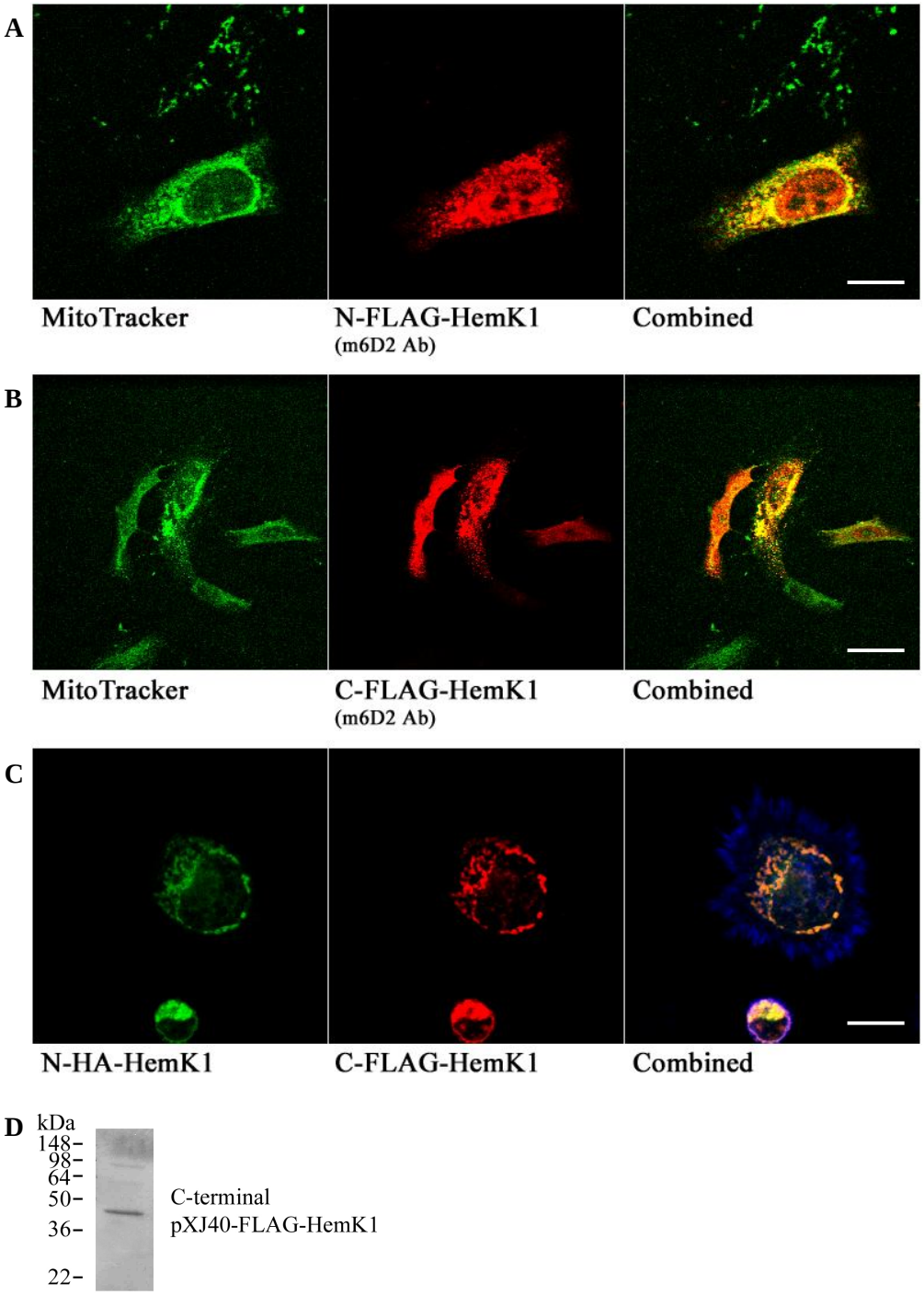

Figure 4.19 N- or C-terminal FLAG-tag fusion does not interfere with HemK1 localisation. The localisation of exogenously expressed N- or C-terminal FLAG-tag fused HemK1 was compared to a mitochondrial stain in HeLa cells (A, B) and to each other when the two constructs were co-expressed (C). (D) Successful cloning of HemK1 in a C-terminal FLAG pXJ40 vector was tested by western blot analysis of lysates of transfected COS-7 cells, with anti-FLAG antibodies. The scale bars represent 10µm.

Channels: (A) FITC(green):MitoTracker and TRITC(red):N-FLAG-HemK1 (mouse 6D2 anti-HemK1 antibody), (B) FITC(green):MitoTracker and TRITC(red):C-FLAG-HemK1 (mouse 6D2 anti-HemK1 antibody), (C) FITC(green):N-HA-HemK1 (mouse anti-HA antibody), TRITC(red):C-FLAG-HemK1 (rabbit anti-FLAG antibody) and Cy5(blue):Phalloidin.

The intracellular localisation of exogenously expressed HemK1 was compared to a stain for cytoplasmic RNA that would reveal RNA localised in the nucleus, mitochondrial and other cytoplasmic locations (Figure 4.20). HemK1 showed some co-localisation with the RNA stain in the cytoplasm in some cells, possibly reflecting mitochondrial RNA.

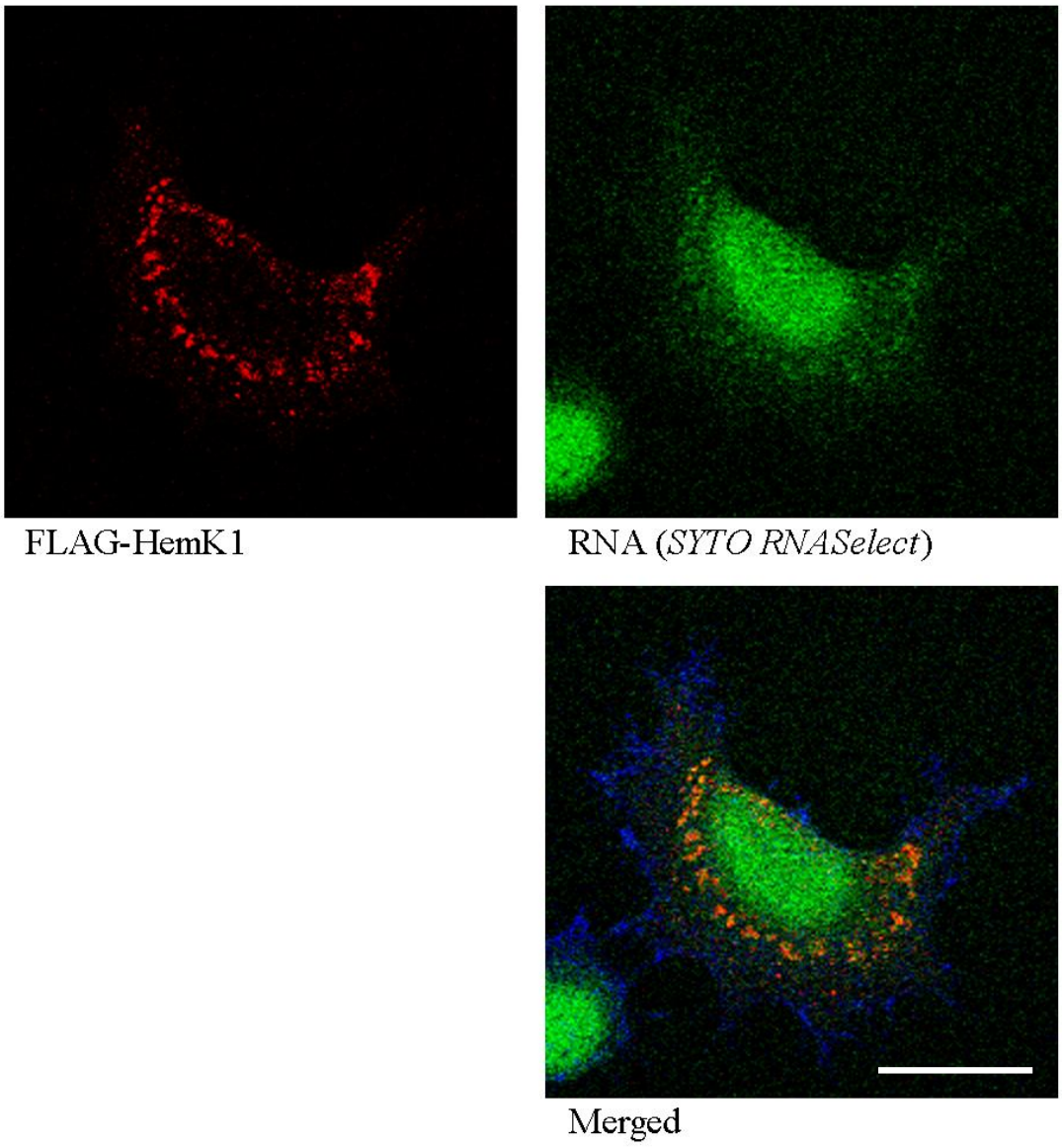

Figure 4.20 HemK1 can co-localise with cytoplasmic RNA. FLAG-HemK1 was expressed in N1E-115 neuroblastoma cells that were fixed and stained with rabbit anti-FLAG (TRITC) antibody as well as the RNA specific stain SYTO RNASelect. The RNA stain revealed a highly nuclear localisation with weaker staining in the cytoplasm. HemK1 showed some co-localisation with RNA in the cytoplasm possibly reflecting mitochondrial structures. The scale bar represents 10µm.

Channels: FITC(green):SYTO RNA select, TRITC(red):FLAG-HemK1 (rabbit anti-FLAG antibody), Cy5(blue):Phalloidin.

Summary

The transcript levels of HemK1 and HemK2 were investigated in the developing rat brain. Real-time PCR revealed higher levels of HemK2 mRNA in e12 rat brain than HemK1. In e18 brain the levels of both N5-methyltransferases were comparable and followed a steady increase through e18, 5d and 20d ages. The levels of the two transcripts in 20d rat cortex were higher to cerebellum tissue of the same age. α2-Chimaerin mRNA was detected at lower levels to HemK1 and HemK2 in e12 rat brain, but followed an increase with development, as previously published.

Characterisation of three monoclonal and two polyclonal antibodies raised against human HemK1 protein sequences was performed on western blots of fractionated e14, e18 and adult rat brain. The bands detected by the antibodies on brain samples were compared to the cloned human HemK1. The 7D7 monoclonal antibody revealed a band of the expected size in fractionated rat brain as well as in lysates of monkey and mouse senescent cells but not in HeLa cells or human brain homogenate. In HemK1 knock-down N1E-115 neuroblastoma cells the protein band detected did not follow the pattern of the knock-down transcript levels, indicating that it may not represent HemK1 protein. Furthermore the band was not detected in human-origin cells and brain, indicating that it is a non-specific antigen that is present in monkey and rat cells but not in human.

The monoclonal 6D2 antibody detected two bands of smaller size than the cloned HemK1 in the mitochondrial fraction of e14 rat brain, at 36-40kDa and at 22-36kDa. One of these bands could represent the product of the mitochondrial leader sequence cleavage upon translocation of HemK1 to mitochondria. MitProtII (v1.101) predicts the cleavage site of HemK1 mitochondrial export at 24 amino acids, which would decrease the size of HemK1 by approximately 2.7kDa, down to a 34.3kDa. The cloned HemK1 is predicted to be 37kDa but on a 10% polyacrylamide gel it runs just below the 50kDa marker. This suggests that the higher of the two bands in the mitochondrial fraction could be mitochondrial HemK1, since a band of similar size is observed in the control lane where lysate of COS-7 cells transfected with FLAG-HemK1 was analysed, possibly representing mitochondrial translocated FLAG-HemK1.

The 8F3 monoclonal antibody detected a series of strong bands of around 64kDa in fractionated rat brain, a pattern reproduced in human brain homogenate. Though this could represent a HemK1-dimer, it is rare for protein dimers to remain associated in denaturing SDS-PAGE. This was not investigated further.

The two polyclonal antibodies showed high background when used on western blots of lysates of cells exogenously expressing HemK1. The antibodies gave more comparable results when used on human brain homogenate, with rabbit-5 antibody revealing a band of the expected size and 6D2, rabbit-6 and a commercial antibody revealing a band of smaller size (36-50kDa) that could represent native HemK1 protein translocated to the mitochondria. All antibodies revealed some endogenous staining when used on fixed mammalian cells and 6D2 and 8F3 detected exogenously expressed protein localising in bright foci in the cytoplasm. The commercially available antibodies against HemK2 failed to detect a clear band of comparable size in rat brain homogenates.

The cellular localisation of HemK1 was compared to markers for lysosomes, golgi, mitochondria, early endosomes and clathrin. Exogenously expressed HemK1 showed strong co-localisation with the mitochondrial marker. In the vast majority of cells analysed HemK1 showed distinct localisation to clathrin and early endosomes. No HemK1 co-localisation was observed with markers for golgi and lysosomes. Furthermore, HemK1 showed partial co-localisation with an RNA stain in areas around the nucleus, possibly revealing RNA contained in mitochondrial structures. HemK1 was cloned as a C-terminal FLAG-fusion protein and cell staining experiments revealed that C- and N-terminal FLAG-fusion HemK1 proteins co-localised with each other and their subcellular localisation was detected in mitochondria, suggesting that the FLAG tag does not interfere with the potential mitochondrial leader sequence of HemK1.

Chapter 5
[Results III]
Functional Associations of HemK proteins with Release Factors and RNA granules

HemK1 and HemK2 association with Release Factors

HemK1 and HemK2 are predicted N5-glutamine methyltransferases suggested to methylate release factors as part of translation termination machinery. When this project started only the function of the bacterial HemK1 homologue PRMC was known mediating translation termination by methylating prokaryotic release factor RF1 at the conserved GGQ motif (Nakahigashi et al, 2002; Heurgué-Hamard et al, 2002). Subsequently, the structure and function of the yeast HemK1 homologue was elucidated (Heurgué-Hamard et al, 2005), and it became evident that the function of HemK1 homologues is conserved in different organisms and the GGQ domain target of methylation in release factor is conserved in evolution. A BLAST search in the human cDNA library had revealed one PRMC homologue, and that was what we now know as HemK2. The clear distinction between the two homologues HemK1 and HemK2 came much later when HemK1 was characterised as a mitochondrial protein with an N5-glutamine methyltransferase activity (Polevoda et al, 2006; Ishizawa et al, 2008). In the meantime cDNA clones of the predicted release factor substrates eRF1 and eRF3 had been acquired and cloned as part of this study and used on enzymatic activity experiments with HemK1. When the mitochondrial release factor mtRF1a was characterised (Soleimanpour-Lichaei et al, 2007) the cDNA clone was acquired and cloned to be used in pull-down experiments with HemK1 to investigate their association.

Cloning of release factors eRF1, eRF3 and mtRF1a

Human cDNA clones of eRF1, eRF3 and mtRF1a release factors were acquired (for details see Materials and Methods). They were cloned in mammalian expression vectors pXJ40 carrying an HA, FLAG and GST tag and sequenced to verify correct cloning. The expression of the cloned constructs was tested on COS-7 cells by western blot analysis of transfected COS-7 cells lysates (Figure 5.1).

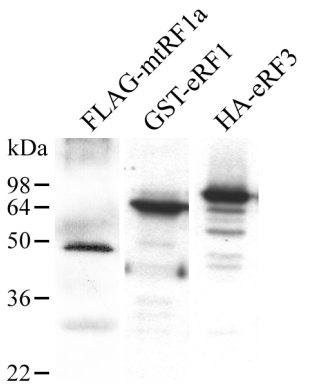

Figure 5.1 Expression of cloned mtRF1a. The expression of the mtRF1a, eRF1 and eRF3 release factors cloned in pXJ40 vectors were tested by western blot. Lysates of COS-7 cells over-expressing the constructs were probed with anti-FLAG, anti-GST and anti-HA antibodies respectively.

Cloning of the human homologue of the yeast zinc finger protein Ynr046w

A study by Heurgué-Hamard and colleagues (Heurgué-Hamard et al, 2006) indicated that the 15 kDa zinc-binding protein Ynr046w was required in the eRF1-eRF3 complex to mediate methylation of eRF1 by HemK in yeast. The human homologue of Ynr046w, TRMT112, was acquired and cloned in pXJ40 mammalian expression vectors to investigate the methyltransferase activity of HemK1 in an enzymatic assay. The expression of TRMT112 was tested by western blot analysis of cell lysates of transfected COS-7 cell (Figure 5.2).

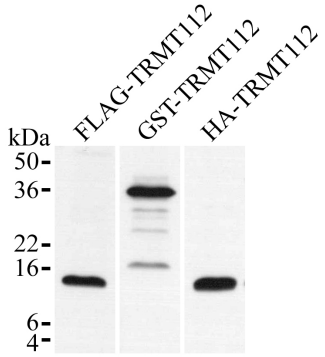

Figure 5.2 Expression of cloned TRMT112. The expression of TRMT112 cloned in pXJ40 vectors was tested by western blot. Lysates of COS-7 cells over-expressing the constructs were probed with anti-FLAG, anti-GST and anti-HA antibodies respectively revealing a protein band of the expected size.

Mutation on the NPPY active site of HemK1

Graille and colleagues have shown that the single amino acid substitution Asn183Ala in the conserved RF1 binding site NPPY of the bacterial HemK1 (PrmC) was adequate to abolish methylation activity down to 2% (Heurgue-Hamard, et al, 2005). To investigate on the methylation activity of HemK1 we raised the Asn239Ala

mutation in the ^{239}NPPY^{242} active site of the human cDNA clone by PCR site-directed mutagenesis, in the mammalian expression vectors pXJ40. The amino acid substitution was verified by DNA sequencing and the expression of HemK1 N239A was tested by western blot of transfected COS-7 cells (Figure 5.3).

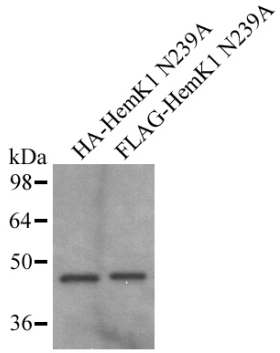

Figure 5.3 Expression of HemK1 N239A. The expression of HemK1 N239A was tested by western blot. Lysates of COS-7 cells over-expressing the constructs were probed with the mouse-6D2 anti-HemK1 antibody revealing a protein band of the expected size.

HemK1 and HemK2 associate with release factors in cells

To investigate the interaction of Hemk1 and HemK2 with the polypeptide chain release factors the human cDNA clones were used in pull-down experiments in COS-7 cells. FLAG tag conjugated HemK1 and HemK2 constructs were used to pull down the HemK2 predicted substrates eRF1 and eRF3 that were GST and HA tag conjugated respectively. HemK2 was able to pull-down eRF1 and eRF3 individually and also when co-expressed with both release factors, though higher amount of eRF3 associated with HemK2 when eRF1 was not present. HemK1 showed some association with eRF1 that increased in the presence of eRF3 (Figure 5.4).

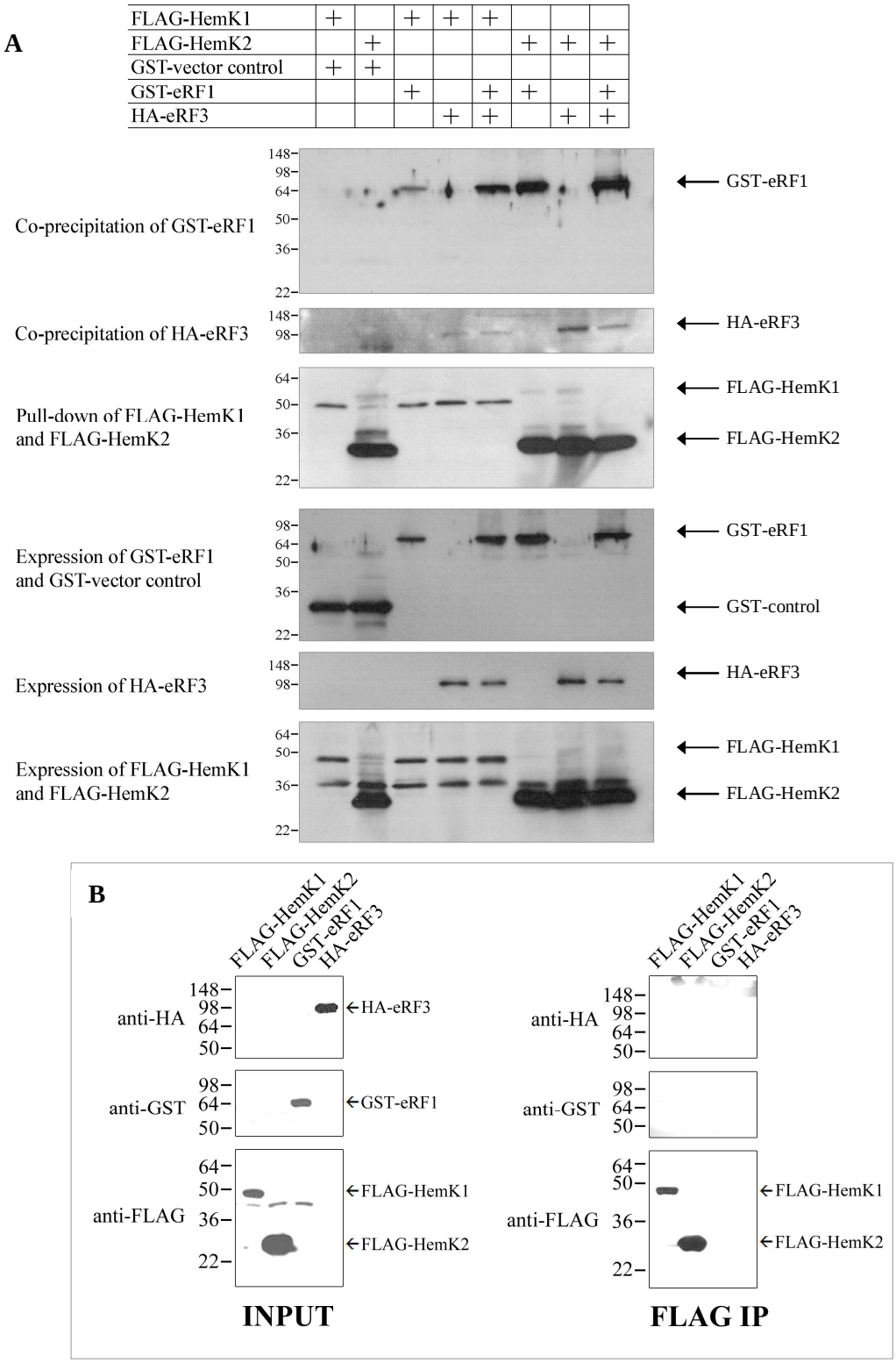

Figure 5.4 HemK1 and HemK2 associate with eRF1 and eRF3 in cells. (A) COS-7 cells were transfected with FLAG-HemK1, FLAG-HemK2, GST-eRF1, HA-eRF3 and GST-vector control constructs and were lysed after over-night expression. FLAG beads were used to affinity purify HemK1 and HemK2 and SDS-PAGE analysis with relevant antibodies revealed eRF1 co-precipitated with both HemK1 and HemK2, while no co-precipitation of the GST-vector control protein was detected. Some co-precipitation of eRF3 was observed with both N5-methyltransferases that increased with HemK2 when co-expressed with its predicted substrate eRF1. (B) Control experiment in COS-7 cells showing that over-expressed GST-eRF1 or HA-eRF3 do not immunoprecipitate with anti-FLAG beads. The left panels show expression of the protein constructs while the FLAG immunoprecipitation samples are presented on the right panels. A contaminating band of approximately 40 kDa size can be seen with the anti-FLAG antibody on cell lysates (bottom right panel).

Next we aimed to investigate the interaction between the two N5-glutamine methyltransferases and the HemK1 mitochondrial predicted substrate mtRF1a. The proteins were over-expressed in COS-7 and pull down analysis revealed that both HemK1 and HemK2 were able to associate with mtRF1a (Figure 5.5).

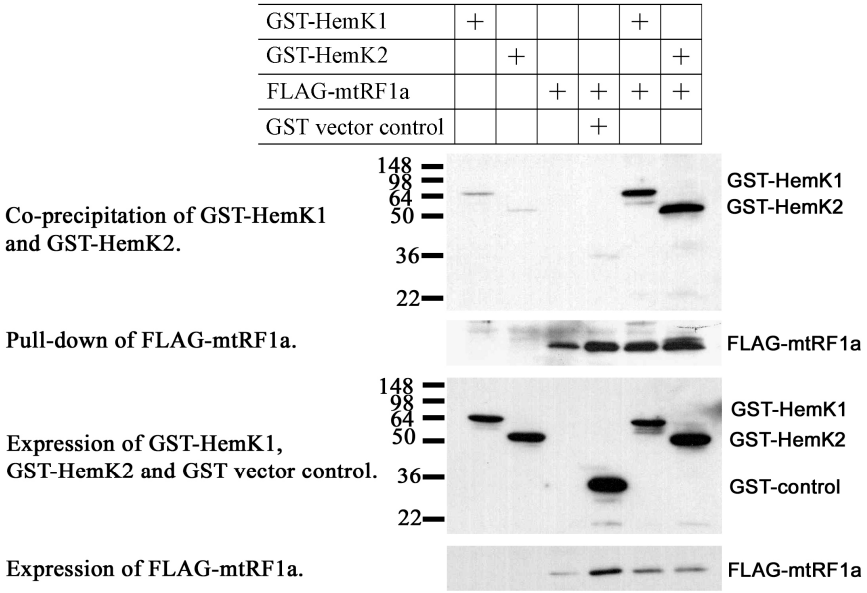

Figure 5.5 HemK1 and HemK2 associate with mtRF1a in cells. COS-7 cells were transfected with GST-HemK1, GST-HemK2, FLAG-mtRF1a and GST-vector control constructs and were lysed after over-night expression. FLAG beads were used to affinity purify mtRF1a and SDS-PAGE analysis with relevant antibodies revealed co-purified HemK1 and HemK2. Only a minimal amount of HemK1, HemK2 and GST-vector control proteins immunoprecipitated with FLAG beads in the control samples verifying the association between the two N5-methyltransferases and HemK1 proposed substrate mtRF1a.

HemK1 and HemK2 localisation in relation to Release Factors

The two N5-methyltransferases HemK1 and HemK2 were shown to associate with both eRF1 and mtRF1a substrates in cells. This poses a question on the cellular localisation of the two enzymes and substrates since HemK1 and mtRF1a localise in the mitochondria, while HemK2 and its substrate eRF1 are not predicted to be mitochondrial. The mitochondrial localisation of mtRF1a (Soleimanpour-Lichaei et al, 2007) was verified in N1E-115 cells, where mtRF1a expression was compared to a mitochondrial stain (Figure 5.6). The localisation of HemK1 and HemK2 in cells was therefore investigated in relation to the localisation of the release factors. The proteins

were over-expressed in cells that were subsequently fixed and stained with the relevant antibodies, and analysed by confocal microscopy to reveal possible co-localisation (Figure 5.7). Strong co-localisation was observed between HemK1 and its proposed substrate mtRF1a and between HemK2 and its proposed substrate eRF1. However, HemK1 also showed some co-localisation with eRF1 in some cells when the two proteins were co-expressed. HemK2 expression was largely cytoplasmic but there were some areas of over-lap with the mtRF1a expression, despite their predominantly distinct expression pattern.

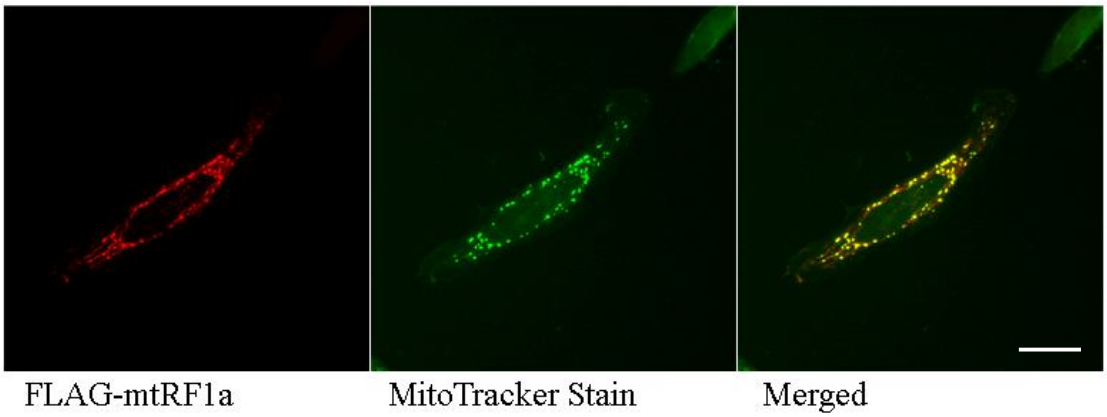

Figure 5.6 mtRF1a localises in mitochondria. N1E-115 neuroblastoma cells were transfected with FLAG-mtRF1a and were fixed and stained after over-night expression. FLAG-mtRF1a (red) was stained with rabbit anti-FLAG (TRITC) antibody while the MitoTracker Green FM marker revealed the localisation of mitochondria under analysis by confocal microscopy. mtRF1a showed a distinct mitochondrial localisation. The scale bar represents 10μm.

Channels: FITC(green):MitoTracker and TRITC(red):FLAG-mtRF1a (rabbit anti-FLAG antibody).

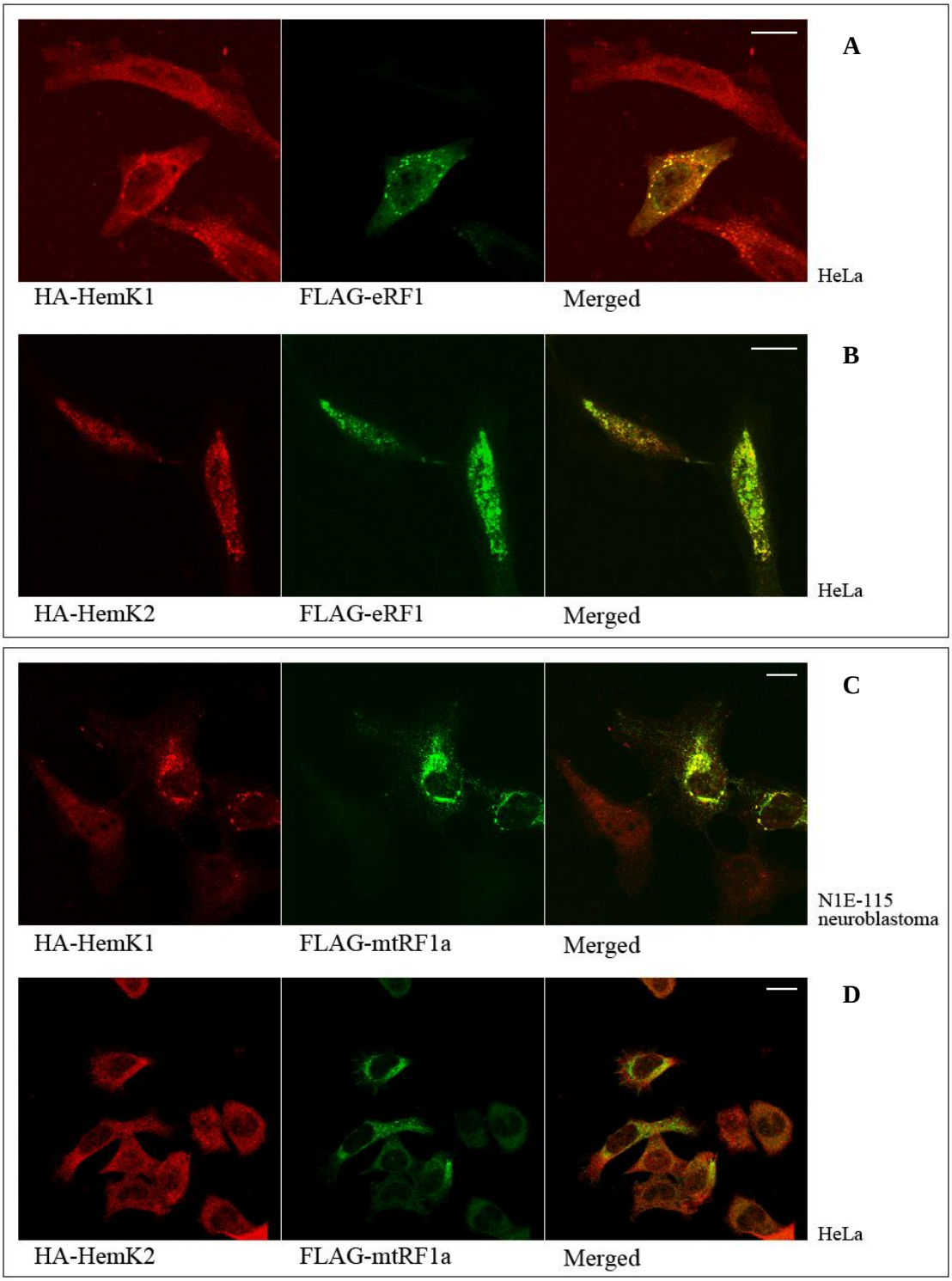

Figure 5.7 HemK1 and HemK2 co-localise with release factors mtRF1a and eRF1 respectively. N1E-115 neuroblastoma and HeLa cells were transfected with HA-HemK1, HA-HemK2 and FLAG-mtRF1a constructs and were fixed and stained after over-night expression. Relevant antibodies were used to stain HemK1 and HemK2 (TRITC, red), and mtRF1a (FITC, green) localisation in the cells that were analysed by confocal microscopy. HemK1 co-localised with proposed mitochondrial substrate mtRF1a (C) and HemK2 with its proposed substrate eRF1 (B). Some co-localisation was observed between HemK1 and eRF1 (A), and also between HemK2 and mtRF1a (D). A close up of the four combined cell images is presented in (E). The scale bars represent 10μm.

Channels: (A) FITC(green):FLAG-eRF1 (rabbit anti-FLAG antibody) and TRITC(red):HA-HemK1 (mouse anti-HA antibody), (B) FITC(green):FLAG-eRF1 (rabbit anti-FLAG antibody) and TRITC(red):HA-HemK2 (mouse anti-HA antibody), (C) FITC(green):FLAG-mtRF1a (rabbit anti-FLAG antibody) and TRITC(red):HA-HemK1 (mouse anti-HA antibody), (D) FITC(green):FLAG-mtRF1a (rabbit anti-FLAG antibody) and TRITC(red):HA-HemK2 (mouse anti-HA antibody).

E

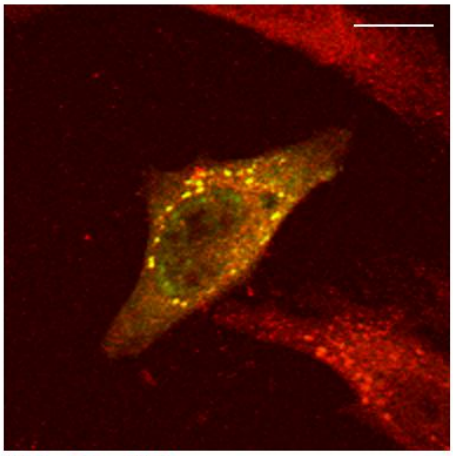

HA-HemK1
FLAG-eRF1

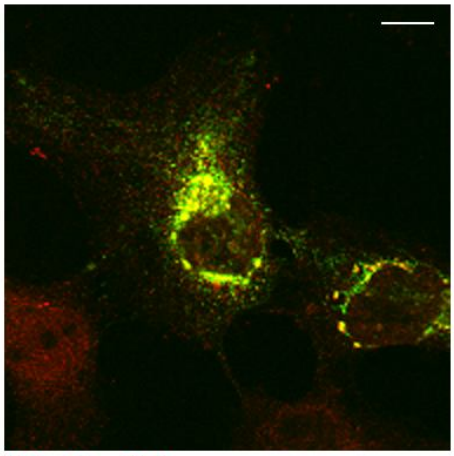

HA-HemK1
FLAG-mtRF1a

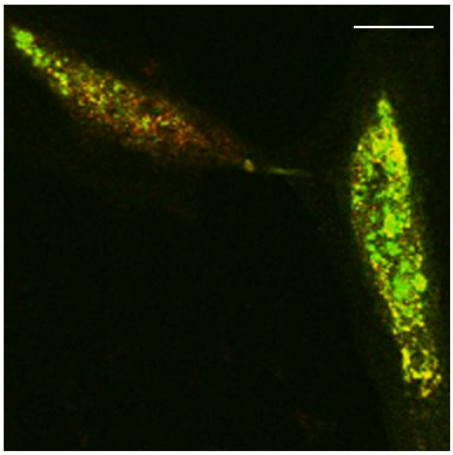

HA-HemK2
FLAG-eRF1

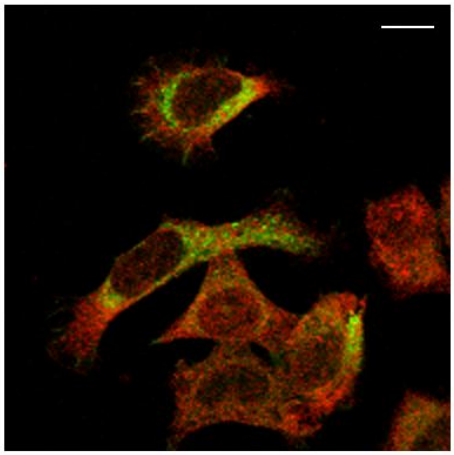

HA-HemK2
FLAG-mtRF1a

HemK1 methyltransferase activity

An enzymatic assay was attempted to investigate the methyltransferase activity of human HemK1. When these experiments were performed the only known homologue of the bacterial PrmC in mammals was HemK1. The hypothesis that the homologue protein of RF1 in mammals, eRF1 would be methylated by HemK1 was tested in an *in vitro* methylation assay. In addition, the human homologue of the yeast Ynr046w, TRMT112 was cloned. Ynr046w has been previously shown to be required for eRF1 methylation in yeast. The methylation assay was performed *in vitro* with immunopurified proteins from transfected COS-7 cells, and S-adenosyl-L-[methyl-^{3}H]methionine was used as a methyl donor to detect methylation by measuring retained radioactivity in a scintillation counter and also by autoradiography of reactions separated by SDS-PAGE and transferred onto PVDF. The reaction conditions were adapted from the work of Heurgué-Hamard and colleagues (Heurgué-Hamard et al, 2002). Figure 5.8 shows the [^{3}H] counts and autoradiography analysis of a representative experiment, where immuno-precipitated release factors GST-eRF1 and HA-eRF3 were incubated with cell lysates of COS-7 cells transfected with HemK1 and TRMT112. After the reaction completion the release factors bound on beads were washed to remove the HemK1(+/-TRMT112) cell lysate, and they were analysed in lanes 1-4. In lanes 5 and 6 the total transfected COS-7 lysates were analysed, presented as positive controls for the methylation reaction conditions. Increased counts are observed with eRF1 and eRF3 (eRFs) incubated with HemK1 transfected cells lysated (lane 2) compared to the no-protein blank control (lane 1) control. In the presence of HemK1 and TRMT112 the release factors show some increased methylation (lane 3) compared to when incubated with HemK1 alone (lane 2). When the HemK1 N239A mutant is used along with TRMT112 the signal drops (lane 4) compared to wt HemK1+TRMT112 (lane 3), suggesting that HemK1 can methylate eRFs and the N239A mutation can affect HemK1 methyltransferase activity (Figure 5.8A). The autoradiography analysis of this experiment revealed a number of bands but did not detect a band at the expected protein size of eRF1. There was an increase in the intensity of the bands in lanes 5 and 6 where lysates of COS-7 cells were analysed, reflecting on the different methyltransferases found in COS-7 lysates.

The enzymatic assay to investigate methylation of eRFs by HemK1 was performed 7 times in total but following different methodologies. In the initial experiments HemK1, eRF1 and eRF3 proteins were produced in *E.coli* and purified using GST and HIS tag affinity beads. They were then eluted to be used in the methylation assay. This methodology did not give promising results as far as detected methylation is concerned, possibly due to incorrect protein folding occurring in the bacterial expression system that did not allow for enzymatic function. The data presented in figure 5.8 represent the only experiment performed with the described methodology, the exact protein combinations in the reactions, and also the single experiment that gave promising results. The experiment was not repeated due to time constraints and also since new data presented in literature described the enzymatic function of HemK1 using mass spectrometry as a more sensitive technique of detection (Ishizawa et al, 2008). Figure 5.8 therefore represents a single experiment and standard deviation bars cannot be applied.

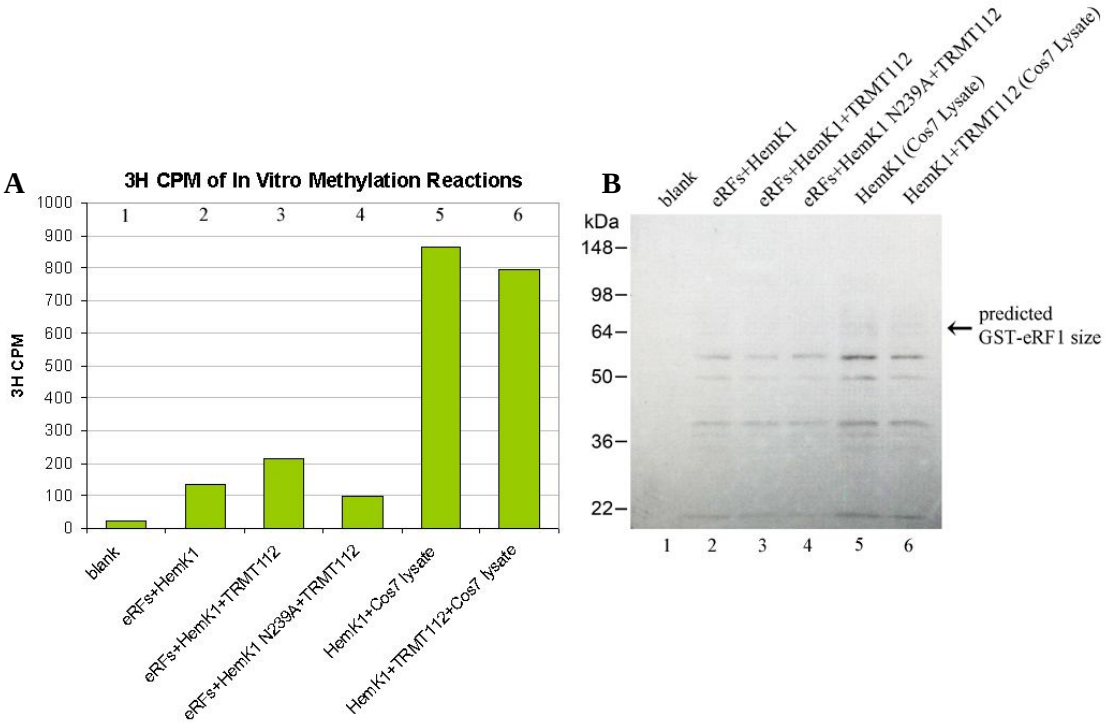

Figure 5.8 HemK1 methylation assay with eRFs. Immunopurified eRFs were incubated with lysate of COS-7 cells transfected with HemK1 and TRMT112, that was washed off after the reaction. (A) Some increase in eRFs [^{3}H] signal is observed when HemK1 and TRMT112 are present (lane 3) while HemK1 N239A affects the incorporation of [^{3}H]-methyl to eRFs with the [^{3}H] counts lowered to control levels (lane 4). (B) Autoradiography did not detect a band at the predicted size of eRF1. The experiment was performed once and each reaction in monoplicate. Lanes 5 and 6, where total COS-7 cell lysates were analysed, represent positive controls for the conditions of the methylation reaction.

In 2007 Soleimanpour-Lichaei and colleagues suggested that the predicted release factor mtRF1 is mitochondrial but it does not show detectable peptide release activity. They were however able to show release activity for another homologue protein, the mitochondrial mtRF1a. The cDNA clones encoding for mtRF1 and mtRF1a were kindly provided by Z. Chrzanowska-Lightowlers and used in a methylation assay with HemK1. GST-HemK1 or FLAG-HemK1 were immuno-precipitated from lysates of transfected COS-7 cells and incubated with purified recombinant proteins GST-mtRF1 or GST-mtRF1a. When the reaction products were analysed by SDS-PAGE and the radioactivity detected by autoradiography, it was possible to detect GST-mtRF1 (a) and GST-mtRF1a (b) in lanes 3, 4, 7 and 8 (Figure 5.9). The two release factor homologues seemed to have been labelled with [^{3}H] in the absence of HemK1 in the reaction (lanes 3 and 4). This is an interesting finding since the only methyltransferases that could possibly exist in the reaction would have been bacterial proteins bound to the release factors during protein purification. A number of bands were detected in the COS-7 lysate-containing reactions reflecting the plethora of active methyltransferases under the reaction conditions (lanes 5, 6 and 9). No increase was detected in the mtRF1 and mtRF1a bands when HemK1 was included in the reaction (comparing lanes 3, 4 with 7,8 and 10,11). An increase in the band intensities of lysate methylated proteins was observed in the presence of FLAG-HemK1 (lane9), a difficult to interpret finding that could suggest that either: a) HemK1 methylates a myriad of proteins in the COS-7 lysate, or b) degraded forms of the successfully methylated substrates of HemK1 can be detected on the film, or c) the difference in band intensities is due to technical error in loading the polyacrylamide gel

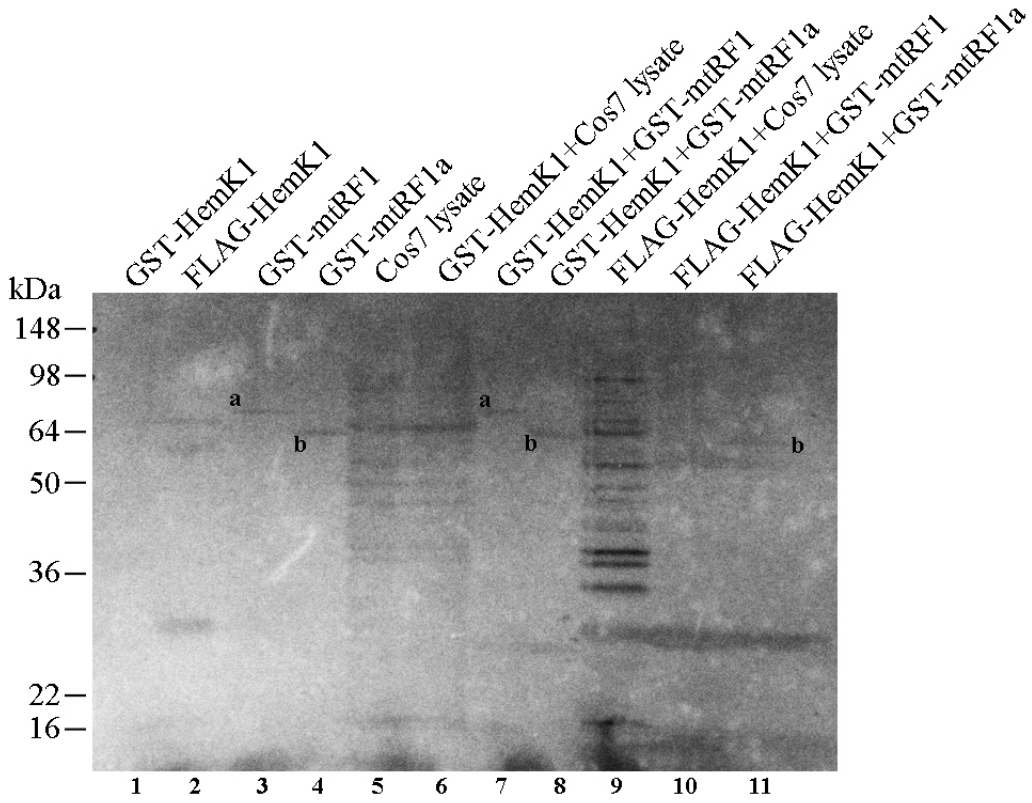

Figure 5.9 Autoradiography detection of methylated mtRF1 and mtRF1a. Autoradiography analysis revealed that radiolabelling of mtRf1 and mtRF1a by [^{3}H]-methyl can be observed even in the absence of enzyme in the reaction (bands are annotated as: mtRf1 (a) and mtRF1a (b)).

The investigation in the methylation activity of HemK1 was not pursued further since the limitations of the technique were considered too critical to allow for an accurate observation of successfully methylated substrate. It was not possible to analyse the reaction product for methylation by mass spectrometry and the detectable levels of [^{3}H] incorporation were believed to be close to the detection thresholds of autoradiography.

HemK functional association with RNA granules

HemK1 and HemK2 are part of translation termination machinery in cells methylating release factors and mediating release of the synthesised peptide chains. HemK2 associates with the release factors eRF1 and eRF3 (see Figure 5.4) and methylates eRF1 in mammalian cells (Figaro et al, 2008). Release factors eRF1 and eRF3 are also part of the nonsense-mediated mRNA decay machinery (NMD) through their association with Upf1 (Ivanov et al, 2008; Kashima et al, 2006).

HemK1 co-localises with P-body protein Dcp1b

When HemK1 was over-expressed in mammalian cells it localised in distinct foci in the cytoplasm not solely confined to the mitochondria, assuming a localisation pattern reminiscent of P-body staining described in literature. In a search to identify possible localisation of HemK1 in RNA processing bodies it was compared to the localisation pattern of Dcp1b, a protein that is localised to and induces the formation of P-bodies (Cougot et al, 2004b). The human cDNA of the p-body component Dcp1b was acquired and cloned in a GFP tag pXJ40 mammalian expression vector (see Materials and Methods). The expression of the cloned GFP-Dcp1b protein was tested by western blotting of lysates of transfected COS-7 cells (Figure 5.18). When HemK1 and Dcp1b were over-expressed in HeLa cells the two proteins showed strong co-localisation as analysed by confocal microscopy, suggesting that HemK1 can localise in RNA processing bodies (Figure 5.10C).

The co-localisation of HemK1 with Dcp1b, albeit a very interesting finding, raised the question if this is actually possible in nature since HemK1 is expected to be mitochondrial and a localisation of HemK1 outside the mitochondria has not been documented in literature. The possibility that Dcp1b can localise in the mitochondria was investigated in HeLa cells where its sub-cellular localisation was compared to that of mtRF1a. Confocal microscopy analysis revealed no co-localisation between Dcp1b and the distinct mitochondrial expression pattern of mtRF1a, indicating that over-expressed Dcp1b does not localise in mitochondria (Figure 5.10B). This indicated that HemK1 and Dcp1b co-localise outside of the mitochondrial space suggesting that either exogenous expression of HemK1 can induce P-bodies, or that

Dcp1b-induced P-bodies recruit HemK1. It was noted that over-expression of HemK1 altered the localisation of Dcp1b to aggregated cytoplasmic foci, an effect that was not observed when Dcp1b was co-expressed with mtRF1a (Figure 5.10C and A). This was observed to at least 70% of the cells analysed and it was reproducible between experiments, but was not quantified. Direct comparison between GFP-Dcp1b and MitoTracker stain was not possible since they both emit on the green wavelength.

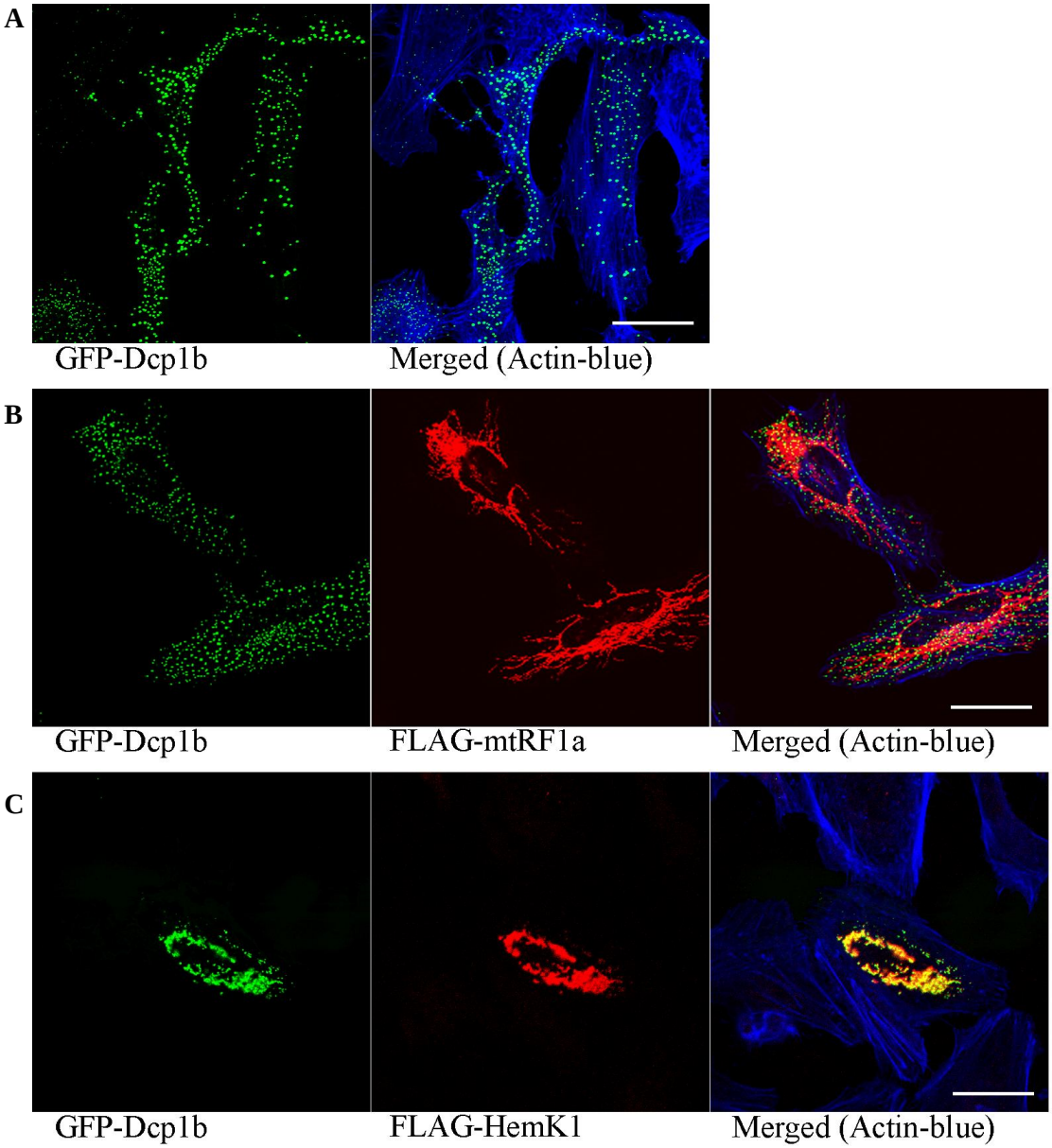

Figure 5.10 HemK1 co-localises with P-body marker Dcp1b. In (A), GFP-Dcp1b was expressed in HeLa cells that were fixed and stained for actin (Phalloidin:Cy5), while in (B) GFP-Dcp1b was co-expressed with FLAG-mtRF1a, subsequently stained with anti-FLAG (TRITC) antibody. Dcp1b, that is believed to localise in RNA processing bodies and also induce their formation when over-expressed, localised in cytoplasmic loci with distinct localisation to mitochondrial mtRF1a. When GFP-Dcp1b was co-expressed with FLAG-HemK1 (TRITC) strong co-localisation was observed between the two protens. It was also noted that GFP-Dcp1b localisation pattern changed in the presence of over-expressed HemK1, concentrating in less distinct cytoplasmic foci and revealing a rather aggregated and irregular cytoplasmic expression pattern. The scale bars represent 10µm.

Channels: (A) FITC(green):GFP-Dcp1b and Cy5(blue):Phalloidin, (B) FITC(green):GFP-Dcp1b, TRITC(red):FLAG-mtRF1a (rabbit anti-FLAG antibody) and Cy5(blue):Phalloidin, and (C) FITC(green):GFP-Dcp1b, TRITC(red):FLAG-HemK1 (rabbit anti-FLAG antibody) and Cy5(blue):Phalloidin.

The data so far indicated that HemK1 can co-localise with its proposed mitochondrial substrate mtRF1a but also with the P-body marker Dcp1b in separate experiments in cells. In fact, in an experiment where all three proteins were co-transfected in cells, HemK1 co-localised with both Dcp1b and mtRF1a in separate areas, while Dcp1b and mtRF1a showed a distinct localisation pattern (Figure 5.11). This indicated that HemK1 intracellular localisation can in fact be shared between P-bodies and mitochondria.

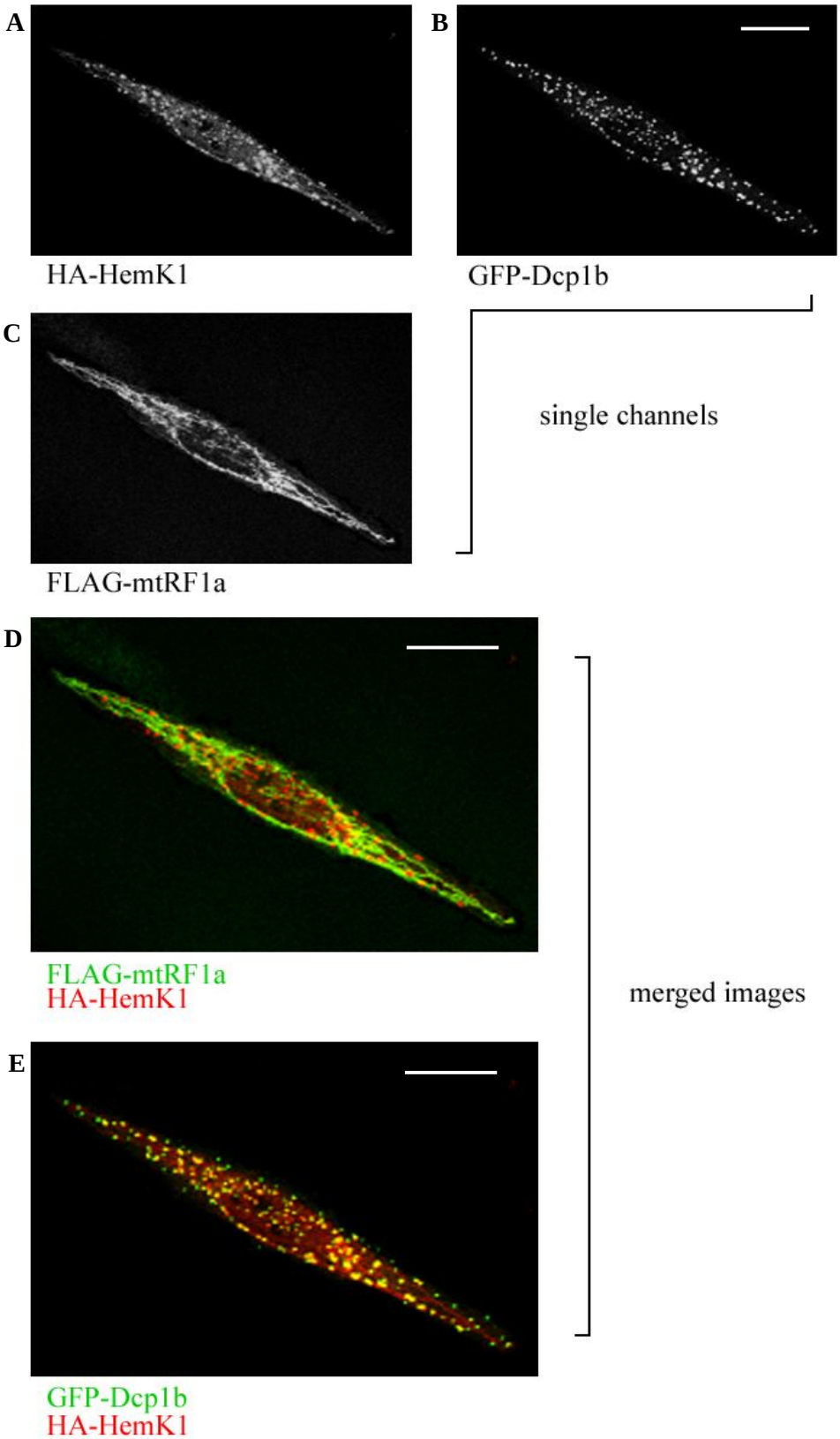

Figure 5.11 HemK1 can localise in mitochondria and P-bodies. HA-HemK1, GFP-Dcp1b and FLAG-mtRF1a were co-expressed in N1E-115 neuroblastoma cells that were subsequently fixed and stained with rabbit anti-FLAG (TRITC) and mouse anti-HA (Cy5) antibodies. Panels (A), (B) and (C) show monochrome images of HA-HemK1 (Cy5), GFp-Dcp1b and FLAG-mtRF1a (TRITC) staining, respectively. Panels (D) and (E) are red/green merge images for comparison, showing HA-HemK1 (red) with FLAG-mtRF1a (green) in (D) and GFP-Dcp1b (green) in (E). The scale bars represent 10µm.
Channels: FITC:GFP-Dcp1b, TRITC-FLAG-mtRF1a (rabbit anti-FLAG antibody) and Cy5:HA-HemK1 (mouse anti-HA antibody).

To investigate whether HemK1 expression can induce P-body formation, P-bodies were visualised in HeLa cells exogenously expressing FLAG-HemK1 using an antibody against endogenous Dcp1a, a homologue of Dcp1b that can localise in P-bodies (Cougot et al, 2004b). At the time of the experiment an antibody against Dcp1b was not available. This commercial antibody raised against human Dcp1a had not been tested for reactivity in other species, so the experiment was performed in HeLa cells. Arsenite treatment was also used to induce P-body formation in untransfected cells (Kedersha et al, 2005). Arsenite treatment induced an increase in Dcp1a staining, compared to untransfected or mock transfected cells, where cells were treated with lipofectamine reagent as in normal transfections but no DNA was added. A similar increase was observed in FLAG-HemK1 transfected cells suggesting that HemK1 expression can induce P-body formation (Figure 5.12). Even though HemK1 exogenous expression seemed to induce an increase in Dcp1a staining no co-localisation was observed.

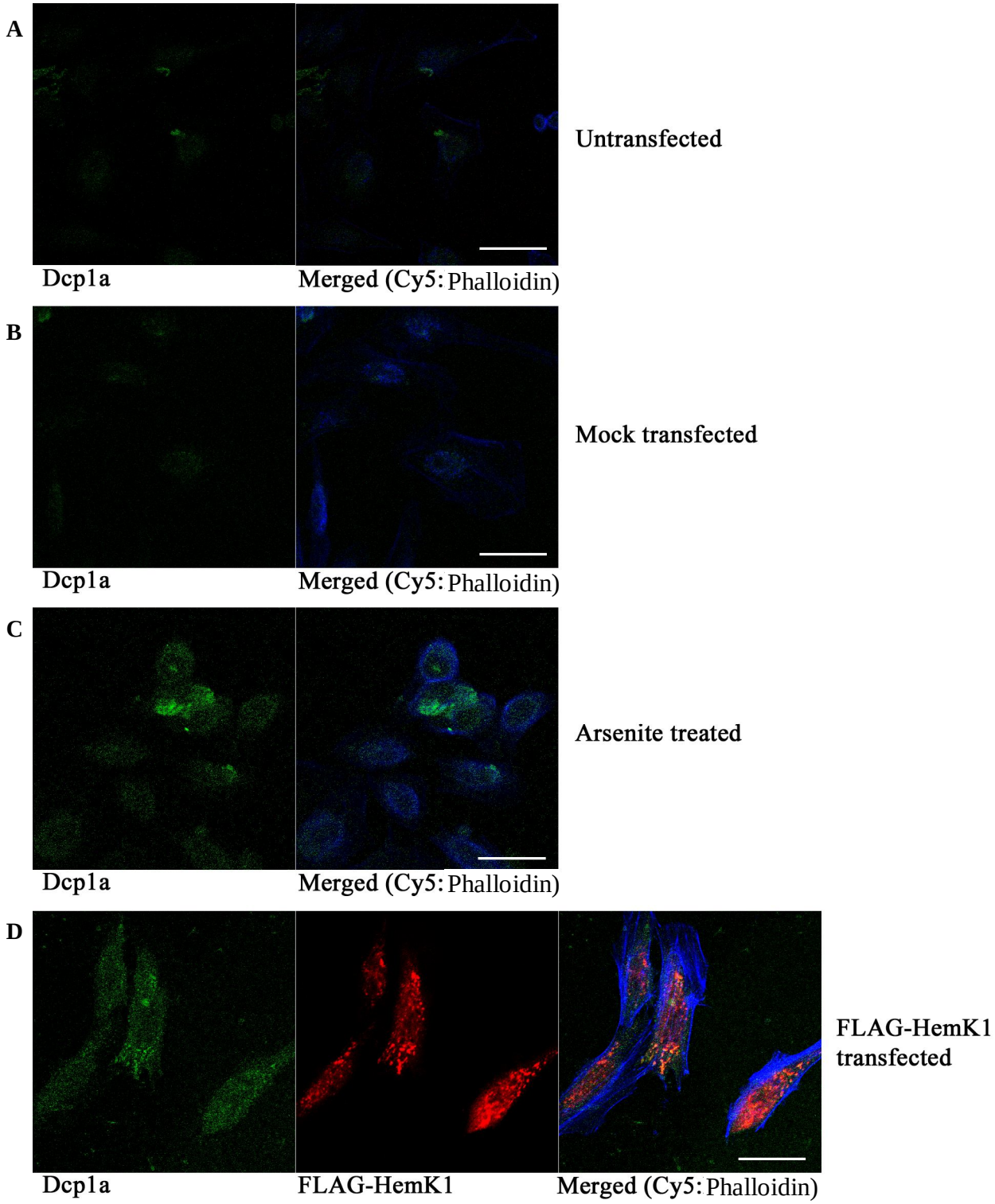

Figure 5.12 Arsenite as well as HemK1 can induce P-body formation. HeLa cells were untreated (A), treated with arsenite (C), mock transfected (B) or tranfected with FLAG-HemK1 (D), and anti-Dcp1a antibody (FITC) was used to detect endogenous Dcp1a localisation under confocal microscopy. An increase in Dcp1a staining was observed in arsenite treated (C) as well as HemK1 transfected cells (D) suggesting that HemK1 can induce the formation of P-bodies. The scale bars represent 10µm.

Channels: (A-C) FITC(green):endogenous Dcp1a (goat anti-Dcp1a antibody) and Cy5(blue):Phalloidin, (D) FITC(green):endogenous Dcp1a (goat anti-Dcp1a antibody), TRITC(red):FLAG-HemK1 (rabbit anti-FLAG antibody) and Cy5(blue):Phalloidin.

The observation that over-expressed HemK1 does not co-localise in Dcp1a-containing bodies while it seems to induce their formation (Figure 5.12) was investigated further by comparing GFP-Dcp1b induced cytoplasmic loci with endogenous Dcp1a. HeLa cells over-expressing GFP-Dcp1b were stained for Dcp1a and even though some over-lapping of the stains was observed the localisation pattern of the two markers was different suggesting that they do not co-localise (Figure 5.13). This could be explained taking in consideration that Dcp1b and Dcp1a do not solely localise in P-body structures (Cougot et al, 2004b).

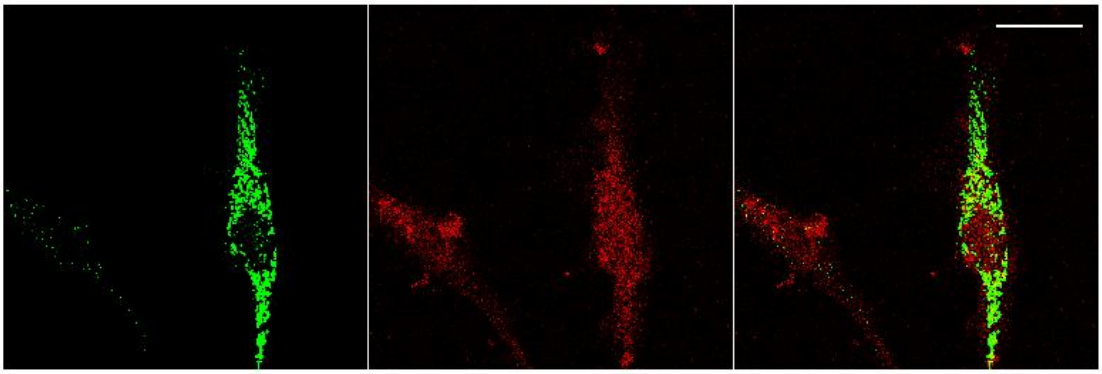

Figure 5.13 Dcp1a is not excusively detected in GFP-Dcp1b-containing cytoplasmic loci. HeLa cells were tranfected with GFP-Dcp1b and anti-Dcp1a antibody (TRITC) was used to detect endogenous Dcp1a localisation under confocal microscopy. Even though some over-lapping of Dcp1a and GFP-Dcp1b was observed the localisation pattern of the two markers does not suggest co-localisation. The scale bars represent 10μm.
Channels: FITC(green):GFP-Dcp1b and TRITC(red):endogenous Dcp1a (goat anti-Dcp1a antibody).

To investigate if Dcp1b-induced P-body formation would recruit endogenous HemK1 in cells the rabbit-5 anti-HemK1 antibody was used on HeLa cells. This antibody was chosen because in other experiments it showed a convincing endogenous staining in untransfected cells and also a clean band corresponding to the cloned HemK1 protein on a western blot of human brain lysate (see Chapter 4). When GFP-Dcp1b was over-expressed in HeLa cells the staining pattern of the rabbit-5 anti-HemK1 antibody did not change compared to that of untransfected cells, and while some over-lapping of the Dcp1b and HemK1 localisation occurred it would not indicate co-localisation (Figure 5.14). These data are hard to interpret since the specificity of the rabbit-5 anti-HemK1 antibody to the endogenous HemK1 protein is still questionable.

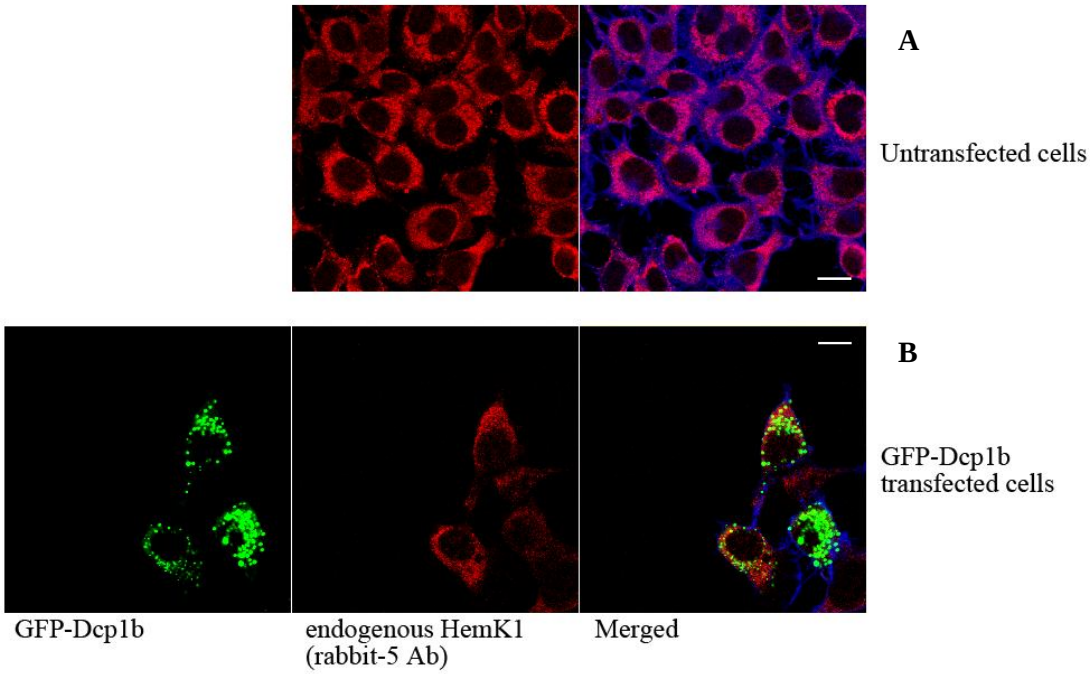

Figure 5.14 Endogenous localisation of HemK1 in GFP-Dcp1b transfected HeLa cells. HeLa cells were transfected with GFP-Dcp1b and the rabbit-5 anti-HemK1 antibody was used to detect endogenous HemK1. No difference was observed in the anti-HemK1 antibody staining between untransfected (A) and GFP-Dcp1b transfected cells (B). The scale bars represent 10μm.
Channels: FITC:GFP-Dcp1b, TRITC(red): endogenous HemK1 (rabbit anti-HemK1) and Cy5(blue):Phalloidin.

Involvement of HemK proteins and Release Factors in P-bodies

Since HemK1 can associate with eRF1 and mtRF1a in cells, and there is a published link between eRF1 and P-bodies through the nonsense-mediated mRNA decay machinery, we aimed to investigate the involvement of the release factors in P-body formation. The localisation of eRF1 in P-bodies was investigated using the Dcp1a antibody and also by inducing P-body formation through GFP-Dcp1b exogenous expression (Figure 5.15A). In cells transfected only with FLAG-eRF1 the Dcp1a localisation showed some over-lap with eRF1 but the two stains followed a distinct pattern not indicating strong co-localisation. However, when FLAG-eRF1 was co-transfected with GFP-Dcp1b the eRF1 localisation changed dramatically in high expressing cells, showing strong co-localisation with Dcp1b (figure 5.15B). Strong co-localisation was not observed in cells expressing low levels of eRF1, but it was persistent in the majority of high expressing cells. Therefore figure 5.15B is a

representative image of cells expressing high levels of eRF1, revealing a consistent alteration in eRF1 localisation in the presence of Dcp1b. This indicated that inducing P-body formation through Dcp1b expression can recruit eRF1 to P-bodies.

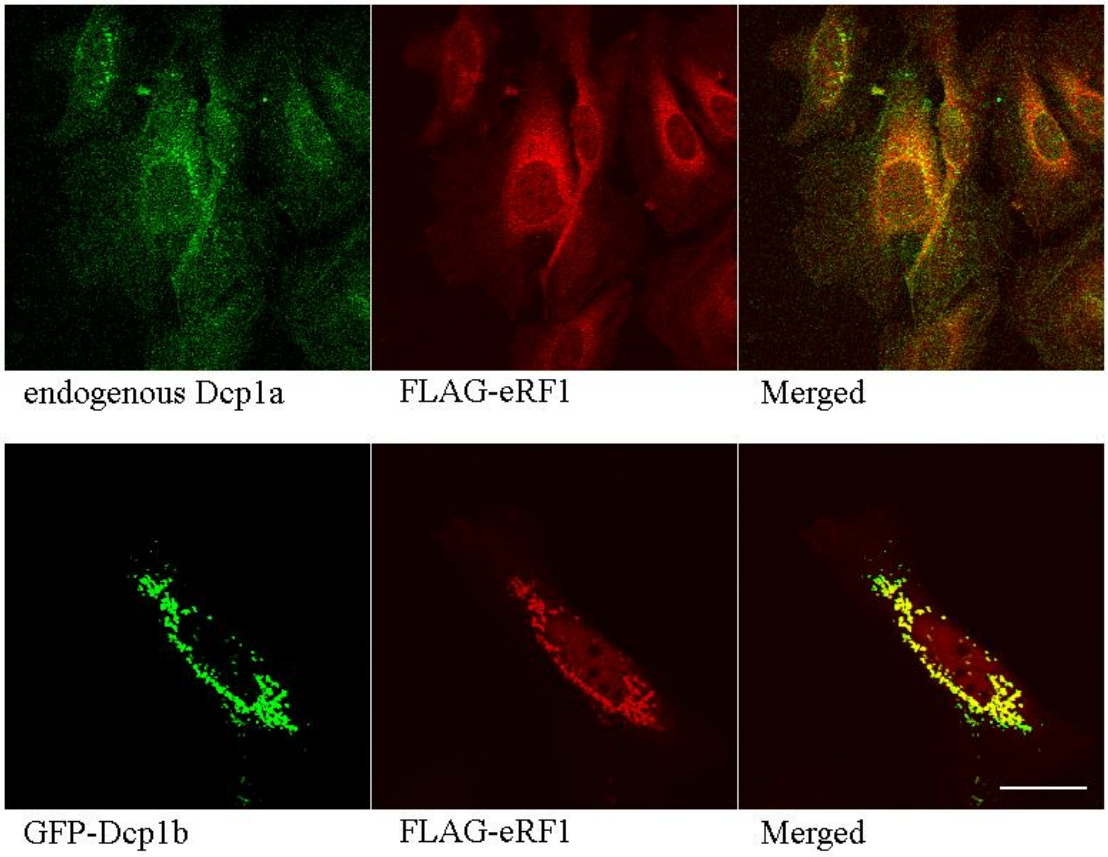

Figure 5.15 GFP-Dcp1b recruits eRF1 in P-bodies. (A) HeLa cells were tranfected with FLAG-eRF1 (TRITC, red) and stained for endogenous Dcp1a (FITC, green). eRF1 localised in the cytoplasm in a particulate localisation pattern. When eRF1 was co-transfected with GFP-Dcp1b, eRF1 localised in large loci in the cytoplasm and revealed a significant co-localisation with Dcp1b in many cells (B). The scale bar represents 10µm.

Channels: (A) FITC(green):endogenous Dcp1a (goat anti-Dcp1a antibody) and TRITC(red):FLAG-eRF1 (rabbit anti-eRF1 antibody), (B) FITC(green):GFP-Dcp1b and TRITC(red):FLAG-eRF1 (rabbit anti-eRF1 antibody).

Next we aimed to investigate the effect of HemK1 in the Dcp1b-induced recruitment of eRF1. Cells expressing HA-HemK1 and FLAG-eRF1 were stained for P-bodies using the Dcp1a antibody or by co-expressing GFP-Dcp1b (Figure 5.16). As previously described in this chapter, over-expressed HA-HemK1 and FLAG-eRF1 co-localised as revealed by confocal analysis. Interestingly the P-body stain as revealed by endogenous Dcp1a antibody co-localised with HemK1 and eRF1 in some cells. This co-localisation is much stronger compared to when HemK1 and eRF1 are expressed individually suggesting that co-expression of HemK1 and eRF1 can induce the formation of Dcp1a-containing P-bodies in some cells (Figure 5.16A). When GFP-Dcp1b was co-expressed with HA-HemK1 and FLAG-eRF1 all three proteins showed partial co-localisation in some cells (Figure 5.16B).

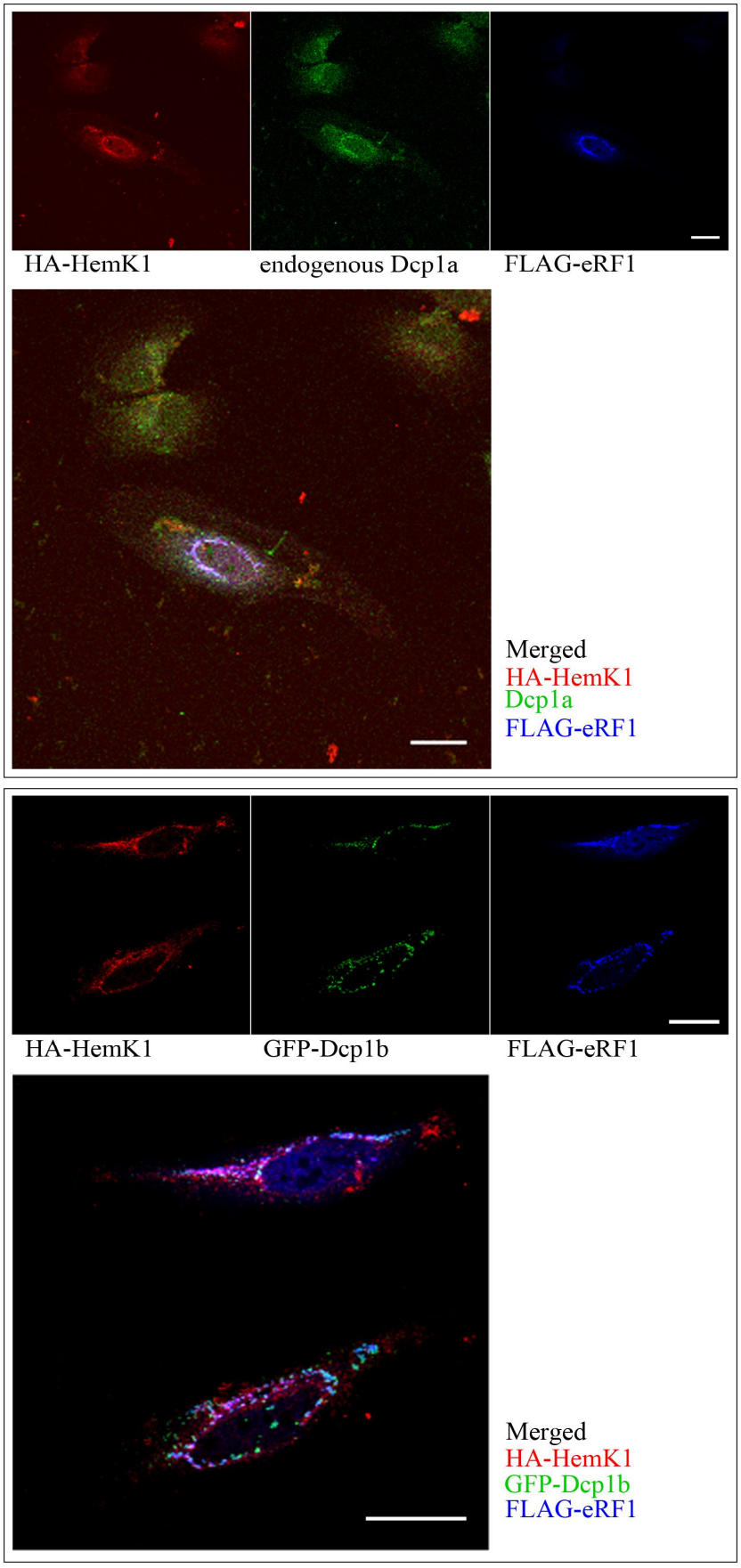

Channels:
(A) FITC(green):endogenous Dcp1a (goat Dcp1a antibody), TRITC(red):HA-HemK1 (mouse anti-HA antibody) and Cy5(blue):FLAG-eRF1 (rabbit anti-FLAG antibody),
(B) FITC(green):GFP-Dcp1b, TRITC(red):HA-HemK1 (mouse anti-HA antibody) and Cy5(blue):FLAG-eRF1 (rabbit anti-FLAG antibody.

Figure 5.16 HemK1 can co-localise with eRF1 and Dcp1b. (A) HeLa cells were tranfected with HA-HemK1 (TRITC) and FLAG-eRF1 (Cy5) and stained with relevant antibodies. Some co-localisation was observed between HemK1 (red), eRF1 (blue) and endogenous Dcp1a (green). When the cells were transfected with HemK1, eRF1 and GFP-Dcp1b partial co-localisation was observed between the three proteins (B). The scale bars represent 10µm.

The localisation pattern of eRF1 and P-bodies was further investigated in a similar experiment in relation to eRF1 *bona fide* partner HemK2. HA-HemK2 and FLAG-eRF1 were exogenously expressed in HeLa cells and were compared to staining of P-bodies stained with the anti-Dcp1a antibody (Figure 5.17A). Some partial co-localisation was observed between HA-HemK2 and FLAG-eRF1 while the localisation distribution of Dcp1a was similar. When GFP-Dcp1b was co-expressed with HA-HemK2 and FLAG-eRF1 the co-localisation of the three proteins was significant in some cells (Figure 5.17B). HemK2 can in fact co-localise with Dcp1b when eRF1 is not present, but the co-localisation is only partial (figure 5.17C).

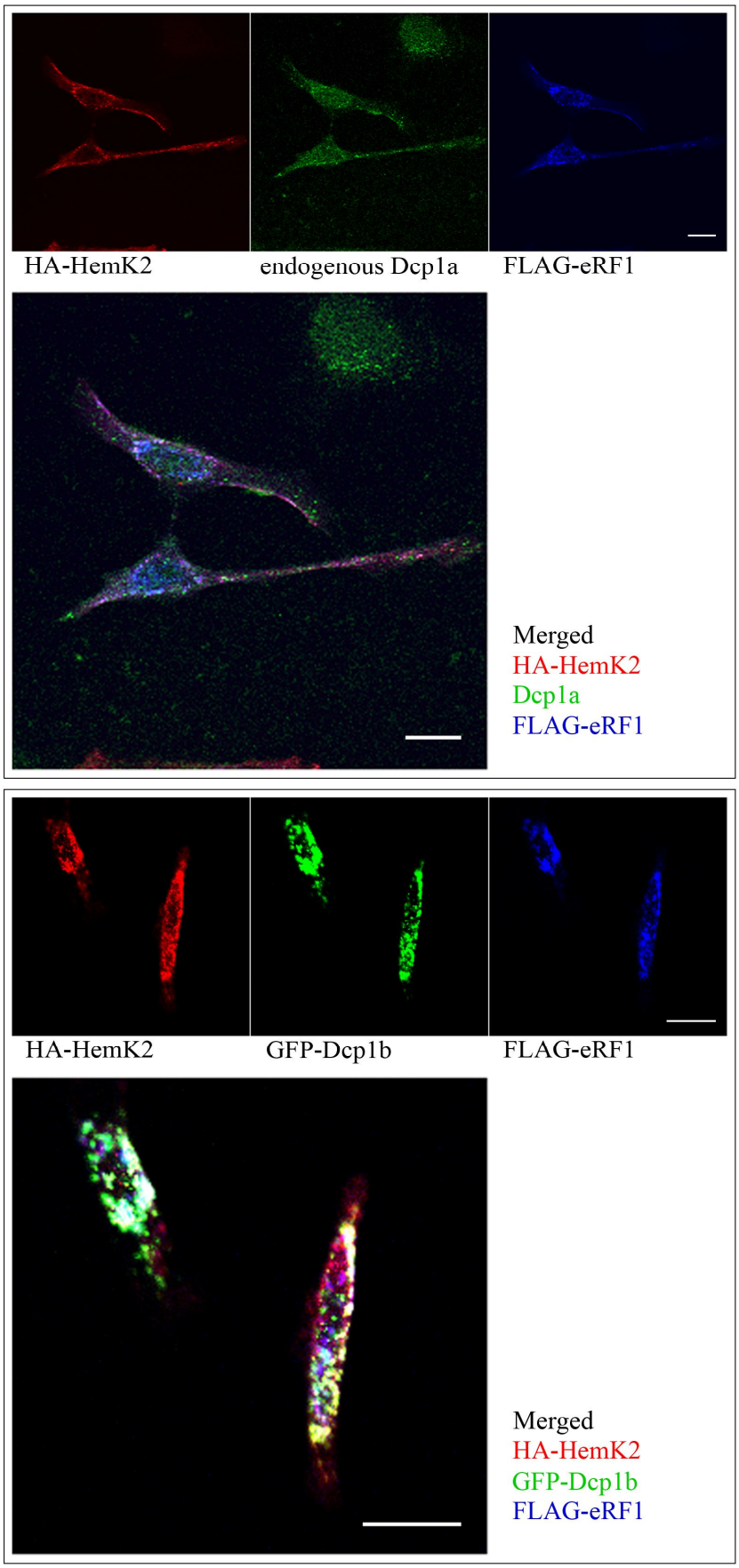

Channels:
(A) FITC(green):endogenous Dcp1a (goat Dcp1a antibody), TRITC(red):HA-HemK2 (mouse anti-HA antibody) and Cy5(blue):FLAG-eRF1 (rabbit anti-FLAG antibody),
(B) FITC(green):GFP-Dcp1b, TRITC(red):HA-HemK2 (mouse anti-HA antibody) and Cy5(blue):FLAG-eRF1 (rabbit anti-FLAG antibody,
(C) FITC(green):GFP-Dcp1b, TRITC(red):HA-HemK2 (mouse anti-HA antibody) and Cy5(blue):Phalloidin.

Figure 5.17 HemK2 can co-localise with eRF1 and Dcp1b. (A) HeLa cells were transfected with HA-HemK2 (TRITC, red) and FLAG-eRF1 (Cy5, blue) and stained with relevant antibodies. Some co-localisation was observed with HemK1, eRF1 and endogenous Dcp1a. When the cells were transfected with HemK2, eRF1 and GFP-Dcp1b significant co-localisation was observed between the three proteins (B). HemK2 can partially co-localise with GFP-Dcp1b in the absence of eRF1 (C). Scale bars: 10µm.

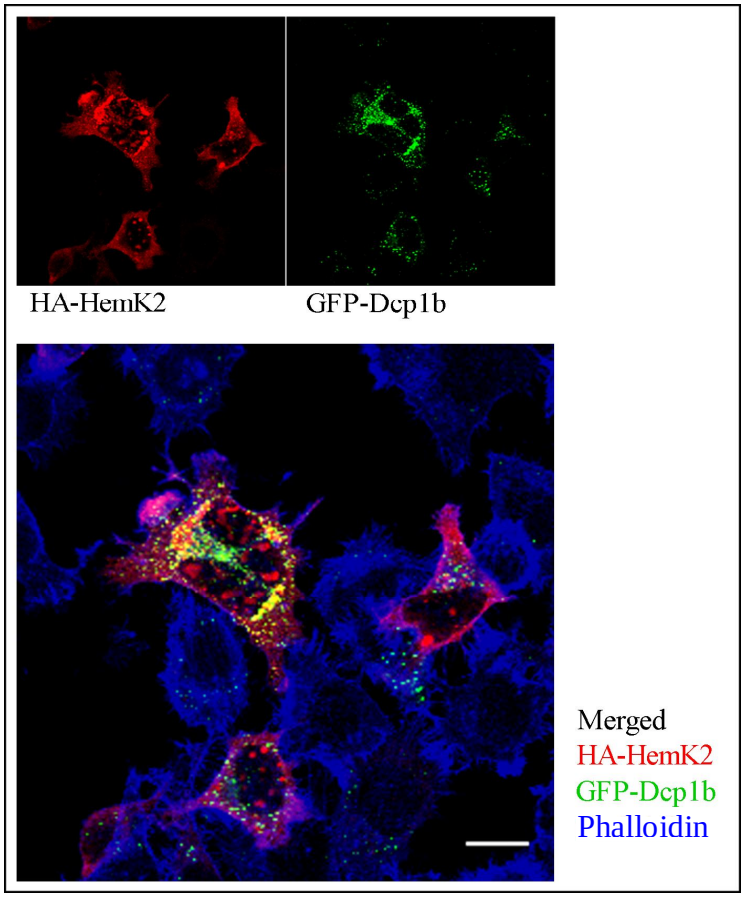

C

Involvement of HemK proteins in stress granules

The data so far indicated that HemK1 and HemK2 are linked to P-bodies as revealed by over-expression experiments and when compared to P-body marker Dcp1b. In an attempt to investigate further the involvement of HemK1 and HemK2 in P-bodies and also to compare their localisation to stress granules an array of proteins involved in RNA processing was obtained and cloned in mammalian expression vectors. The obtained cDNAs and the localisation/function of the encoded proteins are summarised in table 5.1.

Component	Localisation/Associates	Known Functions/Involved in
Dcp1	P-bodies	mRNA decapping enzyme, mRNA decay
G3BP	Stress granules	Ras signalling, Endoribonuclease, mRNA decay, ubiquitin proteosome pathway
FMRP	Associates with microRNA components, P-bodies, SGs	Local translation in dendrites
Staufen1	Localises with ribonucleoprotein complexes, FMRP, PABP. P-bodies	mRNA transport along microtubules, SMD. Recruits UPF1 to SMD.
Upf1	P-bodies? Can co-localise with Dcp1a, Dcp2	NMD

Table 5.1 Proteins involved in RNA processing. A list of proteins involved in RNA processing and transport and their localisation in respect to stress granules and P-bodies. References: Dcp1: (van Dijk et al, 2002; Cougot et al, 2008), G3BP (Tourrière et al, 2003), FMRP: (Antar et al, 2005; Zalfa et al, 2006; Li et al, 2009; Cheever and Ceman, 2009) Staufen: (Johnston et al, 1991; Goetze et al, 2006; Tang et al, 2001b), Upf1: (Lykke-Andersen et al, 2000; Barbee et al, 2006).

The expression of the cloned cDNA constructs was tested in over-expression experiment COS-7 cells where lysates were analysed by SDS-PAGE and immunoblotting. Figure 5.18 shows expression of GFP-Dcp1b and GFP-Staufen1.

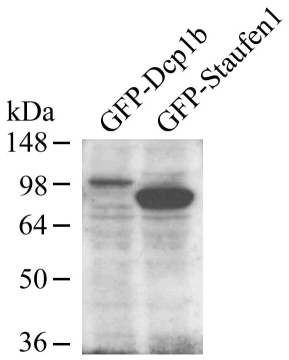

Figure 5.18 Expression of GFP-Dcp1b and GFP-Staufen1. GFP-Dcp1b and GFP-Staufen1 were transfected in COS-7 cells that were lysed after over-night expression. Under SDS-PAGE analysis of the lysates immunoblotting with anti-GFP antibody revealed a single band of the expected size for both cloned constructs.

A survey on the localisation of FMRP, Staufen1 and Upf1 was undertaken in relation to HemK1 and HemK2. The proteins were expressed in N1E-115 cells that were subsequently fixed and stained. The confocal images obtained for Staufen1 were difficult to interpret since a homogeneous cytoplasmic expression was observed at high expression levels. Nevertheless, HemK1 and HemK2 stain over-lapped with Staufen1. Upf1 showed a nuclear localisation in contrast to published research suggesting that Upf1 is mainly cytoplasmic (Brogna et al, 2008). FMRP revealed a dot-like expression in the cytoplasm while in cells expressing a comparable amount of Hemk2 protein no substantial co-localisation was observed between the two proteins (Figure 5.19)

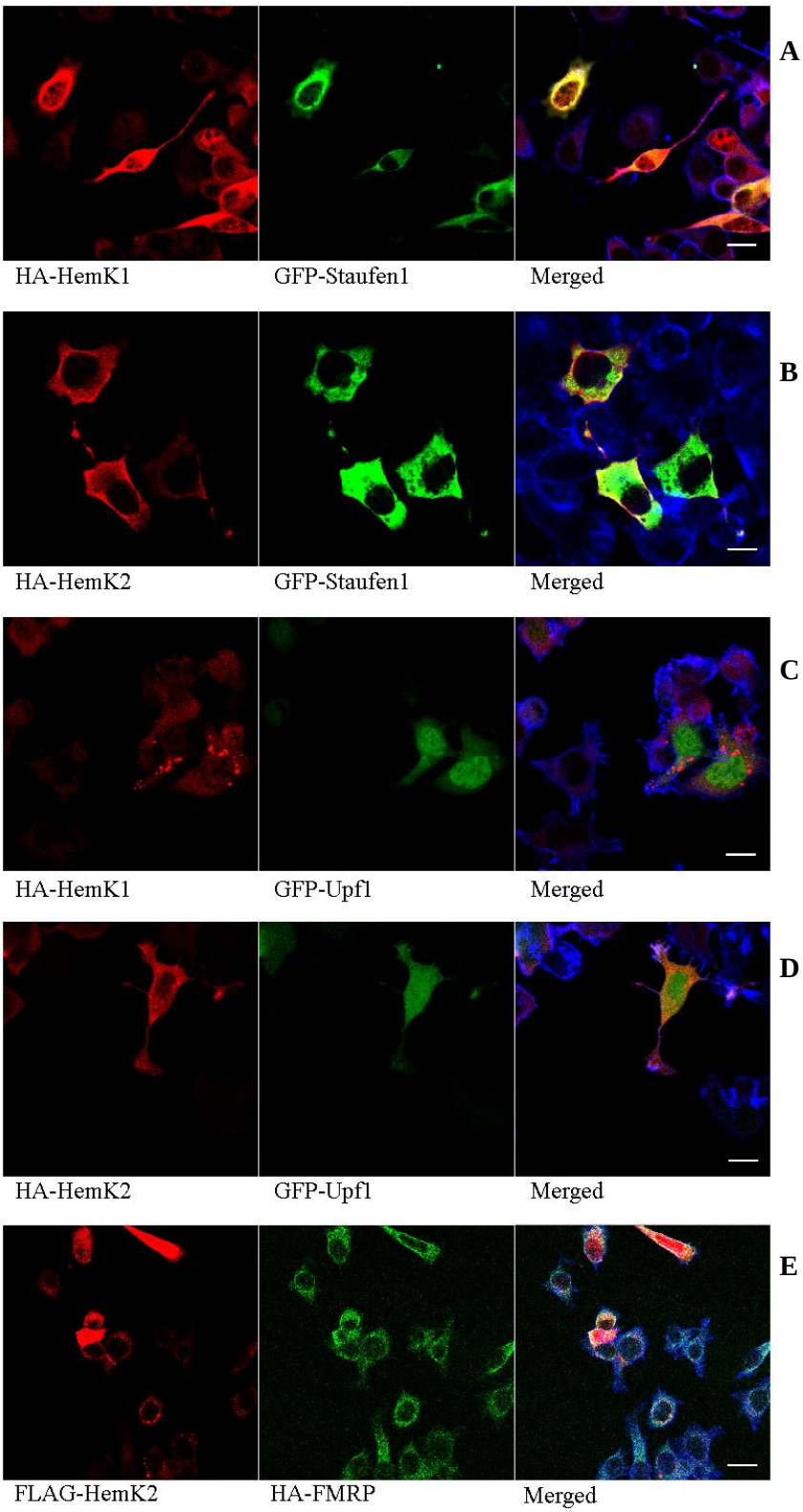

Figure 5.19 Survey on cellular localisation of Staufen1, Upf1 and FMRP. GFP-Staufen1, GFP-Upf1 and HA-FMRP were expressed in N1E-115 neuroblastoma cells along with HemK1 and HemK2. Under confocal analysis of the fixed and stained cells GFP-Staufen1 revealed a diffused cytoplasmic expression pattern, though some over-lap in staining was observed with the co-expressed N5-methyltransferases (A, B). Upf1 expressed largely in the nucleus not co-localising with either HemK1 or HemK2 (C, D). In (E), the cells that show moderate expression of HemK2 revealing its localisation do not suggest co-localisation with FMRP. The scale bars represent 10µm. Channels: (A) FITC:GFP-Staufen1, TRITC:HA-HemK1 (anti-HA) and Cy5:Phalloidin, (B) FITC:GFP-Staufen1, TRITC:HA-HemK2 (anti-HA) and Cy5:Phalloidin, (C) FITC:GFP-Upf1, TRITC:HA-HemK1 (anti-HA) and Cy5:Phalloidin, (D) FITC:GFP-Upf1, TRITC:HA-HemK2 (anti-HA) and Cy5:Phalloidin, (E) FITC:HA-FMRP (anti-HA), TRITC:FLAG-HemK2 (anti-FLAG) and Cy5:Phalloidin.

The stress granule marker G3BP was investigated in terms of subcellular localisation in relation to Hemk1 and HemK2. Initially it was demonstrated that G3BP-containing stress granules are largely distinct to Dcp1b-containing P-bodies in an over-expression experiment in N1E-115 cells, as previously reported by Ohn and colleagues (Ohn et al, 2008) (Figure 5.20).

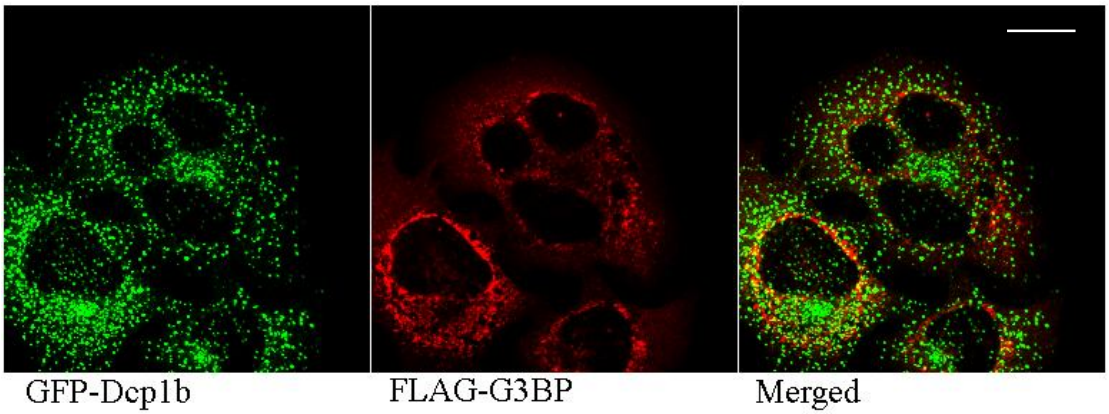

Figure 5.20 P-bodies are distinct to stress granules. The localisation of Dcp1b-induced P-bodies was compared to G3BP-induced stress granules in N1E-115 cells. Both proteins were overexpressed and FLAG-G3BP was stained with anti-FLAG antibody (TRITC, red). The loci induced by the two proteins show largely distinct localisation while some co-localisation is observed, a finding which is in agreement with the current literature suggesting a link between P-bodies and stress granules. The scale bar represents 10μm. Channels: FITC(green):GFP-Dcp1b and TRITC(red):FLAG-G3BP (rabbit anti-FLAG antibody).

The localisation of G3BP was compared to exogenously expressed HemK1 and HemK2 in N1E-115 cells. Over-expressed G3BP showed largely distinct localisation to that of HemK1 and HemK2, but both showed some regions of over-lap (Figure 5.21).

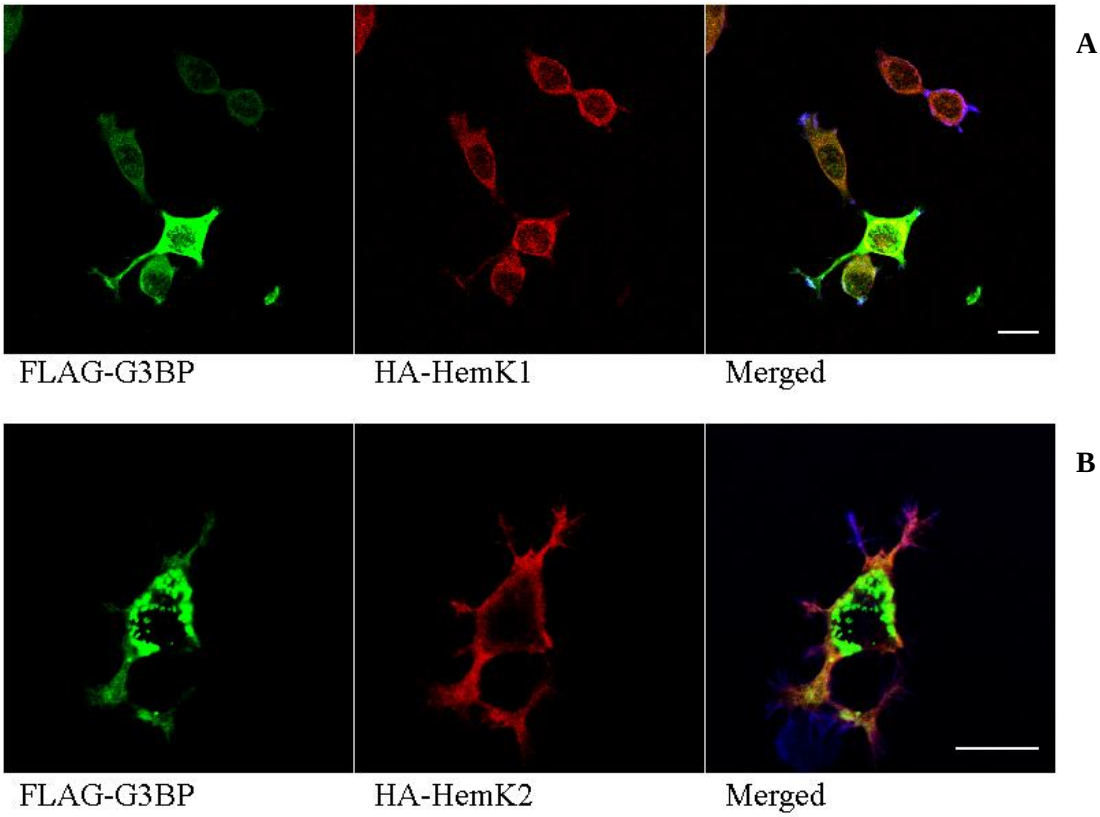

Figure 5.21 G3BP localisation compared to HemK1 and HemK2. The localisation of G3BP-induced stress granules was compared to HemK1 and HemK2 in N1E-115 cells. Even though some over-lap of the stains was observed the localisation pattern of G3BP and the two N5-methyltransferases was distinct therefore not suggesting significant co-localisation. The scale bars represent 10µm.
Channels: (A) FITC(green):FLAG-G3BP (rabbit anti-FLAG antibody), TRITC(red):HA-HemK1 (mouse anti-HA antibody) and Cy5(blue):Phalloidin, (B) FITC(green):FLAG-G3BP (rabbit anti-FLAG antibody), TRITC(red):HA-HemK2 (mouse anti-HA antibody) and Cy5(blue):Phalloidin.

Interestingly, in a pull-down experiment in N1E-115 neuroblastoma cells, HemK1 and HemK2 were able to associate with GFP-G3BP when over-expressed (Figure 5.22).

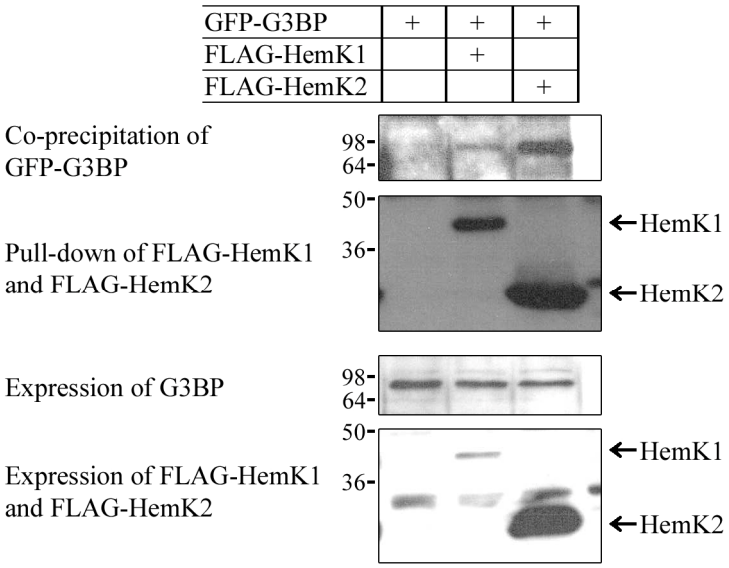

Figure 5.22 G3BP can associate with HemK1 and HemK2 in cells. FLAG-HemK1 and FLAG-HemK2 were co-expressed with GFP-G3BP and were immunopurified using FLAG beads. Western blot analysis revealed a significant amount of co-immunoprecipitated GFP-G3BP in the HemK2 pull-down, while some G3BP was detected co-precipitating with HemK1.

Summary

A possible association between the HemK proteins and peptide release factors eRF1, eRF3 and mtRF1a was investigated. In pull-down assays in cells HemK1 associated with mtRF1a, and with eRF1 which is the predicted substrate of HemK2. HemK2 associated with eRF1 and mtRF1a. To investigate HemK1 and HemK2 intracellular localisation in respect to release factors, the proteins were exogenously expressed in cells that were fixed and stained with relevant antibodies. HemK1 co-localised with mitochondrial release factor mtRF1a and showed some co-localisation with eRF1. HemK2 co-localised with eRF1 and showed some partial co-localisation with mtRF1a. To investigate the methyltransferase activity of HemK1, the NPPY motif of HemK1, that mediates its association with release factors, was mutated to N239A. Methyltransferase assays *in vitro* indicated that eRF1 may be methylated by HemK1 in the presence of TRMT112, while the N239A mutation seemed to have an effect in HemK1 activity.

The subcellular localisation of HemK1 and HemK2 was investigated in respect to markers for P-bodies and stress granules, following published data supporting a role of eRR1 and eRF3 in RNA NMD, that takes place in RNA processing bodies. Table 5.2 summarises the co-localisations observed between the HemK proteins and the components of P-bodies and stress granule investigated. HemK1 co-localised with mtRF1a that was highly mitochondrial. HemK1 also co-localised with P-body protein Dcp1b, in the cytoplasm. Dcp1b showed distinct localisation when compared to a mitochondrial marker, indicating that HemK1 and Dcp1b co-localise outside the mitochondria. Exogenous expression of HemK1 seemed to increase endogenous staining of Dcp1a, a protein involved in RNA processing that can localise in P-bodies. eRF1 localised in foci-like structures in the cytoplasm in the presence of Dcp1b and strong co-localisation between the two proteins was observed. Partial co-localisation between HemK1, eRF1 and Dcp1b was observed when all three proteins were exogenously expressed in HeLa cells. HemK2 showed partial co-localisation with Dcp1b, and this was enhanced in the presence of eRF1. HemK1 and HemK2 showed partial over-lap in staining with Staufen1, possibly suggesting co-localisation. The localisation of stress granule protein G3BP was distinct to the P-body protein Dcp1b, when exogenously expressed in cells. Even though no significant co-localisation was observed between the two N5-glutamine methyltransferases and G3BP, HemK2 was able to associate with G3BP in a pull-down assay in cells. These results collectively demonstrate a possible involvement of HemK1 and HemK2 in RNA processing that takes place in P-bodies and stress granules in the cytoplasm.

	HemK1	HemK2	mtRf1a	eRF1	Dcp1a	Dcp1b	G3BP1	Staufen1
HemK1			strong	partial	partial	strong	partial	partial
HemK2			partial	strong	partial	Partial	partial	partial
mtRF1a	strong	partial				No		
eRF1	partial	strong			partial	strong		
Dcp1a	partial	partial		partial		No		
Dcp1b	strong	partial	No	strong	No		No	
G3BP1	partial	partial				No		
Staufen	partial	partial						

Table 5.2 Summary of the co-localisations observed between the HemK proteins and components of RNA processing machinery. HemK1 and HemK2 were expressed in cells along with proteins involved in RNA processing, and the cells were fixed and stained to visualise any possible co-localisations. Strong co-localisation was observed between the HemK proteins and their corresponding proposed substrates. HemK1 strongly co-localised with Dcp1b, while no co-localisation was observed between mtRF1a and Dcp1b, or Dcp1b and G3BP. The description “partial” in the co-localisation table denotes that further analysis would have to be performed to verify the observation.

Chapter 6

[Results IV]

HemK proteins in neuronal morphology

HemK1 and HemK2 shRNA knock-down

In the course of this study it was discovered that the two N5-glutamine methyltransferases HemK1 and HemK2 are able to associate with the neuronal α2-chimaerin in cells. α2-Chimaerin plays an established role in neurite outgrowth dynamics regulating Rac1 activity and participating in signalling pathways of EphA4-dependent axonal guidance (Wegmeyer et al, 2007). An involvement of the two translation termination machinery proteins in neuritogenesis has not been documented and in fact the role of translation control mechanisms in neuronal outgrowth is still minimally understood. Our real-time PCR data indicate that both HemK1 and HemK2 are expressed in hippocampal neurones of developing rat brain (see figures 4.6, 4.7 in chapter 4). Hippocampal neurones of embryonic day 18 offer an attractive system of tracking the morphology of developing neurones *in vitro* since the hippocampus contains a relatively pure population of neurones that are at the beginning stages of developing cell polarity and the hippocampus is easily distinguishable under a light microscope and therefore easy to excise (Dotti et al, 1988). To examine the effects of the two proteins in neurite development a gene expression knock-down strategy was followed. The expression of the two genes was knocked-down by shRNA in primary hippocampal neurones isolated from e18 rat brains and the morphology of the developing neurones was analysed for complexity assessed by the Sholl analysis method (Sholl, 1953). This gave an indication of dendrite complexity reflecting the effect of the protein knock-down in neurite development. The efficiency of the shRNA sequences used was initially determined in N1E-115 neuroblastoma cells by quantitative real-time PCR, and subsequently in hippocampal primary neurones. mRNA transcript levels instead of protein levels were analysed since western blot experiments with the antibodies against HemK1 generated inconclusive data as far as specificity in detecting the endogenous HemK1 protein is concerned (see Chapter 4).

shRNA protein knock-down system

The expression of HemK1 and HemK2 was knocked down by double-stranded RNA interference. The system used was the siSTRIKE shRNA (Promega) that uses a psiSTRIKE vector incorporating a U6 eukaryotic promoter and an Amp^r gene. The psiSTRIKE vector used in primary neurones carried a GFP expression gene that

allowed us to analyse successfully transfected cells by confocal microscopy. The psiSTRIKE vector used in N1E-115 cells carried a neomycin gene allowing selection of successfully transfected cells for analysis of transcript levels by real-time PCR. Three shRNA sequences and a scrambled sequence control were designed for each protein (see Materials and Methods). The shRNA oligonucleotides used were designed to be complementary to both rat and mouse HemK1 and HemK2 transcript sequences and different from the human sequences. This allowed us to re-introduce expression of the two proteins in shRNA knock-down rat hippocampal neurones by transfecting with the two human cDNA constructs.

Real-Time PCR analysis of HemK1 and HemK2 transcripts

The mRNA levels of the targeted genes were analysed by quantitative real-time PCR based on the standard curve method. The primers used in the quantitative real-time PCR analysis of transcript levels were designed to intercept intron-exon boundaries to eliminate possible genomic amplification. The verification of knock-down experiments was done in triplicate in N1E-115 neuroblastoma cells and in monoplicate in primary hippocampal neurones due to the large number of cells needed to obtain adequate amount of RNA for the analysis.

HemK1 knock-down in N1E-115 neuroblastoma cells

Initially the efficiency of the shRNA sequences in knocking down HemK1 expression was verified in N1E-115 neuroblastoma cells. The cells were transfected with three shRNA constructs, a scrambled sequence control and psiSTRIKE vector control and grown in neomycin G-418 selection. The HemK1 mRNA levels were analysed by real-time PCR after 7 days of psiSTRIKE-shRNA expression, a time window proposed by the shRNA kit manual and supported by preliminary data of different time-points. The experiments were performed in triplicate and real-time PCR data verified knock-down in N1E-115 neuroblastoma cells. The shRNA sequence H1shRNA2 showed the lowest HemK1 transcript levels knocking-down expression by 80% compared to controls (Figure 6.1).

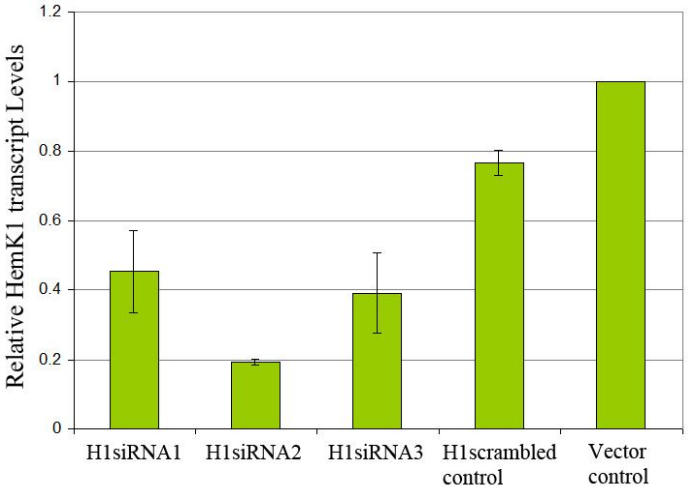

Figure 6.1 Efficient knock-down of HemK1 expression in N1E-115. The HemK1 transcript levels of shRNA transfected N1E-115 cells were analysed by real-time PCR and normalised to β-actin mRNA levels. Sequence H1shRNA2 showed the highest knock-down. The bar graphs represent SDs of three experiments.

Knocking down the expression of HemK1 in N1E-115 cells using the siSTRIKE shRNA system severely affected the growth and morphology of the transfected cells, within 7 days expression and when selected with neomycin G-418. The H1shRNA1 and H1shRNA3 transfected cells showed a 20-30% survival rate, and the surviving cells exhibited a contracted phenotype and did not divide at an observable rate. H1shRNA2 cells survived at a higher rate but exhibited the most severe phenotype effects with many cells spreading to a surface area up to 10 times larger than the control cells (Figure 6.2). The scrambled sequence shRNA transfected cells exhibited only minimal alterations in morphology and growth compared to the empty vector control cells. The image analysis software ImageJ was used to quantify the observed size difference, and examining 11 shRNA2 and 7 Vector Control cells the average cell sizes were calculated as 7,967 μm^2 and 1,803 μm^2 respectively, while a two-tailed *t*-test revealed that the size difference is statistically significant (Figure 6.4A).

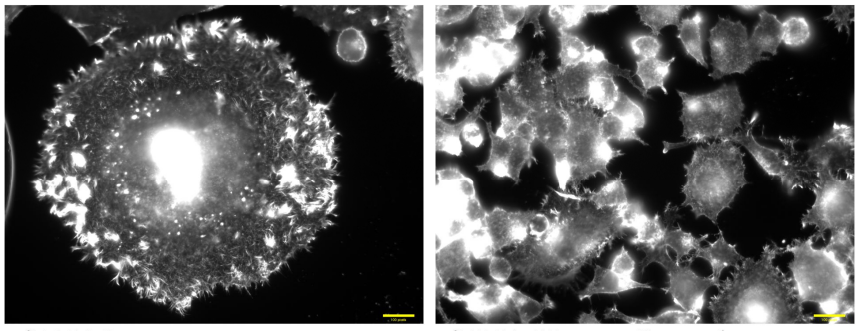

siRNA2 siRNA Vector Control

Figure 6.2 Knocking-down HemK1 expression affected the phenotype of N1E-115 cells. The shRNA knock-down sequence H1shRNA1 affected the phenotype of transfected N1E-115 cells. Along with compromised growth the cells exhibited a much enlarged phenotype when compared to unstransfected or empty vector controls. The scale bar represents 10μm.

In this study a link was indicated between HemK1 and P-body formation, involving Dcp1b as a P-body marker. To investigate the effect of knocking-down HemK1 expression on P-body formation H1shRNA2 knock-down cells were transfected with GFP-Dcp1b and analysed by confocal microscopy (Figure 6.3). The much enlarged knock-down cells exhibited a much higher number of Dcp1b-containing bright foci in the cytoplasm compared to control cells (Figure 6.3). The Dcp1b expression was observed as individual foci as well as in clustered foci. The number of clustered and non-clustered foci was quantified using the ImagePro Plus v7.0 software in 11 shRNA2 and 7 Control Vector cells as analysed by confocal imaging. The numbers of foci counted were divided by the cell size (μm^2) to reveal the foci density, that is, number of foci per μm^2. No statistical difference was observed between total foci numbers of shRNA2 and Control Vector cells or when comparing only the non-clustered foci (Figure 6.4 B and C). The average Dcp1b foci size was calculated using the ImagePro Plus v7.0 and revealed a statistically significant difference, indicating that the foci formed by Dcp1b are smaller when HemK1 expression is knocked-down (average Dcp1b foci: shRNA2=0.32 μm^2, Vector Control=0.41 μm^2) (Figure 6.4D). Futhermore, it was indicated that HemK1 expression can affect clustering of expressed Dcp1b, since in Vector Control cells an average of 70.6% of foci were in clusters while in shRNA2 only 45.6% of total foci was clustered (Figure 6.4E).

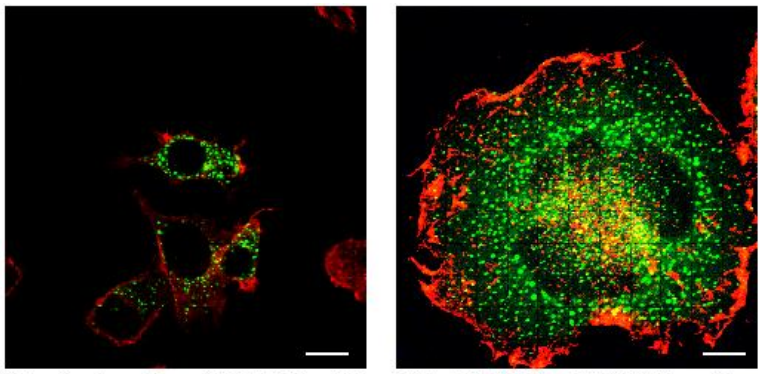

Figure 6.3 Dcp1b-induced P-bodies in HemK1 knock-down cells. HemK1 knock-down N1E-115 cells were transfected with GFP-Dcp1b to induce P-body formation and were analysed by confocal microscopy. The scale bars represent 10µm. Channels: FITC(green):GFP-Dcp1b and TRITC(red):Phalloidin.

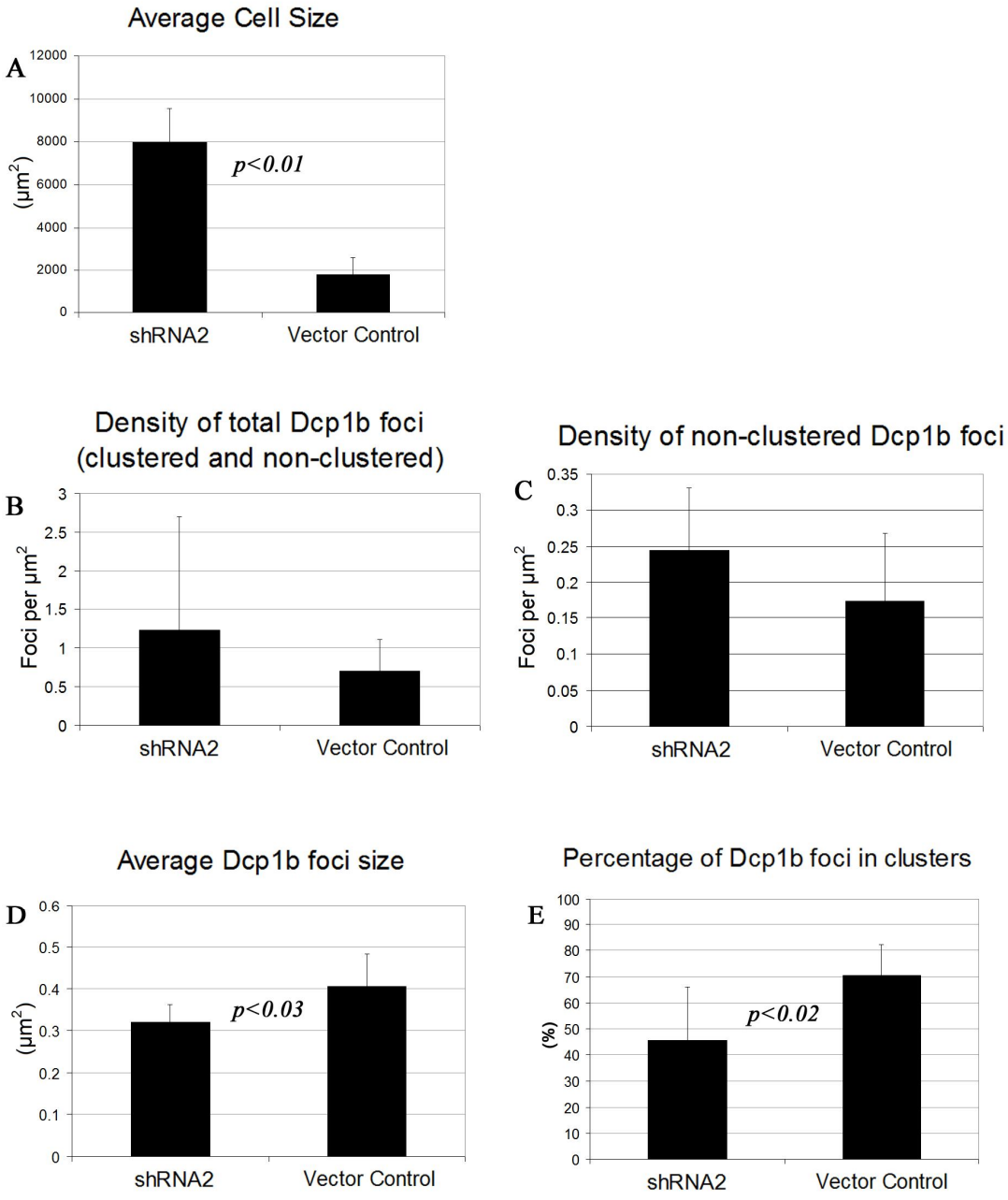

Figure 6.4 Knock-down of HemK1 expression can influence clustering and size of Dcp1b foci, but not foci density, in N1E-115 Neuroblastoma cells. HemK1 expression was knocked-down in N1E-115 cells that were subsequently transfected with GFP-Dcp1b, stained and analysed by confocal microscopy. The ImagePro Plus v7.0 software was used to analyse Dcp1b foci density, foci size and clustering, while the ImageJ software was used to analyse cell size. A total of 11 shRNA2 and 7 Vector Control cells were analysed. Knock-down of HemK1 expression caused a dramatic increase in cell size (A) but did not affect the density of total or non-clustered Dcp1b foci (B and C). A decrease in the average size of Dcp1b foci was observed in knock-down cells (D) while a lower percentage of foci found in clusters were observed in knock-down cells as compared to Vector Control cells (E). [$p(A)$=1.3061x10^{-8}, $p(B)$=0.2882, $p(C)$=0.1330, $p(D)$=0.0251, $p(E)$=0.0131].

HemK1 knock-down in primary hippocampal neurones

The effects of HemK1 knock-down in neurite development were investigated in primary hippocampal neurones isolated from e18 rat brains. The primary neurons were isolated as described in the materials and methods and transfected with the shRNA constructs cloned in a GFP psiSTRIKE, by electroporation. Initially the efficiency of knock-down was investigated, by transfecting primary neurons and plating them at a 400,000 cells per 5cm^2 plate, previously coated with Poly-D-Lysine/Laminin. RNA was isolated and cDNA was transcribed as described in the materials and methods, after three days *in vitro*. FLAG-HemK1 was co-transfected with shRNA2 in one experiment. The efficiency of all three shRNA knock-down sequences was validated by real-time PCR (Figure 6.5).

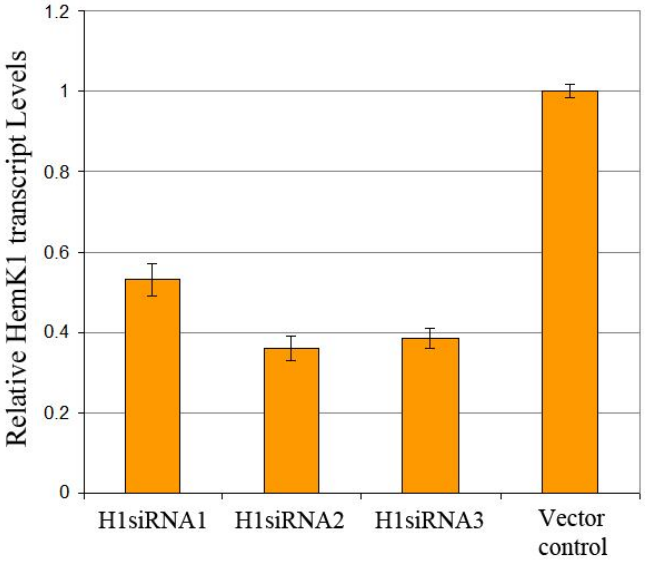

Figure 6.5 Efficient knock-down of HemK1 expression in e18 rat hippocampal neurones. The HemK1 transcript levels of shRNA transfected e18 rat primary hippocampal neurones were analysed by real-time PCR and normalised to β-actin mRNA levels. Sequence H1shRNA2 showed the highest knock-down. The experiment was performed once and the SD bars represent amplification reactions performed in triplicate on the same cDNA samples.

This study focused on the effects of H1shRNA2 which showed the maximum HemK1 knock-down in N1E-115 neuroblastoma cells. We compared the morphology of primary hippocampal neurones transfected with: a) H1shRNA2, b) a scrambled shRNA control sequence, c) GFP vector control and d) H1shRNA2 plus human HemK1, where HemK1 expression was restored by co-transfecting FLAG-HemK1 cDNA. Due to the low efficiency of the standard transfection methods when used on

plated primary neurones (eg lipofectamin, calcium phosphate), the H1shRNA2 and FLAG-HemK1 constructs were co-transfected by electroporation. All the cells were fixed at four days in vitro. The cells were stained with anti-Tau1 (Cy5) antibodies to reveal the developing axons and with phalloidin (TRITC) (Figure 6.6). FLAG-HemK1 was stained with anti-FLAG on the FITC channel. Therefore, both FLAG-HemK1 and GFP-H1shRNA2 occupied the FITC channel due to limitations on secondary antibodies and available channels. Cells successfully expressing FLAG-HemK1 were distinguished under confocal microscopy by the high level of signal on the FITC channel, since GFP-shRNA construct expression shows a distinctivally lower emission, mainly focused on the cell body. FLAG-HemK1 showed strong expression in the neuronal body also localising down axons and dendritic processes. The cells that gave a strong emission on the FITC channel were assumed to be co-expressing GFP-shRNA and FLAG-HemK1 constructs. Cell images obtained by confocal microscopy were analysed for neurite complexity by the Sholl method (Sholl, 1953). No dendrite-specific staining (MAP2) was used due to limitations in the available fluorescence channels. The Tau staining however did not stain for these processes, indicating that they do not constitute axonal processes. It was therefore assumed that the processes observed are immature dendrites (or neurites). Initial observation of the knock-down cells revealed a more complex morphology of a net-like arrangement of presumed dendrites close to the soma, as compared to the empty vector and the scrambled sequence controls. Co-transfection of HemK1 with H1shRNA2 in neurones abolished the complex neurite morphology of the knock-down (Figure 6.6). Tau1 staining revealed no accountable differences in the number or length of neuronal axons between knock-down and controlled cells.

Figure 6.6 Knocking-down HemK1 expression in hippocampal neurones affects their morphology. Rat e18 hippocampal neurones were transfected with knock-down sequences H1shRNA1, H1shRNA2, H1shRNA3, empty vector control, scrambled sequence control and H1shRNA2+HemK1 where HemK1 expression was reintroduced. The knock-down sequences caused a much complex neurite phenotype compared to vector and scrambled sequence controls. The phenotype was restored when HemK1 expression was reintroduced by transfecting with human HemK1 cDNA. This experiment was performed three times and a total of 31 of H1shRNA2, 9 of H1shRNA2+HemK1, 6 of the scrambled sequence control and 21 for GFP vector control cells were analysed. The scale bars represent 20μm.

Channels: (A, B, C, E, F) FITC:GFP-psiSTRIKE-shRNA constructs, TRITC:Phalloidin and Cy5:Tau1,
(D) FITC:GFP-psiSTRIKE-shRNA2 and FLAG-HemK1, TRITC:Phalloidin and Cy5:Tau1.

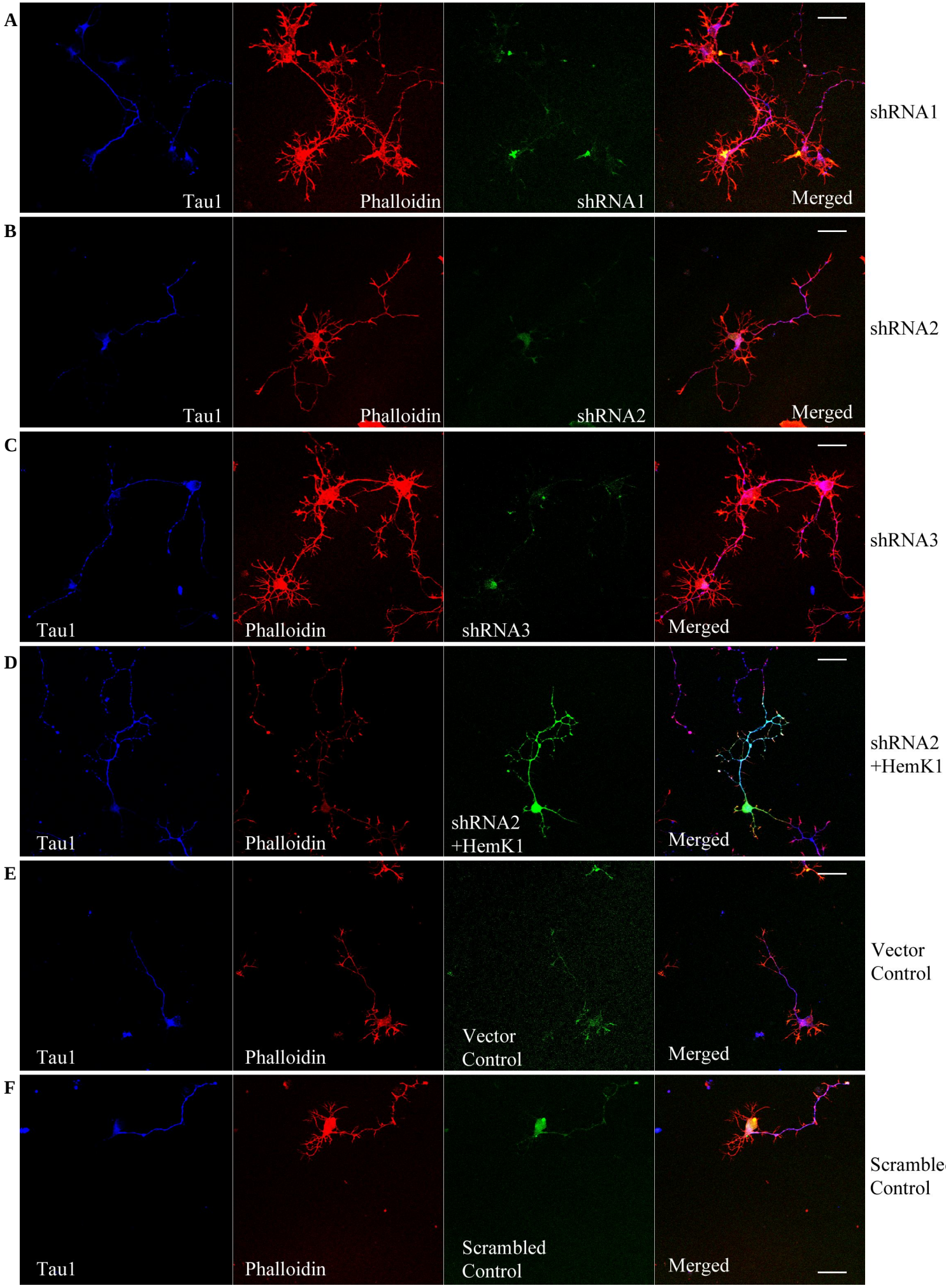
A
Tau1
Phalloidin
shRNA1
Merged
shRNA1
B
Tau1
Phalloidin
shRNA2
Merged
shRNA2
C
Tau1
Phalloidin
shRNA3
Merged
shRNA3
D
Tau1
Phalloidin
shRNA2
+HemK1
Merged
shRNA2
+HemK1
E
Tau1
Phalloidin
Vector
Control
Merged
Vector
Control
F
Tau1
Phalloidin
Scrambled
Control
Merged
Scrambled
Control

Sholl analysis of HemK1 knock-down morphological effects

The Sholl analysis was first developed by D. A. Sholl in 1953 to describe the dendritic organisation in neurones of the visual and motor cortices of cats (Sholl, 1953). The analysis involves drawing a series of concentric circles around the cell soma of a neuron. The circles feature the centroid of the cell soma as the centre and a fixed step in radii increase between them. The number of times that each circle intersects a cell process is counted and the data are plotted as number of intersections versus distance from the cell soma (Figure 6.7). The public domain image processing and analysis program ImageJ along with the Sholl analysis plug-in was used to generate these data. The starting and ending radii used were 0 and 250 µm respectively, with a step size increase of 2 µm. A margin of 0.5 µm radius span around each radius value was used to make continuous measurements of intersections and calculate the median for each radius step (Figure 6.7).

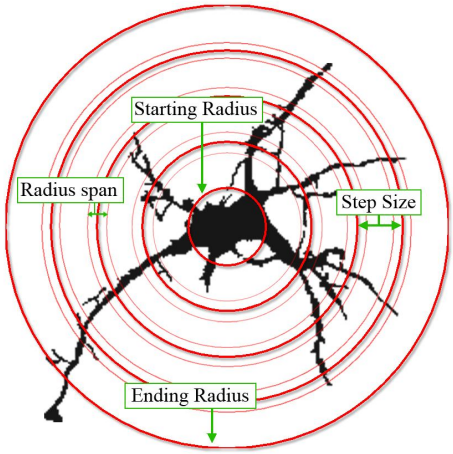

Figure 6.7 Analysis of neuronal morphology complexity by the Sholl method. The Sholl analysis was used to investigate the complexity of shRNA transfected primary neurones. A series of concentric circles are drawn around the soma and the number of intersections with the cell processes per increasing radii gives a measure of dendritic complexity.

The data collected from the Sholl analysis were analysed by the linear Sholl analysis and the semi-log Sholl analysis methods (Ristanović et al, 2006).

In the linear Sholl analysis the data were plotted as number of intersections (N) versus radius (r) (Figure 6.8). The plot represents the average intersection values of each radius of all the cells imaged and analysed. The H1shRNA2 expressing neurones showed much higher dendritic complexity in the range of 10 to 40 µm radius compared to the GFP vector and the scrambled sequence controls. Upon reintroduction of human HemK1 expression the H1shRNA2-induced complexity was abolished and reduced to a level lower than the control cells (Figure 6.8).

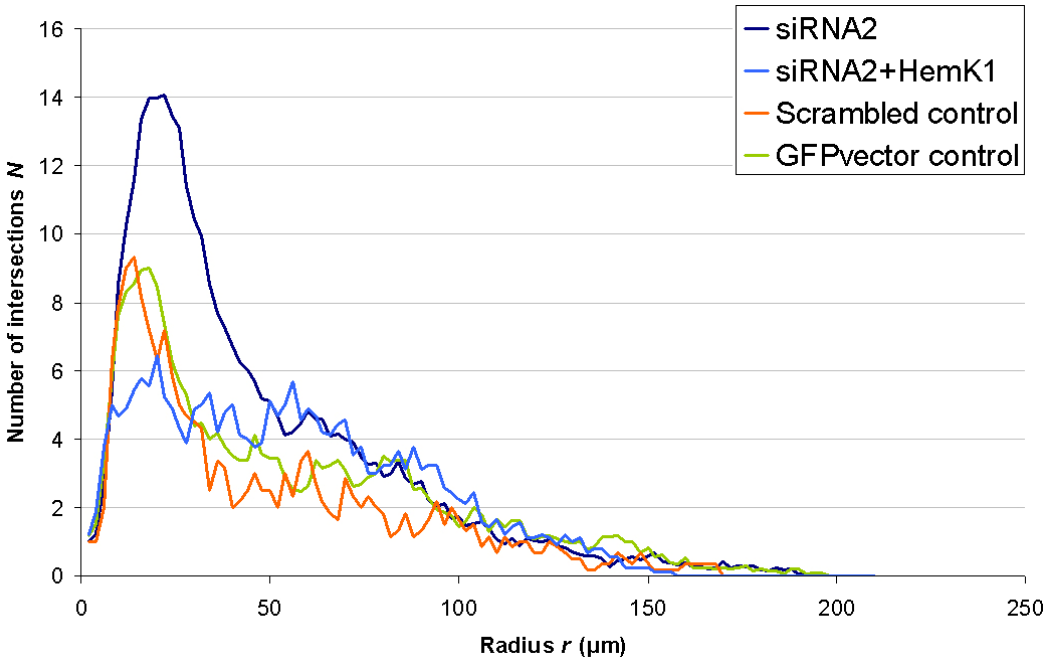

Figure 6.8 Linear Sholl analysis of neurite complexity of HemK1 knock-down rat hippocampal neurones. The data collected from the Sholl analysis were plotted as number of intersections versus the radius (linear analysis). H1shRNA2 (dark blue) showed 1.5 fold increase in intersections compared to empty vectror (green) and scrambled control (orange), between 10-40µm distance from the cell soma. Reintroducing HemK1 expression dropped the complexity to levels lower than the controls (light blue). The number of cells analysed were: a) 31 of H1shRNA2, b) 9 of H1shRNA2+HemK1, c) 6 of the scrambled sequence control and d) 21 for GFP vector control.

To evaluate the statistical significance of the observed difference in complexity between knock-down and control cells, the average intersections of all cells in the radius range 10-40µm was calculated and plotted as a bar graph (Figure 6.9). Two-tailed *t*-tests for a difference in mean intersections revealed that the difference in complexity between H1shRNA2 and the control GFPvector, scrambled and shRNA2+HemK1 is statistically significant.

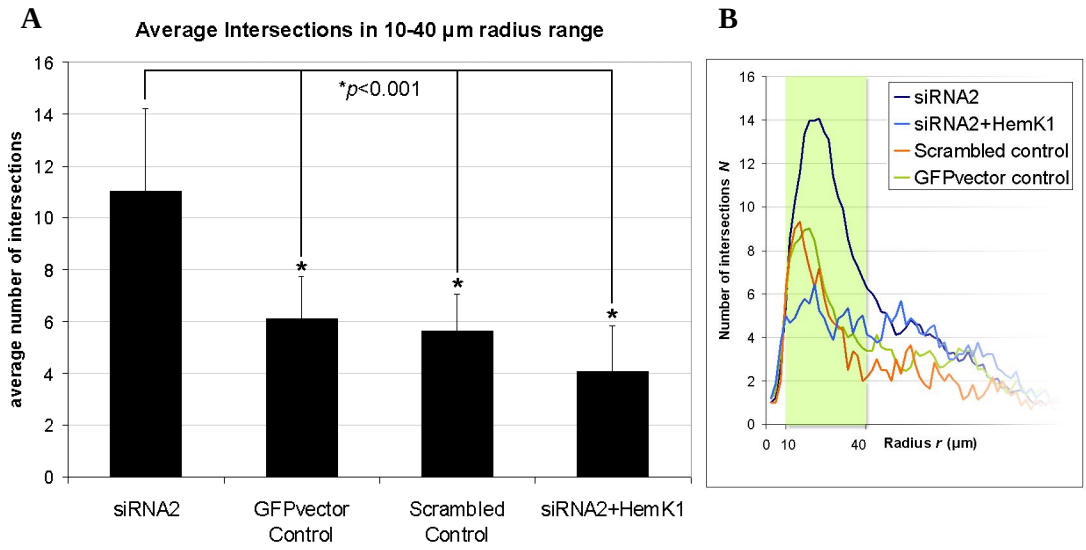

Figure 6.9 Linear Sholl analysis of neurite complexity of HemK1 knock-down rat hippocampal neurones in radius range 10-40µm. The difference in number of intersections between the shRNA constructs was analysed in the radius range 10-40µm shown in light green (B). The average number of intersections (10-40µm radius range) for each shRNA construct was plotted and the difference in complexity between shRNA2 and controls was found to be statistically significant by means of a *t*-test (two-tailed, unequal variance). SDs are indicated. [p=3.034x10^{-8} for shRNA2/GFPv, p=5.088x10^{-6} for shRNA2/Scrambled, p=9.9x10^{-8} for shRNA2/shRNA2+HemK1].

To further evaluate the morphological changes observed between shRNA2 and control cells, the semi-log Sholl analysis method was applied (Sholl, 1953). The data were plotted as the log of the number of intersections per circle area versus the corresponding radius, and the graph presented the data in an approximate straight line (Figure 6.10). The slope of the fitted straight line which is represented by the Sholl regression coefficient *k* is a measure of the rate of decay of branches with the distance from the cell body and it was originally used by Sholl to characterise the morphology of basal dendrites of pyramidal neurones from the cerebral cortex (Sholl, 1953). The data collected from H1shRNA2, H1shRNA2+HemK1, GFPvector control and scrambled control expressing neurones were plotted as log of the number of dendritic intersections/unit area versus circle radius of the cells (Figure 6.11). The rate of decay of branches with the distance was greater for H1shRNA2 neurones as represented in Figure 6.10. The Sholl regression coefficient *k* values were calculated for each cell and the difference between H1shRNA2 and GFPvector control was found to be significant by means of a *t*-test (Figure 6.12).

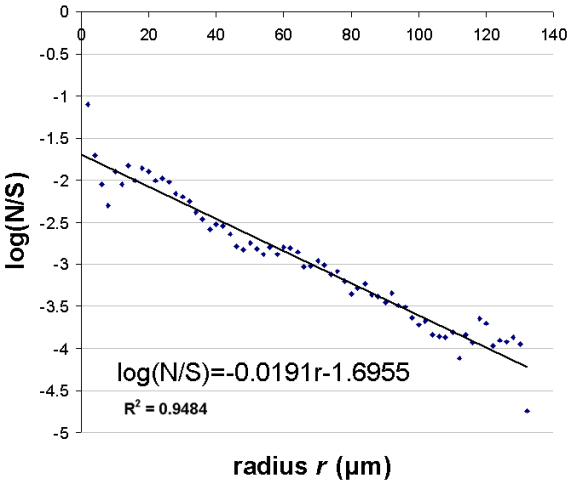

Figure 6.10 Semi-log Sholl analysis of neurite complexity of HemK1 knock-down rat hippocampal neurones. The difference in number of intersections between the shRNA constructs was analysed by the semi-log method where the log of the average number of intersections per circle area (log(N/S)) was plotted versus the radius. This method obtained the Sholl regression coefficient *k* for each group of neurones. This graph is a representative example of the semi-log plot.

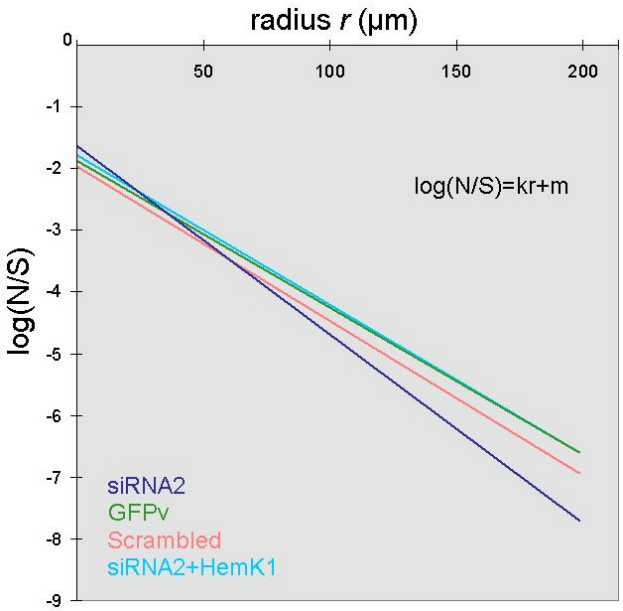

Construct	*k*
shRNA2	-0.03057±0.00959
GFPv	-0.02387±0.008029
Scrambled	-0.02511±0.007029
shRNA2+HemK1	-0.02426±0.006727

Figure 6.11 Distribution of regression lines over the different shRNA constructs. The lines are plotted as the log of number of intersections per circle area (N/S) versus the corresponding radius. The slope of each line is determined by the Sholl regression coefficient *k*. The rate of decay of log(N/S) with the distance *r* from the cell body is largest for H1shRNA2.

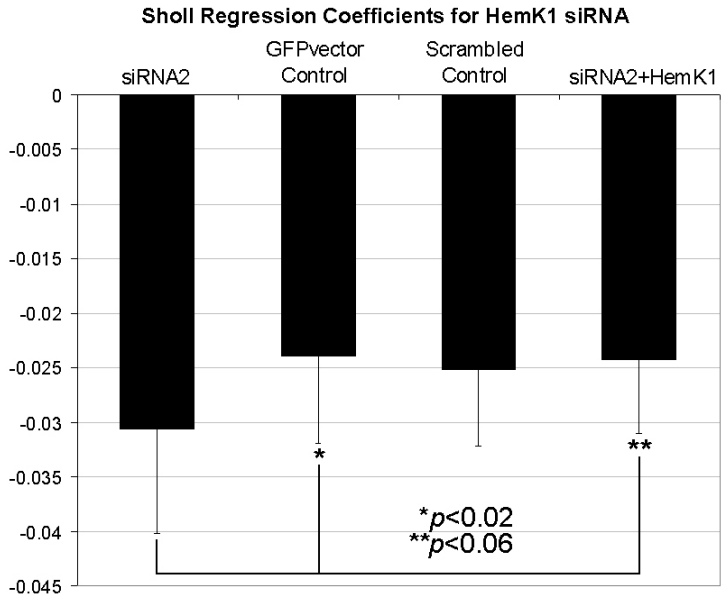

Figure 6.12 Semi-log Sholl analysis of neurite complexity of HemK1 knock-down rat hippocampal neurones. The difference in number of intersections between the shRNA constructs was analysed by the semi-log Sholl method where the mean Sholl regression coefficient was calculated for each group of neurones. Significant difference was found between H1shRNA2 and GFPvector control by means of a *t*-test. [p=0.011 for shRNA2/GFPv, p=0.051 for shRNA2/shRNA2+HemK1].

HemK2 knock-down in N1E-115 neuroblastoma cells

Three shRNA sequences specific to HemK2 were tested in N1E-115 neuroblastoma cells for knock-down efficiency. Real-time PCR analysis indicated that the H2-shRNA1 sequence was the most efficient in knocking-down HemK2 expression, lowering the HemK2 transcript by almost 90% as compared to scrambled sequence and empty GFP vector controls (Figure 6.13).

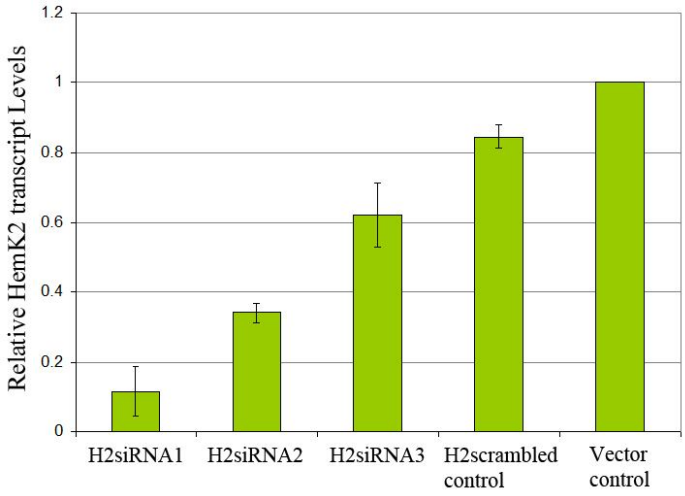

Figure 6.13 Efficient knock-down of HemK2 expression in N1E-115. The HemK2 transcript levels of shRNA transfected N1E-115 cells were analysed by real-time PCR and normalised to β-actin mRNA levels. Sequence H2shRNA1 showed the highest knock-down. The bar graphs represent SDs of three experiments.

The shRNA knock-down transfected N1E-115 neuroblastoma cells featured limited compromised growth compared to the scrambled and GFP vector controls. A similar enlarged phenotype to that of HemK1 knock-down was observed with the HemK2 knock-down H2-shRNA1 sequence that featured the lowest HemK2 transcript levels in real-time analysis (Figure 6.14).

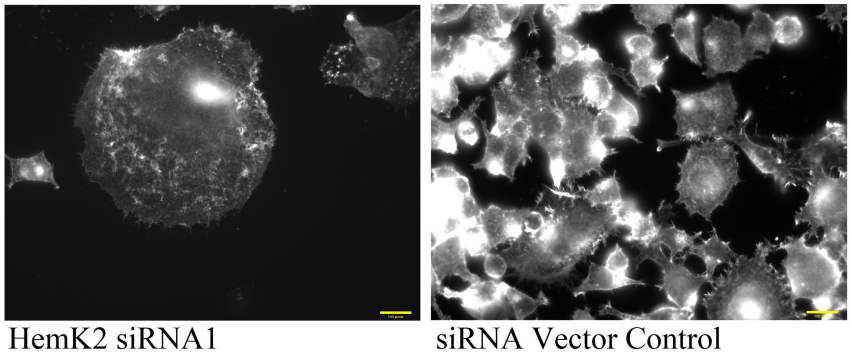

Figure 6.14 Knocking-down HemK2 expression affected the phenotype of N1E-115 cells. The knock-down sequence H2shRNA1 affected the phenotype of transfected N1E-115 cells. Along with some compromised growth the cells exhibited an enlarged phenotype similar to that observed for HemK1 knock-down. The bar represents 10μm.

HemK2 knock-down in primary hippocampal neurones

A similar methodology to the HemK1 knock-down morphological analysis was followed to investigate whether knocking-down HemK2 expression affects the morphology of developing neurones. The efficiency of the shRNA sequences to knock-down HemK2 expression was tested in primary neurones in a single experiment that verified the real-time data collected in N1E-115 neuroblastoma cells that the H2shRNA1 sequence featured the maximum knock-down (Figure 6.15).

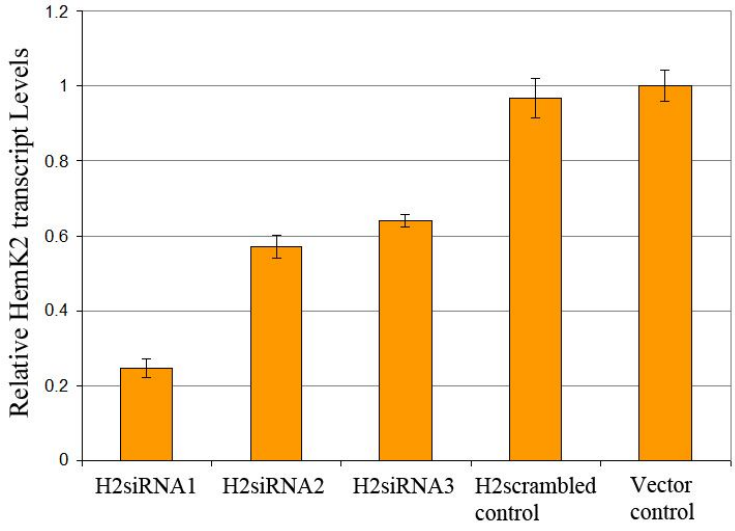

Figure 6.15 Efficient knock-down of HemK2 expression in e18 rat hippocampal neurones. The HemK2 transcript levels of shRNA transfected e18 rat primary hippocampal neurones were analysed by real-time PCR and normalised to β-actin mRNA levels. Sequence H2shRNA1 showed the highest knock-down. The experiment was performed once while the SD bars represent three amplification reactions performed on the same cDNA sample (triplicate).

The morphology of primary hippocampal neurones transfected with the three HemK2 shRNA sequences was investigated by confocal microscopy. The HemK2 shRNA sequences were compared to scrambled control, and to neurones co-transfected with rodent shRNA and human FLAG-HemK2 cDNA (Figure 6.16). The confocal images obtained were analysed by the linear Sholl analysis and the average number of intersections versus the corresponding radii was plotted for each cell group (Figure 6.17). The H2shRNA1 expressing neurones showed higher complexity at a radius between 10 and 40 μm compared to the scrambled sequence control. The morphology of these neurones was distinct to the morphology of HemK1 knock-down neurones, since the presumed dendrites did not form net-like inter-connections. Instead, the HemK2 knock-down neurones exhibited bud-like structures with extending neurites, sprouting from processes mainly close to the cell soma. Upon reintroduction of HemK2 expression the H2shRNA1 complexity abolished to a level comparable to control cells (Figure 6.18).

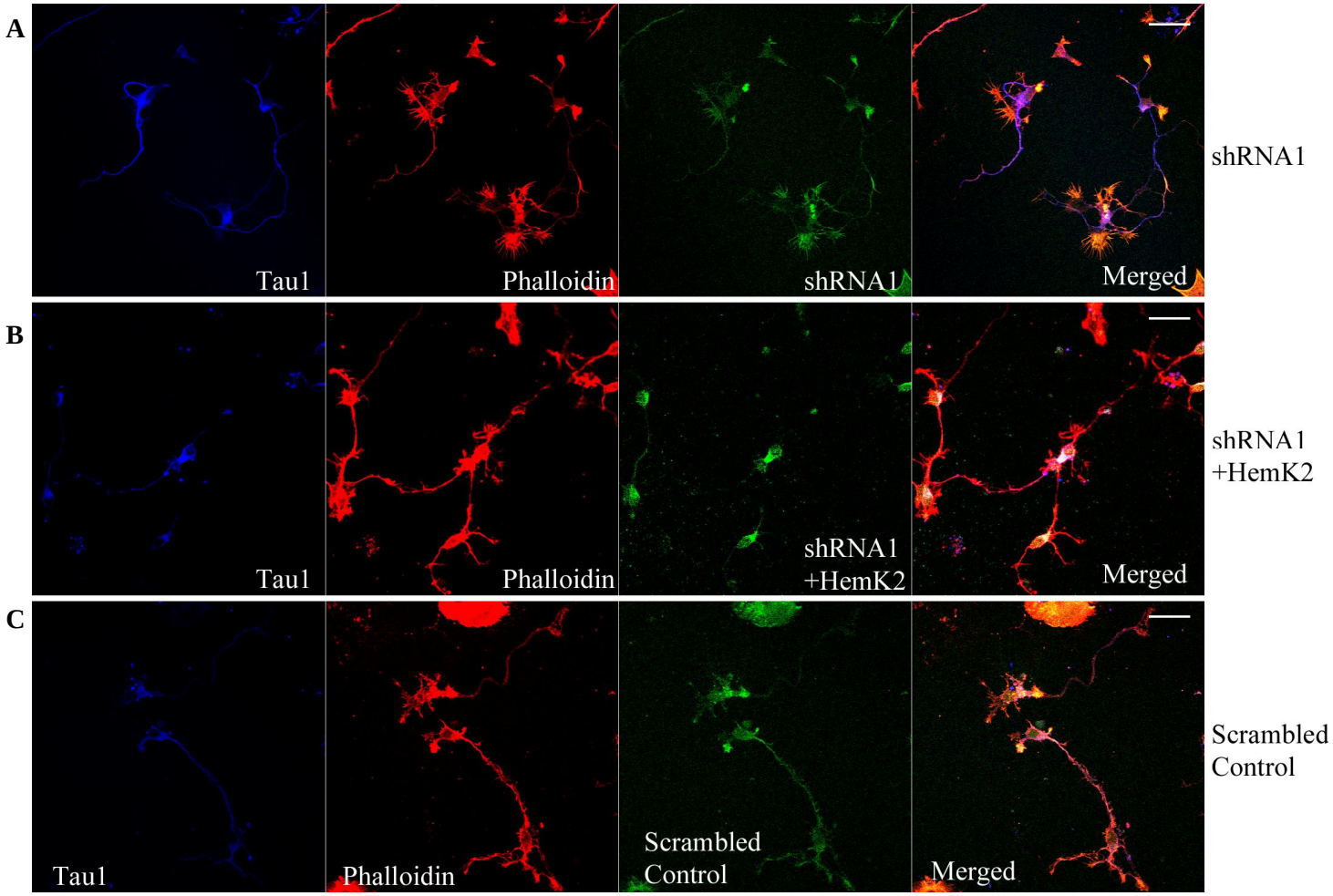

Figure 6.16 Knocking-down HemK2 expression in hippocampal neurones affects their morphology. Rat e18 hippocampal neurones were transfected with knock-down sequences H2shRNA1, scrambled sequence control and H2shRNA1+HemK2 where HemK2 expression was reintroduced. The knock-down sequences caused an increase in dendritic complexity compared to the scrambled sequence controls. The phenotype was restored when HemK2 expression was reintroduced by transfecting with human HemK2 cDNA. This experiment was performed two times and a total of 16 of H2shRNA1, 13 H2shRNA1+HemK2 and 18 of scrambled control cells were analysed. The scale bars represent 20µm.

Channels: (A, C) FITC:GFP-psiSTRIKE-shRNA constructs, TRITC:Phalloidin and Cy5:Tau1, (B) FITC:GFP-psiSTRIKE-shRNA1 and FLAG-HemK2, TRITC:Phalloidin and Cy5:Tau1.

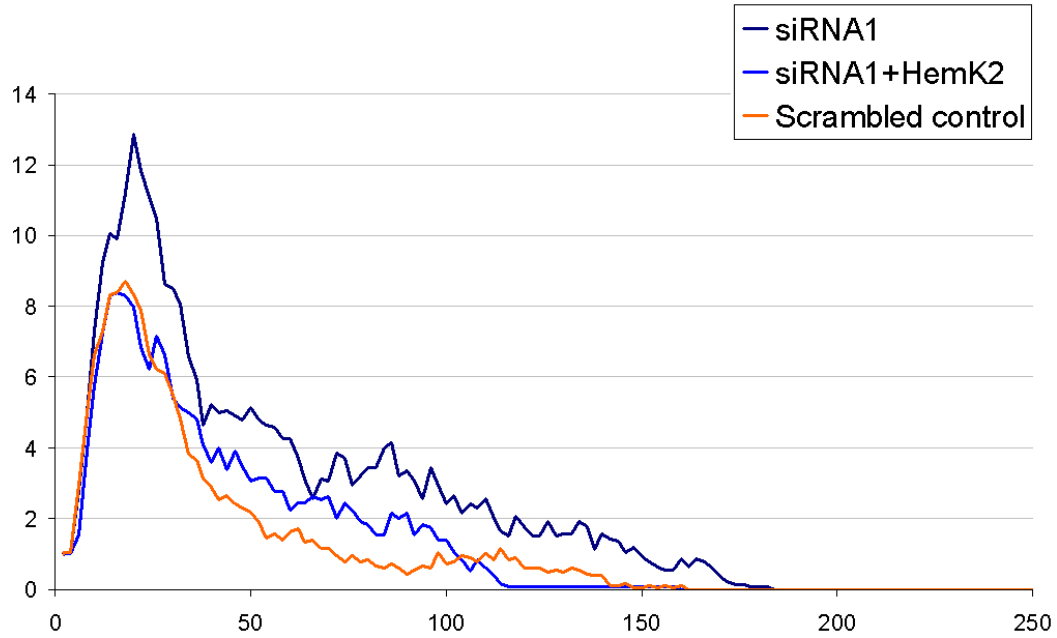

Figure 6.17 Linear Sholl analysis of neurite complexity of HemK2 knock-down rat hippocampal neurones. The data collected from the Sholl analysis were plotted as number of intersections versus the radius (linear analysis). H2shRNA1 (dark blue) showed an increase in intersections compared to scrambled control (orange), between 10-40µm distance from the cell soma. Reintroducing HemK2 expression dropped the complexity to levels comparable to controls (light blue). The number of cell analysed were: 16 of H2shRNA1, 13 H2shRNA1+HemK2 and 18 of scrambled control

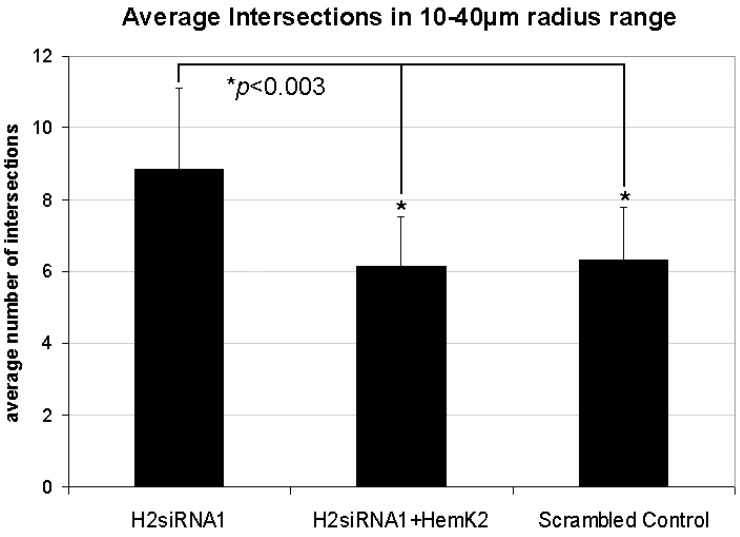

Figure 6.18 Linear Sholl analysis of neurite complexity of HemK2 knock-down rat hippocampal neurones in radius range 10-40µm. The difference in number of intersections between the shRNA constructs was analysed in the radius range 10-40µm. The average number of intersections (10-40µm radius range) for each shRNA construct was plotted and the difference in complexity between H2shRNA1 and the scrambled control was found to be statistically significant by means of a *t*-test (two-tailed, unequal variance). SDs are indicated. [p=0.741x10^{-3} for H2shRNA1/Scrambled, p=0.2x10^{-2} for H2shRNA1/H2shRNA1+HemK2.

Summary

To determine whether HemK1 and HemK2 influence the morphology of differentiating neurones the morphological effects of knocking-down the expression of the two N5-glutamine methyltransferases were examined in e18 rat hippocampal neurones. Efficient knock-down of the shRNA sequences was verified by real-time PCR in N1E-115 transfected cells. For both HemK1 and HemK2, shRNA knock-down resulted in growth compromise and an enlarged phenotype when compared to cells transfected with empty vector or scrambled sequence. The phenotypic effects of knock-down in N1E-115 neuroblastoma cells were most prominent with HemK1 knock-down. In HemK1 knock-down cells significant alterations were observed in the size of Dcp1b foci formed under transient expression of the P-body factor, as well as in Dcp1b foci clustering. This indicates that HemK1 may be involved in the formation of P-bodies as induced by Dcp1b. These results are preliminary as the number of cells analysed were low, and further analysis in a larger cell number and experiments would have to be carried out to evaluate startistical significance.

In primary neurones HemK1 knock-down caused a significant increase in neurite complexity close to the soma, at a 10-40μm distance from the centroid of the neuronal soma, with presumed dendrites forming net-like structures of interconnecting processes. This phenotype was rescued upon reintroduction of HemK1 expression by transient transfection of human HemK1. The effect in neuronal processes morphology was quantified by the Sholl analysis method, where a series of concentric rings with regular radial increments centered in the neuronal soma are traced around the neurone and the number of processes intersecting each ring is counted and plotted against the corresponding radius. Analysis by the semi-log Sholl method revealed that HemK1 knock-down primary neurones exhibit a different rate of decay of neuronal processes with distance from the soma compared to control cells. The increase in neurite complexity and rate of decay of processes with distance between HemK1 knock-down and controls was statistically significant as revealed by a *t*-test, though more cells would need to be analysed before the data are fully reliable.

When HemK2 expression was knocked-down in e18 rat hippocampal neurones an increase in neuronal processes complexity was observed at 10-40μm distance from the neuronal soma centroid, with bud-like structures extending multiple thin neurites from processes close to the soma. This phenotype was restored upon reintroduction of HemK2 expression.

These results indicate that modifying the expression levels of the two N5-methyltransferases can affect neuronal outgrowth in primary neurones. This suggests an involvement of HemK1 and HemK2 in signalling pathways orchestrating dendritic development, but not necessarily involving Rac1 or α2-chimaerin. It is certainly a possibility that the two N5-methyltransferases are involved in morphogenetic events mediated by Rac1 or α2-chimaerin, since both HemK1 and HemK2 can associate with α2-chimaerin in cells, and HemK1 can also associate with CRMP-2. On the other hand, both HemK1 and HemK2 play important roles in maintaining intracellular global translation control, and one would presume that modulating their expression would have severe effects in cell growth and morphology. For this to be analysed further, a neuronal morphology experiment where α2-chimaerin expression is modulated as well as HemK1 or HemK2 would have to be carried out. Furthermore, α2-chimaerin contructs where the functional domains SH2 and GAP have been mutated inhibiting the functional associations mediated by these domains could reveal involvement of HemK1 or HemK2 in pathways of α2-chimaerin morphogenesis.

Chapter 7
[Discussion]

HemK proteins in neurite outgrowth dynamics

A yeast two-hybrid screen on a human cDNA library previously identified HemK1 as a potential interacting partner for α2-chimaerin. This study aimed to characterise this novel interaction between the neuronal α2-chimaerin and the ubiquitously expressed HemK1, which is believed to modulate mitochondrial translation termination. It was shown that both HemK1 and related protein HemK2 can associate with α2-chimaerin, while investigation of HemK1 and HemK2 transcript levels as well as an antibody characterisation study aimed to reveal the expression of these proteins in the brain. A novel functional link of the two N5-glutamine methyltransferases with cytoplasmic RNA processing machinery was suggested by immunocytochemistry and protein association studies in cells, involving factors of P-bodies and stress granules. A possible role of HemK1 and HemK2 in the differentiation of developing neurones was suggested by knock-down experiments in rat hippocampal primary neurones that revealed a selective effect on neurite complexity. Possible roles of HemK1 and HemK2 in morphology of developing neurones are discussed in the context of: a) association with α2-chimaerin, b) effect on mitochondrial translation, and c) dynamics of cytoplasmic RNA processing bodies.

HemK1 and HemK2 associate with α2-chimaerin

α2-Chimaerin is expressed specifically in brain and testis and is involved in pathways of axonal growth cone collapse through EphA4 signalling while it also mediates the activity of the RhoGTPase Rac1 (Hall et al, 1993; Hall et al, 2001; Brown et al, 2004; Shi et al, 2007; Wegmeyer et al, 2007). HemK1 is ubiquitously expressed in nature and is found in a variety of human tissues, while there is evidence that it methylates mitochondrial release factor mtRf1a (NCBI:AceView, Thierry-Mieg et al, 2006; Soleimanpour-Lichaei et al, 2007; Ishizawa et al, 2008). The related protein HemK2, also a homologue of the bacterial PrmC, has been shown to methylate eukaryotic release factor eRF1 (Figaro et al, 2008). In this study it was shown that both HemK1 and HemK2 can associate with α2-chimaerin in pull-down experiments in cells. In fact, in an experiment where partial constructs of α2-chimaerin were tested for

association with HemK1, the strongest association was observed between HemK1 and the SH2 domain of α2-chimaerin, indicating a phospho-tyrosine-dependent interaction. In a similar experiment it was shown that HemK1 protein that co-immunoprecipitated with the SH2 domain of α2-chimaerin is tyrosine phosphorylated in cells (Figure 3.4). An *in silico* tyrosine phosphorylation analysis predicted a few strong candidate residues on both proteins (Figure 7.1). Interestingly, the tyrosine on the NPPY motifs of both HemK1 and HemK2 showed the highest score on tyrosine phosphorylation prediction, that if true, it would suggest a further functional significance on their association with α2-chimaerin. It is possible that the association observed occurs between the SH2 domain of α2-chimaerin and the NPPY motif of HemK upon tyrosine phosphorylation. Furthermore, if tyrosine phosphorylation on the release factor binding motif NPPY occurs in nature, it could affect substrate binding and methyltransferase activity and possibly constitute a control mechanism for HemK activity and translation termination. This would raise implications on a possible involvement of α2-chimaerin in the proposed function of the N5-methyltransferases.

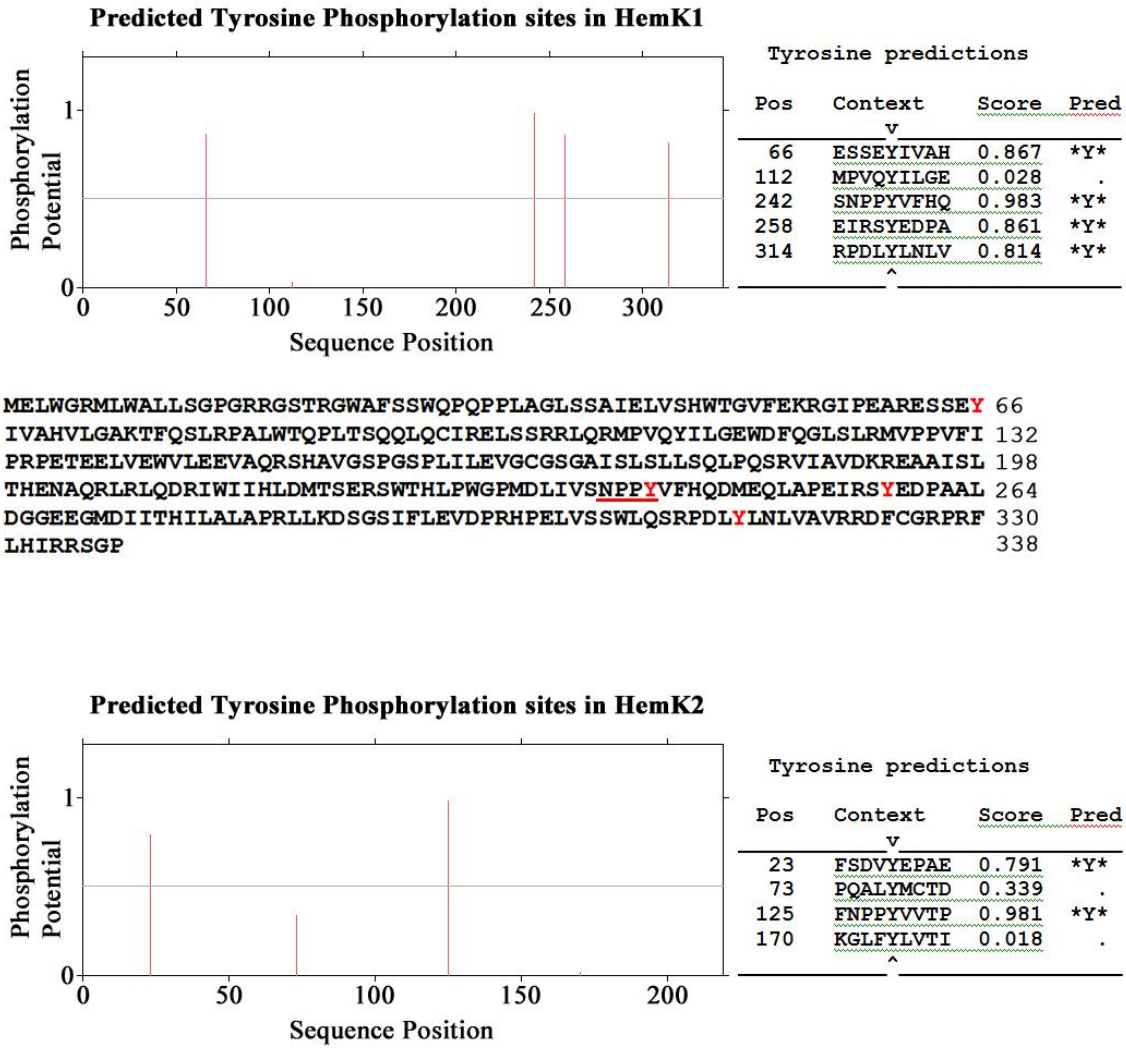

Figure 7.1 *In silico* tyrosine phosphorylation analysis of human HemK1 and HemK2. A tyrosine phosphorylation prediction was performed on the human HemK1 (NM_01617.3) and HemK2 (BI520047) sequences on the NetPhos 2.0 Server (www.cbs.dtu.dk/services/NetPhos/). Interestingly, the tyrosine on the NPPY motif of both HemK1 and HemK2 gave the highest score for predicted phosphorylation, raising the possibility of a phospho-tyrosine-dependent association between the SH2 domain of α2-chimaerin and the release factor binding site of the two N5-methyltransferases.

HemK1 is predicted to bear a mitochondrial localisation sequence (TargetP) and in experiments by Ishizawa and colleagues Myc-tagged HemK1 co-localised with the MitoTracker stain for mitochondria, in transiently transfected HeLa cells (Ishizawa et al, 2008). Binding of diacylglycerol to the C1 domain of chimaerins is thought to mediate their translocation to membranes. α2-Chimaerin is known to translocate to the plasma membrane where it can bind the EphA4 receptor, while β2-chimaerin can translocate to the Golgi apparatus (Shi et al, 2007; Caloca et al, 2001; Colón-González et al, 2008). This poses the question if the association observed between HemK1 and α2-chimaerin is actually possible in nature, since the two proteins may be expressed in and confined to different subcellular spaces. HemK2 is believed to be part of the translation machinery ordered by the ribosomes in the endoplasmic reticulum, and this would give higher chances for HemK2 to meet α2-chimaerin intracellularly and therefore be its real biological partner. However, unpublished data in our lab have suggested that α2-chimaerin can be found in mitochondria co-localising with mitochondrial marker HSP60 in N1E-115 neuroblastoma cells permanently expressing the EphA4 receptor while native α2-chimaerin has been detected in purified mitochondria (C. Hall and C. Porchetta, personal communication). The observation that HemK1 but not HemK2 can associate with CRMP-2, an established a2-chimaerin partner reinforces the hypothesis that HemK1 is a *bona fide* interacting partner of α2-chimaerin possibly part of a signalling pathway involving CRMP-2. It is still possible however that the association of α2-chimaerin with the two N5-glutamine methyltransferases is not biological and is a result of the high exogenous expression of the proteins driven by the CMV promoter of the mammalian expression vectors used. To address this, an endogenous immunoprecipitation would have to be performed in neurones or brain tissue where chimaerin is expressed. Anti-chimaerin antibodies coupled on beads could be used to immunoprecipitate endogenous α2-chimaerin from brain homogenates and western blot analysis would reveal if native HemK1 protein was co-precipitated. The limitation of this technique is that the available anti-HemK1 and anti-HemK2 antibodies cannot reliably detect endogenous protein. To over-come this, mass spectrometry could be used to identify the proteins co-precipitated with α2-chimaerin. Furthermore, the association could be mapped on the two N5-glutamine methyltransferases, generating a series of HemK1 and HemK2 deletion mutants to be used in pull-down experiments in cells. This could indicate if the substrate binding site and/or the catalytic site of the two proteins are involved in

the association with α2-chimaerin and could help characterise the interaction in terms of a biological function. Following the effect of HemK1 knock-down in primary neurones where a significant increase in dendritic complexity was observed, the effect of the two HemKs on the GAP activity of α2-chimaerin should be investigated, that could offer a direct link to neurite outgrowth dynamics through modulating the activity of Rac1. The effect of HemK1 and HemK2 in the GAP activity of α2-chimaerin could be explored by means of an assay that measures the dissociation of Rac1-bound GTP to GDP+Pi, in the presence of α2-chimaerin and HemK proteins. Furthermore, the levels of normal or phosphorylated levels of α2-chimaerin in HemK1 knock-down neurones could be investigated, since increase in phosphorylation of α2-chimaerin and GAP activity towards Rac1 have been linked to its association to the EphA4 receptor in the context of growth cone collapse (Shi et al, 2007).

Possible Morphogenetic Signalling Pathways

The morphological effects of HemK1 or HemK2 knock-down in cultured primary neurons are quite distinct with an increase in complexity of processes close to the soma, but no significant effect on axonal length. A review of the literature on cultured hippocampal neurons can give some clues as to which signalling pathways could be affected that may be relevant to HemK proteins. Even though the literature on cultured hippocampal neurons morphology is a vast one, with a wide variety of proteins attributed an involvement in signalling pathways affecting outgrowth of neuronal processes, the phenotype observed for HemK1 knock-down still appears quite unique in terms of its neurite complexity. In a recent large-scale gain-of-function screen done in primary hippocampal neurons by Buchser and colleagues, a wide spectrum of proteins was identified affecting neuronal morphology (Buchser et al, 2010). These included protein kinases and phosphatases, and HemK1 was also identified in this screen, causing a moderate decrease in total neurite length (Buchser et al, 2010). A prime example of a signalling pathway involved in neuronal morphogenetic events is the PI3K pathway that is activated upon binding of growth factors to membrane receptors, and mediates remodelling events on both actin and microtubules via activation of GSK-3β, Akt and the Rho GTPases (Cosker and Eickholt, 2007). In a recent paper it was demontrated that the phosphatidylinositol

transfer protein PITPα induces increase in axonal length of e18 hippocampal neurons, an effect mediated by the PI3K pathway (Cosker et al, 2008). Furthermore, the PI3K pathway has been involved in dendritic development through the action of tyrosine receptor kinase B TrkB, affecting dendritic growth cone dynamics and filopodia motility in cultured hippocampal neurons (Luikart et al, 2008). A phenotype that shows some similarity to the HemK1 knock-down phenotype is provided by a study by Kumar and colleagues, where activation of the PI3K-Akt-mTOR pathway increased the dendritic size in cultured hippocampal neurons, while a coordinated activation together with the Ras-MAPK pathway increased dendrite complexity (Kumar et al, 2005). In a different study, an increase in the number of primary dendrites in cultured hippocampal neurons was observed under over-expression of glutamate receptor interacting protein 1 GRIP1, while knock-down had the opposite effect, and it was suggested that GRIP1 controls dendrite morphogenesis by mediating the transport of EphB receptors to dendrites (Hoogenraad et al, 2005). This phenotype is distinct to the HemK1 knock-down phenotype, in which primary dendrites could not be counted since the processes sprouting from the cell soma formed net-like structures, making the identification of primary dendrites impossible. The phenotype of HemK2 knock-down is perhaps even more difficult to interpret, since it is a subtle effect but still statistically significant in the number of cells analysed. The growth cone-like structures observed near the soma could relate the phenotype to the function proteins involved in actin and microtubule polymerisation, such as the Arp2/3 complex and CRMP-2 mediating the effects of Rho GTPases.

HemK1 expression and function is not confined to the mitochondria

The human Hemk1 bears a mitochondrial localisation sequence as predicted by TargetP with a probability of 0.808, but this prediction is not consistent across other mitochondrial localisation prediction logarithms. MitProtII (v1.101) predicted a 0.4597 probability of HemK1 to be mitochondrial while Mitpred (v2.0) could not detect a mitochondrial leader sequence at all when used in default settings (Kumar et al, 2006). It is therefore possible that the transport of HemK1 to mitochondria is not the sole possible fate of the native protein, and HemK1 can have a function outside the mitochondria. It was shown that HemK1 can localise with mitochondrial mtRF1a but also with eRF1 that is believed to associate with ribosomes in the cytoplasm. HemK1 also co-localised with Dcp1b, a protein that constitutes an important marker for cytoplasmic P-bodies, even in the presence of its substrate mtRF1a. This clearly demonstrates that HemK1 intracellular expression, and possibly function, is not confined to the mitochondria.

HemK1 could affect neuronal morphology through mitochondrial function

In preliminary experiments, a significant increase in dendritic complexity in range of 10-40µm distance from the neuronal soma centroid was observed when HemK1 expression was knocked-down in e18 rat hippocampal primary neurones. Furthermore knock-down of HemK1 expression in N1E-115 for 7 days with antibiotic selection cells caused a large phenotype and compromised growth suggesting impaired mitochondrial function (McBride et al, 2006). Since antibiotics such as gentamicin and neomycin also affect translational fidelity this may also have contributed to the severity of the phenotype in HemK1 knockdown in these cells (Schroeder et al, 2000; Mehta and Champney, 2003). These data indicate obvious and severe morphological effects of shRNA knock-down of HemK1 in N1E-115 neuroblastoma cells. Taking in consideration that HemK1 has been found to localise in mitochondria as part of the translation machinery and HemK1 knockdown cells show a significant reduction in

mitochondrial protein synthesis (Ishizawa et al, 2008), the morphological effect of abolishing HemK1 expression could be due to alteration of mitochondrial protein translation functions. When eukaryotic cells are grown in glucose-free galactose-containing media glycolysis is inhibited and the cells are forced to produce ATP by oxidative phosphorylation that takes place in the mitochondria. The process of oxidative phosphorylation requires proteins encoded by the mitochondrial genome and therefore non-compromised mitochondrial translation machinery is imperative for cell growth under these conditions (Anderson et al, 1981). In fact, a study has shown that depletion of the HemK1 mitochondrial substrate mtRF1a in HeLa cells compromised cell growth in galactose and promoted increased production of reactive oxygen species (Soleimanpour-Lichaei et al, 2007). To investigate further the effect of HemK1 knock-down in mitochondrial function, HemK1 shRNA cells could be cultured in galactose-containing media, and their rate of division compared to untransfected cells. Furthermore, a possible mitochondrial dysfunction in HemK1 knock-down N1E-115 cells could be investigated in live cell imaging by tracking the accumulation of ROS. This can be done using a MitoSOX Mitochondrial Superoxide Indicator that translocates to mitochondria and emits red fluorescence under oxidation by superoxide ion, the predominant ROS in mitochondria (Kudin et al, 2004). (http://products.invitrogen.com/ivgn/product/M36008).

Mitochondria are important for cell survival and death and impaired function can lead to increased generation of reactive oxygen species (ROS) and reduced ATP production (Beal, 2005). Many lines of evidence suggest that mitochondrial dysfunction and oxidative stress are causative to the pathogenesis of neurodegenerative diseases (Lin and Beal, 2006). Impaired energy metabolism and mitochondrial dysfunction are a feature of autopsied brain tissue from Alzheimer's disease patients while cell damage from ROS can occur before the development of plaque pathology (Pratico and Delanty, 2000; Small et al, 1995). Biochemical studies have suggested that mitochondria function is also involved in the pathogenesis of Parkinson's disease (Schapira et al, 1990), and mutations in mitochondrial genes have been associated with parkinsonism (Casali et al, 2001; Thyagarajan et al, 2000). HemK1 could affect mitochondrial function or ROS signalling by modulating the expression of mitochondrial proteins being part of the mitochondrial translation machinery.

In neurones, mitochondria are found in the cell soma as well as in distal dendritic and axonal sites where they are believed to have a direct effect in neurite arborisation and synaptic activity (Li et al, 2004; Verstreken et al, 2005). Studies have suggested that reduction of dendritic mitochondrial content leads to loss of spines and synapses while increase in mitochondrial content and activity leads to increased number of dendritic spines and synapses (Li et al, 2004). A direct link between mitochondrial translation and dendritic morphology was set by Chihata and colleagues in a study of the *GARS* gene encoding for glycyl-tRNA synthetase (Chihara et al, 2007). Glycyl-tRNA synthetase catalyses the synthesis of glycyl-tRNA that mediates the addition of glycine during protein synthesis. (Freist et al, 1996). In experiments in Drosophila olfactory projection neurones, *GARS* mutants showed compromised terminal branching of both axons and dendrites (Chihara et al, 2007). Combined with data of mitochondrial ribosomal protein S12 null mutants affecting mitochondrial translation, the authors propose that cytoplasmic translation is required for arborisation of both developing dendrites and axons while mitochondrial translation preferentially affects dendritic arborisation (Chihara et al, 2007). A role of HemK1 in neuronal morphology through an effect in mitochondrial translation and/or function is a plausible hypothesis that could account for the complex dendritic morphology observed in HemK1 knock-down neurones.

HemK1 could affect neuronal morphology by modulating P-body assembly

An effect of HemK1 in neuronal morphology could be linked to its involvement in P-body dynamics. It was found that HemK1 expression can induce the formation of Dcp1a-containing cytoplasmic foci while exogenously expressed HemK1 co-localises with P-body protein Dcp1b. Knock-down of HemK1 expression affected the clustering and size of Dcp1b-induced P-bodies, and this was statistically significant in a small number of analysed cells. HemK1 also associated with eRF1 that is part of the nonsense mediated mRNA decay machinery and was shown to co-localise with Dcp1b suggesting its presence in P-bodies and indicating a possible role in mRNA degradation. P-bodies are cytoplasmic sites of RNA processing and have been implicated in nonsense mediated mRNA decay and local translation in distal neuronal

sites where translationally repressed mRNA can be expressed in response to synaptic activity (Cougot et al, 2008). Furthermore P-bodies have been shown to contain translationally silent mRNA that can return to polysomes to resume translation (Brengues et al, 2005). If HemK1 can induce P-body assembly it could have an effect on synaptic-induced translation and mediate morphological changes in the developing neurite. One hypothesis is that HemK1 is directly involved in P-body assembly as part of the RNA processing machinery found in these cytoplasmic foci, as suggested by the strong co-localisation of HemK1 with Dcp1b. On the other hand, the induction in Dcp1a-containing cytoplasmic foci in HemK1 transfected cells could also be due to an effect of HemK1 in mitochondrial translation, possibly causing cell stress that is linked to P-body and stress granule assembly.

A link between mitochondrial translation and P-bodies has been previously set with Rpm2p, a protein subunit of mitochondrial RNase P (Stribinskis and Ramos, 2007; Dang et al, 1993). RNase P is involved in processing ribosomal RNA and subunit Rpm2p has also been implicated in the translation of mitochondrially encoded cytochrome c oxidase subunits in mitochondria (Stribinskis et al, 2001). In a recent study Rpm2p was found to localise in cytoplasmic P-bodies and regulate their stability while it was also able to associate with mRNA decapping protein Dcp2 (Stribinskis and Ramos, 2007). It is therefore evident that an interplay between different factors primarily localised in different intracellular organelles is occurring in the formation of cytoplasmic RNA processing bodies. This reinforces the hypothesis that HemK1 has a new previously unknown function linked to RNA degradation and cytoplasmic P-bodies function and dynamics.

HemK2 knock-down could affect neuronal morphology through modulating stress granules function

P-bodies show similarities with stress granules sharing a subset of identical component proteins and also through their involvement in miRNA-mediated gene silencing (Anderson and Kedersha, 2008). Both stress granules and P-bodies are in equilibrium with polysomes as suggested by experiments that show the dissociation of these cytoplasmic foci when polysomes are stabilised (Brengues et al, 2005; Eulalio et al, 2007b). Stress granules have been involved in holding translationally silent

mRNAs that can either be degraded or retargeted to the translation machinery (Kedersha et al, 2000). Staufen is thought to regulate the equilibrium between polysomes and stress granules by stabilising polysomes under stress conditions (Thomas et al, 2009), while the two human Staufen homologues have been involved in mRNA transport and localised translation control in dendritic spines (Villacé et al, 2004; Goetze et al, 2006; Tang et al, 2001b). G3BP has been implicated in the localised translation of proteins involved in cellular proliferation and migration (Solomon et al, 2007), while it has been shown to be required for stress granule assembly (Tourrière et al, 2003). In preliminary experiments, HemK2 was shown to associate with G3BP in cells and some partial co-localisation between the two proteins was observed in N1E-115 cells. Furthermore, some partial co-localisation was observed between HemK2 and Staufen1. Together with the observation that HemK2 shRNA knock-down in primary hippocampal neurones causes an increase in neurite complexity, these results could indicate a link between HemK2 and RNA processing proteins involved in transport of mRNA to distal dendritic sites and control of local translation. The formation and dynamics of stress granules and P-bodies have been shown to be regulated by the proteins dynein and kinesin suggesting an important role of these two microtubule associated proteins in the shuttling of ribonucleoproteins and RNA processing factors in these RNA regulation foci (Loschi et al, 2009). CRMP-2, a binding partner of α2-chimaerin that is involved in microtubule assemblies and axonal outgrowth, directly binds to dynein and modulates its activity (Brown et al, 2004; Fukata et al, 2002; Yoshimura et al, 2005; Arimura et al, 2009). It is therefore possible that the HemK2 could hold a role in the assembly of RNA processing bodies through its association with α2-chimaerin. The role of HemK1 or HemK2 in the assembly of stress granules could be investigated by looking at endogenous G3BP by means of an immunocytochemistry on knock-down cells as well as cells exogenously expressing HemK1 or HemK2.

HemK1 could play a role in escort complexes linking it to Chimaerin

Results have shown that exogenously expressed HemK1 can show partial over-lap with markers for clathrin and early endosomes in some cells. Endosomes order the

cellular processes of endocytosis that mediate the uptake of nutrients and the transmission of neuronal and proliferative signals. Clathrin is a key player in internalisation of membrane-bound ligands ordering the formation of endoplasmic vesicles that selectively sort cargo at the cell membrane, endosomes and trans-Golgi network for various membrane traffic pathways (Mellman, 1996). The endocytotic pathway sees the delivery of internalised membrane receptors to early endosomes, where they can be targeted for degradation in lysosomes by ubiquitination, recycled back to the plasma membrane or destined to the trans-Golgi network (Jovic et al, 2010). A molecule that follows this endocytotic pathway is the epidermal growth hormone (EGF) that plays a key role in cell proliferation, growth and differentiation. Studies in yeast have suggested that the process of sorting ubiquitinated proteins for degradation in late endosomes requires the recruitment of the ESCRT (endosomal sorting complex required for transport) complexes (Hurley, 2008). The ESCRT-I complex is composed of Vps23, Vps28, and Vps37 (Katzmann et al, 2001). A yeast two-hybrid screen in our lab has previously identified Vps28 as a potential interacting partner for α2-chimaerin. Furthermore, the chimaerin-related protein Bcr has been shown to be required for the turnover of EGF receptor through its interaction with Vps28 and other components of ESCRT-I complex, implicating it in processes of cellular trafficking at growth cone receptors (Raiborg et al, 2003). It is therefore possible that α2-chimaerin plays a role in processes of endocytosis in recycling membrane receptors, and partial co-localisation of HemK1 with molecules representing these cellular pathways could also indicate a possible involvement of HemK1 as a chimaerin interacting partner.

A possible role of HemK in endosomal trafficking could also be linked to a function in P-bodies and RNA processing. A link between P-bodies and the ESCRT complexes has been set with the P-body proteins GW182 and Argonaute 2 (AGO2), two main components of the RNA-induced silencing complex (RISC) (Liu et al, 2005). GW182 and AGO2 have been shown to localise in late endosomes while miRNA silencing and the formation of GW182-containing bodies is dependant on the presence of ESCRT complexes (Gibbings et al, 2009; Lee et al, 2009).

Endogenous HemK1 detection

The expression of HemK1 and HemK2 mRNA in brain development was investigated by real-time PCR in rat brains, and compared to α2-chimaerin. Results showed a parallel increase in transcript levels between the three proteins with development, in e12 and e18 whole brains, and 5d and 20d cortices. The transcript levels of the two N5-glutamine methyltransferases were generally comparable to those of α2-chimaerin, as detected by real-time PCR. Specifically for the 20d rat brains cerebellum, the expression of the three transcripts was similar, with HemK1 being the lowest, followed by of α2-chimaerin and HemK2. In the 20d cortex, α2-chimaerin was detected at much lower levels to HemK1 and HemK2. However the Allen Brain Atlas revealed very low levels of HemK1 in cerebellum and cortex compared to HemK2 and α2-chimaerin in 55 days old mice (Figure 7.2A and B). The difference in transcript levels as presented by the Allen Brain Atlas is not consistent with the findings of this project, probably reflecting the intrinsic differences and limitations of the two techniques in comparison, *in situ* hybridisation and real-time PCR.

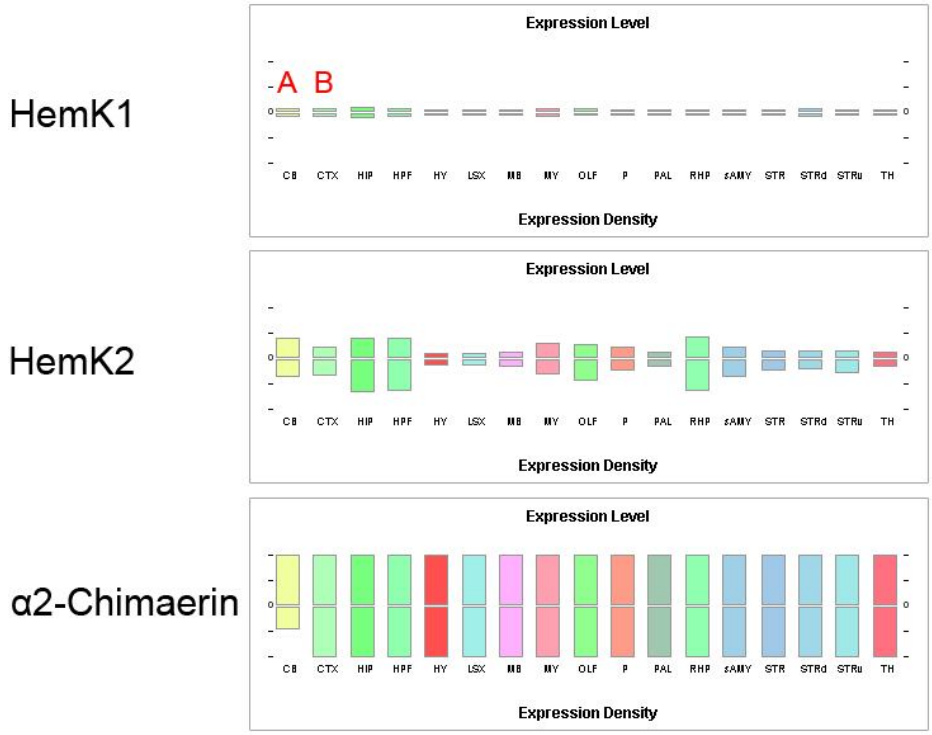

Figure 7.2 Relative transcript levels of HemK1, HemK2 and α2-chimaerin in mouse brain as described by the Allen Brain Atlas. The relative transcript levels of HemK1, HemK2 and α2-chimaerin in (A) cerebellum and (B) cortex in adult mice as revealed by *in situ* hybridisation are not consistent to the comparable levels obtained by real-time PCR in adult rat brains in this study. Picture adapted from the Allen Brain Atlas. [(http://mouse.brain-map.org) *in situ* analyses: (Strain: C57BL/6J, Sex: M, Plane of Section: sagittal. Mouse age: 55 days for HemK1, 56 days for HemK2 and α2-chimaerin); Lein et al, 2007]

In an attempt to characterise three monoclonal and two polyclonal antibodies raised against HemK1, western blots of fractionated e14, 18 and adult rat brain obtained different results between the antibodies. The monoclonal antibodies have been raised against the C terminal of human HemK1 while the two polyclonal ones were raised against a synthesised peptide of the last 16 amino acids of the human protein. In these experiments an anomalous separation of recombinant HemK1 in 10% polyacrylamide gel was observed since the protein was detected just below the 50kDa size marker. The human HemK1 protein is predicted to be 37kDa.

The monoclonal 7D7 antibody detected a strong band corresponding to the expected size of the cloned HemK1 in rat brain, as well as in untransfected mouse and monkey cell lines, but not in human brain or HeLa cells. In the western blot experiment of fractionated rat brains the control lane was lysate of COS-7 cells transfected with HA-HemK1. Since 7D7 could detect a strong band of the expected size in untransfected COS-7 cells, the band detected in this experiment is not believed to be exogenously expressed HA-HemK1. This means that to date there is no indication that this antibody can detect cloned HemK1 protein. Furthermore, the band detected in N1E-115 neuroblastoma cells did not decrease in intensity when HemK1 was knocked-down by shRNA as verified by real-time PCR. These data indicate that the band recognised by 7D7 is a non-specific antigen not detected in human origin cells.

The most promising antibody was 6D2 that detected a band of lower molecular weight than the cloned HemK1 in the mitochondrial fraction of e14 rat brain as well as in human brain homogenate of frontal cortex, possibly representing native HemK1 protein translocated to the mitochondria. This band was also detected by the polyclonal rabbit-5 and the commercially available monoclonal antibody (Cat#: H00051409-B01 from Abnova). The different results obtained with the 7D7, rabbit-5 and rabbit-6 antibodies when used in rat or human brain indicates that they show species specificity but not necessarily their ability to detect native protein. The synthesised peptide that the rabbit-5 and rabbit-6 polyclonal antibodies were raised against shows 62.5% residue identity to the corresponding rat sequence (Figure 7.3). This could account for the inconsistent results when used cross-species.

Figure 7.3 The C-terminal HemK1 synthetic peptide that the two polyclonal antibodies were raised against. The two polyclonal antibodies rabbit-5 and rabbit-6 were raised against a 16 amino acid synthetic peptide of the human HemK1 C-terminal that shows 62.5% sequence identity to the rat sequence.

To further characterise these antibodies one would map the epitope recognised by the monoclonal antibodies on human HemK1 sequence, and compare to the rat sequence. Furthermore, the proteins detected by the antibodies could be analysed by mass spectrometry that would confirm their identity and the specificity of the antibodies. Lastly, the antibodies should be used on fractionated human brain to reveal the localisation of native HemK1, since an obvious difference in detected proteins is observed across species. This could also detect a size difference between the mitochondrial and the cytoplasmic HemK1 proteins.

Interchangeability of HemK1 and HemK2 substrates

An interesting finding of this project was that HemK1 can associate and also partially co-localise with eRF1 as well as its proposed substrate mtRF1a. Also HemK2 was shown to associate and partially co-localise with its proposed substrate eRF1 as well as mtRF1a. This suggests interchangeability between the release factor substrates of HemK1 and HemK2. Even though the two N5-glutamine methyltransferases share the conserved NPPY substrate-binding motif and the GxGxG AdoMet-binding motif, their primary structure only shows a 25.7% residue identity. It is therefore possible that interchangeability of substrates is based on similar tertiary structure. Comparing the described tertiary structure of *Thermotoga maritima* HemK1 to the predicted structure of human HemK2 reveals the conservation of the a five helix bundle containing the NPPY motif, as well as the seven-stranded β-sheet that harbours the AdoMet binding sequence (Figure 7.4).

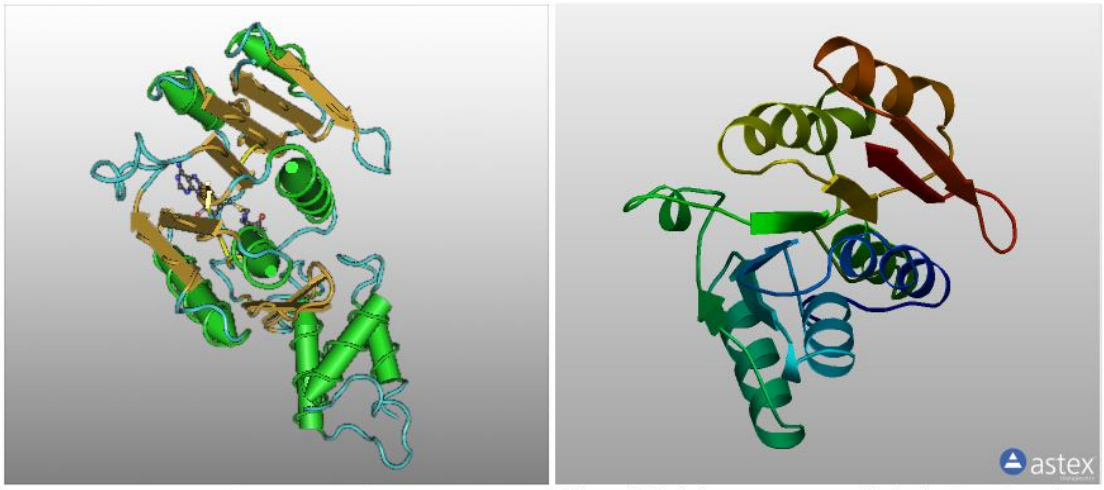

Figure 7.4 Comparison of HemK1 and HemK2 predicted structures. The published structure of HemK1 in *Thermotoga maritime* is shown (left) and compared to the predicted tertiary structure of human HemK2 (right). The seven-stranded β-sheet and the five helix bundle that harbour the catalytic domain and the susbtrate binding motif respectively are conserved. The structure prediction was done by the SwissModel online algorithm based on the human HemK2 sequence NCBI: NM_013240. [(http://swissmodel.expasy.org); Arnold et al, 2006; Schwede et al, 2003; Guex et al, 1997]. [HemK1 structure: (PDB ID:1NV9); Schubert et al, 2003; Yang et al, 2004a).

Conclusion

This study investigated the interaction between α2-chimaerin and HemK1, initially observed in a yeast two-hybrid screen in our lab. At first, an association between a protein that is specifically expressed in the brain and is involved in pathways affecting neuronal morphogenesis, with a protein that is expressed in every cell and holds the ubiquitous and important function of mediating translation termination, seemed unlikely to be reflecting a real biological function. During the course of this study however, a number of interacting partners and cellular processes have been involved in what seems to be a complex interplay of different factors that could bridge distinct cellular pathways to mediate morphogenetic events in the developing neurone (Figure 7.5).

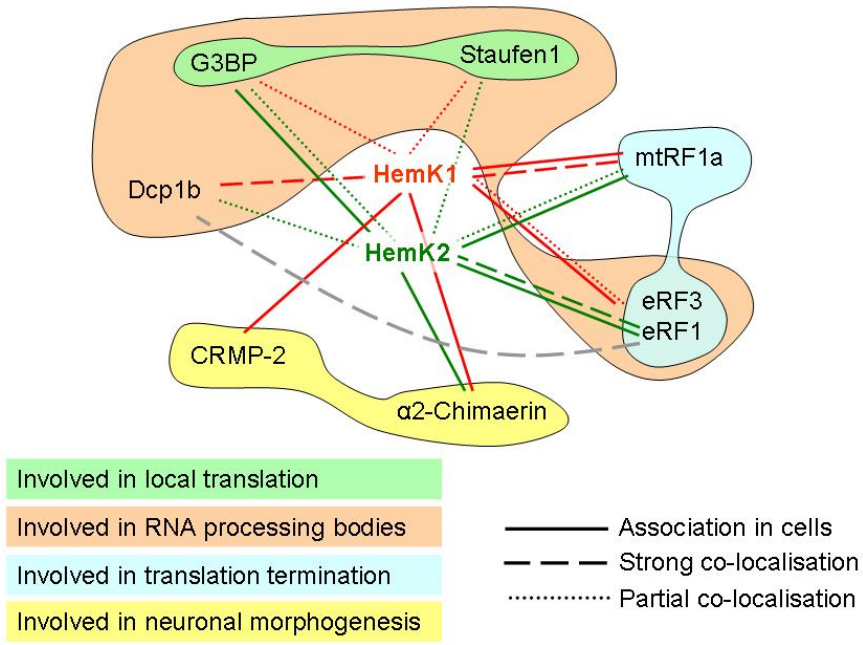

Figure 7.5 Protein associations and co-localisations observed in this study. A number of associations and protein co-localisation in cells were suggested by this study. HemK1 and HemK2 could bridge previously distinct pathways of translation termination, RNA processing and localised translation to mediate morphogenetic events in developing neurones through α2-chimaerin.

It was found that α2-chimaerin can associate with HemK1 and related protein HemK2. HemK1 also associated with CRMP-2, a *bona fide* interacting partner of α2-chimaerin and showed strong co-localisation with P-body protein Dcp1b, involved in RNA degradation. HemK2 also associated with G3BP, a protein involved in localised translation. HemK1 and HemK2 were able to associate and co-localise with both eRF1 and mtRF1a release factors, possibly reflecting their conserved secondary structure. Furthermore, both HemK1 and HemK2 showed some over-lap in cell staining for Staufen1, a protein involved in localised mRNA translation in dendritic spines and axons. ShRNA knock-down of HemK1 in primary hippocampal neurones caused a significant increase in dendritic complexity close to the soma. Knock-down of HemK2 by shRNA caused a similar effect though of much less amplitude. It has to be noted that the N numbers for some of the experiments presented in this work are relatively low and the data are therefore presented as preliminary and would have to be repeated before their evaluation would be statistically significant. These data shed a pioneer light to a complex interplay between RNA processing and neuronal morphogenetic pathways, possibly choreographed by HemK1 and HemK2, while rediscovering the beautiful economy of nature.

References

Ahmed, S.; Kozma, R.; Monfries, C.; Hall, C.; Lim, H. H.; Smith, P. & Lim, L. (1990), 'Human brain n-chimaerin cDNA encodes a novel phorbol ester receptor.', *Biochem J* **272**(3), 767-773.

Alkalaeva, E. Z.; Pisarev, A. V.; Frolova, L. Y.; Kisselev, L. L. & Pestova, T. V. (2006), 'In vitro reconstitution of eukaryotic translation reveals cooperativity between release factors eRF1 and eRF3.', *Cell* **125**(6), 1125-1136.

Amos, L. & Klug, A. (1974), 'Arrangement of subunits in flagellar microtubules.', *J Cell Sci* **14**(3), 523-549.

Amrani, N.; Ganesan, R.; Kervestin, S.; Mangus, D. A.; Ghosh, S. & Jacobson, A. (2004), 'A faux 3'-UTR promotes aberrant termination and triggers nonsense-mediated mRNA decay.', *Nature* **432**(7013), 112-118.

Amrani, N.; Ghosh, S.; Mangus, D. A. & Jacobson, A. (2008), 'Translation factors promote the formation of two states of the closed-loop mRNP.', *Nature* **453**(7199), 1276-1280.

Andersen, S. S. & Bi, G. Q. (2000), 'Axon formation: a molecular model for the generation of neuronal polarity.', *Bioessays* **22**(2), 172-179.

Andersen, G. R.; Valente, L.; Pedersen, L.; Kinzy, T. G. & Nyborg, J. (2001), 'Crystal structures of nucleotide exchange intermediates in the eEF1A-eEF1Balpha complex.', *Nat Struct Biol* **8**(6), 531-534.

Anderson, P. & Kedersha, N. (2009), 'Stress granules.', *Curr Biol* **19**(10), R397-R398.

Anderson, P. & Kedersha, N. (2008), 'Stress granules: the Tao of RNA triage.', *Trends Biochem Sci* **33**(3), 141-150.

Anderson, P. & Kedersha, N. (2006), 'RNA granules.', *J Cell Biol* **172**(6), 803-808.

Anderson, P. & Kedersha, N. (2002), 'Visibly stressed: the role of eIF2, TIA-1, and stress granules in protein translation.', *Cell Stress Chaperones* **7**(2), 213-221.

Anderson, S.; Bankier, A. T.; Barrell, B. G.; de Bruijn, M. H.; Coulson, A. R.; Drouin, J.; Eperon, I. C.; Nierlich, D. P.; Roe, B. A.; Sanger, F.; Schreier, P. H.; Smith, A. J.; Staden, R. & Young, I. G. (1981), 'Sequence and organization of the human mitochondrial genome.', *Nature* **290**(5806), 457-465.

Aoto, J.; Ting, P.; Maghsoodi, B.; Xu, N.; Henkemeyer, M. & Chen, L. (2007), 'Postsynaptic ephrinB3 promotes shaft glutamatergic synapse formation.', *J Neurosci* **27**(28), 7508-7519.

Arimura, N.; Hattori, A.; Kimura, T.; Nakamuta, S.; Funahashi, Y.; Hirotsune, S.; Furuta, K.; Urano, T.; Toyoshima, Y. Y. & Kaibuchi, K. (2009), 'CRMP-2 directly binds to cytoplasmic dynein and interferes with its activity.', *J Neurochem* **111**(2), 380-390.

Arimura, N.; Inagaki, N.; Chihara, K.; Ménager, C.; Nakamura, N.; Amano, M.; Iwamatsu, A.; Goshima, Y. & Kaibuchi, K. (2000), 'Phosphorylation of collapsin response mediator protein-2 by Rho-kinase. Evidence for two separate signalling pathways for growth cone collapse.', *J Biol Chem* **275**(31), 23973-23980.

Arimura, N. & Kaibuchi, K. (2007), 'Neuronal polarity: from extracellular signals to intracellular mechanisms.', *Nat Rev Neurosci* **8**(3), 194-205.

Arnold, D. B. (2009), 'Actin and microtubule-based cytoskeletal cues direct polarized targeting of proteins in neurones.', *Sci Signal* **2**(83), pe49.

Arnold, K.; Bordoli, L.; Kopp, J. & Schwede, T. (2006), 'The SWISS-MODEL workspace: a web-based environment for protein structure homology modelling.', *Bioinformatics* **22**(2), 195-201.

Atlas, R.; Behar, L.; Sapoznik, S. & Ginzburg, I. (2007), 'Dynamic association with polysomes during P19 neuronal differentiation and an untranslated-region-dependent translation regulation of the tau mRNA by the tau mRNA-associated proteins IMP1, HuD, and G3BP1.', *J Neurosci Res* **85**(1), 173-183.

Azevedo, F. A. C.; Carvalho, L. R. B.; Grinberg, L. T.; Farfel, J. M.; Ferretti, R. E. L.; Leite, R. E. P.; Filho, W. J.; Lent, R. & Herculano-Houzel, S. (2009), 'Equal numbers of neuronal and nonneuronal cells make the human brain an isometrically scaled-up primate brain.', *J Comp Neurol* **513**(5), 532-541.

Banko, J. L.; Hou, L. & Klann, E. (2004), 'NMDA receptor activation results in PKA- and ERK-dependent Mnk1 activation and increased eIF4E phosphorylation in hippocampal area CA1.', *J Neurochem* **91**(2), 462-470.

Barbee, S. A.; Estes, P. S.; Cziko, A.-M.; Hillebrand, J.; Luedeman, R. A.; Coller, J. M.; Johnson, N.; Howlett, I. C.; Geng, C.; Ueda, R.; Brand, A. H.; Newbury, S. F.; Wilhelm, J. E.; Levine, R. B.; Nakamura, A.; Parker, R. & Ramaswami, M. (2006), 'Staufen- and FMRP-containing neuronal RNPs are structurally and functionally related to somatic P bodies.', *Neurone* **52**(6), 997-1009.

Barrell, B. G.; Bankier, A. T. & Drouin, J. (1979), 'A different genetic code in human mitochondria.', *Nature* **282**(5735), 189-194.

Bassell, G. J. & Warren, S. T. (2008), 'Fragile X syndrome: loss of local mRNA regulation alters synaptic development and function.', *Neurone* **60**(2), 201-214.

Beal, M. F. (2005), 'Mitochondria take center stage in aging and neurodegeneration.', *Ann Neurol* **58**(4), 495-505.

Beg, A. A.; Sommer, J. E.; Martin, J. H. & Scheiffele, P. (2007), 'alpha2-Chimaerin is an essential EphA4 effector in the assembly of neuronal locomotor circuits.', *Neurone* **55**(5), 768-778.

Bellanger, J. M.; Lazaro, J. B.; Diriong, S.; Fernandez, A.; Lamb, N. & Debant, A. (1998), 'The two guanine nucleotide exchange factor domains of Trio link the Rac1 and the RhoA pathways in vivo.', *Oncogene* **16**(2), 147-152.

Benson, M. D.; Romero, M. I.; Lush, M. E.; Lu, Q. R.; Henkemeyer, M. & Parada, L. F. (2005), 'Ephrin-B3 is a myelin-based inhibitor of neurite outgrowth.', *Proc Natl Acad Sci U S A* **102**(30), 10694-10699.

Bernards, A. & Settleman, J. (2004), 'GAP control: regulating the regulators of small GTPases.', *Trends Cell Biol* **14**(7), 377-385.

Bernhardt, R. & Matus, A. (1984), 'Light and electron microscopic studies of the distribution of microtubule-associated protein 2 in rat brain: a difference between dendritic and axonal cytoskeletons.', *J Comp Neurol* **226**(2), 203-221.

Blanchoin, L.; Amann, K. J.; Higgs, H. N.; Marchand, J. B.; Kaiser, D. A. & Pollard, T. D. (2000), 'Direct observation of dendritic actin filament networks nucleated by Arp2/3 complex and WASP/Scar proteins.', *Nature* **404**(6781), 1007-1011.

Blangy, A.; Vignal, E.; Schmidt, S.; Debant, A.; Gauthier-Rouvière, C. & Fort, P. (2000), 'TrioGEF1 controls Rac- and Cdc42-dependent cell structures through the direct activation of rhoG.', *J Cell Sci* **113 (Pt 4)**, 729-739.

Booth, R. F. & Clark, J. B. (1978), 'A rapid method for the preparation of relatively pure metabolically competent synaptosomes from rat brain.', *Biochem J* **176**(2), 365-370.

Bouakaz, L.; Bouakaz, E.; Murgola, E. J.; Ehrenberg, M. & Sanyal, S. (2006), 'The role of ribosomal protein L11 in class I release factor-mediated translation termination and translational accuracy.', *J Biol Chem* **281**(7), 4548-4556.

Bradke, F. & Dotti, C. G. (2000), 'Establishment of neuronal polarity: lessons from cultured hippocampal neurones.', *Curr Opin Neurobiol* **10**(5), 574-581.

Brengues, M.; Teixeira, D. & Parker, R. (2005), 'Movement of eukaryotic mRNAs between polysomes and cytoplasmic processing bodies.', *Science* **310**(5747), 486-489.

Briançon-Marjollet, A.; Ghogha, A.; Nawabi, H.; Triki, I.; Auziol, C.; Fromont, S.; Piché, C.; Enslen, H.; Chebli, K.; Cloutier, J.-F.; Castellani, V.; Debant, A. & Lamarche-Vane, N. (2008), 'Trio mediates netrin-1-induced Rac1 activation in axon outgrowth and guidance.', *Mol Cell Biol* **28**(7), 2314-2323.

Brogna, S.; Ramanathan, P. & Wen, J. (2008), 'UPF1 P-body localization.', *Biochem Soc Trans* **36**(Pt 4), 698-700.

Brown, M.; Jacobs, T.; Eickholt, B.; Ferrari, G.; Teo, M.; Monfries, C.; Qi, R. Z.; Leung, T.; Lim, L. & Hall, C. (2004), 'Alpha2-chimaerin, cyclin-dependent Kinase 5/p35, and its target collapsin response mediator protein-2 are essential components in semaphorin 3A-induced growth-cone collapse.', *J Neurosci* **24**(41), 8994-9004.

Bruinsma, S. P.; Cagan, R. L. & Baranski, T. J. (2007), 'Chimaerin and Rac regulate cell number, adherens junctions, and ERK MAP kinase signalling in the Drosophila eye.', *Proc Natl Acad Sci U S A* **104**(17), 7098-7103.

Bryant, S. S.; Briggs, S.; Smithgall, T. E.; Martin, G. A.; McCormick, F.; Chang, J. H.; Parsons, S. J. & Jove, R. (1995), 'Two SH2 domains of p120 Ras GTPase-activating protein bind synergistically to tyrosine phosphorylated p190 Rho GTPase-activating protein.', *J Biol Chem* **270**(30), 17947-17952.

Bujnicki, J. M. & Radlinska, M. (1999), 'Is the HemK family of putative S-adenosylmethionine-dependent methyltransferases a "missing" zeta subfamily of adenine methyltransferases? A hypothesis.', *IUBMB Life* **48**(3), 247-249.

Burns, R. G. (1991), 'Assembly of chick brain MAP2-tubulin microtubule protein. Characterization of the protein and the MAP2-dependent addition of tubulin dimers.', *Biochem J* **277 (Pt 1)**, 231-238.

Bustelo, X. R.; Sauzeau, V. & Berenjeno, I. M. (2007), 'GTP-binding proteins of the Rho/Rac family: regulation, effectors and functions in vivo.', *Bioessays* **29**(4), 356-370.

Buttery, P.; Beg, A. A.; Chih, B.; Broder, A.; Mason, C. A. & Scheiffele, P. (2006), 'The diacylglycerol-binding protein alpha1-chimaerin regulates dendritic morphology.', *Proc Natl Acad Sci U S A* **103**(6), 1924-1929.

Caloca, M. J.; Garcia-Bermejo, M. L.; Blumberg, P. M.; Lewin, N. E.; Kremmer, E.; Mischak, H.; Wang, S.; Nacro, K.; Bienfait, B.; Marquez, V. E. & Kazanietz, M. G. (1999), 'beta2-chimaerin is a novel target for diacylglycerol: binding properties and changes in subcellular localization mediated by ligand binding to its C1 domain.', *Proc Natl Acad Sci U S A* **96**(21), 11854-11859.

Caloca, M. J.; Wang, H.; Delemos, A.; Wang, S. & Kazanietz, M. G. (2001), 'Phorbol esters and related analogs regulate the subcellular localization of beta 2-chimaerin, a non-protein kinase C phorbol ester receptor.', *J Biol Chem* **276**(21), 18303-18312.

Campbell, D. S. & Holt, C. E. (2001), 'Chemotropic responses of retinal growth cones mediated by rapid local protein synthesis and degradation.', *Neurone* **32**(6), 1013-1026.

Canagarajah, B.; Leskow, F. C.; Ho, J. Y. S.; Mischak, H.; Saidi, L. F.; Kazanietz, M. G. & Hurley, J. H. (2004), 'Structural mechanism for lipid activation of the Rac-specific GAP, beta2-chimaerin.', *Cell* **119**(3), 407-418.

Capecchi, M. R. (1967), 'Polypeptide chain termination in vitro: isolation of a release factor.', *Proc Natl Acad Sci U S A* **58**(3), 1144-1151.

Casali, C.; Bonifati, V.; Santorelli, F. M.; Casari, G.; Fortini, D.; Patrignani, A.; Fabbrini, G.; Carrozzo, R.; D'Amati, G.; Locuratolo, N.; Vanacore, N.; Damiano, M.; Pierallini, A.; Pierelli, F.; Amabile, G. A. & Meco, G. (2001), 'Mitochondrial myopathy, parkinsonism, and multiple mtDNA deletions in a Sephardic Jewish family.', *Neurology* **56**(6), 802-805.

Cheever, A. & Ceman, S. (2009), 'Translation regulation of mRNAs by the fragile X family of proteins through the microRNA pathway.', *RNA Biol* **6**(2), 175-178.

Chen, J.; Deng, F.; Li, J. & Wang, Q. J. (2008), 'Selective binding of phorbol esters and diacylglycerol by individual C1 domains of the PKD family.', *Biochem J* **411**(2), 333-342.

Chhatriwala, M. K.; Betts, L.; Worthylake, D. K. & Sondek, J. (2007), 'The DH and PH domains of Trio coordinately engage Rho GTPases for their efficient activation.', *J Mol Biol* **368**(5), 1307-1320.

Chiaberge, S.; Cassarino, E. & Mangiarotti, G. (1998), 'The phosphorylation of protein S6 modulates the interaction of the 40 S ribosomal subunit with the 5'-untranslated region of a dictyostelium pre-spore-specific mRNA and controls its stability.', *J Biol Chem* **273**(42), 27070-27075.

Chihara, T.; Luginbuhl, D. & Luo, L. (2007), 'Cytoplasmic and mitochondrial protein translation in axonal and dendritic terminal arborization.', *Nat Neurosci* **10**(7), 828-837.

Cho, H.; Kim, K. M. & Kim, Y. K. (2009), 'Human proline-rich nuclear receptor coregulatory protein 2 mediates an interaction between mRNA surveillance machinery and decapping complex.', *Mol Cell* **33**(1), 75-86.

Chung, H.; Nairn, A. C.; Murata, K. & Brautigan, D. L. (1999), 'Mutation of Tyr307 and Leu309 in the protein phosphatase 2A catalytic subunit favors association with the alpha 4 subunit which promotes dephosphorylation of elongation factor-2.', *Biochemistry* **38**(32), 10371-10376.

Colson, C.; Lhoest, J. & Urlings, C. (1979), 'Genetics of ribosomal protein methylation in Escherichia coli. III. Map position of two genes, prmA and prmB, governing methylation of proteins L11 and L3.', *Mol Gen Genet* **169**(3), 245-250.

Colón-González, F. & Kazanietz, M. G. (2006), 'C1 domains exposed: from diacylglycerol binding to protein-protein interactions.', *Biochim Biophys Acta* **1761**(8), 827-837.

Colón-González, F.; Leskow, F. C. & Kazanietz, M. G. (2008), 'Identification of an autoinhibitory mechanism that restricts C1 domain-mediated activation of the Rac-GAP alpha2-chimaerin.', *J Biol Chem* **283**(50), 35247-35257.

Conde, C. & Cáceres, A. (2009), 'Microtubule assembly, organization and dynamics in axons and dendrites.', *Nat Rev Neurosci* **10**(5), 319-332.

Conti, E. & Izaurralde, E. (2005), 'Nonsense-mediated mRNA decay: molecular insights and mechanistic variations across species.', *Curr Opin Cell Biol* **17**(3), 316-325.

Cosker, K. E. & Eickholt, B. J. (2007), 'Phosphoinositide 3-kinase signalling events controlling axonal morphogenesis.', *Biochem Soc Trans* **35**(Pt 2), 207-210.

Cosker, K. E.; Shadan, S.; van Diepen, M.; Morgan, C.; Li, M.; Allen-Baume, V.; Hobbs, C.; Doherty, P.; Cockcroft, S. & Eickholt, B. J. (2008), 'Regulation of PI3K signalling by the phosphatidylinositol transfer protein PITPalpha during axonal extension in hippocampal neurons.', *J Cell Sci* **121**(Pt 6), 796-803.

Cougot, N.; Babajko, S. & Séraphin, B. (2004b), 'Cytoplasmic foci are sites of mRNA decay in human cells.', *J Cell Biol* **165**(1), 31-40.

Cougot, N.; Bhattacharyya, S. N.; Tapia-Arancibia, L.; Bordonné, R.; Filipowicz, W.; Bertrand, E. & Rage, F. (2008), 'Dendrites of mammalian neurones contain specialized P-body-like structures that respond to neuronal activation.', *J Neurosci* **28**(51), 13793-13804.

Cougot, N.; van Dijk, E.; Babajko, S. & Séraphin, B. (2004a), "Cap-tabolism'.', *Trends Biochem Sci* **29**(8), 436-444.

Crick, F. (1970), 'Central dogma of molecular biology.', *Nature* **227**(5258), 561-563.

D'Hulst, C. & Kooy, R. F. (2009), 'Fragile X syndrome: from molecular genetics to therapy.', *J Med Genet* **46**(9), 577-584.

Dahm, R.; Zeitelhofer, M.; Götze, B.; Kiebler, M. A. & Macchi, P. (2008), 'Visualizing mRNA localization and local protein translation in neurones.', *Methods Cell Biol* **85**, 293-327.

Dang, Y. L. & Martin, N. C. (1993), 'Yeast mitochondrial RNase P. Sequence of the RPM2 gene and demonstration that its product is a protein subunit of the enzyme.', *J Biol Chem* **268**(26), 19791-19796.

Daub, H.; Gevaert, K.; Vandekerckhove, J.; Sobel, A. & Hall, A. (2001), 'Rac/Cdc42 and p65PAK regulate the microtubule-destabilizing protein stathmin through phosphorylation at serine 16.', *J Biol Chem* **276**(3), 1677-1680.

DerMardirossian, C. & Bokoch, G. M. (2005), 'GDIs: central regulatory molecules in Rho GTPase activation.', *Trends Cell Biol* **15**(7), 356-363.

Desai, A. & Mitchison, T. J. (1997), 'Microtubule polymerization dynamics.', *Annu Rev Cell Dev Biol* **13**, 83-117.

van Dijk, E.; Cougot, N.; Meyer, S.; Babajko, S.; Wahle, E. & Séraphin, B. (2002), 'Human Dcp2: a catalytically active mRNA decapping enzyme located in specific cytoplasmic structures.', *EMBO J* **21**(24), 6915-6924.

Ding, L. & Han, M. (2007), 'GW182 family proteins are crucial for microRNA-mediated gene silencing.', *Trends Cell Biol* **17**(8), 411-416.

Dotti, C. G. & Banker, G. A. (1987), 'Experimentally induced alteration in the polarity of developing neurones.', *Nature* **330**(6145), 254-256.

Dotti, C. G.; Sullivan, C. A. & Banker, G. A. (1988), 'The establishment of polarity by hippocampal neurones in culture.', *J Neurosci* **8**(4), 1454-1468.

Dugré-Brisson, S.; Elvira, G.; Boulay, K.; Chatel-Chaix, L.; Mouland, A. J. & DesGroseillers, L. (2005), 'Interaction of Staufen1 with the 5' end of mRNA facilitates translation of these RNAs.', *Nucleic Acids Res* **33**(15), 4797-4812.

Dunckley, T. & Parker, R. (1999), 'The DCP2 protein is required for mRNA decapping in Saccharomyces cerevisiae and contains a functional MutT motif.', *EMBO J* **18**(19), 5411-5422.

Ebihara, K. & Nakamura, Y. (1999), 'C-terminal interaction of translational release factors eRF1 and eRF3 of fission yeast: G-domain uncoupled binding and the role of conserved amino acids.', *RNA* **5**(6), 739-750.

Edwards, D. C.; Sanders, L. C.; Bokoch, G. M. & Gill, G. N. (1999), 'Activation of LIM-kinase by Pak1 couples Rac/Cdc42 GTPase signalling to actin cytoskeletal dynamics.', *Nat Cell Biol* **1**(5), 253-259.

Elzanowski, A. & Ostell, J. (2008), 'The Genetic Codes'. Retrieved April 5 2010 from http://www.ncbi.nlm.nih.gov/Taxonomy/Utils/wprintgc.cgi?mode=c#SG32000

Eng, C. H.; Huckaba, T. M. & Gundersen, G. G. (2006), 'The formin mDia regulates GSK3beta through novel PKCs to promote microtubule stabilization but not MTOC reorientation in migrating fibroblasts.', *Mol Biol Cell* **17**(12), 5004-5016.

Eng, L. F. (1985), 'Glial fibrillary acidic protein (GFAP): the major protein of glial intermediate filaments in differentiated astrocytes.', *J Neuroimmunol* **8**(4-6), 203-214.

Estrach, S.; Schmidt, S.; Diriong, S.; Penna, A.; Blangy, A.; Fort, P. & Debant, A. (2002), 'The Human Rho-GEF trio and its target GTPase RhoG are involved in the NGF pathway, leading to neurite outgrowth.', *Curr Biol* **12**(4), 307-312.

Eulalio, A.; Behm-Ansmant, I. & Izaurralde, E. (2007a), 'P bodies: at the crossroads of post-transcriptional pathways.', *Nat Rev Mol Cell Biol* **8**(1), 9-22.

Eulalio, A.; Behm-Ansmant, I.; Schweizer, D. & Izaurralde, E. (2007b), 'P-body formation is a consequence, not the cause, of RNA-mediated gene silencing.', *Mol Cell Biol* **27**(11), 3970-3981.

Eystathioy, T.; Jakymiw, A.; Chan, E. K. L.; Séraphin, B.; Cougot, N. & Fritzler, M. J. (2003), 'The GW182 protein colocalizes with mRNA degradation associated proteins hDcp1 and hLSm4 in cytoplasmic GW bodies.', *RNA* **9**(10), 1171-1173.

Feng, Y.; Gutekunst, C. A.; Eberhart, D. E.; Yi, H.; Warren, S. T. & Hersch, S. M. (1997), 'Fragile X mental retardation protein: nucleocytoplasmic shuttling and association with somatodendritic ribosomes.', *J Neurosci* **17**(5), 1539-1547.

Ferrandon, D.; Elphick, L.; Nüsslein-Volhard, C. & Johnston, D. S. (1994), 'Staufen protein associates with the 3'UTR of bicoid mRNA to form particles that move in a microtubule-dependent manner.', *Cell* **79**(7), 1221-1232.

Figaro, S.; Scrima, N.; Buckingham, R. H. & Heurgué-Hamard, V. (2008), 'HemK2 protein, encoded on human chromosome 21, methylates translation termination factor eRF1.', *FEBS Lett* **582**(16), 2352-2356.

Foster, K. G. & Fingar, D. C. (2010), 'Mammalian target of rapamycin (mTOR): conducting the cellular signaling symphony.', *J Biol Chem* **285**(19), 14071-14077.

Franks, T. M. & Lykke-Andersen, J. (2007), 'TTP and BRF proteins nucleate processing body formation to silence mRNAs with AU-rich elements.', *Genes Dev* **21**(6), 719-735.

Freist, W.; Logan, D. T. & Gauss, D. H. (1996), 'Glycyl-tRNA synthetase.', *Biol Chem Hoppe Seyler* **377**(6), 343-356.

Freistroffer, D. V.; Pavlov, M. Y.; MacDougall, J.; Buckingham, R. H. & Ehrenberg, M. (1997), 'Release factor RF3 in E.coli accelerates the dissociation of release factors RF1 and RF2 from the ribosome in a GTP-dependent manner.', *EMBO J* **16**(13), 4126-4133.

Frolova, L.; Goff, X. L.; Rasmussen, H. H.; Cheperegin, S.; Drugeon, G.; Kress, M.; Arman, I.; Haenni, A. L.; Celis, J. E. & Philippe, M. (1994), 'A highly conserved eukaryotic protein family possessing properties of polypeptide chain release factor.', *Nature* **372**(6507), 701-703.

Frolova, L. Y.; Tsivkovskii, R. Y.; Sivolobova, G. F.; Oparina, N. Y.; Serpinsky, O. I.; Blinov, V. M.; Tatkov, S. I. & Kisselev, L. L. (1999), 'Mutations in the highly conserved GGQ motif of class 1 polypeptide release factors abolish ability of human eRF1 to trigger peptidyl-tRNA hydrolysis.', *RNA* **5**(8), 1014-1020.

Fuchs, E. & Cleveland, D. W. (1998), 'A structural scaffolding of intermediate filaments in health and disease.', *Science* **279**(5350), 514-519.

Fukata, M.; Watanabe, T.; Noritake, J.; Nakagawa, M.; Yamaga, M.; Kuroda, S.; Matsuura, Y.; Iwamatsu, A.; Perez, F. & Kaibuchi, K. (2002), 'Rac1 and Cdc42 capture microtubules through IQGAP1 and CLIP-170.', *Cell* **109**(7), 873-885.

Fukata, Y.; Itoh, T. J.; Kimura, T.; Ménager, C.; Nishimura, T.; Shiromizu, T.; Watanabe, H.; Inagaki, N.; Iwamatsu, A.; Hotani, H. & Kaibuchi, K. (2002), 'CRMP-2 binds to tubulin heterodimers to promote microtubule assembly.', *Nat Cell Biol* **4**(8), 583-591.

Fukumoto, Y.; Kaibuchi, K.; Hori, Y.; Fujioka, H.; Araki, S.; Ueda, T.; Kikuchi, A. & Takai, Y. (1990), 'Molecular cloning and characterization of a novel type of regulatory protein (GDI) for the rho proteins, ras p21-like small GTP-binding proteins.', *Oncogene* **5**(9), 1321-1328.

Gallouzi, I. E.; Parker, F.; Chebli, K.; Maurier, F.; Labourier, E.; Barlat, I.; Capony, J. P.; Tocque, B. & Tazi, J. (1998), 'A novel phosphorylation-dependent RNase activity

of GAP-SH3 binding protein: a potential link between signal transduction and RNA stability.', *Mol Cell Biol* **18**(7), 3956-3965.

Gao, H.; Zhou, Z.; Rawat, U.; Huang, C.; Bouakaz, L.; Wang, C.; Cheng, Z.; Liu, Y.; Zavialov, A.; Gursky, R.; Sanyal, S.; Ehrenberg, M.; Frank, J. & Song, H. (2007), 'RF3 induces ribosomal conformational changes responsible for dissociation of class I release factors.', *Cell* **129**(5), 929-941.

Gebauer, F. & Hentze, M. W. (2004), 'Molecular mechanisms of translational control.', *Nat Rev Mol Cell Biol* **5**(10), 827-835.

Geraldo, S. & Gordon-Weeks, P. R. (2009), 'Cytoskeletal dynamics in growth-cone steering.', *J Cell Sci* **122**(Pt 20), 3595-3604.

Gibbings, D. J.; Ciaudo, C.; Erhardt, M. & Voinnet, O. (2009), 'Multivesicular bodies associate with components of miRNA effector complexes and modulate miRNA activity.', *Nat Cell Biol* **11**(9), 1143-1149.

Gilbert, S. F. (2003), *Developmental Biology*, Sinauer Associates, Inc.

Gingras, A. C.; Raught, B. & Sonenberg, N. (1999), 'eIF4 initiation factors: effectors of mRNA recruitment to ribosomes and regulators of translation.', *Annu Rev Biochem* **68**, 913-963.

Gingras, A. C.; Raught, B. & Sonenberg, N. (2004), 'mTOR signaling to translation.', *Curr Top Microbiol Immunol* **279**, 169-197.

Girard, P. R. & Kuo, J. F. (1990), 'Protein kinase C and its 80-kilodalton substrate protein in neuroblastoma cell neurite outgrowth.', *J Neurochem* **54**(1), 300-306.

Goetze, B.; Tuebing, F.; Xie, Y.; Dorostkar, M. M.; Thomas, S.; Pehl, U.; Boehm, S.; Macchi, P. & Kiebler, M. A. (2006), 'The brain-specific double-stranded RNA-binding protein Staufen2 is required for dendritic spine morphogenesis.', *J Cell Biol* **172**(2), 221-231.

Gong, C.; Kim, Y. K.; Woeller, C. F.; Tang, Y. & Maquat, L. E. (2009), 'SMD and NMD are competitive pathways that contribute to myogenesis: effects on PAX3 and myogenin mRNAs.', *Genes Dev* **23**(1), 54-66.

Goshima, Y.; Nakamura, F.; Strittmatter, P. & Strittmatter, S. M. (1995), 'Collapsin-induced growth cone collapse mediated by an intracellular protein related to UNC-33.', *Nature* **376**(6540), 509-514.

Goslin, K. & Banker, G. (1989), 'Experimental observations on the development of polarity by hippocampal neurones in culture.', *J Cell Biol* **108**(4), 1507-1516.

Gotzmann, J. & Foisner, R. (2006), 'A-type lamin complexes and regenerative potential: a step towards understanding laminopathic diseases?', *Histochem Cell Biol* **125**(1-2), 33-41.

Govek, E.-E.; Newey, S. E. & Aelst, L. V. (2005), 'The role of the Rho GTPases in neuronal development.', *Genes Dev* **19**(1), 1-49.

Govind, S.; Kozma, R.; Monfries, C.; Lim, L. & Ahmed, S. (2001), 'Cdc42Hs facilitates cytoskeletal reorganization and neurite outgrowth by localizing the 58-kD insulin receptor substrate to filamentous actin.', *J Cell Biol* **152**(3), 579-594.

Guen, L. L.; Santos, R. & Camadro, J. M. (1999), 'Functional analysis of the hemK gene product involvement in protoporphyrinogen oxidase activity in yeast.', *FEMS Microbiol Lett* **173**(1), 175-182.

Guitard, E.; Parker, F.; Millon, R.; Abecassis, J. & Tocqué, B. (2001), 'G3BP is overexpressed in human tumors and promotes S phase entry.', *Cancer Lett* **162**(2), 213-221.

Hall, C.; Brown, M.; Jacobs, T.; Ferrari, G.; Cann, N.; Teo, M.; Monfries, C. & Lim, L. (2001), 'Collapsin response mediator protein switches RhoA and Rac1 morphology

in N1E-115 neuroblastoma cells and is regulated by Rho kinase.', *J Biol Chem* **276**(46), 43482-43486.

Hall, C.; Lim, L. & Leung, T. (2005), 'C1, see them all.', *Trends Biochem Sci* **30**(4), 169-171.

Hall, C.; Michael, G. J.; Cann, N.; Ferrari, G.; Teo, M.; Jacobs, T.; Monfries, C. & Lim, L. (2001), 'alpha2-chimaerin, a Cdc42/Rac1 regulator, is selectively expressed in the rat embryonic nervous system and is involved in neuritogenesis in N1E-115 neuroblastoma cells.', *J Neurosci* **21**(14), 5191-5202.

Hall, C.; Monfries, C.; Smith, P.; Lim, H. H.; Kozma, R.; Ahmed, S.; Vanniasingham, V.; Leung, T. & Lim, L. (1990), 'Novel human brain cDNA encoding a 34,000 Mr protein n-chimaerin, related to both the regulatory domain of protein kinase C and BCR, the product of the breakpoint cluster region gene.', *J Mol Biol* **211**(1), 11-16.

Hall, C.; Sin, W. C.; Teo, M.; Michael, G. J.; Smith, P.; Dong, J. M.; Lim, H. H.; Manser, E.; Spurr, N. K. & Jones, T. A. (1993), 'Alpha 2-chimerin, an SH2-containing GTPase-activating protein for the ras-related protein p21rac derived by alternate splicing of the human n-chimerin gene, is selectively expressed in brain regions and testes.', *Mol Cell Biol* **13**(8), 4986-4998.

de Haro, C.; Méndez, R. & Santoyo, J. (1996), 'The eIF-2alpha kinases and the control of protein synthesis.', *FASEB J* **10**(12), 1378-1387.

He, F.; Brown, A. H. & Jacobson, A. (1997), 'Upf1p, Nmd2p, and Upf3p are interacting components of the yeast nonsense-mediated mRNA decay pathway.', *Mol Cell Biol* **17**(3), 1580-1594.

Herrmann, H.; Strelkov, S. V.; Burkhard, P. & Aebi, U. (2009), 'Intermediate filaments: primary determinants of cell architecture and plasticity.', *J Clin Invest* **119**(7), 1772-1783.

Heurgué-Hamard, V.; Champ, S.; Engström, A.; Ehrenberg, M. & Buckingham, R. H. (2002), 'The hemK gene in Escherichia coli encodes the N(5)-glutamine methyltransferase that modifies peptide release factors.', *EMBO J* **21**(4), 769-778.

Heurgué-Hamard, V.; Champ, S.; Mora, L.; Merkulova-Rainon, T.; Merkoulova-Rainon, T.; Kisselev, L. L. & Buckingham, R. H. (2005), 'The glutamine residue of the conserved GGQ motif in Saccharomyces cerevisiae release factor eRF1 is methylated by the product of the YDR140w gene.', *J Biol Chem* **280**(4), 2439-2445.

Heurgué-Hamard, V.; Graille, M.; Scrima, N.; Ulryck, N.; Champ, S.; van Tilbeurgh, H. & Buckingham, R. H. (2006), 'The zinc finger protein Ynr046w is plurifunctional and a component of the eRF1 methyltransferase in yeast.', *J Biol Chem* **281**(47), 36140-36148.

Hillebrand, J.; Barbee, S. A. & Ramaswami, M. (2007), 'P-body components, microRNA regulation, and synaptic plasticity.', *ScientificWorldJournal* **7**, 178-190.

Hinds, H. L.; Ashley, C. T.; Sutcliffe, J. S.; Nelson, D. L.; Warren, S. T.; Housman, D. E. & Schalling, M. (1993), 'Tissue specific expression of FMR-1 provides evidence for a functional role in fragile X syndrome.', *Nat Genet* **3**(1), 36-43.

Hir, H. L.; Izaurralde, E.; Maquat, L. E. & Moore, M. J. (2000), 'The spliceosome deposits multiple proteins 20-24 nucleotides upstream of mRNA exon-exon junctions.', *EMBO J* **19**(24), 6860-6869.

Hirokawa, N. (1998), 'Kinesin and dynein superfamily proteins and the mechanism of organelle transport.', *Science* **279**(5350), 519-526.

Holbrook, J. A.; Neu-Yilik, G.; Hentze, M. W. & Kulozik, A. E. (2004), 'Nonsense-mediated decay approaches the clinic.', *Nat Genet* **36**(8), 801-808.

Hoogenraad, C. C.; Milstein, A. D.; Ethell, I. M.; Henkemeyer, M. & Sheng, M. (2005), 'GRIP1 controls dendrite morphogenesis by regulating EphB receptor trafficking.', *Nat Neurosci* **8**(7), 906-915.

Hoshino, S.; Imai, M.; Kobayashi, T.; Uchida, N. & Katada, T. (1999), 'The eukaryotic polypeptide chain releasing factor (eRF3/GSPT) carrying the translation termination signal to the 3'-Poly(A) tail of mRNA. Direct association of erf3/GSPT with polyadenylate-binding protein.', *J Biol Chem* **274**(24), 16677-16680.

Hosoda, N.; Kobayashi, T.; Uchida, N.; Funakoshi, Y.; Kikuchi, Y.; Hoshino, S. & Katada, T. (2003), 'Translation termination factor eRF3 mediates mRNA decay through the regulation of deadenylation.', *J Biol Chem* **278**(40), 38287-38291.

Howard, J. & Hyman, A. A. (2003), 'Dynamics and mechanics of the microtubule plus end.', *Nature* **422**(6933), 753-758.

Hurley, J. H. (2008), 'ESCRT complexes and the biogenesis of multivesicular bodies.', *Curr Opin Cell Biol* **20**(1), 4-11.

Hyman, A. A.; Salser, S.; Drechsel, D. N.; Unwin, N. & Mitchison, T. J. (1992), 'Role of GTP hydrolysis in microtubule dynamics: information from a slowly hydrolyzable analogue, GMPCPP.', *Mol Biol Cell* **3**(10), 1155-1167.

Iden, S. & Collard, J. G. (2008), 'Crosstalk between small GTPases and polarity proteins in cell polarization.', *Nat Rev Mol Cell Biol* **9**(11), 846-859.

Inagaki, N.; Chihara, K.; Arimura, N.; Ménager, C.; Kawano, Y.; Matsuo, N.; Nishimura, T.; Amano, M. & Kaibuchi, K. (2001), 'CRMP-2 induces axons in cultured hippocampal neurones.', *Nat Neurosci* **4**(8), 781-782.

Ingelfinger, D.; Arndt-Jovin, D. J.; Lührmann, R. & Achsel, T. (2002), 'The human LSm1-7 proteins colocalize with the mRNA-degrading enzymes Dcp1/2 and Xrnl in distinct cytoplasmic foci.', *RNA* **8**(12), 1489-1501.

Iqbal, K.; Liu, F.; Gong, C.-X.; Alonso, A. D. C. & Grundke-Iqbal, I. (2009), 'Mechanisms of tau-induced neurodegeneration.', *Acta Neuropathol* **118**(1), 53-69.

Ishizawa, T.; Nozaki, Y.; Ueda, T. & Takeuchi, N. (2008), 'The human mitochondrial translation release factor HMRF1L is methylated in the GGQ motif by the methyltransferase HMPrmC.', *Biochem Biophys Res Commun* **373**(1), 99-103.

Isken, O. & Maquat, L. E. (2007), 'Quality control of eukaryotic mRNA: safeguarding cells from abnormal mRNA function.', *Genes Dev* **21**(15), 1833-1856.

Ito, K.; Uno, M. & Nakamura, Y. (2000), 'A tripeptide 'anticodon' deciphers stop codons in messenger RNA.', *Nature* **403**(6770), 680-684.

Ivanov, P. V.; Gehring, N. H.; Kunz, J. B.; Hentze, M. W. & Kulozik, A. E. (2008), 'Interactions between UPF1, eRFs, PABP and the exon junction complex suggest an integrated model for mammalian NMD pathways.', *EMBO J* **27**(5), 736-747.

Iwasato, T.; Katoh, H.; Nishimaru, H.; Ishikawa, Y.; Inoue, H.; Saito, Y. M.; Ando, R.; Iwama, M.; Takahashi, R.; Negishi, M. & Itohara, S. (2007), 'Rac-GAP alpha-chimerin regulates motor-circuit formation as a key mediator of EphrinB3/EphA4 forward signalling.', *Cell* **130**(4), 742-753.

Jacobs, H. T. & Turnbull, D. M. (2005), 'Nuclear genes and mitochondrial translation: a new class of genetic disease.', *Trends Genet* **21**(6), 312-314.

Jacobson, A. & Peltz, S. W. (1996), 'Interrelationships of the pathways of mRNA decay and translation in eukaryotic cells.', *Annu Rev Biochem* **65**, 693-739.

Jiang, H.; Guo, W.; Liang, X. & Rao, Y. (2005), 'Both the establishment and the maintenance of neuronal polarity require active mechanisms: critical roles of GSK-3beta and its upstream regulators.', *Cell* **120**(1), 123-135.

Jin, Z. & Strittmatter, S. M. (1997), 'Rac1 mediates collapsin-1-induced growth cone collapse.', *J Neurosci* **17**(16), 6256-6263.

Johnston, D. S.; Beuchle, D. & Nüsslein-Volhard, C. (1991), 'Staufen, a gene required to localize maternal RNAs in the Drosophila egg.', *Cell* **66**(1), 51-63.

Jovic, M.; Sharma, M.; Rahajeng, J. & Caplan, S. (2010), 'The early endosome: a busy sorting station for proteins at the crossroads.', *Histol Histopathol* **25**(1), 99-112.

Kadison, S. R.; Mäkinen, T.; Klein, R.; Henkemeyer, M. & Kaprielian, Z. (2006), 'EphB receptors and ephrin-B3 regulate axon guidance at the ventral midline of the embryonic mouse spinal cord.', *J Neurosci* **26**(35), 8909-8914.

Kashima, I.; Yamashita, A.; Izumi, N.; Kataoka, N.; Morishita, R.; Hoshino, S.; Ohno, M.; Dreyfuss, G. & Ohno, S. (2006), 'Binding of a novel SMG-1-Upf1-eRF1-eRF3 complex (SURF) to the exon junction complex triggers Upf1 phosphorylation and nonsense-mediated mRNA decay.', *Genes Dev* **20**(3), 355-367.

Kasri, N. N. & Aelst, L. V. (2008), 'Rho-linked genes and neurological disorders.', *Pflugers Arch* **455**(5), 787-797.

Kataoka, N.; Yong, J.; Kim, V. N.; Velazquez, F.; Perkinson, R. A.; Wang, F. & Dreyfuss, G. (2000), 'Pre-mRNA splicing imprints mRNA in the nucleus with a novel RNA-binding protein that persists in the cytoplasm.', *Mol Cell* **6**(3), 673-682.

Katzmann, D. J.; Babst, M. & Emr, S. D. (2001), 'Ubiquitin-dependent sorting into the multivesicular body pathway requires the function of a conserved endosomal protein sorting complex, ESCRT-I.', *Cell* **106**(2), 145-155.

Kedersha, N.; Chen, S.; Gilks, N.; Li, W.; Miller, I. J.; Stahl, J. & Anderson, P. (2002), 'Evidence that ternary complex (eIF2-GTP-tRNA(i)(Met))-deficient preinitiation complexes are core constituents of mammalian stress granules.', *Mol Biol Cell* **13**(1), 195-210.

Kedersha, N.; Cho, M. R.; Li, W.; Yacono, P. W.; Chen, S.; Gilks, N.; Golan, D. E. & Anderson, P. (2000), 'Dynamic shuttling of TIA-1 accompanies the recruitment of mRNA to mammalian stress granules.', *J Cell Biol* **151**(6), 1257-1268.

Kedersha, N.; Stoecklin, G.; Ayodele, M.; Yacono, P.; Lykke-Andersen, J.; Fritzler, M. J.; Scheuner, D.; Kaufman, R. J.; Golan, D. E. & Anderson, P. (2005), 'Stress granules and processing bodies are dynamically linked sites of mRNP remodeling.', *J Cell Biol* **169**(6), 871-884.

Kedersha, N. L.; Gupta, M.; Li, W.; Miller, I. & Anderson, P. (1999), 'RNA-binding proteins TIA-1 and TIAR link the phosphorylation of eIF-2 alpha to the assembly of mammalian stress granules.', *J Cell Biol* **147**(7), 1431-1442.

Kim, A. S.; Kakalis, L. T.; Abdul-Manan, N.; Liu, G. A. & Rosen, M. K. (2000), 'Autoinhibition and activation mechanisms of the Wiskott-Aldrich syndrome protein.', *Nature* **404**(6774), 151-158.

Kim, V. N.; Kataoka, N. & Dreyfuss, G. (2001), 'Role of the nonsense-mediated decay factor hUpf3 in the splicing-dependent exon-exon junction complex.', *Science* **293**(5536), 1832-1836.

Kim, Y. K.; Furic, L.; Desgroseillers, L. & Maquat, L. E. (2005), 'Mammalian Staufen1 recruits Upf1 to specific mRNA 3'UTRs so as to elicit mRNA decay.', *Cell* **120**(2), 195-208.

Kim, Y. K.; Furic, L.; Parisien, M.; Major, F.; DesGroseillers, L. & Maquat, L. E. (2007), 'Staufen1 regulates diverse classes of mammalian transcripts.', *EMBO J* **26**(11), 2670-2681.

Kim-Ha, J.; Kerr, K. & Macdonald, P. M. (1995), 'Translational regulation of oskar mRNA by bruno, an ovarian RNA-binding protein, is essential.', *Cell* **81**(3), 403-412.

Kimball, S. R.; Horetsky, R. L.; Ron, D.; Jefferson, L. S. & Harding, H. P. (2003), 'Mammalian stress granules represent sites of accumulation of stalled translation initiation complexes.', *Am J Physiol Cell Physiol* **284**(2), C273-C284.

Kloc, M.; Zearfoss, N. R. & Etkin, L. D. (2002), 'Mechanisms of subcellular mRNA localization.', *Cell* **108**(4), 533-544.

Kofuji, S.; Sakuno, T.; Takahashi, S.; Araki, Y.; Doi, Y.; ichi Hoshino, S. & Katada, T. (2006), 'The decapping enzyme Dcp1 participates in translation termination through its interaction with the release factor eRF3 in budding yeast.', *Biochem Biophys Res Commun* **344**(2), 547-553.

Kollins, K. M.; Bell, R. L.; Butts, M. & Withers, G. S. (2009), 'Dendrites differ from axons in patterns of microtubule stability and polymerization during development.', *Neural Dev* **4**, 26.

Konecki, D. S.; Aune, K. C.; Tate, W. & Caskey, C. T. (1977), 'Characterization of reticulocyte release factor.', *J Biol Chem* **252**(13), 4514-4520.

Kononenko, A. V.; Mitkevich, V. A.; Atkinson, G. C.; Tenson, T.; Dubovaya, V. I.; Frolova, L. Y.; Makarov, A. A. & Hauryliuk, V. (2010), 'GTP-dependent structural rearrangement of the eRF1:eRF3 complex and eRF3 sequence motifs essential for PABP binding.', *Nucleic Acids Res* **38**(2), 548-558.

Kozma, R.; Sarner, S.; Ahmed, S. & Lim, L. (1997), 'Rho family GTPases and neuronal growth cone remodelling: relationship between increased complexity induced by Cdc42Hs, Rac1, and acetylcholine and collapse induced by RhoA and lysophosphatidic acid.', *Mol Cell Biol* **17**(3), 1201-1211.

Kudin, A. P.; Bimpong-Buta, N. Y.-B.; Vielhaber, S.; Elger, C. E. & Kunz, W. S. (2004), 'Characterization of superoxide-producing sites in isolated brain mitochondria.', *J Biol Chem* **279**(6), 4127-4135.

Kumar, M.; Verma, R. & Raghava, G. P. S. (2006), 'Prediction of mitochondrial proteins using support vector machine and hidden Markov model.', *J Biol Chem* **281**(9), 5357-5363.

Kumar, V.; Zhang, M.-X.; Swank, M. W.; Kunz, J. & Wu, G.-Y. (2005), 'Regulation of dendritic morphogenesis by Ras-PI3K-Akt-mTOR and Ras-MAPK signaling pathways.', *J Neurosci* **25**(49), 11288-11299.

Kusaba, A.; Ansai, T.; Akifusa, S.; Nakahigashi, K.; Inokuchi, H. & Takehara, T. (2003), 'Cloning and sequencing a HemK-family gene in Porphyromonas gingivalis.', *DNA Seq* **14**(1), 71-74.

Lai, K.-O. & Ip, N. Y. (2009), 'Synapse development and plasticity: roles of ephrin/Eph receptor signalling.', *Curr Opin Neurobiol* **19**(3), 275-283.

Lasko, P. (1999), 'RNA sorting in Drosophila oocytes and embryos.', *FASEB J* **13**(3), 421-433.

Lebeau, G.; Maher-Laporte, M.; Topolnik, L.; Laurent, C. E.; Sossin, W.; Desgroseillers, L. & Lacaille, J.-C. (2008), 'Staufen1 regulation of protein synthesis-dependent long-term potentiation and synaptic function in hippocampal pyramidal cells.', *Mol Cell Biol* **28**(9), 2896-2907.

Lee, A.; Li, W.; Xu, K.; Bogert, B. A.; Su, K. & Gao, F.-B. (2003), 'Control of dendritic development by the Drosophila fragile X-related gene involves the small GTPase Rac1.', *Development* **130**(22), 5543-5552.

Lee, Y. S.; Pressman, S.; Andress, A. P.; Kim, K.; White, J. L.; Cassidy, J. J.; Li, X.; Lubell, K.; Lim, D. H.; Cho, I. S.; Nakahara, K.; Preall, J. B.; Bellare, P.; Sontheimer, E. J. & Carthew, R. W. (2009), 'Silencing by small RNAs is linked to endosomal trafficking.', *Nat Cell Biol* **11**(9), 1150-1156.

Lee, Y.-H. & Stallcup, M. R. (2009), 'Minireview: protein arginine methylation of nonhistone proteins in transcriptional regulation.', *Mol Endocrinol* **23**(4), 425-433.

Lei, M.; Lu, W.; Meng, W.; Parrini, M. C.; Eck, M. J.; Mayer, B. J. & Harrison, S. C. (2000), 'Structure of PAK1 in an autoinhibited conformation reveals a multistage activation switch.', *Cell* **102**(3), 387-397.

Lein, E. S.; Hawrylycz, M. J.; Ao, N.; Ayres, M.; Bensinger, A.; Bernard, A.; Boe, A. F.; Boguski, M. S.; Brockway, K. S.; Byrnes, E. J.; Chen, L.; Chen, L.; Chen, T.-M.; Chin, M. C.; Chong, J.; Crook, B. E.; Czaplinska, A.; Dang, C. N.; Datta, S.; Dee, N.

R.; Desaki, A. L.; Desta, T.; Diep, E.; Dolbeare, T. A.; Donelan, M. J.; Dong, H.-W.; Dougherty, J. G.; Duncan, B. J.; Ebbert, A. J.; Eichele, G.; Estin, L. K.; Faber, C.; Facer, B. A.; Fields, R.; Fischer, S. R.; Fliss, T. P.; Frensley, C.; Gates, S. N.; Glattfelder, K. J.; Halverson, K. R.; Hart, M. R.; Hohmann, J. G.; Howell, M. P.; Jeung, D. P.; Johnson, R. A.; Karr, P. T.; Kawal, R.; Kidney, J. M.; Knapik, R. H.; Kuan, C. L.; Lake, J. H.; Laramee, A. R.; Larsen, K. D.; Lau, C.; Lemon, T. A.; Liang, A. J.; Liu, Y.; Luong, L. T.; Michaels, J.; Morgan, J. J.; Morgan, R. J.; Mortrud, M. T.; Mosqueda, N. F.; Ng, L. L.; Ng, R.; Orta, G. J.; Overly, C. C.; Pak, T. H.; Parry, S. E.; Pathak, S. D.; Pearson, O. C.; Puchalski, R. B.; Riley, Z. L.; Rockett, H. R.; Rowland, S. A.; Royall, J. J.; Ruiz, M. J.; Sarno, N. R.; Schaffnit, K.; Shapovalova, N. V.; Sivisay, T.; Slaughterbeck, C. R.; Smith, S. C.; Smith, K. A.; Smith, B. I.; Sodt, A. J.; Stewart, N. N.; Stumpf, K.-R.; Sunkin, S. M.; Sutram, M.; Tam, A.; Teemer, C. D.; Thaller, C.; Thompson, C. L.; Varnam, L. R.; Visel, A.; Whitlock, R. M.; Wohnoutka, P. E.; Wolkey, C. K.; Wong, V. Y.; Wood, M.; Yaylaoglu, M. B.; Young, R. C.; Youngstrom, B. L.; Yuan, X. F.; Zhang, B.; Zwingman, T. A. & Jones, A. R. (2007), 'Genome-wide atlas of gene expression in the adult mouse brain.', *Nature* **445**(7124), 168-176.

Leung, T.; Manser, E.; Tan, L. & Lim, L. (1995), 'A novel serine/threonine kinase binding the Ras-related RhoA GTPase which translocates the kinase to peripheral membranes.', *J Biol Chem* **270**(49), 29051-29054.

Lewis, B. P.; Green, R. E. & Brenner, S. E. (2003), 'Evidence for the widespread coupling of alternative splicing and nonsense-mediated mRNA decay in humans.', *Proc Natl Acad Sci U S A* **100**(1), 189-192.

Li, R.; Messing, A.; Goldman, J. E. & Brenner, M. (2002), 'GFAP mutations in Alexander disease.', *Int J Dev Neurosci* **20**(3-5), 259-268.

Li, X. & Jin, P. (2009), 'Macro role(s) of microRNAs in fragile X syndrome?', *Neuromolecular Med* **11**(3), 200-207.

Li, Z.; Okamoto, K.-I.; Hayashi, Y. & Sheng, M. (2004), 'The importance of dendritic mitochondria in the morphogenesis and plasticity of spines and synapses.', *Cell* **119**(6), 873-887.

Lin, M. T. & Beal, M. F. (2006), 'Mitochondrial dysfunction and oxidative stress in neurodegenerative diseases.', *Nature* **443**(7113), 787-795.

Liu, Y.; Nie, D.; Huang, Y. & Lu, G. (2009), 'RNAi-mediated knock-down of gene mN6A1 reduces cell proliferation and decreases protein translation.', *Mol Biol Rep* **36**(4), 767-774.

Liu, J.; Rivas, F. V.; Wohlschlegel, J.; Yates, J. R.; Parker, R. & Hannon, G. J. (2005), 'A role for the P-body component GW182 in microRNA function.', *Nat Cell Biol* **7**(12), 1261-1266.

Lorenzo, P. S.; Kung, J. W.; Bottorff, D. A.; Garfield, S. H.; Stone, J. C. & Blumberg, P. M. (2001), 'Phorbol esters modulate the Ras exchange factor RasGRP3.', *Cancer Res* **61**(3), 943-949.

Loschi, M.; Leishman, C. C.; Berardone, N. & Boccaccio, G. L. (2009), 'Dynein and kinesin regulate stress-granule and P-body dynamics.', *J Cell Sci* **122**(Pt 21), 3973-3982.

Lu, R.; Wang, H.; Liang, Z.; Ku, L.; O'donnell, W. T.; Li, W.; Warren, S. T. & Feng, Y. (2004), 'The fragile X protein controls microtubule-associated protein 1B translation and microtubule stability in brain neurone development.', *Proc Natl Acad Sci U S A* **101**(42), 15201-15206.

Luikart, B. W.; Zhang, W.; Wayman, G. A.; Kwon, C.-H.; Westbrook, G. L. & Parada, L. F. (2008), 'Neurotrophin-dependent dendritic filopodial motility: a convergence on PI3K signaling.', *J Neurosci* **28**(27), 7006-7012.

Lykke-Andersen, J. (2002), 'Identification of a human decapping complex associated with hUpf proteins in nonsense-mediated decay.', *Mol Cell Biol* **22**(23), 8114-8121.

Lykke-Andersen, J.; Shu, M. D. & Steitz, J. A. (2000), 'Human Upf proteins target an mRNA for nonsense-mediated decay when bound downstream of a termination codon.', *Cell* **103**(7), 1121-1131.

Lécuyer, E.; Yoshida, H.; Parthasarathy, N.; Alm, C.; Babak, T.; Cerovina, T.; Hughes, T. R.; Tomancak, P. & Krause, H. M. (2007), 'Global analysis of mRNA localization reveals a prominent role in organizing cellular architecture and function.', *Cell* **131**(1), 174-187.

Machesky, L. M. & Gould, K. L. (1999), 'The Arp2/3 complex: a multifunctional actin organizer.', *Curr Opin Cell Biol* **11**(1), 117-121.

Machesky, L. M.; Mullins, R. D.; Higgs, H. N.; Kaiser, D. A.; Blanchoin, L.; May, R. C.; Hall, M. E. & Pollard, T. D. (1999), 'Scar, a WASp-related protein, activates nucleation of actin filaments by the Arp2/3 complex.', *Proc Natl Acad Sci U S A* **96**(7), 3739-3744.

Maeda, M.; Kato, S.; Fukushima, S.; Kaneyuki, U.; Fujii, T.; Kazanietz, M. G.; Oshima, K. & Shigemori, M. (2006), 'Regulation of vascular smooth muscle proliferation and migration by beta2-chimaerin, a non-protein kinase C phorbol ester receptor.', *Int J Mol Med* **17**(4), 559-566.

Manser, E.; Leung, T.; Salihuddin, H.; Zhao, Z. S. & Lim, L. (1994), 'A brain serine/threonine protein kinase activated by Cdc42 and Rac1.', *Nature* **367**(6458), 40-46.

Manuvakhova, M.; Keeling, K. & Bedwell, D. M. (2000), 'Aminoglycoside antibiotics mediate context-dependent suppression of termination codons in a mammalian translation system.', *RNA* **6**(7), 1044-1055.

McBride, H. M.; Neuspiel, M. & Wasiak, S. (2006), 'Mitochondria: more than just a powerhouse.', *Curr Biol* **16**(14), R551-R560.

Mehta, R. & Champney, W. S. (2003), 'Neomycin and paromomycin inhibit 30S ribosomal subunit assembly in Staphylococcus aureus.', *Curr Microbiol* **47**(3), 237-243.

Mellman, I. (1996), 'Endocytosis and molecular sorting.', *Annu Rev Cell Dev Biol* **12**, 575-625.

Meskauskas, A. & Dinman, J. D. (2007), 'Ribosomal protein L3: gatekeeper to the A site.', *Mol Cell* **25**(6), 877-888.

Miki, H.; Suetsugu, S. & Takenawa, T. (1998), 'WAVE, a novel WASP-family protein involved in actin reorganization induced by Rac.', *EMBO J* **17**(23), 6932-6941.

Miki, H. & Takenawa, T. (2002), 'WAVE2 serves a functional partner of IRSp53 by regulating its interaction with Rac.', *Biochem Biophys Res Commun* **293**(1), 93-99.

Moffat, J. G. & Tate, W. P. (1994), 'A single proteolytic cleavage in release factor 2 stabilizes ribosome binding and abolishes peptidyl-tRNA hydrolysis activity.', *J Biol Chem* **269**(29), 18899-18903.

Mora, L.; Heurgué-Hamard, V.; de Zamaroczy, M.; Kervestin, S. & Buckingham, R. H. (2007), 'Methylation of bacterial release factors RF1 and RF2 is required for normal translation termination in vivo.', *J Biol Chem* **282**(49), 35638-35645.

Mounkes, L. C. & Stewart, C. L. (2004), 'Aging and nuclear organization: lamins and progeria.', *Curr Opin Cell Biol* **16**(3), 322-327.

Mowen, K. A.; Tang, J.; Zhu, W.; Schurter, B. T.; Shuai, K.; Herschman, H. R. & David, M. (2001), 'Arginine methylation of STAT1 modulates IFNalpha/beta-induced transcription.', *Cell* **104**(5), 731-741.

Nakahigashi, K.; Kubo, N.; ichiro Narita, S.; Shimaoka, T.; Goto, S.; Oshima, T.; Mori, H.; Maeda, M.; Wada, C. & Inokuchi, H. (2002), 'HemK, a class of protein

methyl transferase with similarity to DNA methyl transferases, methylates polypeptide chain release factors, and hemK knockout induces defects in translational termination.', *Proc Natl Acad Sci U S A* **99**(3), 1473-1478.

Nakayashiki, T.; Nishimura, K. & Inokuchi, H. (1995), 'Cloning and sequencing of a previously unidentified gene that is involved in the biosynthesis of heme in Escherichia coli.', *Gene* **153**(1), 67-70.

Nie, D.-S.; Liu, Y.-B. & Lu, G.-X. (2009), 'Cloning and primarily function study of two novel putative N5-glutamine methyltransferase (Hemk) splice variants from mouse stem cells.', *Mol Biol Rep* **36**(8), 2221-2228.

Nobes, C. & Hall, A. (1994), 'Regulation and function of the Rho subfamily of small GTPases.', *Curr Opin Genet Dev* **4**(1), 77-81.

Nozaki, Y.; Matsunaga, N.; Ishizawa, T.; Ueda, T. & Takeuchi, N. (2008), 'HMRF1L is a human mitochondrial translation release factor involved in the decoding of the termination codons UAA and UAG.', *Genes Cells* **13**(5), 429-438.

Ohn, T.; Kedersha, N.; Hickman, T.; Tisdale, S. & Anderson, P. (2008), 'A functional RNAi screen links O-GlcNAc modification of ribosomal proteins to stress granule and processing body assembly.', *Nat Cell Biol* **10**(10), 1224-1231.

Ohnishi, T.; Yamashita, A.; Kashima, I.; Schell, T.; Anders, K. R.; Grimson, A.; Hachiya, T.; Hentze, M. W.; Anderson, P. & Ohno, S. (2003), 'Phosphorylation of hUPF1 induces formation of mRNA surveillance complexes containing hSMG-5 and hSMG-7.', *Mol Cell* **12**(5), 1187-1200.

Palazzo, A. F.; Cook, T. A.; Alberts, A. S. & Gundersen, G. G. (2001), 'mDia mediates Rho-regulated formation and orientation of stable microtubules.', *Nat Cell Biol* **3**(8), 723-729.

Pan, Q.; Shai, O.; Lee, L. J.; Frey, B. J. & Blencowe, B. J. (2008), 'Deep surveying of alternative splicing complexity in the human transcriptome by high-throughput sequencing.', *Nat Genet* **40**(12), 1413-1415.

Pannekoek, Y.; Heurgué-Hamard, V.; Langerak, A. A. J.; Speijer, D.; Buckingham, R. H. & van der Ende, A. (2005), 'The N5-glutamine S-adenosyl-L-methionine-dependent methyltransferase PrmC/HemK in Chlamydia trachomatis methylates class 1 release factors.', *J Bacteriol* **187**(2), 507-511.

Parker, F.; Maurier, F.; Delumeau, I.; Duchesne, M.; Faucher, D.; Debussche, L.; Dugue, A.; Schweighoffer, F. & Tocque, B. (1996), 'A Ras-GTPase-activating protein SH3-domain-binding protein.', *Mol Cell Biol* **16**(6), 2561-2569.

Parker, R. & Sheth, U. (2007), 'P bodies and the control of mRNA translation and degradation.', *Mol Cell* **25**(5), 635-646.

Pestova, T. V.; Kolupaeva, V. G.; Lomakin, I. B.; Pilipenko, E. V.; Shatsky, I. N.; Agol, V. I. & Hellen, C. U. (2001), 'Molecular mechanisms of translation initiation in eukaryotes.', *Proc Natl Acad Sci U S A* **98**(13), 7029-7036.

Piper, M.; Anderson, R.; Dwivedy, A.; Weinl, C.; van Horck, F.; Leung, K. M.; Cogill, E. & Holt, C. (2006), 'Signalling mechanisms underlying Slit2-induced collapse of Xenopus retinal growth cones.', *Neurone* **49**(2), 215-228.

Pisareva, V. P.; Pisarev, A. V.; Hellen, C. U. T.; Rodnina, M. V. & Pestova, T. V. (2006), 'Kinetic analysis of interaction of eukaryotic release factor 3 with guanine nucleotides.', *J Biol Chem* **281**(52), 40224-40235.

Polevoda, B.; Span, L. & Sherman, F. (2006), 'The yeast translation release factors Mrf1p and Sup45p (eRF1) are methylated, respectively, by the methyltransferases Mtq1p and Mtq2p.', *J Biol Chem* **281**(5), 2562-2571.

Pollard, T. D.; Blanchoin, L. & Mullins, R. D. (2000), 'Molecular mechanisms controlling actin filament dynamics in nonmuscle cells.', *Annu Rev Biophys Biomol Struct* **29**, 545-576.

Praticò, D. & Delanty, N. (2000), 'Oxidative injury in diseases of the central nervous system: focus on Alzheimer's disease.', *Am J Med* **109**(7), 577-585.

Raiborg, C.; Rusten, T. E. & Stenmark, H. (2003), 'Protein sorting into multivesicular endosomes.', *Curr Opin Cell Biol* **15**(4), 446-455.

Ramakers, G. M.; McNamara, R. K.; Lenox, R. H. & Graan, P. N. D. (1999), 'Differential changes in the phosphorylation of the protein kinase C substrates myristoylated alanine-rich C kinase substrate and growth-associated protein-43/B-50 following Schaffer collateral long-term potentiation and long-term depression.', *J Neurochem* **73**(5), 2175-2183.

Ratel, D.; Ravanat, J.-L.; Charles, M.-P.; Platet, N.; Breuillaud, L.; Lunardi, J.; Berger, F. & Wion, D. (2006), 'Undetectable levels of N6-methyl adenine in mouse DNA: Cloning and analysis of PRED28, a gene coding for a putative mammalian DNA adenine methyltransferase.', *FEBS Lett* **580**(13), 3179-3184.

Reeve, S. P.; Bassetto, L.; Genova, G. K.; Kleyner, Y.; Leyssen, M.; Jackson, F. R. & Hassan, B. A. (2005), 'The Drosophila fragile X mental retardation protein controls actin dynamics by directly regulating profilin in the brain.', *Curr Biol* **15**(12), 1156-1163.

Ren, X. R.; Du, Q. S.; Huang, Y. Z.; Ao, S. Z.; Mei, L. & Xiong, W. C. (2001), 'Regulation of CDC42 GTPase by proline-rich tyrosine kinase 2 interacting with PSGAP, a novel pleckstrin homology and Src homology 3 domain containing rhoGAP protein.', *J Cell Biol* **152**(5), 971-984.

Ridley, A. J. & Hall, A. (1992), 'The small GTP-binding protein rho regulates the assembly of focal adhesions and actin stress fibers in response to growth factors.', *Cell* **70**(3), 389-399.

Ridley, A. J.; Paterson, H. F.; Johnston, C. L.; Diekmann, D. & Hall, A. (1992), 'The small GTP-binding protein rac regulates growth factor-induced membrane ruffling.', *Cell* **70**(3), 401-410.

Ristanović, D.; Milosević, N. T. & Stulić, V. (2006), 'Application of modified Sholl analysis to neuronal dendritic arborization of the cat spinal cord.', *J Neurosci Methods* **158**(2), 212-218.

Robinson, R. C.; Turbedsky, K.; Kaiser, D. A.; Marchand, J. B.; Higgs, H. N.; Choe, S. & Pollard, T. D. (2001), 'Crystal structure of Arp2/3 complex.', *Science* **294**(5547), 1679-1684.

Rohatgi, R.; Ho, H. Y. & Kirschner, M. W. (2000), 'Mechanism of N-WASP activation by CDC42 and phosphatidylinositol 4, 5-bisphosphate.', *J Cell Biol* **150**(6), 1299-1310.

Rozengurt, E.; Rey, O. & Waldron, R. T. (2005), 'Protein kinase D signalling.', *J Biol Chem* **280**(14), 13205-13208.

Sadowski, I.; Stone, J. C. & Pawson, T. (1986), 'A noncatalytic domain conserved among cytoplasmic protein-tyrosine kinases modifies the kinase function and transforming activity of Fujinami sarcoma virus P130gag-fps.', *Mol Cell Biol* **6**(12), 4396-4408.

Saito, Y.; Oinuma, I.; Fujimoto, S. & Negishi, M. (2009), 'Plexin-B1 is a GTPase activating protein for M-Ras, remodelling dendrite morphology.', *EMBO Rep* **10**(6), 614-621.

Sakuno, T.; Araki, Y.; Ohya, Y.; Kofuji, S.; Takahashi, S.; ichi Hoshino, S. & Katada, T. (2004), 'Decapping reaction of mRNA requires Dcp1 in fission yeast: its characterization in different species from yeast to human.', *J Biochem* **136**(6), 805-812.

Sasaki, Y.; Cheng, C.; Uchida, Y.; Nakajima, O.; Ohshima, T.; Yagi, T.; Taniguchi, M.; Nakayama, T.; Kishida, R.; Kudo, Y.; Ohno, S.; Nakamura, F. & Goshima, Y. (2002), 'Fyn and Cdk5 mediate semaphorin-3A signalling, which is involved in regulation of dendrite orientation in cerebral cortex.', *Neurone* **35**(5), 907-920.

Schapira, A. H.; Mann, V. M.; Cooper, J. M.; Dexter, D.; Daniel, S. E.; Jenner, P.; Clark, J. B. & Marsden, C. D. (1990), 'Anatomic and disease specificity of NADH CoQ1 reductase (complex I) deficiency in Parkinson's disease.', *J Neurochem* **55**(6), 2142-2145.

Scheid, M. P. & Woodgett, J. R. (2001), 'PKB/AKT: functional insights from genetic models.', *Nat Rev Mol Cell Biol* **2**(10), 760-768.

Schenck, A.; Bardoni, B.; Langmann, C.; Harden, N.; Mandel, J. L. & Giangrande, A. (2003), 'CYFIP/Sra-1 controls neuronal connectivity in Drosophila and links the Rac1 GTPase pathway to the fragile X protein.', *Neurone* **38**(6), 887-898.

Schmidt, A. & Hall, A. (2002), 'Guanine nucleotide exchange factors for Rho GTPases: turning on the switch.', *Genes Dev* **16**(13), 1587-1609.

Schroeder, R.; Waldsich, C. & Wank, H. (2000), 'Modulation of RNA function by aminoglycoside antibiotics.', *EMBO J* **19**(1), 1-9.

Schubert, H. L.; Phillips, J. D. & Hill, C. P. (2003), 'Structures along the catalytic pathway of PrmC/HemK, an N5-glutamine AdoMet-dependent methyltransferase.', *Biochemistry* **42**(19), 5592-5599.

Schuman, E. M.; Dynes, J. L. & Steward, O. (2006), 'Synaptic regulation of translation of dendritic mRNAs.', *J Neurosci* **26**(27), 7143-7146.

Schwede, T.; Diemand, A.; Guex, N. & Peitsch, M. C. (2000), 'Protein structure computing in the genomic era.', *Res Microbiol* **151**(2), 107-112.

Schwede, T.; Kopp, J.; Guex, N. & Peitsch, M. C. (2003), 'SWISS-MODEL: An automated protein homology-modeling server.', *Nucleic Acids Res* **31**(13), 3381-3385.

Scolnick, E.; Tompkins, R.; Caskey, T. & Nirenberg, M. (1968), 'Release factors differing in specificity for terminator codons.', *Proc Natl Acad Sci U S A* **61**(2), 768-774.

Scoumanne, A.; Zhang, J. & Chen, X. (2009), 'PRMT5 is required for cell-cycle progression and p53 tumor suppressor function.', *Nucleic Acids Res* **37**(15), 4965-4976.

She, M.; Decker, C. J.; Svergun, D. I.; Round, A.; Chen, N.; Muhlrad, D.; Parker, R. & Song, H. (2008), 'Structural basis of dcp2 recognition and activation by dcp1.', *Mol Cell* **29**(3), 337-349.

Shi, L.; Fu, W.-Y.; Hung, K.-W.; Porchetta, C.; Hall, C.; Fu, A. K. Y. & Ip, N. Y. (2007), 'Alpha2-chimaerin interacts with EphA4 and regulates EphA4-dependent growth cone collapse.', *Proc Natl Acad Sci U S A* **104**(41), 16347-16352.

Shi, S.-H.; Jan, L. Y. & Jan, Y.-N. (2003), 'Hippocampal neuronal polarity specified by spatially localized mPar3/mPar6 and PI 3-kinase activity.', *Cell* **112**(1), 63-75.

SHOLL, D. A. (1953), 'Dendritic organization in the neurones of the visual and motor cortices of the cat.', *J Anat* **87**(4), 387-406.

Silva, A. L.; Ribeiro, P.; Inácio, A.; Liebhaber, S. A. & Romão, L. (2008), 'Proximity of the poly(A)-binding protein to a premature termination codon inhibits mammalian nonsense-mediated mRNA decay.', *RNA* **14**(3), 563-576.

Singh, G.; Rebbapragada, I. & Lykke-Andersen, J. (2008), 'A competition between stimulators and antagonists of Upf complex recruitment governs human nonsense-mediated mRNA decay.', *PLoS Biol* **6**(4), e111.

Small, G. W.; Mazziotta, J. C.; Collins, M. T.; Baxter, L. R.; Phelps, M. E.; Mandelkern, M. A.; Kaplan, A.; Rue, A. L.; Adamson, C. F. & Chang, L. (1995), 'Apolipoprotein E type 4 allele and cerebral glucose metabolism in relatives at risk for familial Alzheimer disease.', *JAMA* **273**(12), 942-947.

Smith, L. G. & Li, R. (2004), 'Actin polymerization: riding the wave.', *Curr Biol* **14**(3), R109-R111.

Soleimanpour-Lichaei, H. R.; Kühl, I.; Gaisne, M.; Passos, J. F.; Wydro, M.; Rorbach, J.; Temperley, R.; Bonnefoy, N.; Tate, W.; Lightowlers, R. & Chrzanowska-Lightowlers, Z. (2007), 'mtRF1a is a human mitochondrial translation release factor decoding the major termination codons UAA and UAG.', *Mol Cell* **27**(5), 745-757.

Solomon, S.; Xu, Y.; Wang, B.; David, M. D.; Schubert, P.; Kennedy, D. & Schrader, J. W. (2007), 'Distinct structural features of caprin-1 mediate its interaction with G3BP-1 and its induction of phosphorylation of eukaryotic translation initiation factor 2alpha, entry to cytoplasmic stress granules, and selective interaction with a subset of mRNAs.', *Mol Cell Biol* **27**(6), 2324-2342.

Soncini, C.; Berdo, I. & Draetta, G. (2001), 'Ras-GAP SH3 domain binding protein (G3BP) is a modulator of USP10, a novel human ubiquitin specific protease.', *Oncogene* **20**(29), 3869-3879.

Songyang, Z.; Shoelson, S. E.; Chaudhuri, M.; Gish, G.; Pawson, T.; Haser, W. G.; King, F.; Roberts, T.; Ratnofsky, S. & Lechleider, R. J. (1993), 'SH2 domains recognize specific phosphopeptide sequences.', *Cell* **72**(5), 767-778.

Stalder, L. & Mühlemann, O. (2008), 'The meaning of nonsense.', *Trends Cell Biol* **18**(7), 315-321.

Stansfield, I.; Jones, K. M.; Kushnirov, V. V.; Dagkesamanskaya, A. R.; Poznyakovski, A. I.; Paushkin, S. V.; Nierras, C. R.; Cox, B. S.; Ter-Avanesyan, M. D. & Tuite, M. F. (1995), 'The products of the SUP45 (eRF1) and SUP35 genes

interact to mediate translation termination in Saccharomyces cerevisiae.', *EMBO J* **14**(17), 4365-4373.

Steward, O. & Levy, W. B. (1982), 'Preferential localization of polyribosomes under the base of dendritic spines in granule cells of the dentate gyrus.', *J Neurosci* **2**(3), 284-291.

Stribinskis, V.; Gao, G. J.; Ellis, S. R. & Martin, N. C. (2001), 'Rpm2, the protein subunit of mitochondrial RNase P in Saccharomyces cerevisiae, also has a role in the translation of mitochondrially encoded subunits of cytochrome c oxidase.', *Genetics* **158**(2), 573-585.

Stribinskis, V. & Ramos, K. S. (2007), 'Rpm2p, a protein subunit of mitochondrial RNase P, physically and genetically interacts with cytoplasmic processing bodies.', *Nucleic Acids Res* **35**(4), 1301-1311.

Takeuchi, S.; Yamaki, N.; Iwasato, T.; Negishi, M. & Katoh, H. (2009), 'Beta2-chimaerin binds to EphA receptors and regulates cell migration.', *FEBS Lett* **583**(8), 1237-1242.

Tang, S. J.; Meulemans, D.; Vazquez, L.; Colaco, N. & Schuman, E. (2001b), 'A role for a rat homolog of staufen in the transport of RNA to neuronal dendrites.', *Neurone* **32**(3), 463-475.

Tang, Y.; Nyengaard, J. R.; Groot, D. M. D. & Gundersen, H. J. (2001a), 'Total regional and global number of synapses in the human brain neocortex.', *Synapse* **41**(3), 258-273.

Tarpey, P. S.; Raymond, F. L.; Nguyen, L. S.; Rodriguez, J.; Hackett, A.; Vandeleur, L.; Smith, R.; Shoubridge, C.; Edkins, S.; Stevens, C.; O'Meara, S.; Tofts, C.; Barthorpe, S.; Buck, G.; Cole, J.; Halliday, K.; Hills, K.; Jones, D.; Mironenko, T.; Perry, J.; Varian, J.; West, S.; Widaa, S.; Teague, J.; Dicks, E.; Butler, A.; Menzies, A.; Richardson, D.; Jenkinson, A.; Shepherd, R.; Raine, K.; Moon, J.; Luo, Y.; Parnau, J.; Bhat, S. S.; Gardner, A.; Corbett, M.; Brooks, D.; Thomas, P.; Parkinson-

Lawrence, E.; Porteous, M. E.; Warner, J. P.; Sanderson, T.; Pearson, P.; Simensen, R. J.; Skinner, C.; Hoganson, G.; Superneau, D.; Wooster, R.; Bobrow, M.; Turner, G.; Stevenson, R. E.; Schwartz, C. E.; Futreal, P. A.; Srivastava, A. K.; Stratton, M. R. & Gécz, J. (2007), 'Mutations in UPF3B, a member of the nonsense-mediated mRNA decay complex, cause syndromic and nonsyndromic mental retardation.', *Nat Genet* **39**(9), 1127-1133.

Tcherkezian, J. & Lamarche-Vane, N. (2007), 'Current knowledge of the large RhoGAP family of proteins.', *Biol Cell* **99**(2), 67-86.

Thierry-Mieg, D. & Thierry-Mieg, J. (2006), 'AceView: a comprehensive cDNA-supported gene and transcripts annotation.', *Genome Biol* **7 Suppl 1**, S12.1-S1214.

Thomas, M. G.; Tosar, L. J. M.; Desbats, M. A.; Leishman, C. C. & Boccaccio, G. L. (2009), 'Mammalian Staufen 1 is recruited to stress granules and impairs their assembly.', *J Cell Sci* **122**(Pt 4), 563-573.

Thomas, M. G.; Tosar, L. J. M.; Loschi, M.; Pasquini, J. M.; Correale, J.; Kindler, S. & Boccaccio, G. L. (2005), 'Staufen recruitment into stress granules does not affect early mRNA transport in oligodendrocytes.', *Mol Biol Cell* **16**(1), 405-420.

Thyagarajan, D.; Bressman, S.; Bruno, C.; Przedborski, S.; Shanske, S.; Lynch, T.; Fahn, S. & DiMauro, S. (2000), 'A novel mitochondrial 12SrRNA point mutation in parkinsonism, deafness, and neuropathy.', *Ann Neurol* **48**(5), 730-736.

Tourrière, H.; Chebli, K.; Zekri, L.; Courselaud, B.; Blanchard, J. M.; Bertrand, E. & Tazi, J. (2003), 'The RasGAP-associated endoribonuclease G3BP assembles stress granules.', *J Cell Biol* **160**(6), 823-831.

Tourrière, H.; Gallouzi, I. E.; Chebli, K.; Capony, J. P.; Mouaikel, J.; van der Geer, P. & Tazi, J. (2001), 'RasGAP-associated endoribonuclease G3Bp: selective RNA degradation and phosphorylation-dependent localization.', *Mol Cell Biol* **21**(22), 7747-7760.

Troca-Marín, J. A.; Alves-Sampaio, A.; Tejedor, F. J. & Montesinos, M. L. (2010), 'Local translation of dendritic RhoA revealed by an improved synaptoneurosome preparation.', *Mol Cell Neurosci* **43**(3), 308-314.

Twiss, J. L. & van Minnen, J. (2006), 'New insights into neuronal regeneration: the role of axonal protein synthesis in pathfinding and axonal extension.', *J Neurotrauma* **23**(3-4), 295-308.

Uchida, N.; Hoshino, S.-I.; Imataka, H.; Sonenberg, N. & Katada, T. (2002), 'A novel role of the mammalian GSPT/eRF3 associating with poly(A)-binding protein in Cap/Poly(A)-dependent translation.', *J Biol Chem* **277**(52), 50286-50292.

Vale, R. D. & Fletterick, R. J. (1997), 'The design plan of kinesin motors.', *Annu Rev Cell Dev Biol* **13**, 745-777.

Valente, L.; Tiranti, V.; Marsano, R. M.; Malfatti, E.; Fernandez-Vizarra, E.; Donnini, C.; Mereghetti, P.; Gioia, L. D.; Burlina, A.; Castellan, C.; Comi, G. P.; Savasta, S.; Ferrero, I. & Zeviani, M. (2007), 'Infantile encephalopathy and defective mitochondrial DNA translation in patients with mutations of mitochondrial elongation factors EFG1 and EFTu.', *Am J Hum Genet* **80**(1), 44-58.

Vanet, A.; Plumbridge, J. A.; Guérin, M. F. & Alix, J. H. (1994), 'Ribosomal protein methylation in Escherichia coli: the gene prmA, encoding the ribosomal protein L11 methyltransferase, is dispensable.', *Mol Microbiol* **14**(5), 947-958.

de Ven, T. J. V.; VanDongen, H. M. A. & VanDongen, A. M. J. (2005), 'The nonkinase phorbol ester receptor alpha 1-chimerin binds the NMDA receptor NR2A subunit and regulates dendritic spine density.', *J Neurosci* **25**(41), 9488-9496.

Verkerk, A. J.; Pieretti, M.; Sutcliffe, J. S.; Fu, Y. H.; Kuhl, D. P.; Pizzuti, A.; Reiner, O.; Richards, S.; Victoria, M. F. & Zhang, F. P. (1991), 'Identification of a gene (FMR-1) containing a CGG repeat coincident with a breakpoint cluster region exhibiting length variation in fragile X syndrome.', *Cell* **65**(5), 905-914.

Verstreken, P.; Ly, C. V.; Venken, K. J. T.; Koh, T.-W.; Zhou, Y. & Bellen, H. J. (2005), 'Synaptic mitochondria are critical for mobilization of reserve pool vesicles at Drosophila neuromuscular junctions.', *Neurone* **47**(3), 365-378.

Vessey, J. P.; Macchi, P.; Stein, J. M.; Mikl, M.; Hawker, K. N.; Vogelsang, P.; Wieczorek, K.; Vendra, G.; Riefler, J.; Tübing, F.; Aparicio, S. A. J.; Abel, T. & Kiebler, M. A. (2008), 'A loss of function allele for murine Staufen1 leads to impairment of dendritic Staufen1-RNP delivery and dendritic spine morphogenesis.', *Proc Natl Acad Sci U S A* **105**(42), 16374-16379.

Villacé, P.; Marión, R. M. & Ortín, J. (2004), 'The composition of Staufen-containing RNA granules from human cells indicates their role in the regulated transport and translation of messenger RNAs.', *Nucleic Acids Res* **32**(8), 2411-2420.

Wegmeyer, H.; Egea, J.; Rabe, N.; Gezelius, H.; Filosa, A.; Enjin, A.; Varoqueaux, F.; Deininger, K.; Schnütgen, F.; Brose, N.; Klein, R.; Kullander, K. & Betz, A. (2007), 'EphA4-dependent axon guidance is mediated by the RacGAP alpha2-chimaerin.', *Neurone* **55**(5), 756-767.

Wegmeyer, H.; Egea, J.; Rabe, N.; Gezelius, H.; Filosa, A.; Enjin, A.; Varoqueaux, F.; Deininger, K.; Schnütgen, F.; Brose, N.; Klein, R.; Kullander, K. & Betz, A. (2007), 'EphA4-dependent axon guidance is mediated by the RacGAP alpha2-chimaerin.', *Neurone* **55**(5), 756-767.

Wegner, A. (1976), 'Head to tail polymerization of actin.', *J Mol Biol* **108**(1), 139-150.

Weng, Y.; Czaplinski, K. & Peltz, S. W. (1996), 'Identification and characterization of mutations in the UPF1 gene that affect nonsense suppression and the formation of the Upf protein complex but not mRNA turnover.', *Mol Cell Biol* **16**(10), 5491-5506.

Whittaker, V. & Barker, L. (1972), The subcellular fractionation of brain tissue with special reference to the preparation of synaptosomes and their component organelles, *in* R. Fried, ed.,'Methods of Neurochemistry', Marcel Dekker, New York, , pp. 1-52.

Wickham, L.; Duchaîne, T.; Luo, M.; Nabi, I. R. & DesGroseillers, L. (1999), 'Mammalian staufen is a double-stranded-RNA- and tubulin-binding protein which localizes to the rough endoplasmic reticulum.', *Mol Cell Biol* **19**(3), 2220-2230.

Wilkinson, D. G. (2001), 'Multiple roles of EPH receptors and ephrins in neural development.', *Nat Rev Neurosci* **2**(3), 155-164.

Witte, H.; Neukirchen, D. & Bradke, F. (2008), 'Microtubule stabilization specifies initial neuronal polarization.', *J Cell Biol* **180**(3), 619-632.

Wu, K. Y.; Hengst, U.; Cox, L. J.; Macosko, E. Z.; Jeromin, A.; Urquhart, E. R. & Jaffrey, S. R. (2005), 'Local translation of RhoA regulates growth cone collapse.', *Nature* **436**(7053), 1020-1024.

Yamashita, A.; Izumi, N.; Kashima, I.; Ohnishi, T.; Saari, B.; Katsuhata, Y.; Muramatsu, R.; Morita, T.; Iwamatsu, A.; Hachiya, T.; Kurata, R.; Hirano, H.; Anderson, P. & Ohno, S. (2009), 'SMG-8 and SMG-9, two novel subunits of the SMG-1 complex, regulate remodeling of the mRNA surveillance complex during nonsense-mediated mRNA decay.', *Genes Dev* **23**(9), 1091-1105.

Yamashita, A.; Ohnishi, T.; Kashima, I.; Taya, Y. & Ohno, S. (2001), 'Human SMG-1, a novel phosphatidylinositol 3-kinase-related protein kinase, associates with components of the mRNA surveillance complex and is involved in the regulation of nonsense-mediated mRNA decay.', *Genes Dev* **15**(17), 2215-2228.

Yan, C.; Martinez-Quiles, N.; Eden, S.; Shibata, T.; Takeshima, F.; Shinkura, R.; Fujiwara, Y.; Bronson, R.; Snapper, S. B.; Kirschner, M. W.; Geha, R.; Rosen, F. S. & Alt, F. W. (2003), 'WAVE2 deficiency reveals distinct roles in embryogenesis and Rac-mediated actin-based motility.', *EMBO J* **22**(14), 3602-3612.

Yang, C.; Liu, Y.; Leskow, F. C.; Weaver, V. M. & Kazanietz, M. G. (2005), 'Rac-GAP-dependent inhibition of breast cancer cell proliferation by beta2-chimerin.', *J Biol Chem* **280**(26), 24363-24370.

Yang, J.; Zhang, Z.; Roe, S. M.; Marshall, C. J. & Barford, D. (2009a), 'Activation of Rho GTPases by DOCK exchange factors is mediated by a nucleotide sensor.', *Science* **325**(5946), 1398-1402.

Yang, N.; Higuchi, O.; Ohashi, K.; Nagata, K.; Wada, A.; Kangawa, K.; Nishida, E. & Mizuno, K. (1998), 'Cofilin phosphorylation by LIM-kinase 1 and its role in Rac-mediated actin reorganization.', *Nature* **393**(6687), 809-812.

Yang, X.-Y.; Guan, M.; Vigil, D.; Der, C. J.; Lowy, D. R. & PopescuYang2009, N. C. (2009b), 'p120Ras-GAP binds the DLC1 Rho-GAP tumor suppressor protein and inhibits its RhoA GTPase and growth-suppressing activities.', *Oncogene* **28**(11), 1401-1409.

Yang, Z.; Jakymiw, A.; Wood, M. R.; Eystathioy, T.; Rubin, R. L.; Fritzler, M. J. & Chan, E. K. L. (2004b), 'GW182 is critical for the stability of GW bodies expressed during the cell cycle and cell proliferation.', *J Cell Sci* **117**(Pt 23), 5567-5578.

Yang, Z.; Shipman, L.; Zhang, M.; Anton, B. P.; Roberts, R. J. & Cheng, X. (2004a), 'Structural characterization and comparative phylogenetic analysis of Escherichia coli HemK, a protein (N5)-glutamine methyltransferase.', *J Mol Biol* **340**(4), 695-706.

Yao, J.; Sasaki, Y.; Wen, Z.; Bassell, G. J. & Zheng, J. Q. (2006), 'An essential role for beta-actin mRNA localization and translation in Ca2+-dependent growth cone guidance.', *Nat Neurosci* **9**(10), 1265-1273.

Yoshimoto, T.; Boehm, M.; Olive, M.; Crook, M. F.; San, H.; Langenickel, T. & Nabel, E. G. (2006), 'The arginine methyltransferase PRMT2 binds RB and regulates E2F function.', *Exp Cell Res* **312**(11), 2040-2053.

Yoshimura, T.; Arimura, N. & Kaibuchi, K. (2006), 'Molecular mechanisms of axon specification and neuronal disorders.', *Ann N Y Acad Sci* **1086**, 116-125.

Yoshimura, T.; Kawano, Y.; Arimura, N.; Kawabata, S.; Kikuchi, A. & Kaibuchi, K. (2005), 'GSK-3beta regulates phosphorylation of CRMP-2 and neuronal polarity.', *Cell* **120**(1), 137-149.

Zalfa, F.; Achsel, T. & Bagni, C. (2006), 'mRNPs, polysomes or granules: FMRP in neuronal protein synthesis.', *Curr Opin Neurobiol* **16**(3), 265-269.

Zalfa, F.; Giorgi, M.; Primerano, B.; Moro, A.; Penta, A. D.; Reis, S.; Oostra, B. & Bagni, C. (2003), 'The fragile X syndrome protein FMRP associates with BC1 RNA and regulates the translation of specific mRNAs at synapses.', *Cell* **112**(3), 317-327.

Zavialov, A. V.; Buckingham, R. H. & Ehrenberg, M. (2001), 'A posttermination ribosomal complex is the guanine nucleotide exchange factor for peptide release factor RF3.', *Cell* **107**(1), 115-124.

Zhang, H.-Z.; Liu, J.-G.; Wei, Y.-P.; Wu, C.; Cao, Y.-K. & Wang, M. (2007), 'Expression of G3BP and RhoC in esophageal squamous carcinoma and their effect on prognosis.', *World J Gastroenterol* **13**(30), 4126-4130.

Zhao, Z.-S.; Lim, J. P.; Ng, Y.-W.; Lim, L. & Manser, E. (2005), 'The GIT-associated kinase PAK targets to the centrosome and regulates Aurora-A.', *Mol Cell* **20**(2), 237-249.

Zhong, J.; Zhang, T. & Bloch, L. M. (2006), 'Dendritic mRNAs encode diversified functionalities in hippocampal pyramidal neurones.', *BMC Neurosci* **7**, 17.

Zhong, N.; Ju, W.; Nelson, D.; Dobkin, C. & Brown, W. T. (1999), 'Reduced mRNA for G3BP in fragile X cells: evidence of FMR1 gene regulation.', *Am J Med Genet* **84**(3), 268-271.